LIPEI DU

UC BERKELEY / LBNL / MCGILL U

ELECTROMAGNETIC AND WEAK PROBES: THEORY

THE 12TH INTERNATIONAL CONFERENCE ON HARD AND ELECTROMAGNETIC PROBES OF HIGH-ENERGY NUCLEAR COLLISIONS

NAGASAKI, JAPAN

SEPTEMBER 26, 2024

Weak probes covered in *Nuclear PDFs* by Petja Paakkinen

INTRODUCTION

Electromagnetic probes

real photon

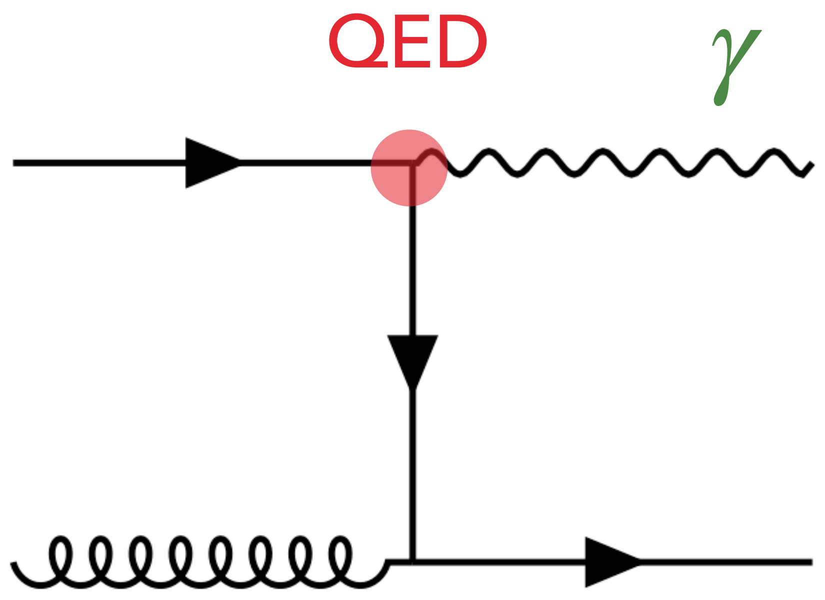

Compton scattering

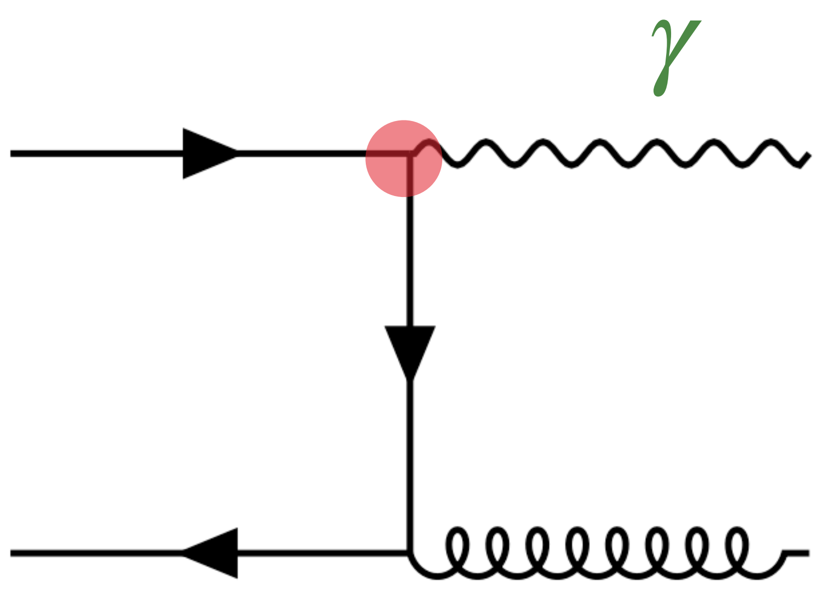

quark-antiquark annihilation

virtual photon

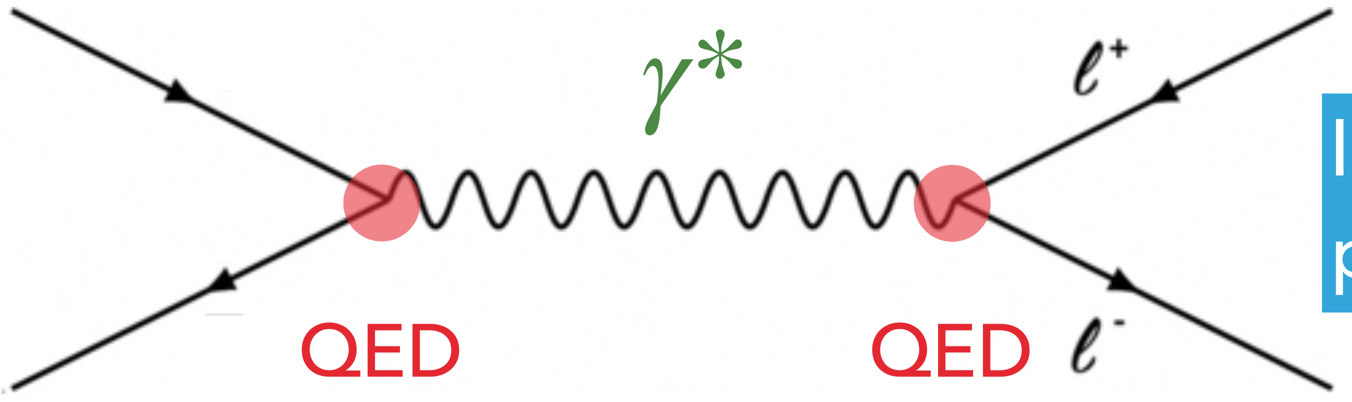

lepton–anti-lepton pair (dilepton)

quark-antiquark annihilation

Four momentum $K^\mu = (\omega, \boldsymbol{k})$. real photon: massless, $\omega = k$; dilepton: invariant mass $M = \sqrt{\omega^2 - k^2}$

Electromagnetic probes

real photon

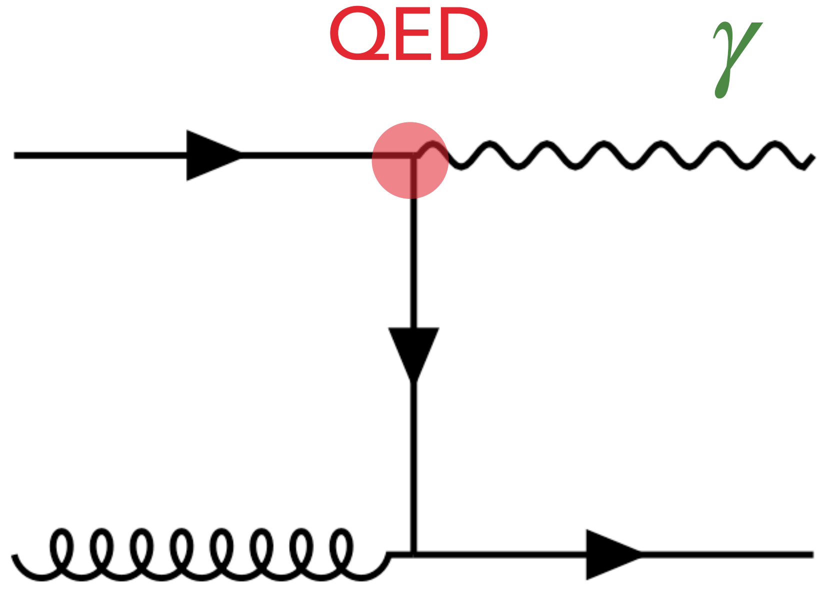

Compton scattering

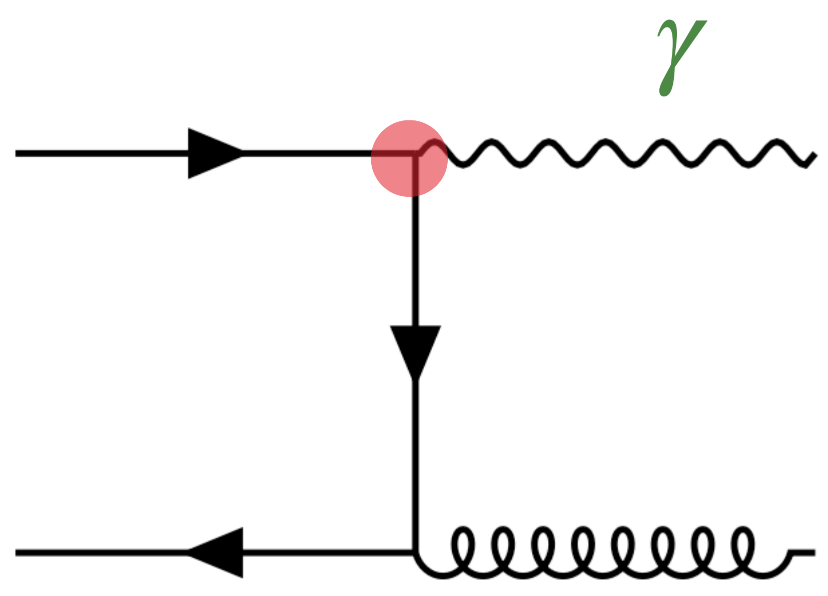

quark-antiquark annihilation

virtual photon

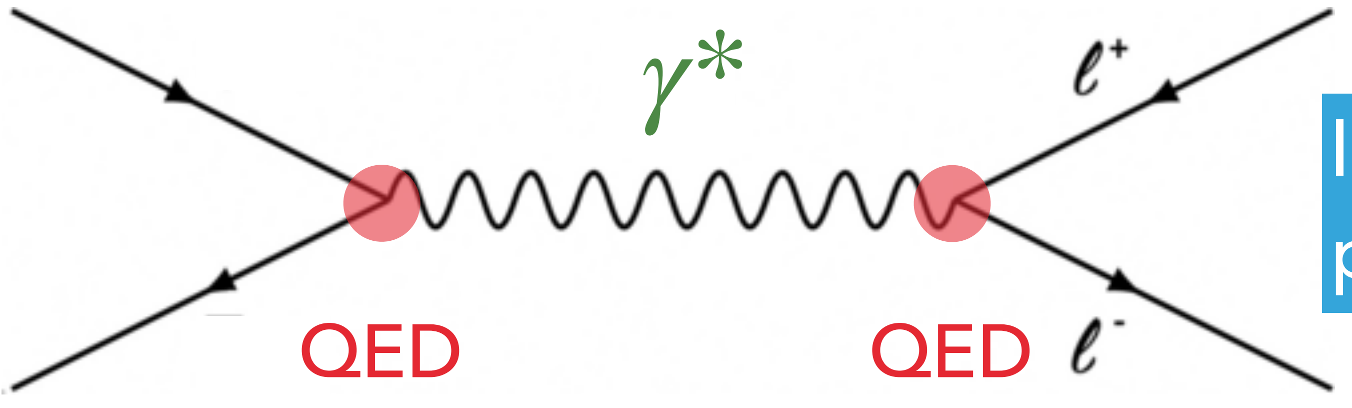

lepton–anti-lepton pair (dilepton)

quark-antiquark annihilation

Four momentum $K^\mu = (\omega, \boldsymbol{k})$. real photon: massless, $\omega = k$; dilepton: invariant mass $M = \sqrt{\omega^2 - k^2}$

- The electromagnetic (EM) interaction is much weaker than the strong interaction; $L_{\rm mfp}^{\rm em} \gg$ system size.

Electromagnetic probes

real photon

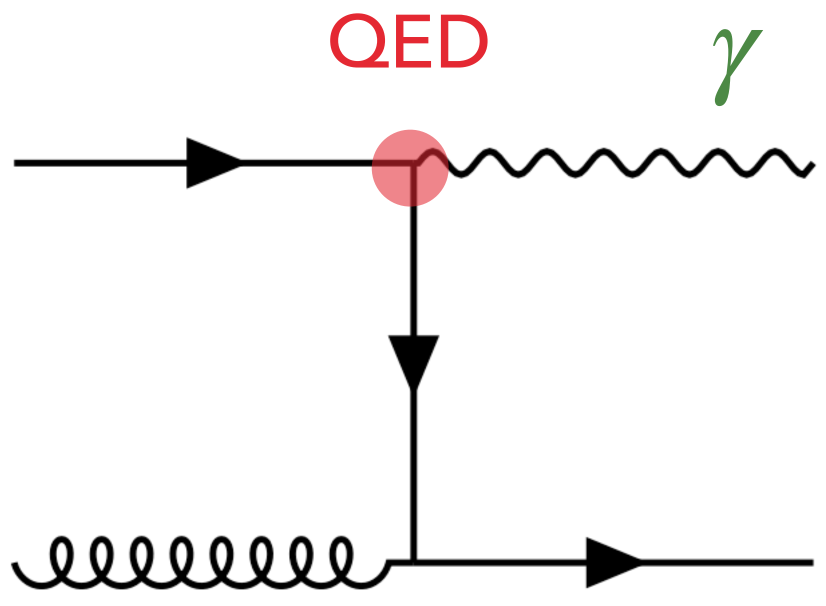

Compton scattering

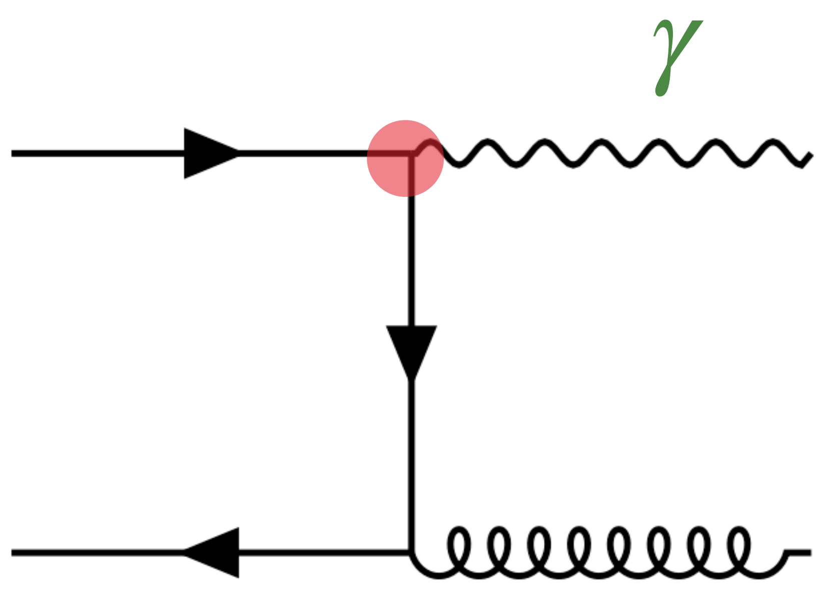

quark-antiquark annihilation

virtual photon

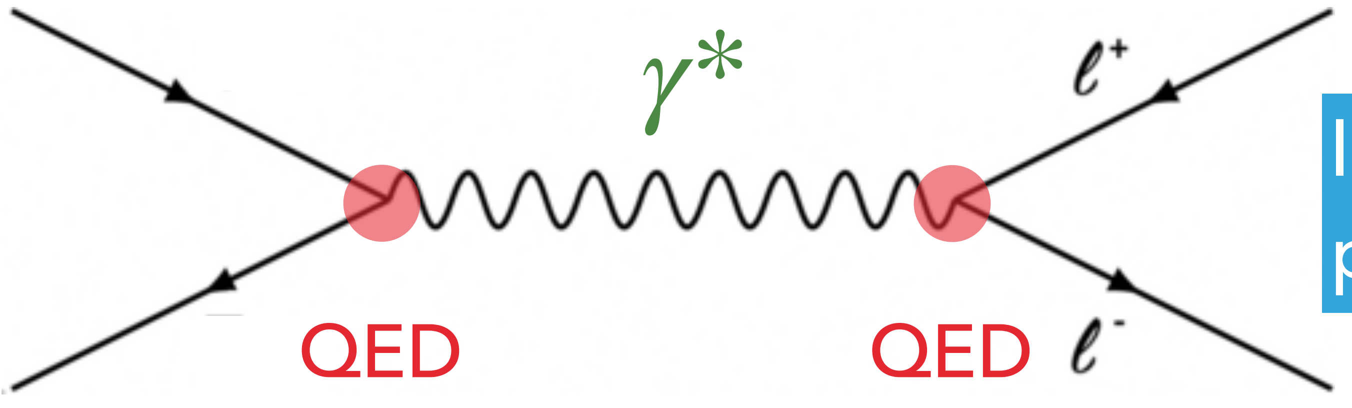

lepton–anti-lepton pair (dilepton)

quark-antiquark annihilation

Four momentum $K^\mu = (\omega, \boldsymbol{k})$. real photon: massless, $\omega = k$; dilepton: invariant mass $M = \sqrt{\omega^2 - k^2}$

- The electromagnetic (EM) interaction is much weaker than the strong interaction; $L_{\rm mfp}^{\rm em} \gg$ system size.
- EM probes penetrate the QCD environment undisturbed, carrying information at their production points.

Electromagnetic probes

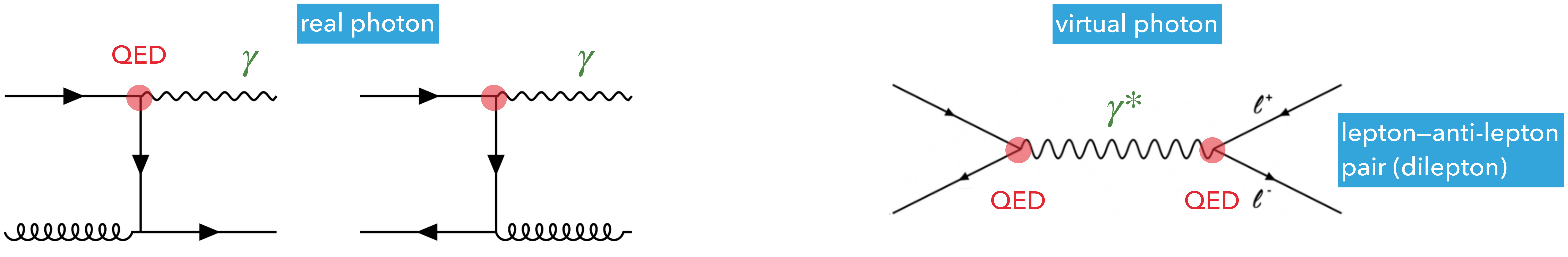

Compton scattering quark-antiquark annihilation quark-antiquark annihilation

Four momentum $K^\mu = (\omega, \boldsymbol{k})$. real photon: massless, $\omega = k$; dilepton: invariant mass $M = \sqrt{\omega^2 - k^2}$

- The electromagnetic (EM) interaction is much weaker than the strong interaction; $L^{\mathrm{em}}_{\mathrm{mfp}} \gg$ system size.
- EM probes penetrate the QCD environment undisturbed, carrying information at their production points.
- Dilepton M-spectra are unaffected by the dynamics and thus not blue-shifted.

Electromagnetic radiation

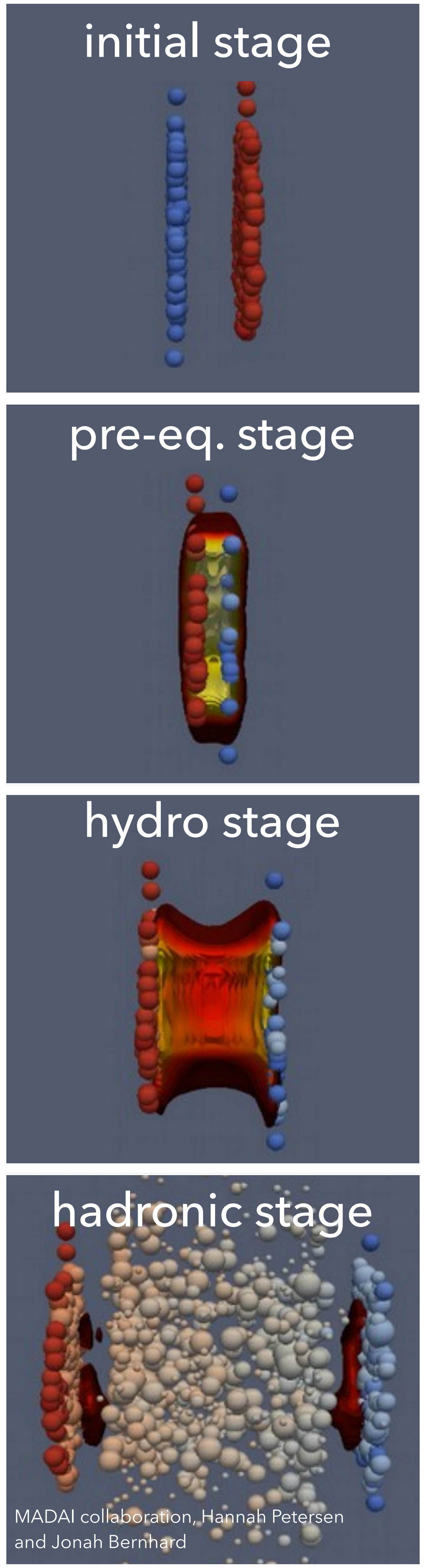

Electromagnetic radiation

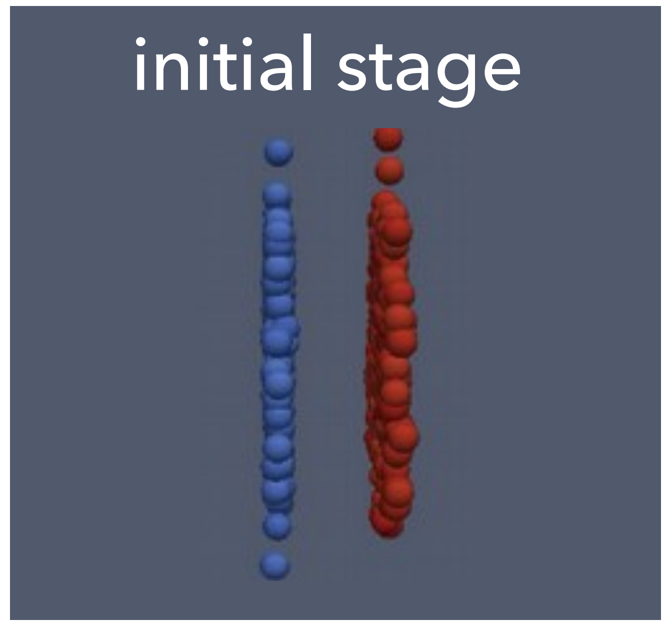

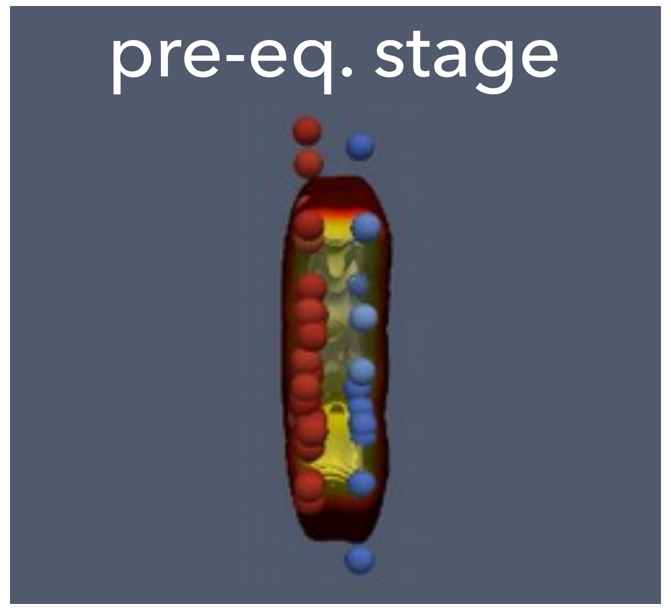

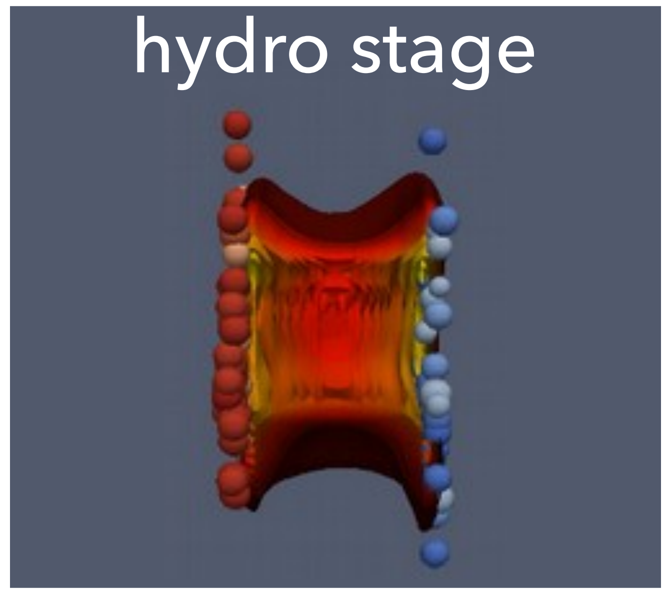

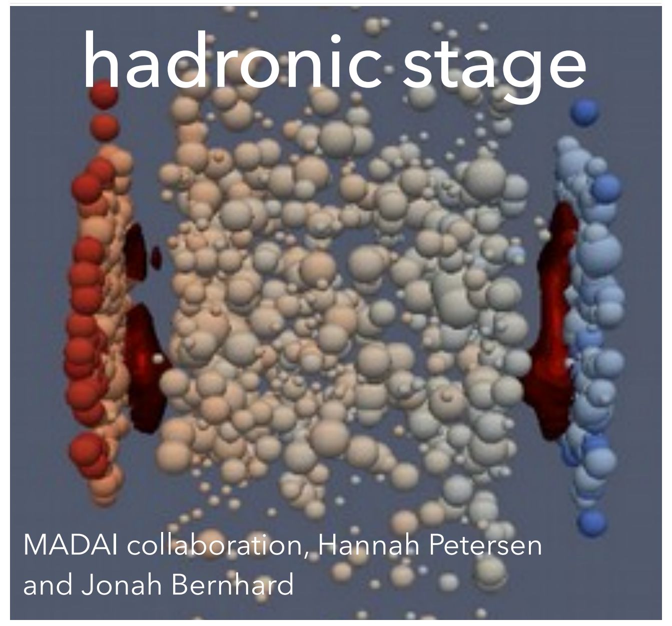

photon

Electromagnetic radiation

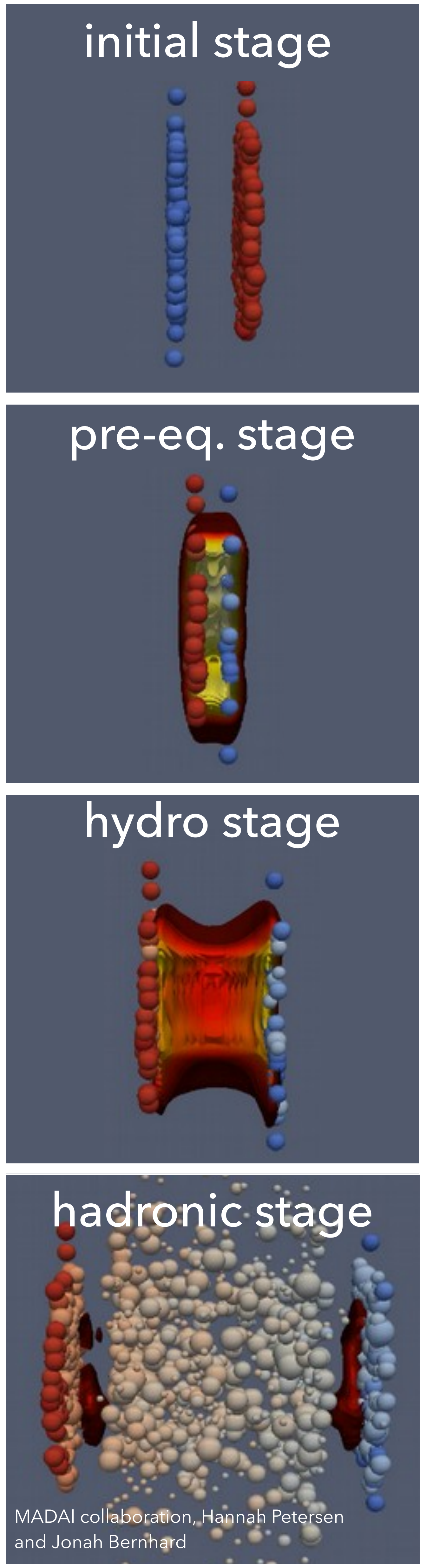

photon

- initial hard scattering or fragmentation ('prompt' photons)

Electromagnetic radiation

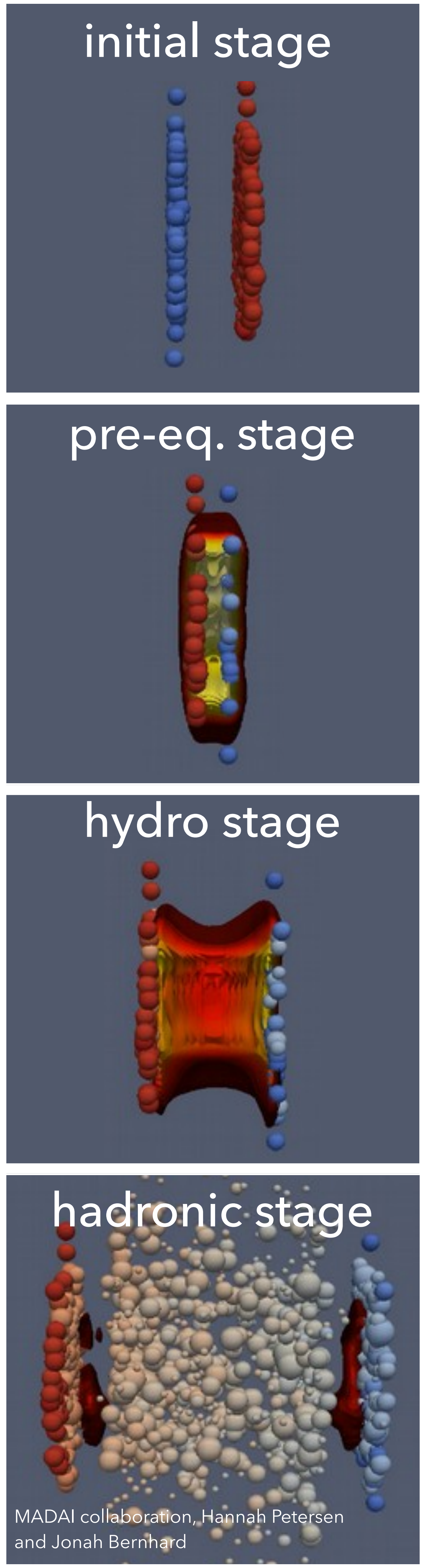

photon

- initial hard scattering or fragmentation ('prompt' photons)

- pre-equilibrium photons

Electromagnetic radiation

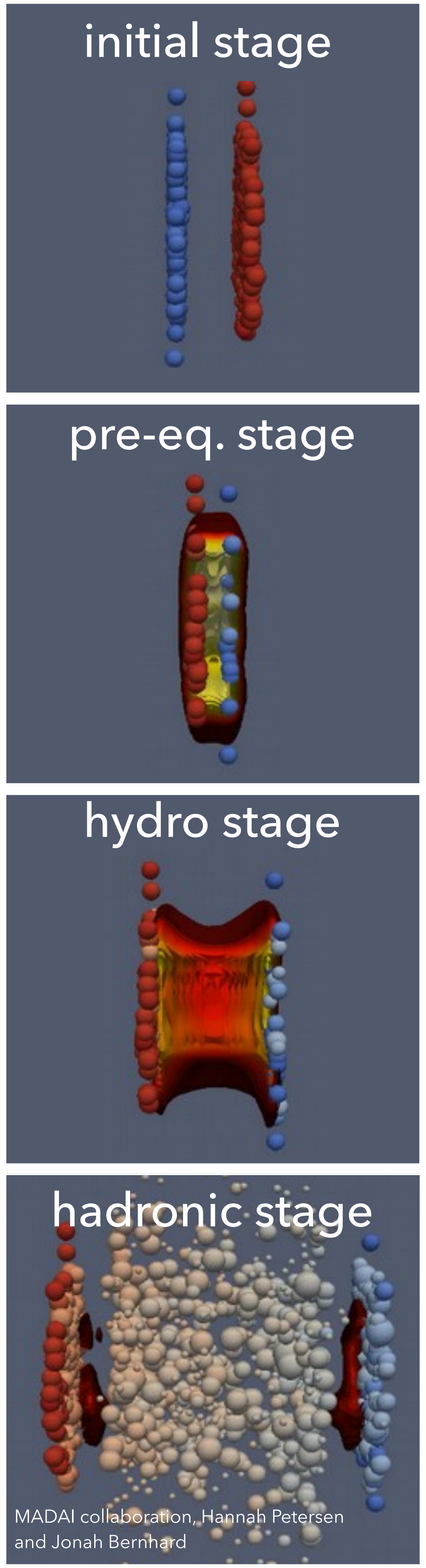

photon

- initial hard scattering or fragmentation (‘prompt’ photons)
- pre-equilibrium photons
- thermal emission from QGP
- jet-medium interaction

Electromagnetic radiation

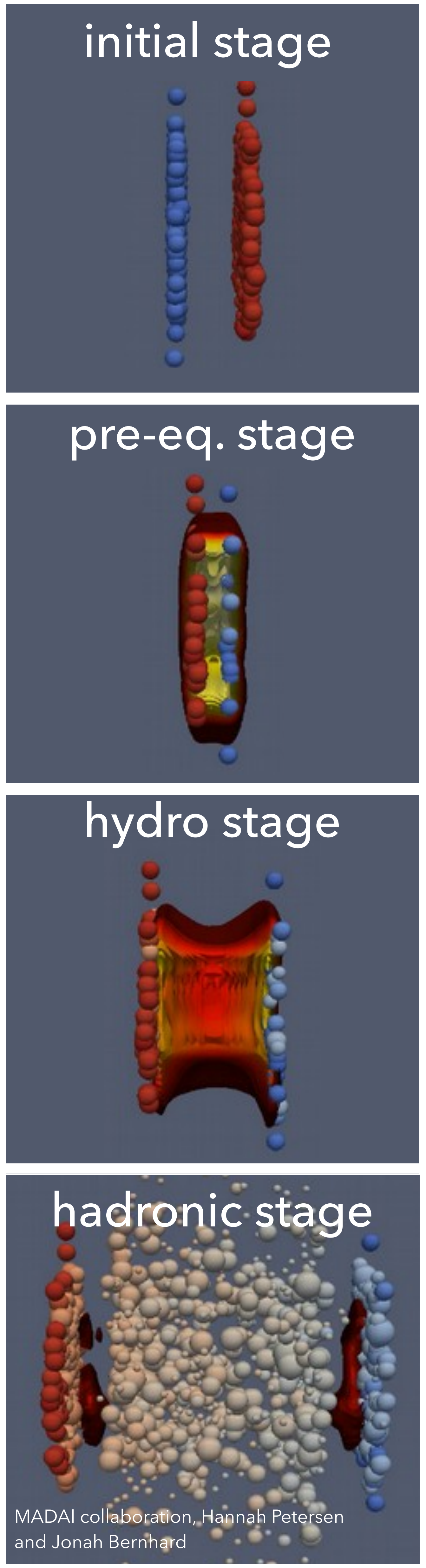

photon

- initial hard scattering or fragmentation (‘prompt’ photons)
- pre-equilibrium photons
- thermal emission from QGP
- jet-medium interaction
- thermal emission from hadronic matter
- hadronic decays

Electromagnetic radiation

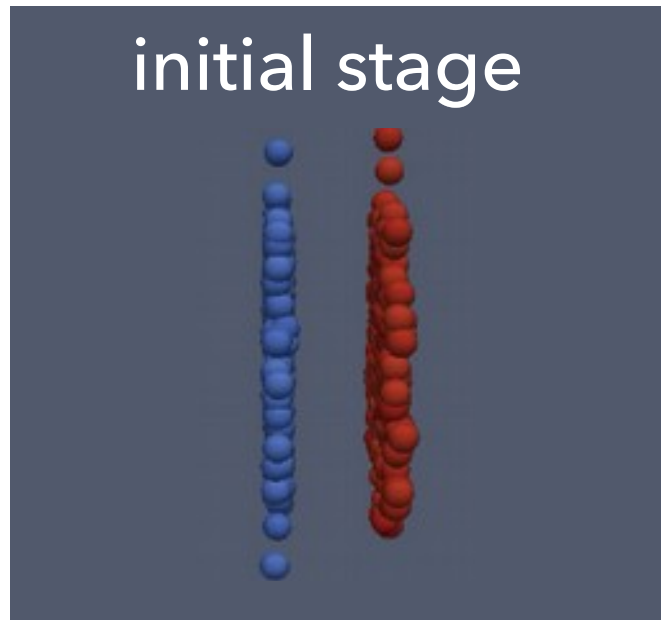

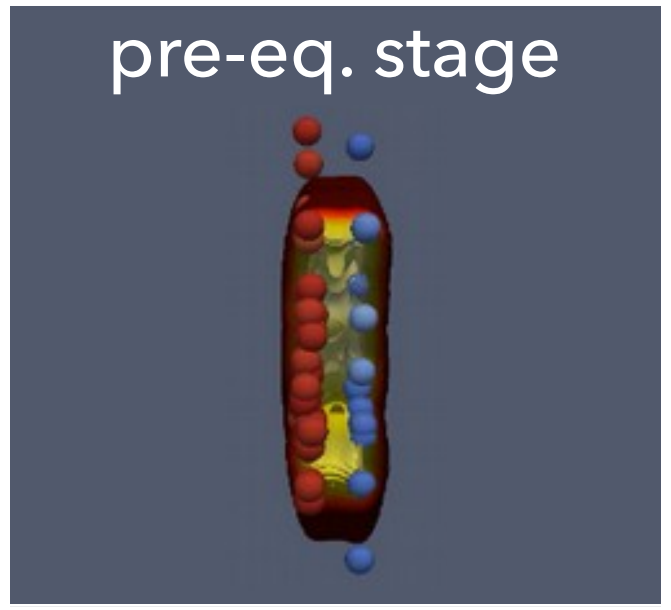

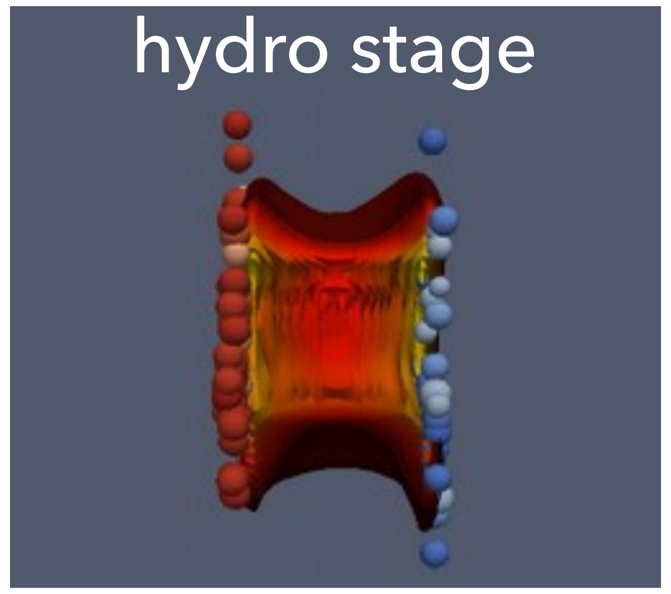

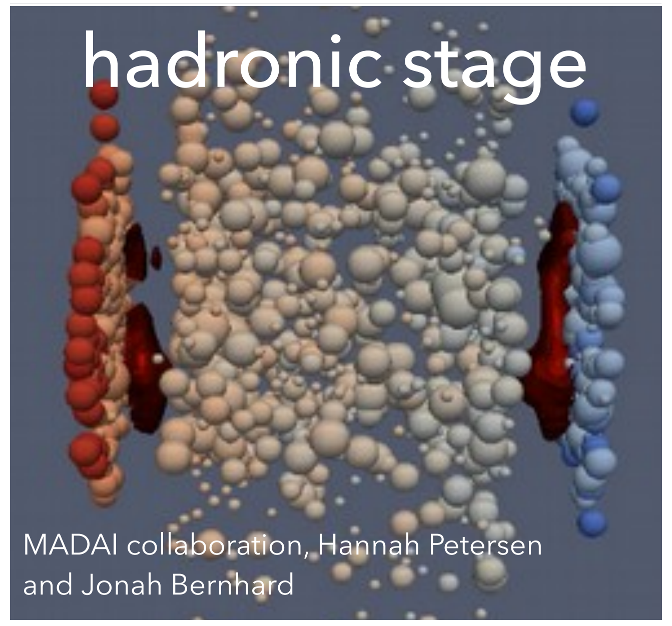

photon

- initial hard scattering or fragmentation ('prompt' photons)
- pre-equilibrium photons
- thermal emission from QGP
- jet-medium interaction
- thermal emission from hadronic matter
- hadronic decays

dilepton

- Drell-Yan process
- pre-equilibrium dileptons
- thermal emission from QGP
- semi-leptonic decays of open heavy flavor
- thermal emission from hadronic matter
- hadronic decays

Electromagnetic radiation

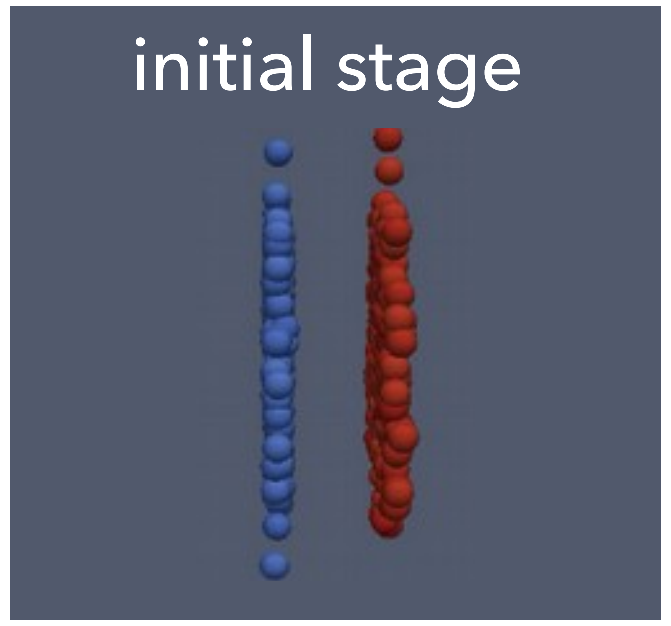

photon

- initial hard scattering or fragmentation ('prompt' photons)

dilepton

- Drell-Yan process

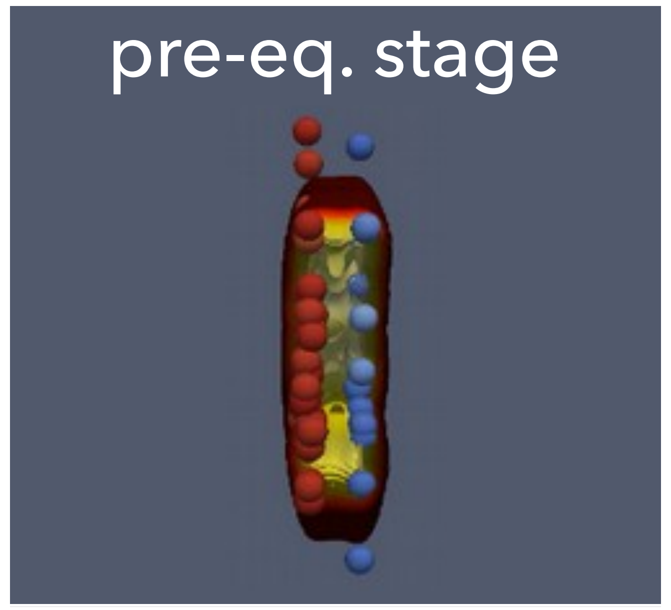

- pre-equilibrium photons

- pre-equilibrium dileptons

pre-eq.: provide information on thermalization and equilibration

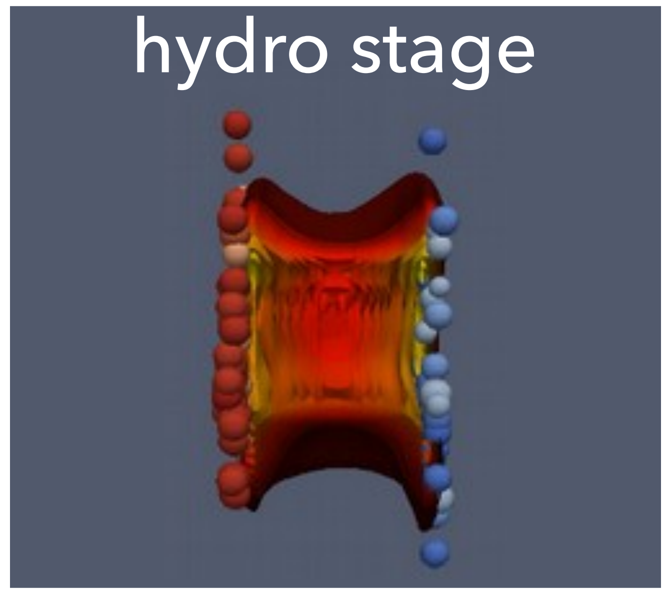

- thermal emission from QGP
- jet-medium interaction

- thermal emission from QGP
- semi-leptonic decays of open heavy flavor

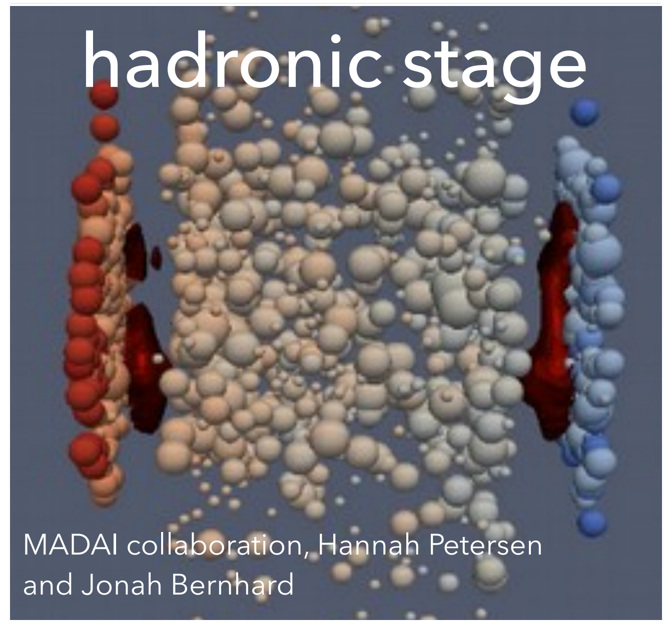

- thermal emission from hadronic matter
- hadronic decays

- thermal emission from hadronic matter
- hadronic decays

Electromagnetic radiation

photon | dilepton

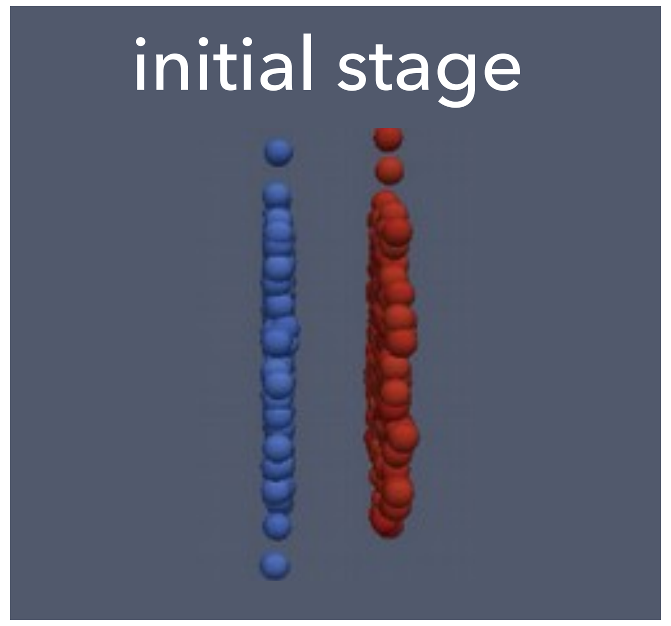

- initial hard scattering or fragmentation (‘prompt’ photons)
- Drell-Yan process

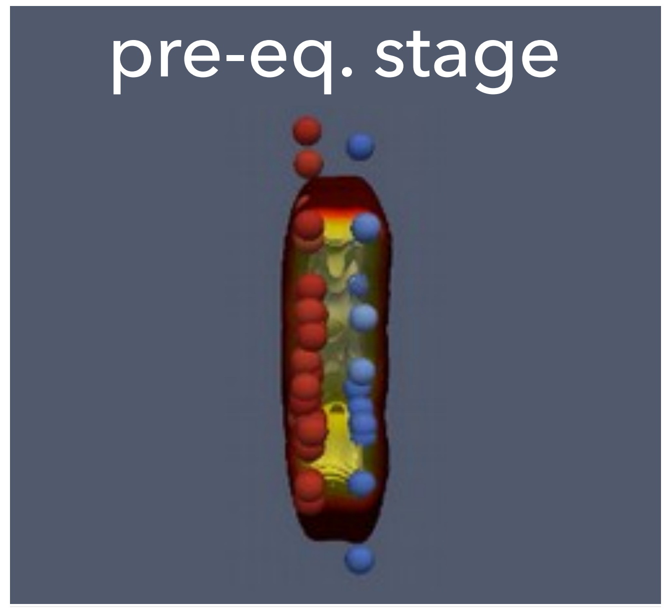

- pre-equilibrium photons
- pre-equilibrium dileptons

pre-eq.: provide information on thermalization and equilibration

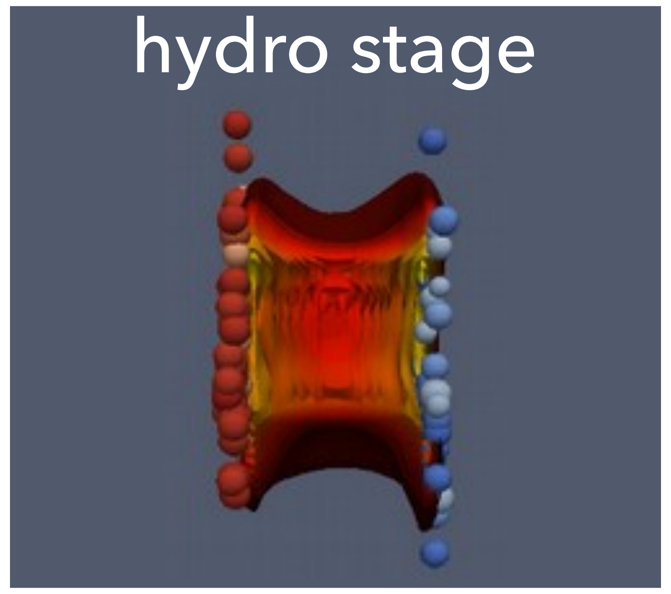

- thermal emission from QGP
- jet-medium interaction
- thermal emission from QGP
- semi-leptonic decays of open heavy flavor

thermal: provide information on thermodynamic properties

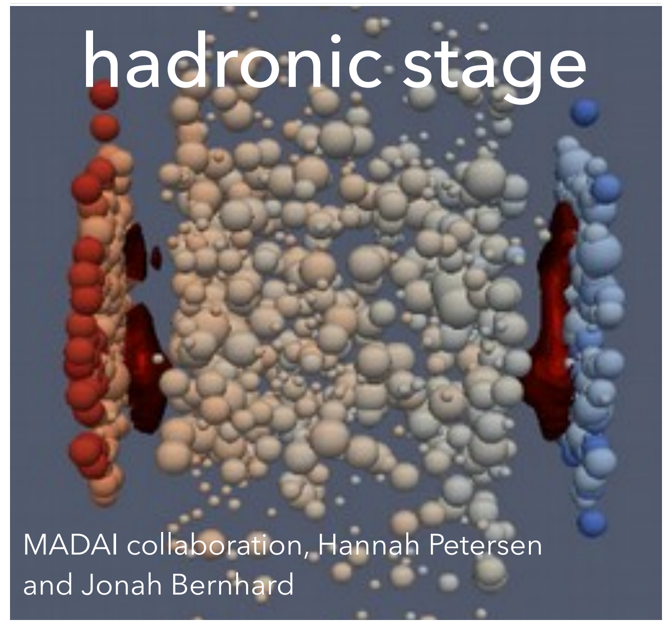

- thermal emission from hadronic matter
- hadronic decays
- thermal emission from hadronic matter
- hadronic decays

Spectra measurements in experiments

direct photons

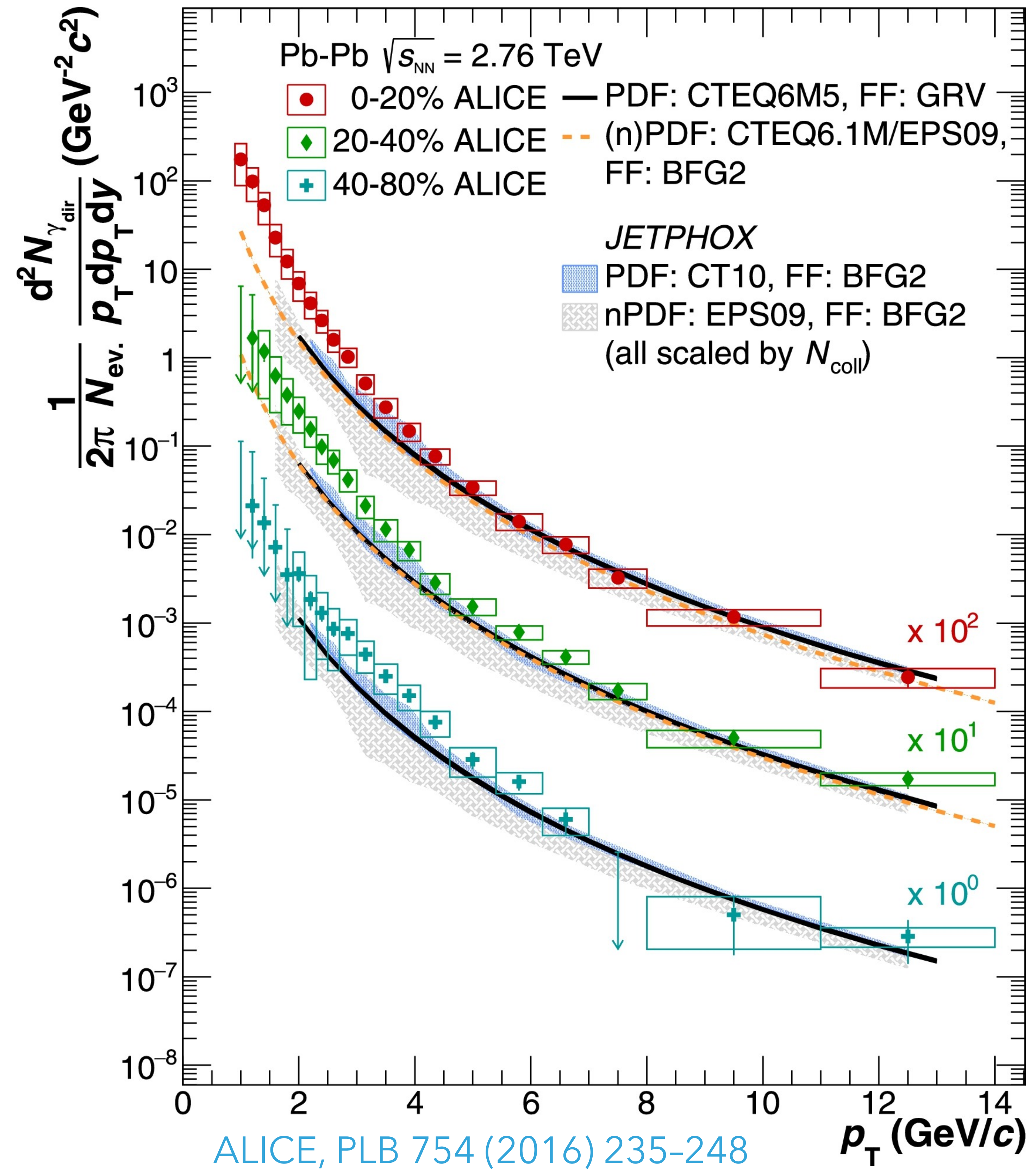

ALICE, PLB 754 (2016) 235–248

inclusive dileptons

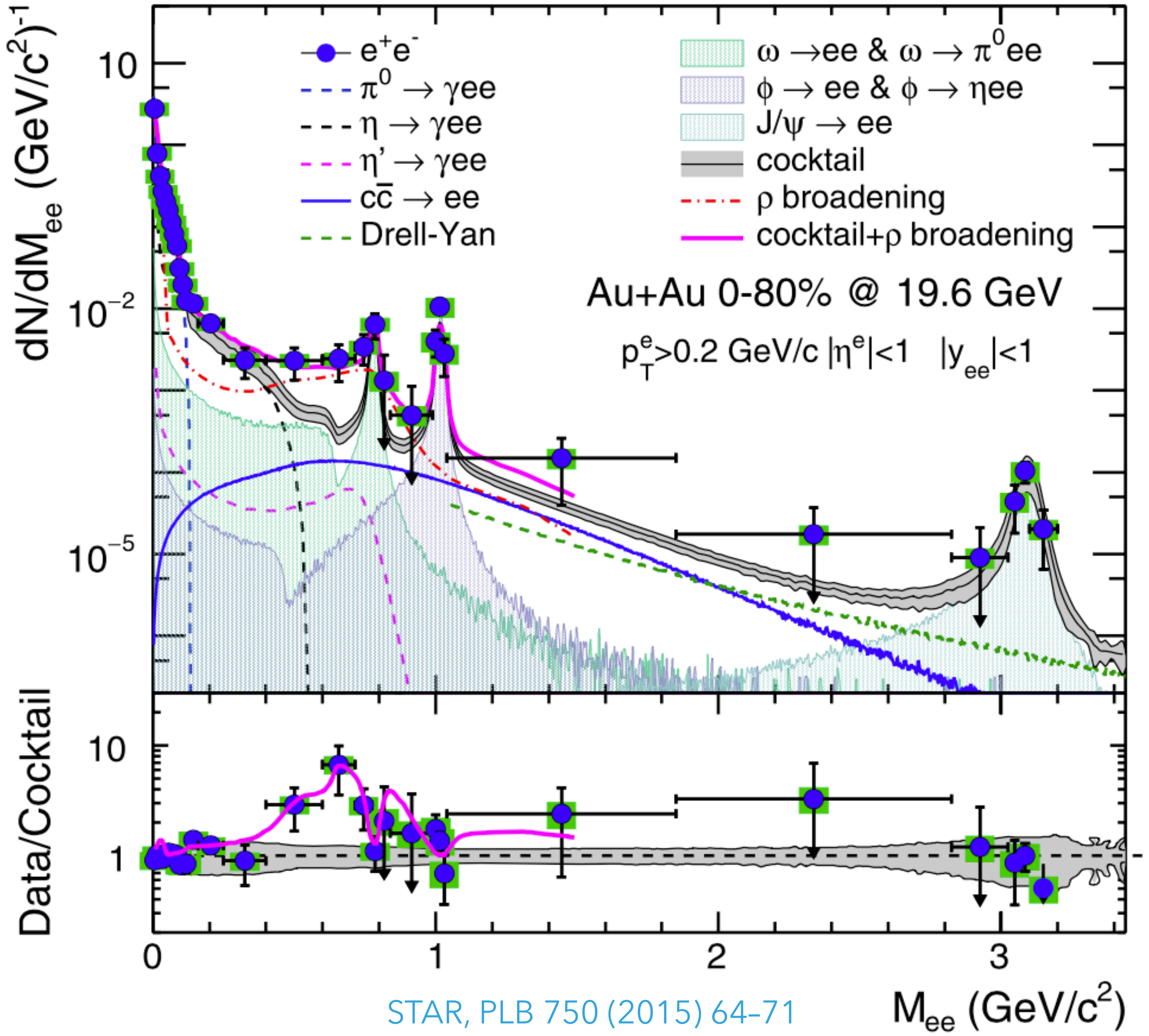

STAR, PLB 750 (2015) 64–71

- EM are produced throughout the evolution, so isolating productions from different stages is challenging.
- However, selecting p_T or M windows can be helpful. On average, the larger p_T or M the EM probes have, the earlier they are produced.

Spectra measurements in experiments

direct photons

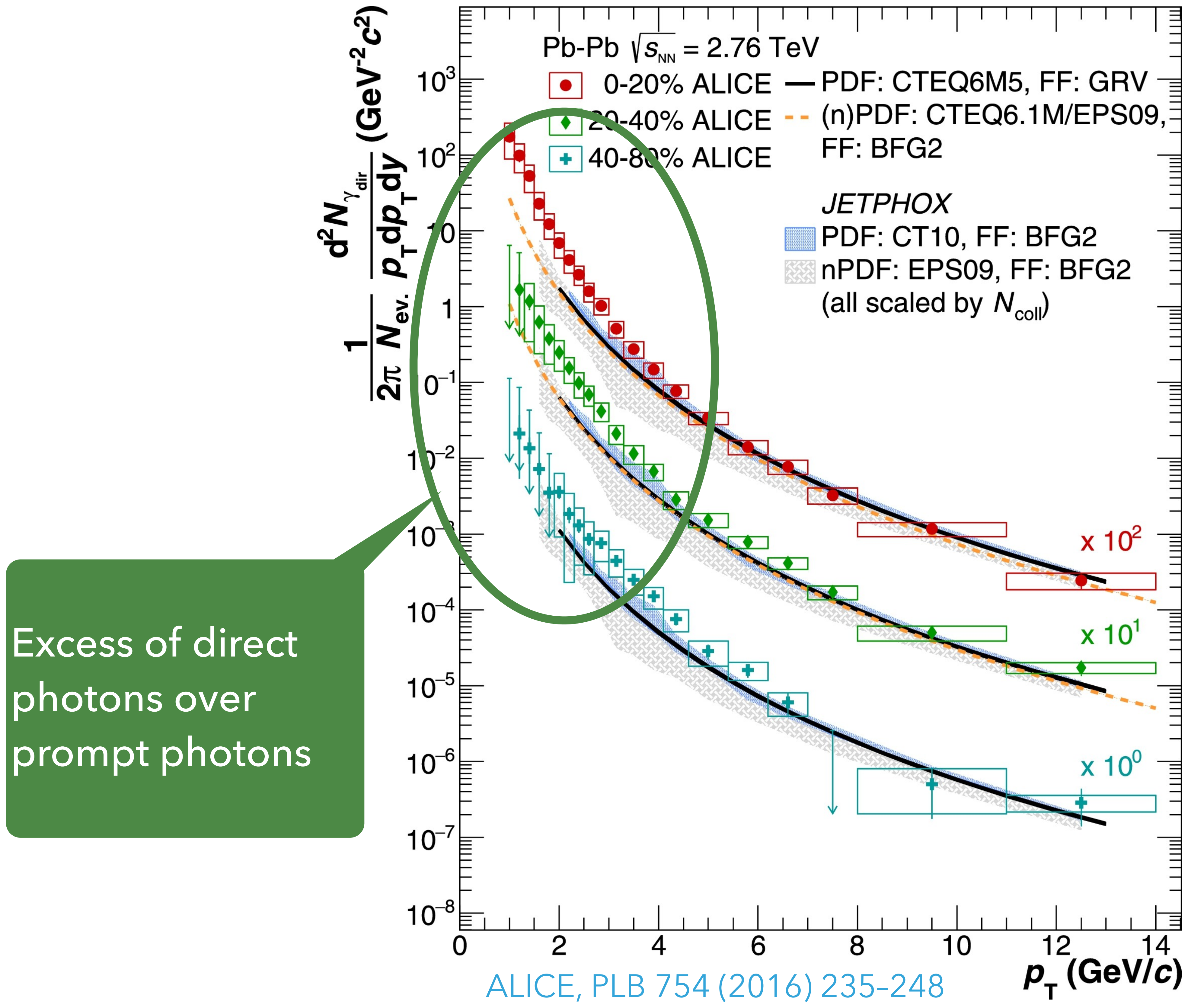

ALICE, PLB 754 (2016) 235–248

inclusive dileptons

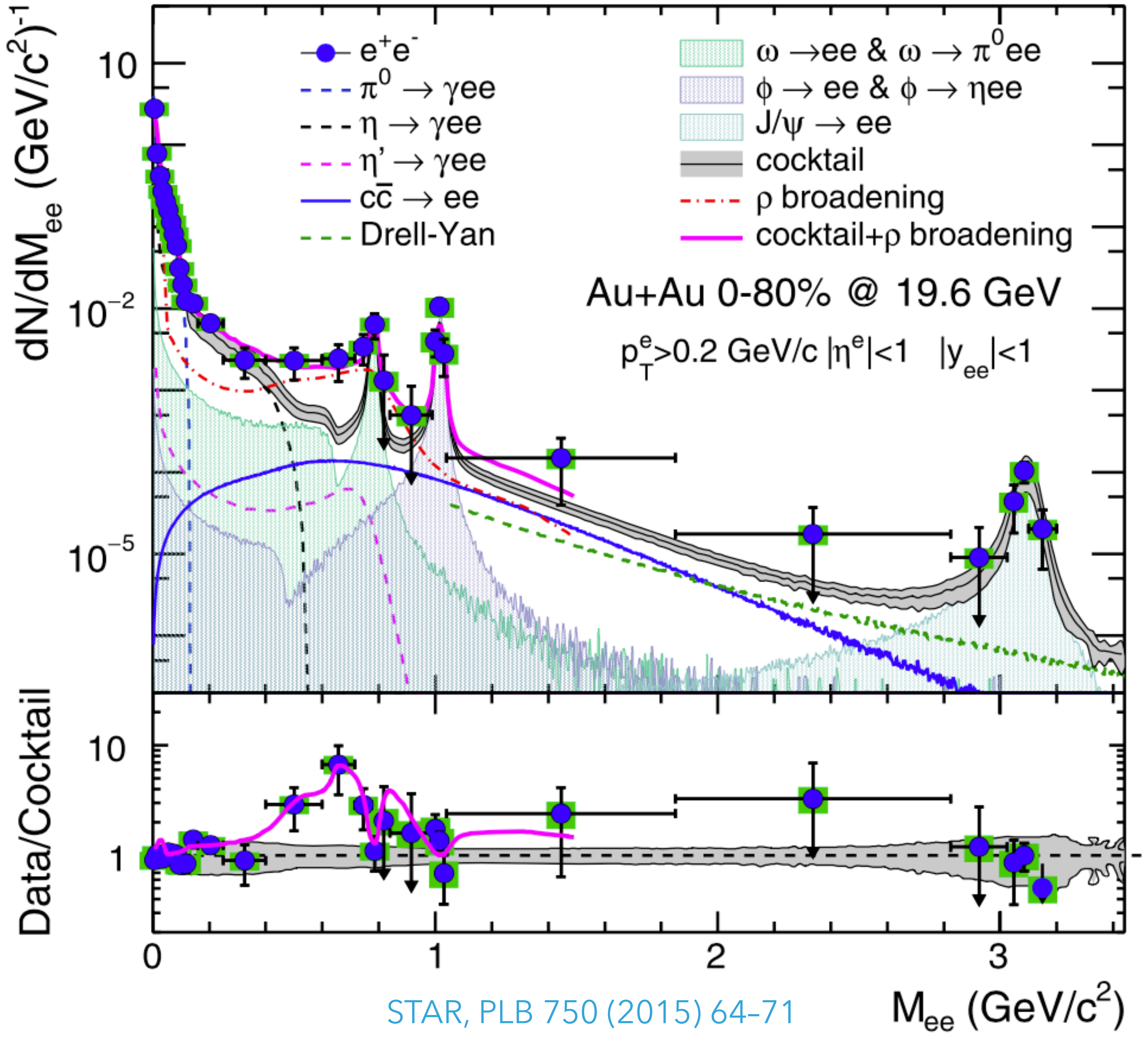

STAR, PLB 750 (2015) 64–71

- EM are produced throughout the evolution, so isolating productions from different stages is challenging.
- However, selecting p_T or M windows can be helpful. On average, the larger p_T or M the EM probes have, the earlier they are produced.

Spectra measurements in experiments

direct photons

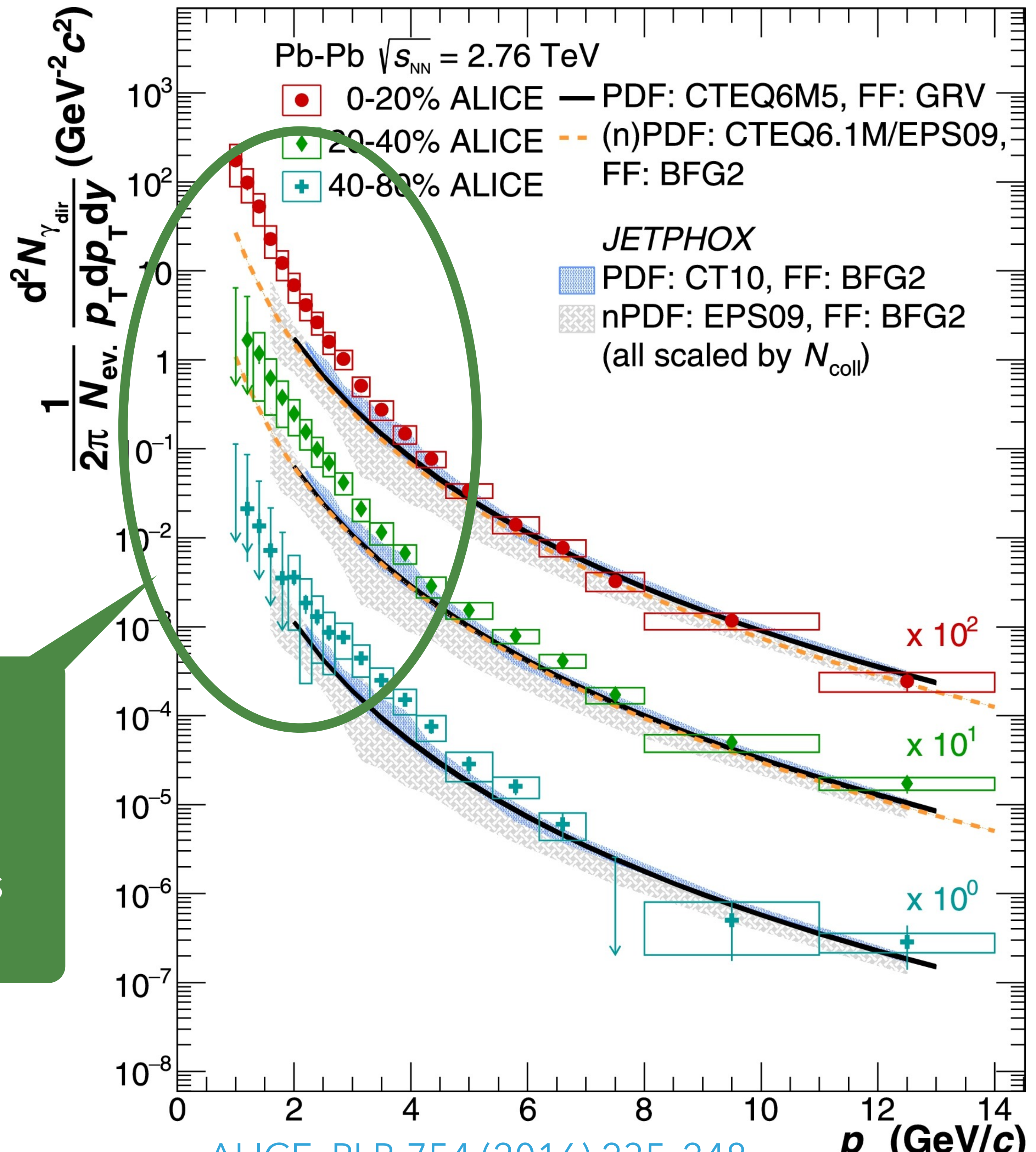

ALICE, PLB 754 (2016) 235–248

Excess of direct photons over prompt photons

inclusive dileptons

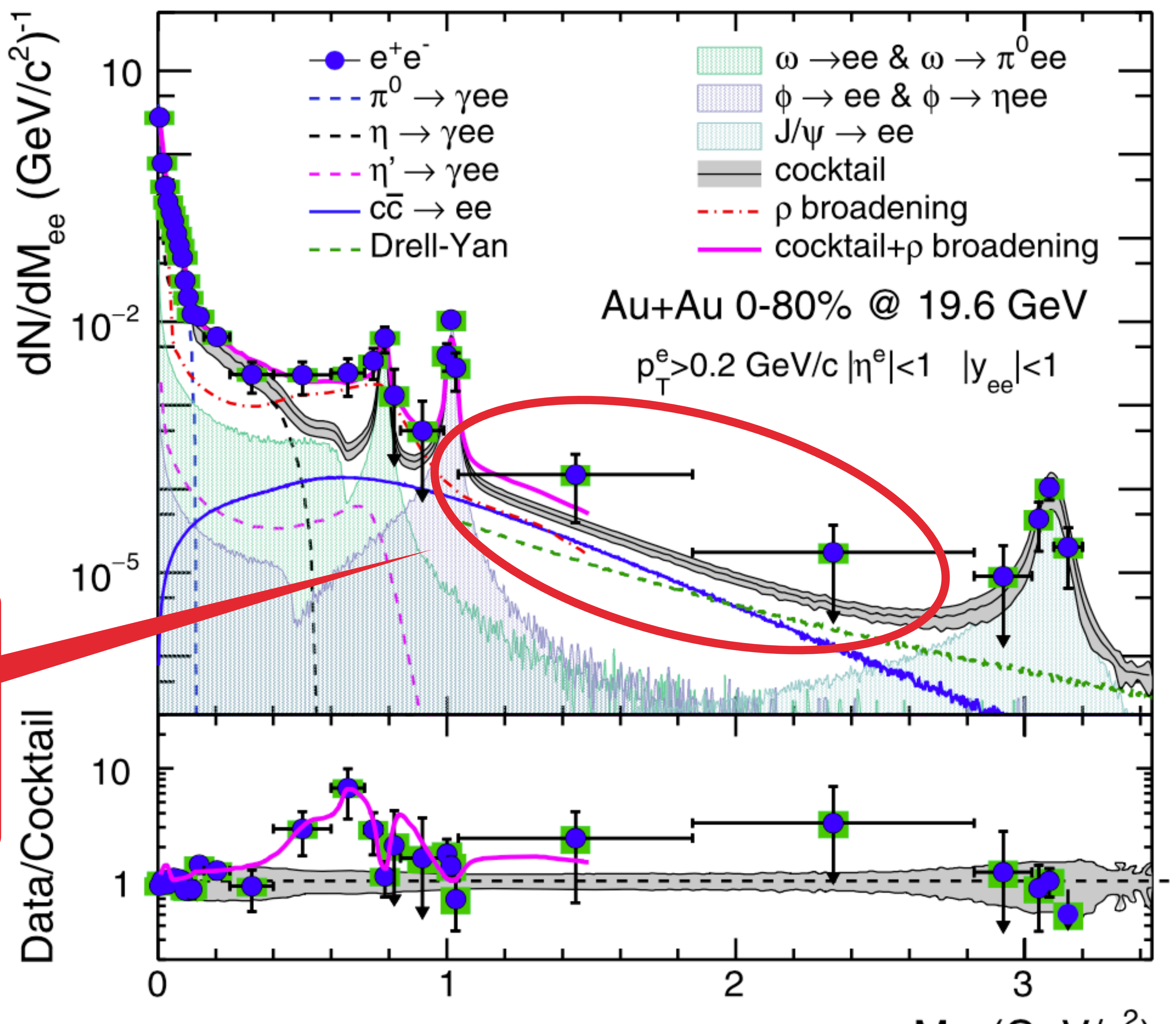

STAR, PLB 750 (2015) 64–71

Excess of inclusive dileptons over the cocktail

- EM are produced throughout the evolution, so isolating productions from different stages is challenging.
- However, selecting p_T or M windows can be helpful. On average, the larger p_T or M the EM probes have, the earlier they are produced.

Theoretical calculation of thermal spectra

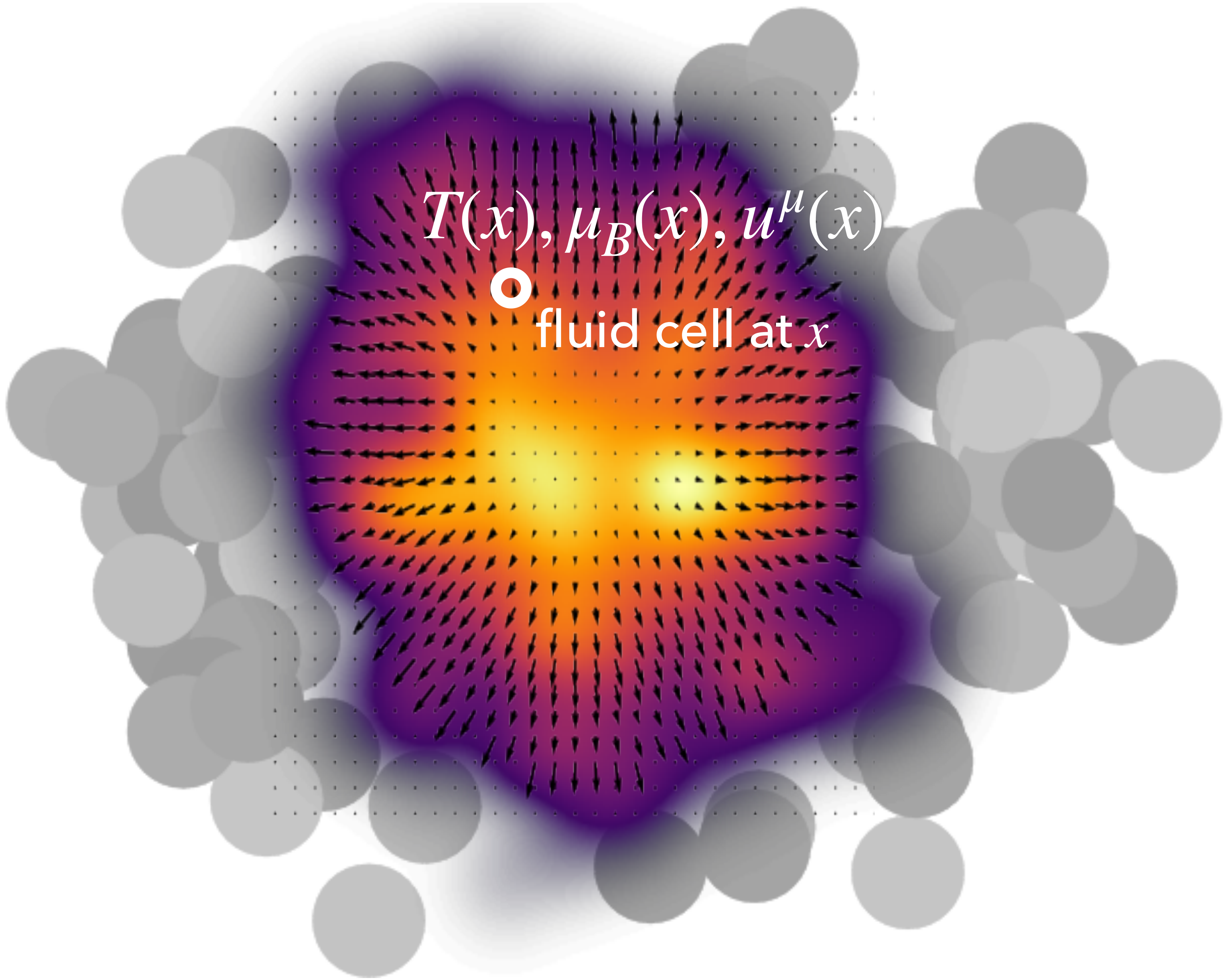

Theoretical calculation of thermal spectra

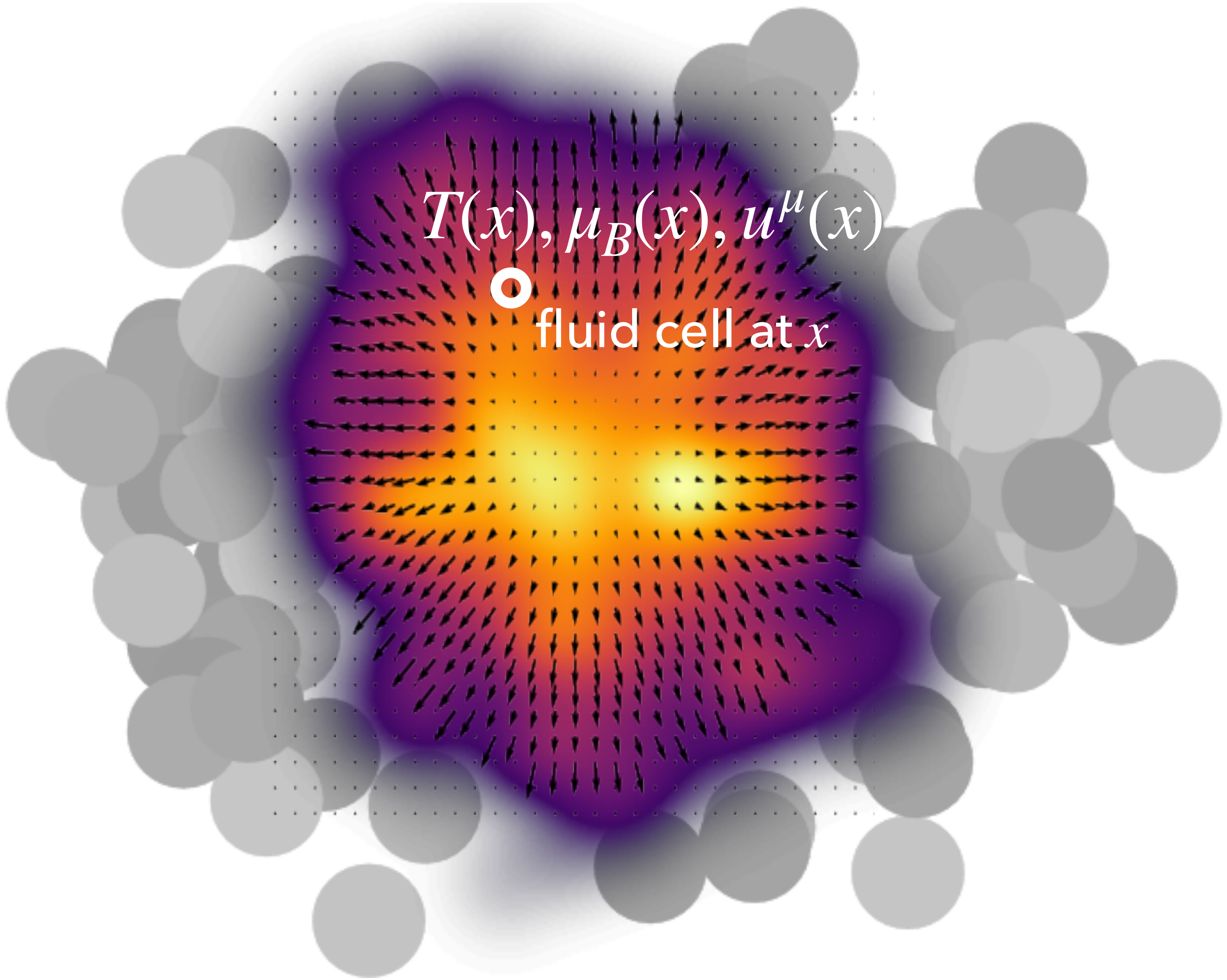

- Fully differential (dilepton) production rate of a static thermal source

$$\frac{\mathrm{d}\Gamma_{\ell\bar{\ell}}}{\mathrm{d}\omega\,\mathrm{d}^3\boldsymbol{k}} = \frac{\mathrm{d}N_{\ell\bar{\ell}}}{\mathrm{d}t\,\mathrm{d}^3\boldsymbol{x}\,\mathrm{d}\omega\,\mathrm{d}^3\boldsymbol{k}} = \frac{2\alpha_{\mathrm{em}}^2 f_B(\omega)}{9\pi^3 M^2} B\left(\frac{m_l^2}{M^2}\right) \rho_{\mathrm{em}}(\omega, \boldsymbol{k}; T, \mu_B)$$

Theoretical calculation of thermal spectra

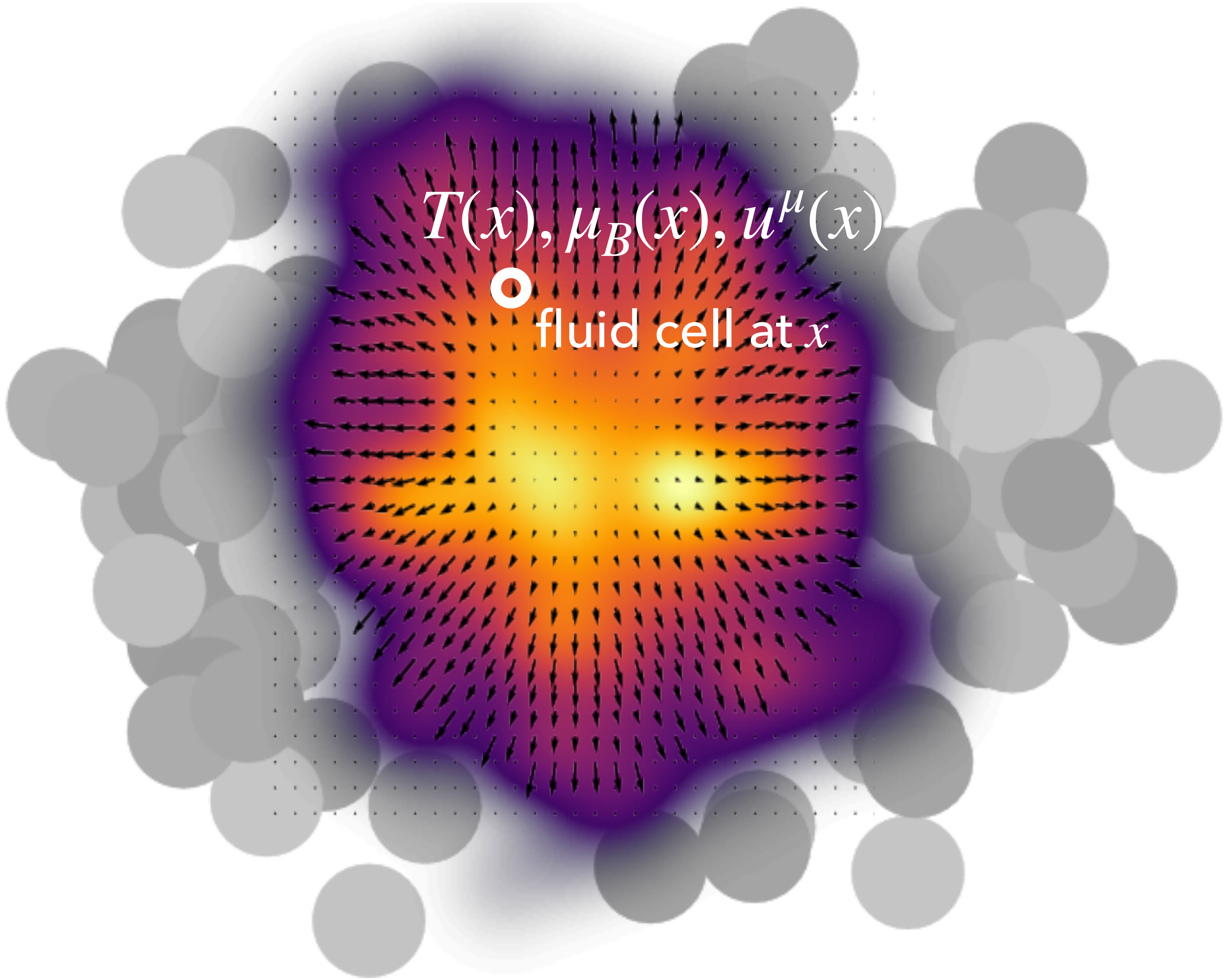

- Fully differential (dilepton) production rate of a static thermal source

Bose distribution

all the QCD information

$$\frac{\mathrm{d}\Gamma_{\ell\bar{\ell}}}{\mathrm{d}\omega\,\mathrm{d}^3\boldsymbol{k}} = \frac{\mathrm{d}N_{\ell\bar{\ell}}}{\mathrm{d}t\,\mathrm{d}^3\boldsymbol{x}\,\mathrm{d}\omega\,\mathrm{d}^3\boldsymbol{k}} = \frac{2\alpha_{\mathrm{em}}^2 f_B(\omega)}{9\pi^3 M^2} B\left(\frac{m_l^2}{M^2}\right) \rho_{\mathrm{em}}(\omega, \boldsymbol{k}; T, \mu_B)$$

Theoretical calculation of thermal spectra

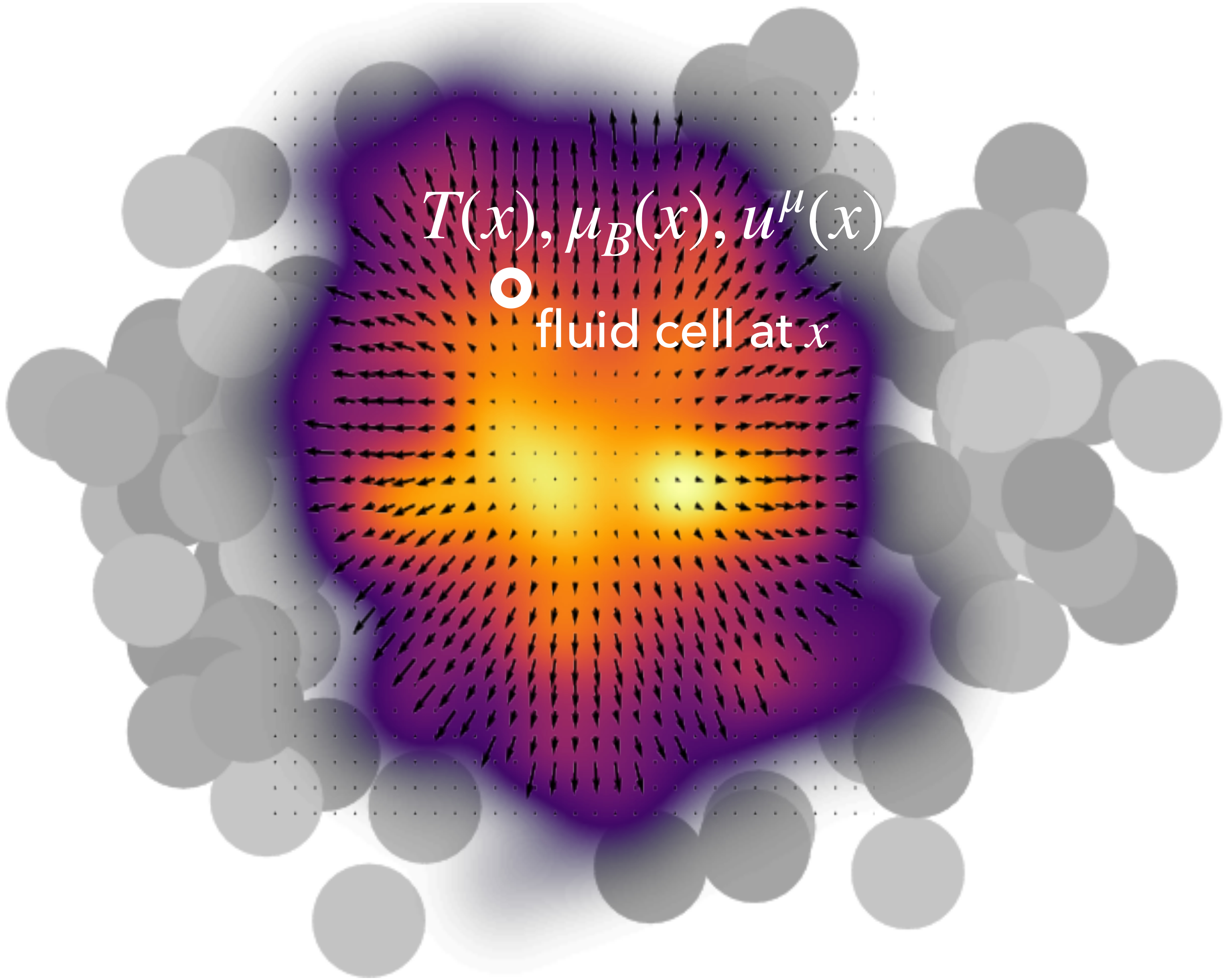

- Fully differential (dilepton) production rate of a static thermal source

Bose distribution

all the QCD information

$$\frac{\mathrm{d}\Gamma_{\ell\bar{\ell}}}{\mathrm{d}\omega\,\mathrm{d}^3\boldsymbol{k}} = \frac{\mathrm{d}N_{\ell\bar{\ell}}}{\mathrm{d}t\,\mathrm{d}^3\boldsymbol{x}\,\mathrm{d}\omega\,\mathrm{d}^3\boldsymbol{k}} = \frac{2\alpha_{\mathrm{em}}^2 f_B(\omega)}{9\pi^3 M^2} B\left(\frac{m_l^2}{M^2}\right) \rho_{\mathrm{em}}(\omega, \boldsymbol{k}; T, \mu_B)$$

- Emission rate in the lab frame

$$\frac{\mathrm{d}\Gamma_{\ell\bar{\ell}}}{\mathrm{d}^4K'} = \left.\frac{\mathrm{d}\Gamma_{\ell\bar{\ell}}}{\mathrm{d}\omega\,\mathrm{d}^3\boldsymbol{k}}\right|_{K^\mu=\Lambda^{\mu\nu}K'_\nu}$$

Theoretical calculation of thermal spectra

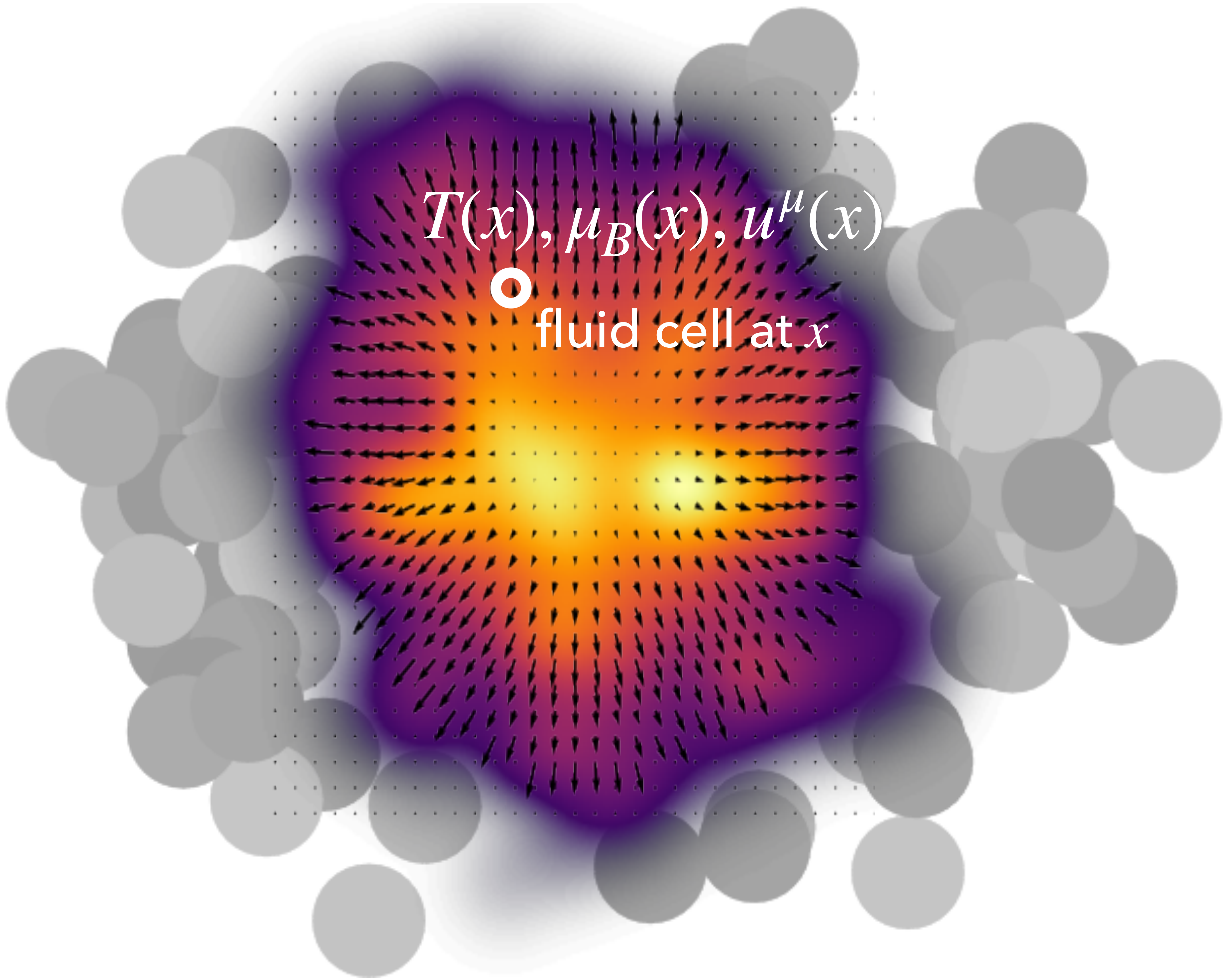

- Fully differential (dilepton) production rate of a static thermal source

Bose distribution

all the QCD information

$$\frac{d\Gamma_{\ell\bar{\ell}}}{d\omega\, d^3\boldsymbol{k}} = \frac{dN_{\ell\bar{\ell}}}{dt\, d^3\boldsymbol{x}\, d\omega\, d^3\boldsymbol{k}} = \frac{2\alpha_{\text{em}}^2 f_B(\omega)}{9\pi^3 M^2} B\left(\frac{m_l^2}{M^2}\right) \rho_{\text{em}}(\omega, \boldsymbol{k}; T, \mu_B)$$

- Emission rate in the lab frame

Local rest frame

Lab frame

$$\frac{d\Gamma_{\ell\bar{\ell}}}{d^4K'} = \left.\frac{d\Gamma_{\ell\bar{\ell}}}{d\omega\, d^3\boldsymbol{k}}\right|_{K^\mu = \Lambda^{\mu\nu} K'_\nu}$$

Theoretical calculation of thermal spectra

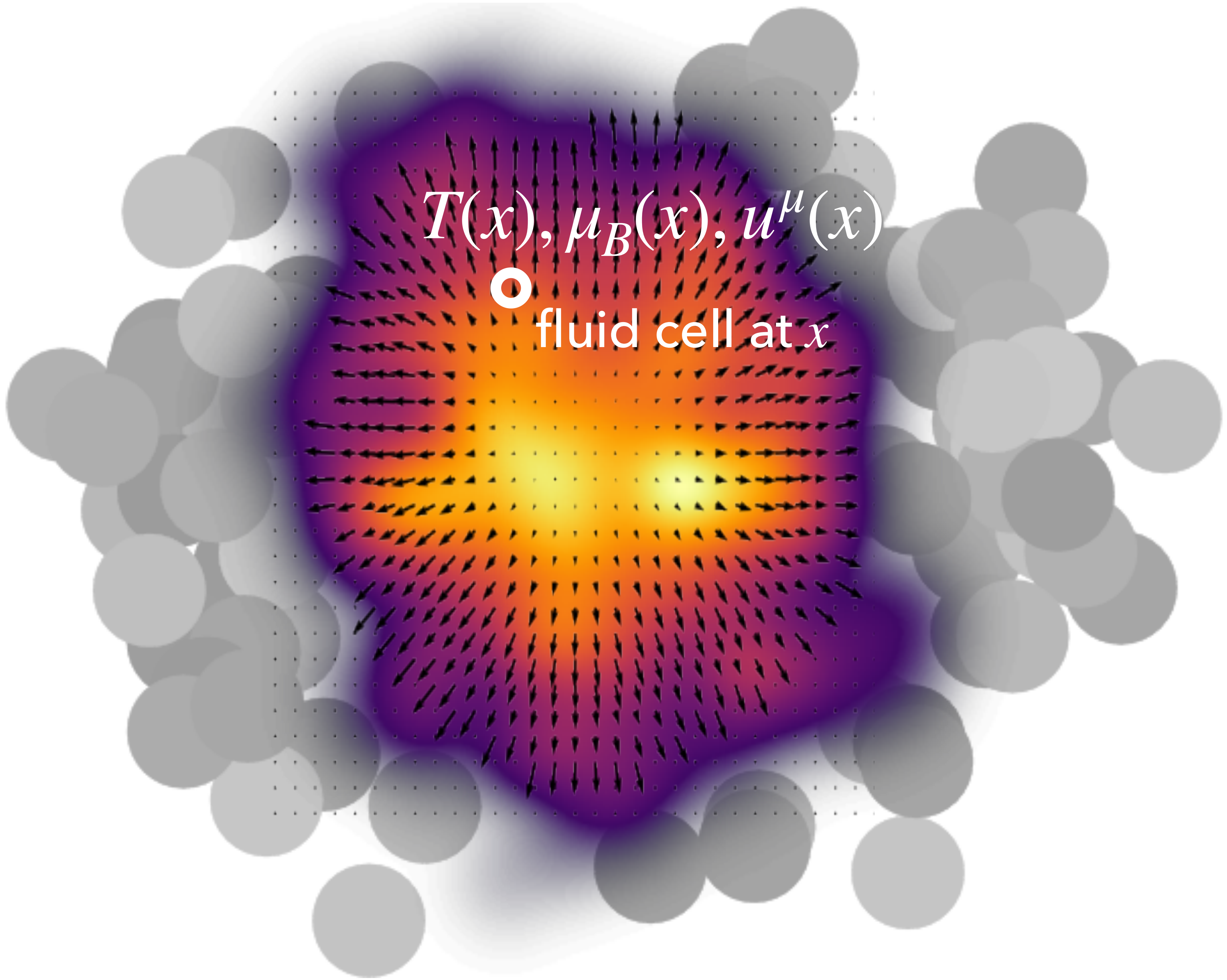

- Fully differential (dilepton) production rate of a static thermal source

Bose distribution

all the QCD information

$$\frac{d\Gamma_{\ell\bar{\ell}}}{d\omega\, d^3\boldsymbol{k}} = \frac{dN_{\ell\bar{\ell}}}{dt\, d^3\boldsymbol{x}\, d\omega\, d^3\boldsymbol{k}} = \frac{2\alpha_{\rm em}^2 f_B(\omega)}{9\pi^3 M^2} B\left(\frac{m_l^2}{M^2}\right) \rho_{\rm em}(\omega, \boldsymbol{k}; T, \mu_B)$$

- Emission rate in the lab frame

Local rest frame

essential for p_T spectra, anisotropic flows v_n, and correct kinematics

Lab frame

$$\frac{d\Gamma_{\ell\bar{\ell}}}{d^4K'} = \frac{d\Gamma_{\ell\bar{\ell}}}{d\omega\, d^3\boldsymbol{k}}\Bigg|_{K^\mu = \Lambda^{\mu\nu}K'_\nu}$$

Lorentz boost

Theoretical calculation of thermal spectra

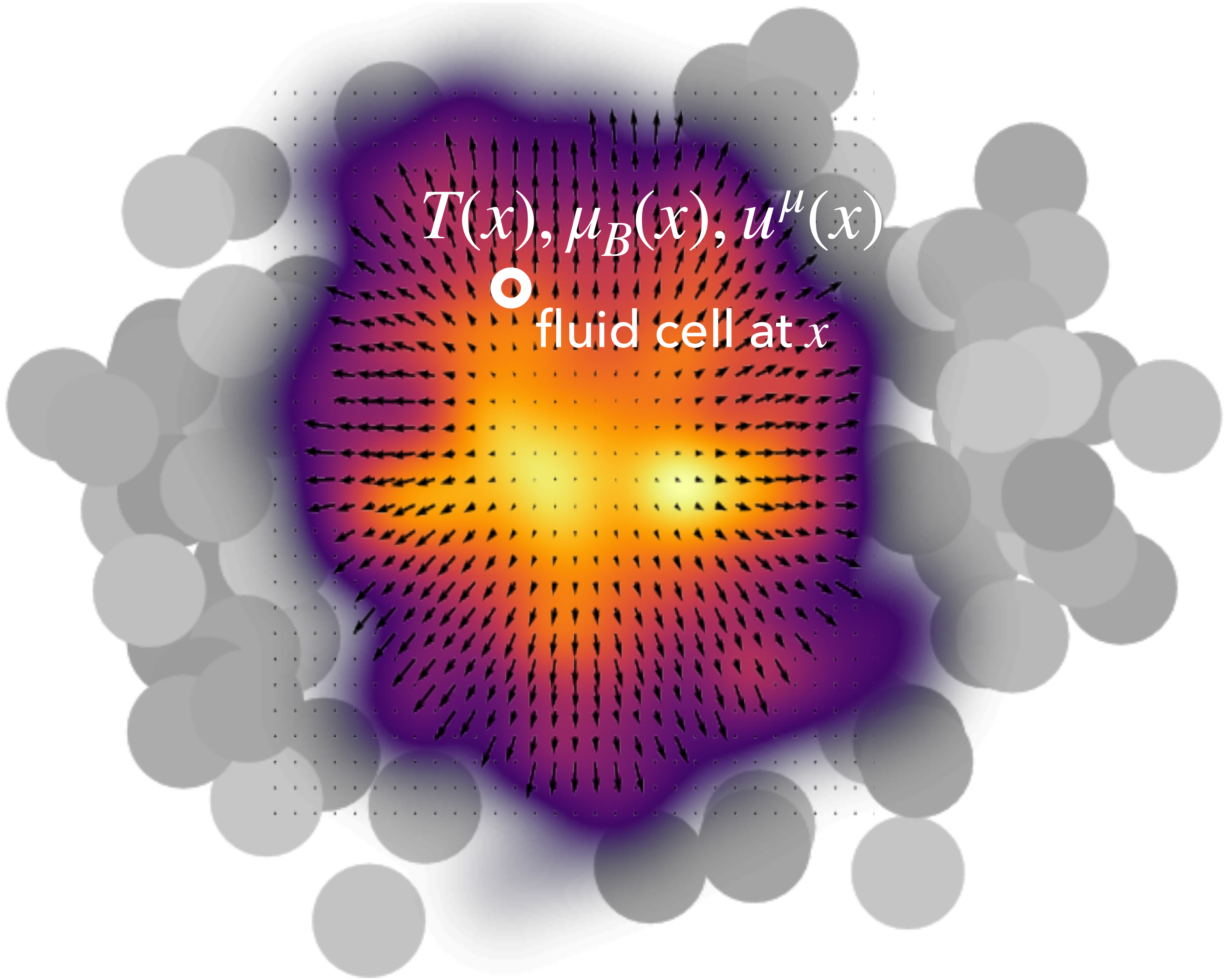

- Fully differential (dilepton) production rate of a static thermal source

Bose distribution

all the QCD information

$$\frac{d\Gamma_{\ell\bar{\ell}}}{d\omega\, d^3\boldsymbol{k}} = \frac{dN_{\ell\bar{\ell}}}{dt\, d^3\boldsymbol{x}\, d\omega\, d^3\boldsymbol{k}} = \frac{2\alpha_{em}^2 f_B(\omega)}{9\pi^3 M^2} B\left(\frac{m_l^2}{M^2}\right) \rho_{em}(\omega, \boldsymbol{k}; T, \mu_B)$$

- Emission rate in the lab frame

Local rest frame

essential for p_T spectra, anisotropic flows v_n, and correct kinematics

Lab frame

$$\frac{d\Gamma_{\ell\bar{\ell}}}{d^4K'} = \left.\frac{d\Gamma_{\ell\bar{\ell}}}{d\omega\, d^3\boldsymbol{k}}\right|_{K^\mu = \Lambda^{\mu\nu} K'_\nu}$$

Lorentz boost

- Spectra in the lab frame

$$\frac{dN_{\ell\bar{\ell}}}{dM\, dy} = M \int_{k_{min}}^{k_{max}} dk_\perp\, k_\perp \int_0^{2\pi} d\phi \int d^4x \frac{d\Gamma_{\ell\bar{\ell}}}{d^4K'}$$

Theoretical calculation of thermal spectra

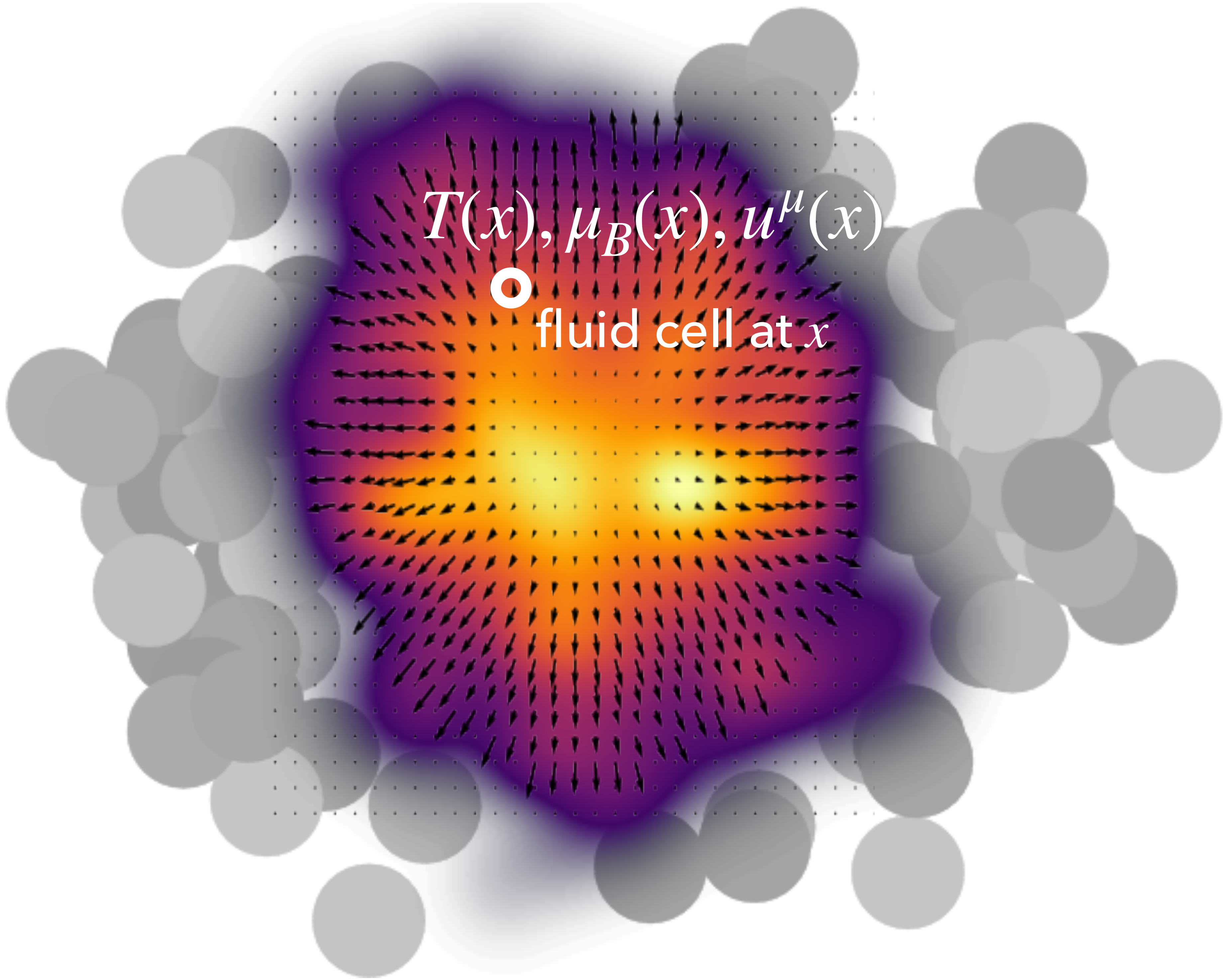

- Fully differential (dilepton) production rate of a static thermal source

Bose distribution

all the QCD information

$$\frac{d\Gamma_{\ell\bar{\ell}}}{d\omega\, d^3\boldsymbol{k}} = \frac{dN_{\ell\bar{\ell}}}{dt\, d^3\boldsymbol{x}\, d\omega\, d^3\boldsymbol{k}} = \frac{2\alpha_{em}^2 f_B(\omega)}{9\pi^3 M^2} B\left(\frac{m_l^2}{M^2}\right) \rho_{em}(\omega, \boldsymbol{k}; T, \mu_B)$$

- Emission rate in the lab frame

Lab frame — Local rest frame

$$\frac{d\Gamma_{\ell\bar{\ell}}}{d^4K'} = \left.\frac{d\Gamma_{\ell\bar{\ell}}}{d\omega\, d^3\boldsymbol{k}}\right|_{K^\mu = \Lambda^{\mu\nu} K'_\nu}$$

Lorentz boost

essential for p_T spectra, anisotropic flows v_n, and correct kinematics

- Spectra in the lab frame

$$\frac{dN_{\ell\bar{\ell}}}{dM\, dy} = M \int_{k_{min}}^{k_{max}} dk_\perp\, k_\perp \int_0^{2\pi} d\phi \int d^4x \frac{d\Gamma_{\ell\bar{\ell}}}{d^4K'}$$

match experimental kinematic cuts

Theoretical calculation of thermal spectra

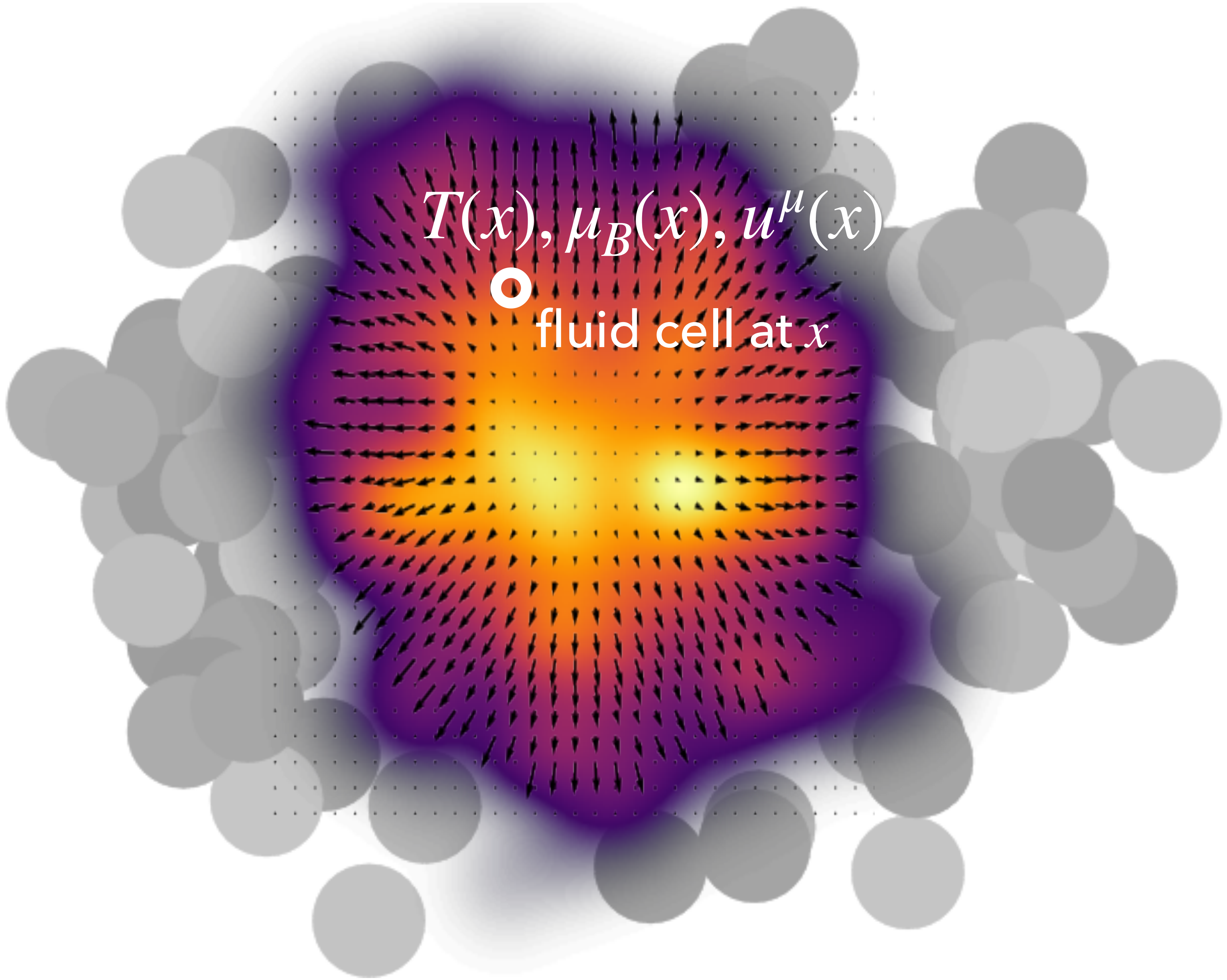

- Fully differential (dilepton) production rate of a static thermal source

Bose distribution — all the QCD information

$$\frac{d\Gamma_{\ell\bar{\ell}}}{d\omega\, d^3\boldsymbol{k}} = \frac{dN_{\ell\bar{\ell}}}{dt\, d^3\boldsymbol{x}\, d\omega\, d^3\boldsymbol{k}} = \frac{2\alpha_{em}^2 f_B(\omega)}{9\pi^3 M^2} B\left(\frac{m_l^2}{M^2}\right) \rho_{em}(\omega, \boldsymbol{k}; T, \mu_B)$$

- Emission rate in the lab frame

Lab frame — Local rest frame

$$\frac{d\Gamma_{\ell\bar{\ell}}}{d^4K'} = \frac{d\Gamma_{\ell\bar{\ell}}}{d\omega\, d^3\boldsymbol{k}}\Bigg|_{K^\mu = \Lambda^{\mu\nu}K'_\nu}$$

Lorentz boost: essential for p_T spectra, anisotropic flows v_n, and correct kinematics

- Spectra in the lab frame

$$\frac{dN_{\ell\bar{\ell}}}{dM\, dy} = M \int_{k_{min}}^{k_{max}} dk_\perp\, k_\perp \int_0^{2\pi} d\phi \int d^4x \frac{d\Gamma_{\ell\bar{\ell}}}{d^4K'}$$

match experimental kinematic cuts

- In non-relativistic approximation ($M \gg T$), the emission rate of dileptons $\propto (MT)^{3/2} e^{-M/T}$; similarly, for photons, when $p_T \gg T$, the rate $\propto e^{-p_T/T}$; the exponential term is from $f_B(\omega) = 1/(e^{\omega/T} - 1)$.

Theoretical calculation of thermal spectra

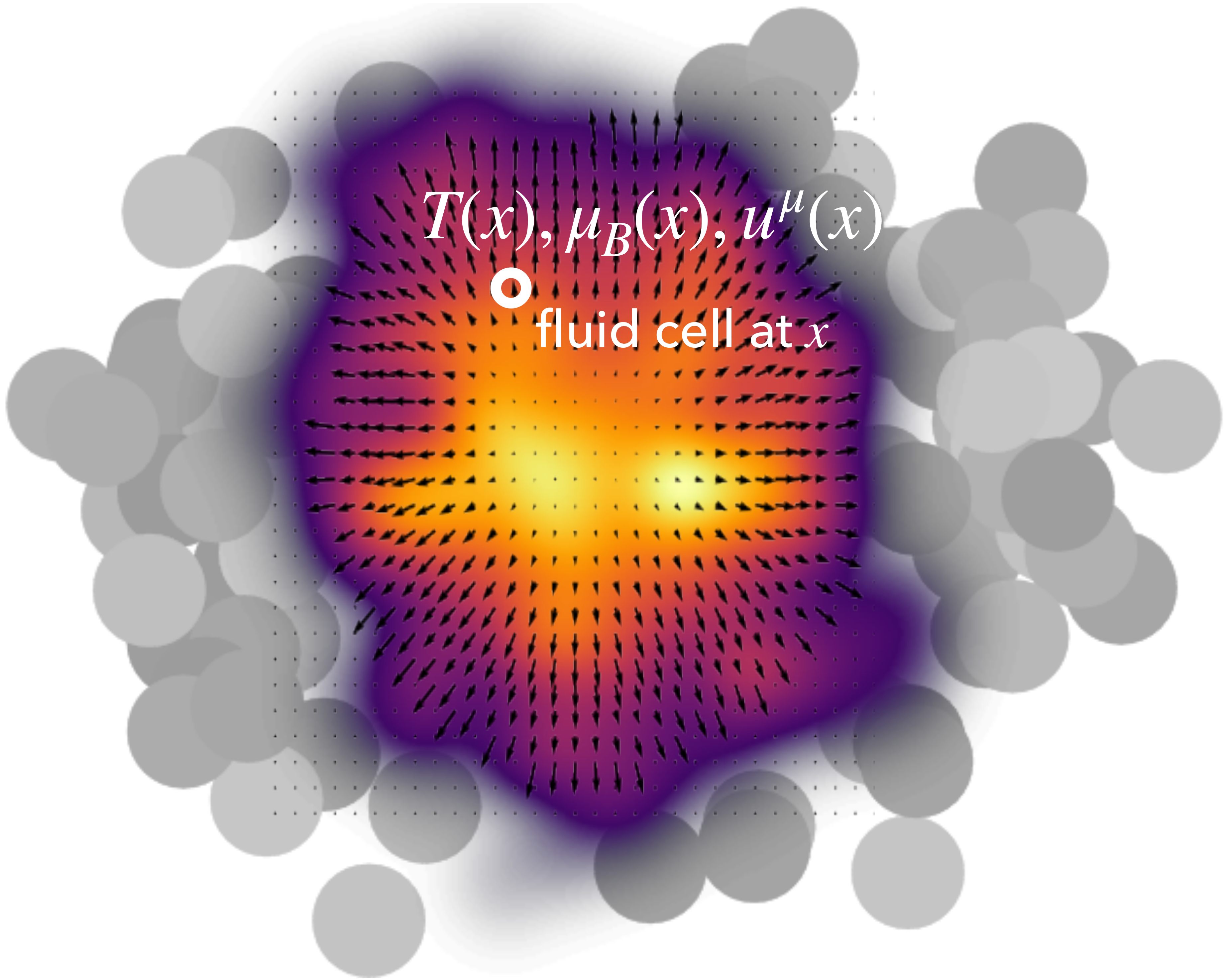

- Fully differential (dilepton) production rate of a static thermal source

Bose distribution — all the QCD information

$$\frac{d\Gamma_{\ell\bar{\ell}}}{d\omega\, d^3\boldsymbol{k}} = \frac{dN_{\ell\bar{\ell}}}{dt\, d^3\boldsymbol{x}\, d\omega\, d^3\boldsymbol{k}} = \frac{2\alpha_{em}^2 f_B(\omega)}{9\pi^3 M^2} B\left(\frac{m_l^2}{M^2}\right) \rho_{em}(\omega, \boldsymbol{k}; T, \mu_B)$$

- Emission rate in the lab frame

Lab frame — Local rest frame

$$\frac{d\Gamma_{\ell\bar{\ell}}}{d^4K'} = \left.\frac{d\Gamma_{\ell\bar{\ell}}}{d\omega\, d^3\boldsymbol{k}}\right|_{K^\mu = \Lambda^{\mu\nu} K'_\nu}$$

Lorentz boost

essential for p_T spectra, anisotropic flows v_n, and correct kinematics

- Spectra in the lab frame

$$\frac{dN_{\ell\bar{\ell}}}{dM\, dy} = M \int_{k_{min}}^{k_{max}} dk_\perp\, k_\perp \int_0^{2\pi} d\phi \int d^4x \frac{d\Gamma_{\ell\bar{\ell}}}{d^4K'}$$

match experimental kinematic cuts

- In non-relativistic approximation ($M \gg T$), the emission rate of dileptons $\propto (MT)^{3/2} e^{-M/T}$; similarly, for photons, when $p_T \gg T$, the rate $\propto e^{-p_T/T}$; the exponential term is from $f_B(\omega) = 1/(e^{\omega/T} - 1)$.
- Off-equilibrium corrections (such as viscous effects, B-field); … Han Gao, 9:20 am, Tue

PRE-HYDRO STAGE

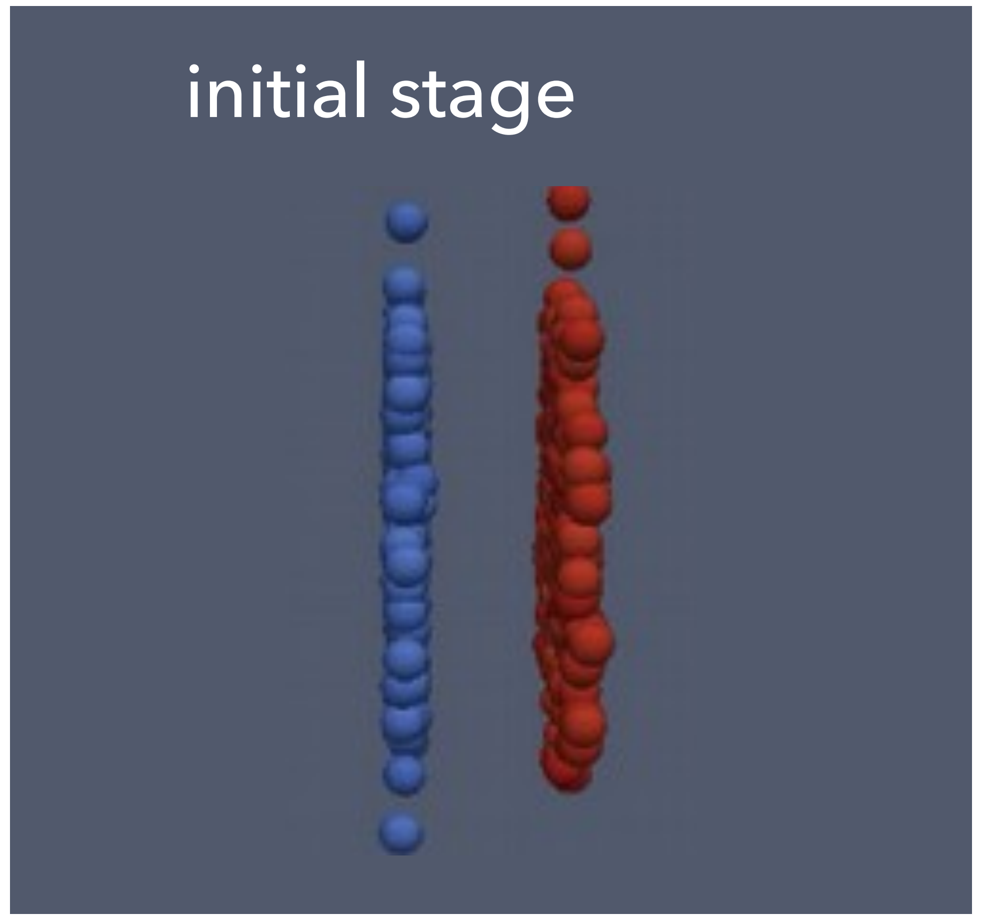

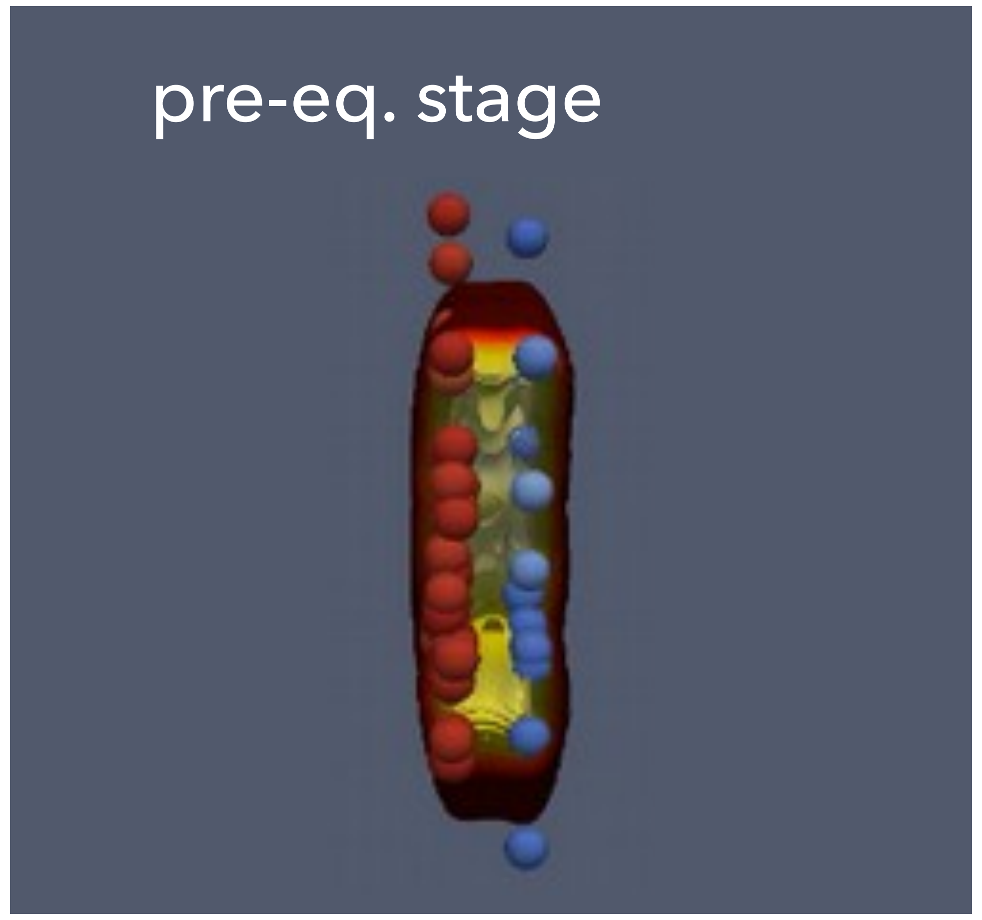

Thermalization in QCD kinetic theory

Kurkela, Mazeliauskas, PRD 99 (2019) 054018; X. Du, Schlichting, PRD 104 (2021) 054011; Garcia-Montero, Mazeliauskas, Plaschke, Schlichting, JHEP03(2024)053

Thermalization in QCD kinetic theory

$\cos\theta = p_z/p$

thermal non-equilibrium

Gluon evolution

time

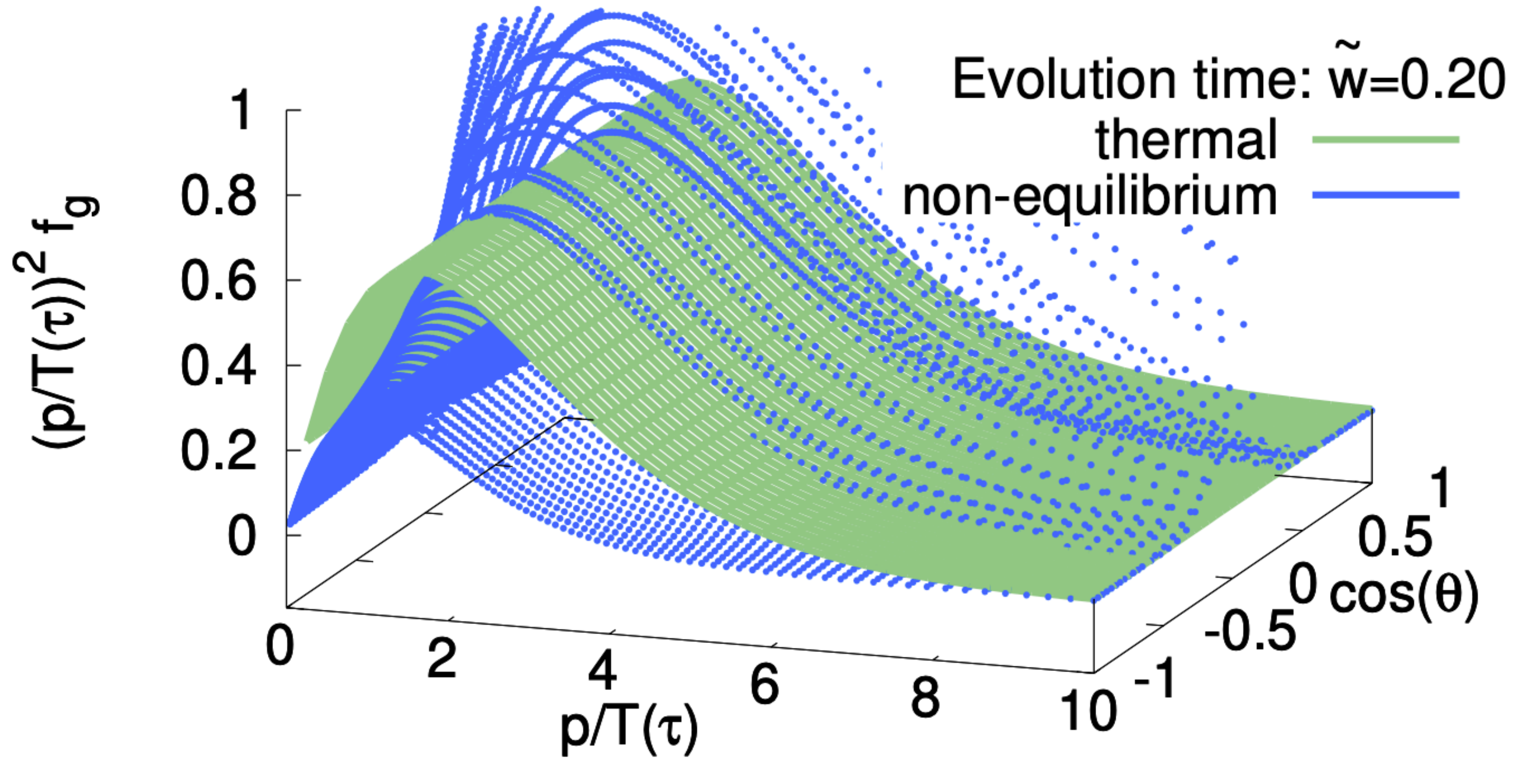

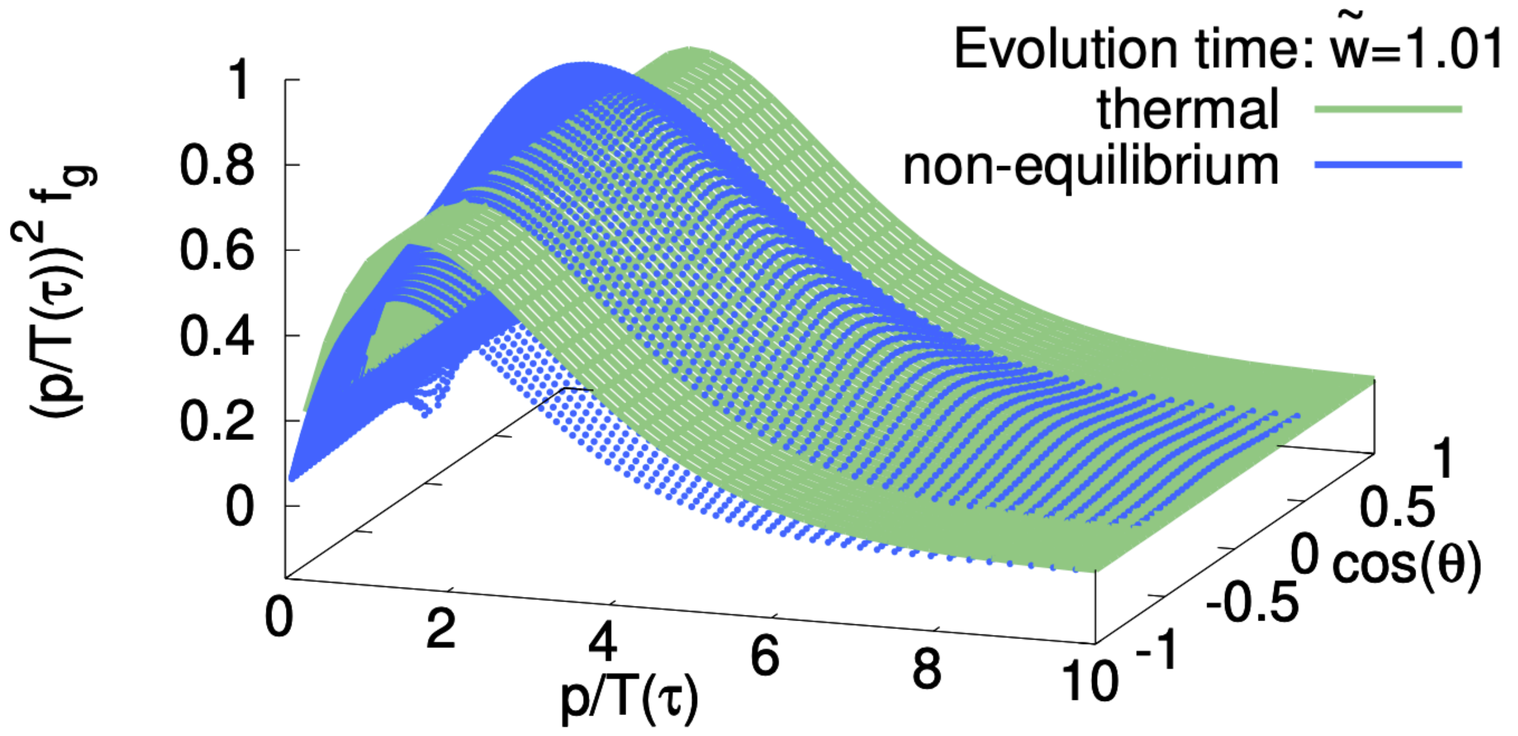

Kurkela, Mazeliauskas, PRD 99 (2019) 054018; X. Du, Schlichting, PRD 104 (2021) 054011; Garcia-Montero, Mazeliauskas, Plaschke, Schlichting, JHEP03(2024)053

Thermalization in QCD kinetic theory

$\cos\theta = p_z/p$ thermal non-equilibrium

Gluon evolution

time

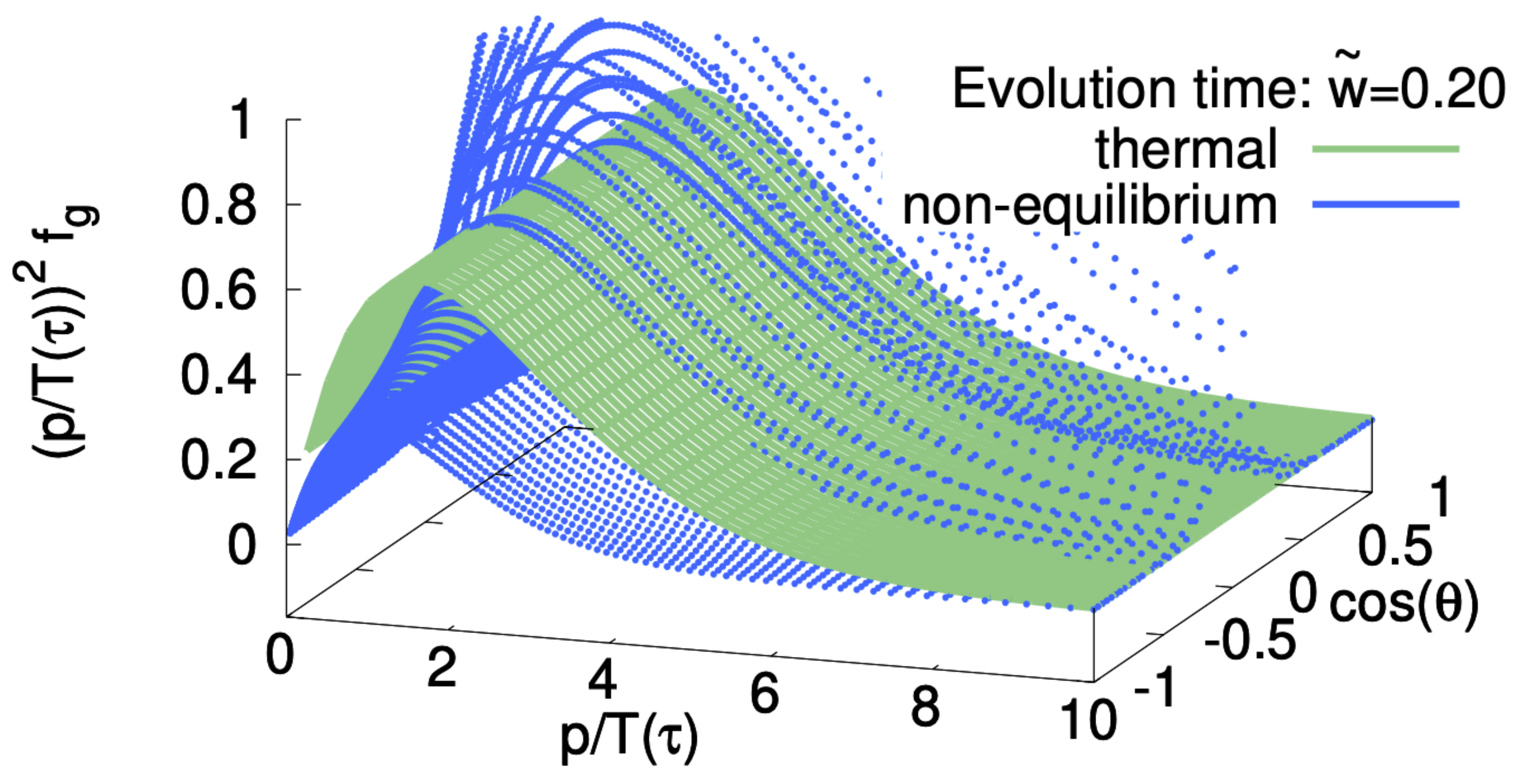

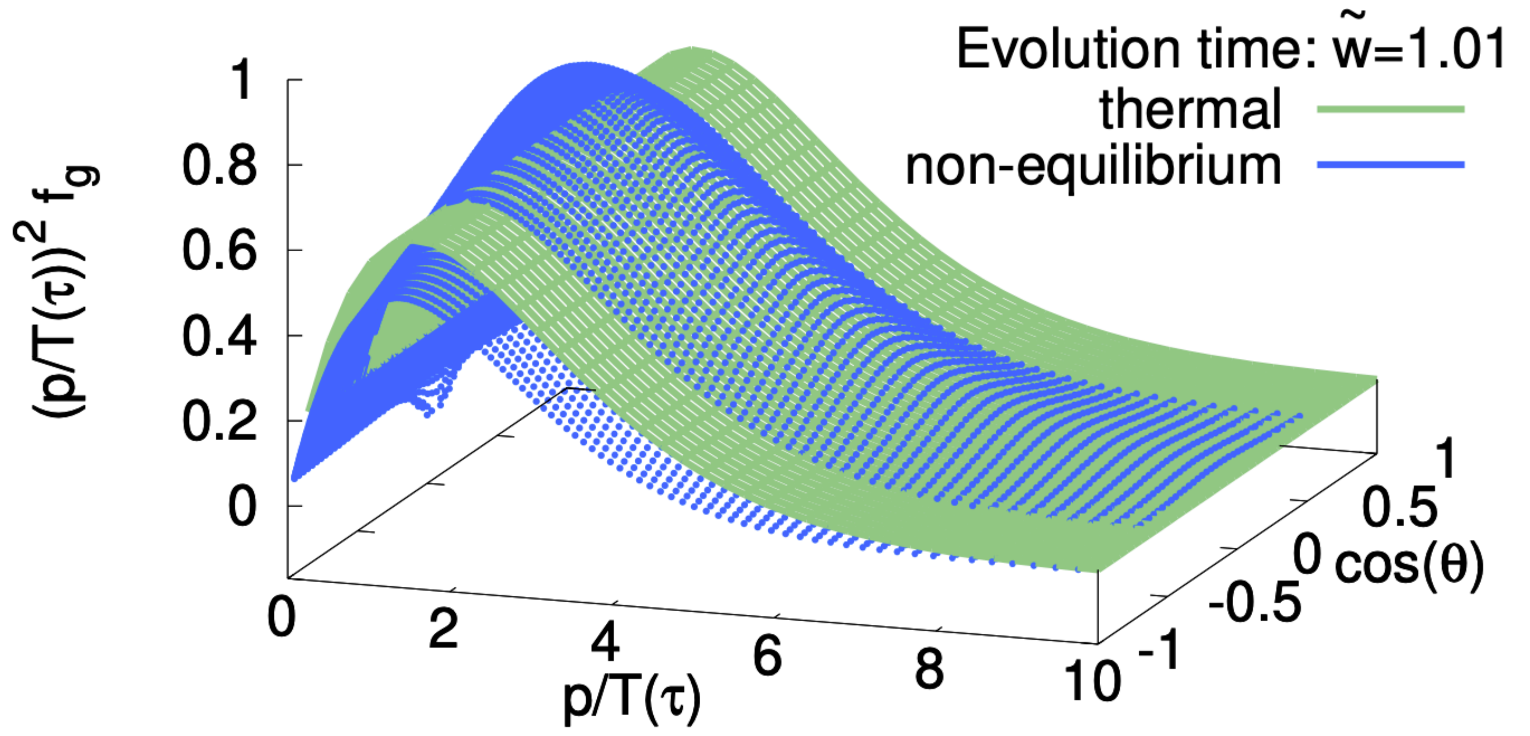

- The system starts with a gluon-dominated initial state; quarks are produced via gluon fusion $gg \to q\bar{q}$ and gluon splitting $g \to q\bar{q}$.

Kurkela, Mazeliauskas, PRD 99 (2019) 054018; X. Du, Schlichting, PRD 104 (2021) 054011; Garcia-Montero, Mazeliauskas, Plaschke, Schlichting, JHEP03(2024)053

Thermalization in QCD kinetic theory

$\cos\theta = p_z/p$

thermal non-equilibrium

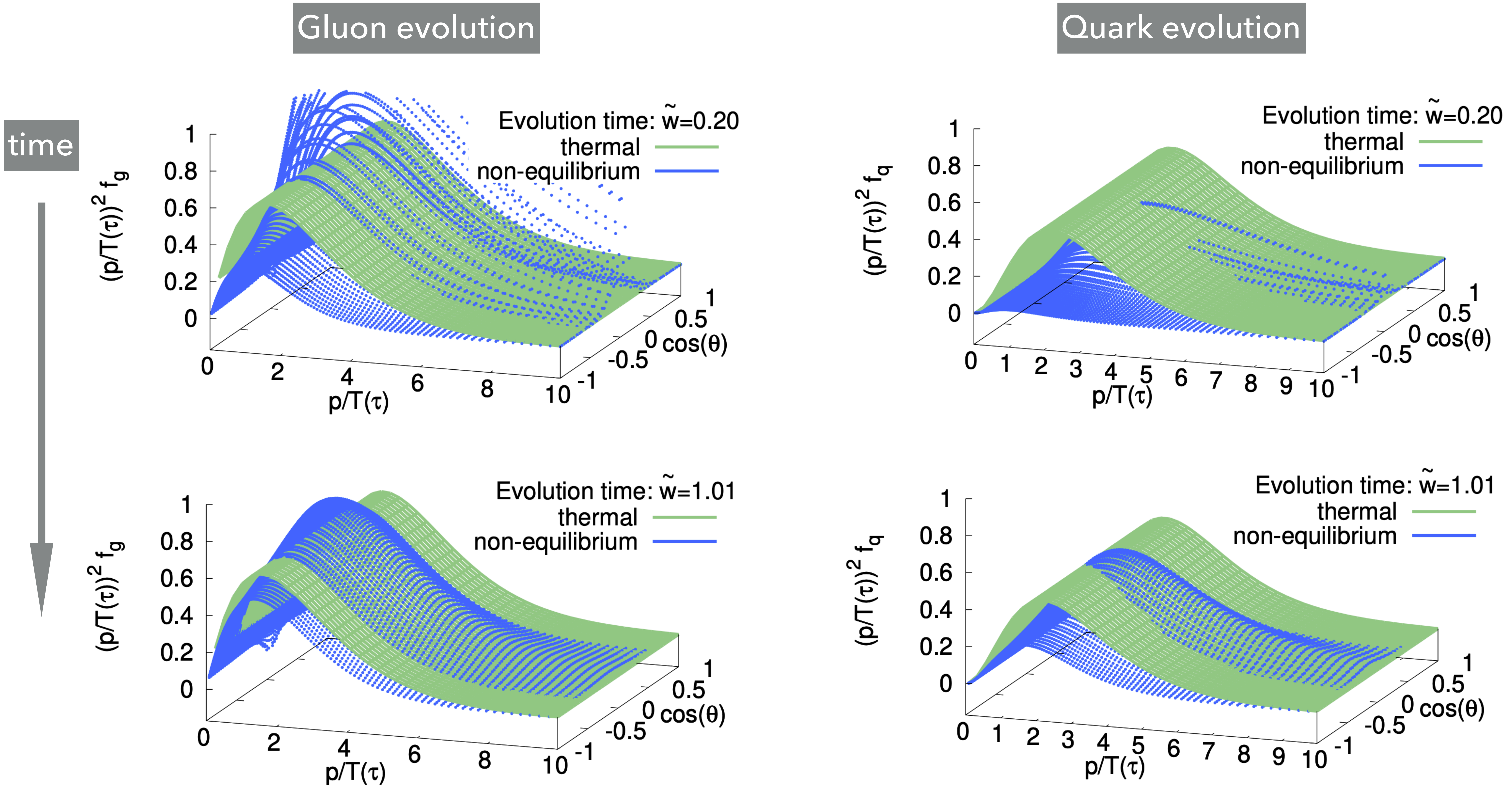

- The system starts with a gluon-dominated initial state; quarks are produced via gluon fusion $gg \to q\bar{q}$ and gluon splitting $g \to q\bar{q}$.

Kurkela, Mazeliauskas, PRD 99 (2019) 054018; X. Du, Schlichting, PRD 104 (2021) 054011; Garcia-Montero, Mazeliauskas, Plaschke, Schlichting, JHEP03(2024)053

Thermalization in QCD kinetic theory

$\cos\theta = p_z/p$ thermal non-equilibrium

Gluon evolution | Quark evolution | Photon emission rate

- The system starts with a gluon-dominated initial state; quarks are produced via gluon fusion $gg \to q\bar{q}$ and gluon splitting $g \to q\bar{q}$.

Kurkela, Mazeliauskas, PRD 99 (2019) 054018; X. Du, Schlichting, PRD 104 (2021) 054011; Garcia-Montero, Mazeliauskas, Plaschke, Schlichting, JHEP03(2024)053

Thermalization in QCD kinetic theory

$\cos\theta = p_z/p$ thermal non-equilibrium

Gluon evolution

Quark evolution

Photon emission rate

time

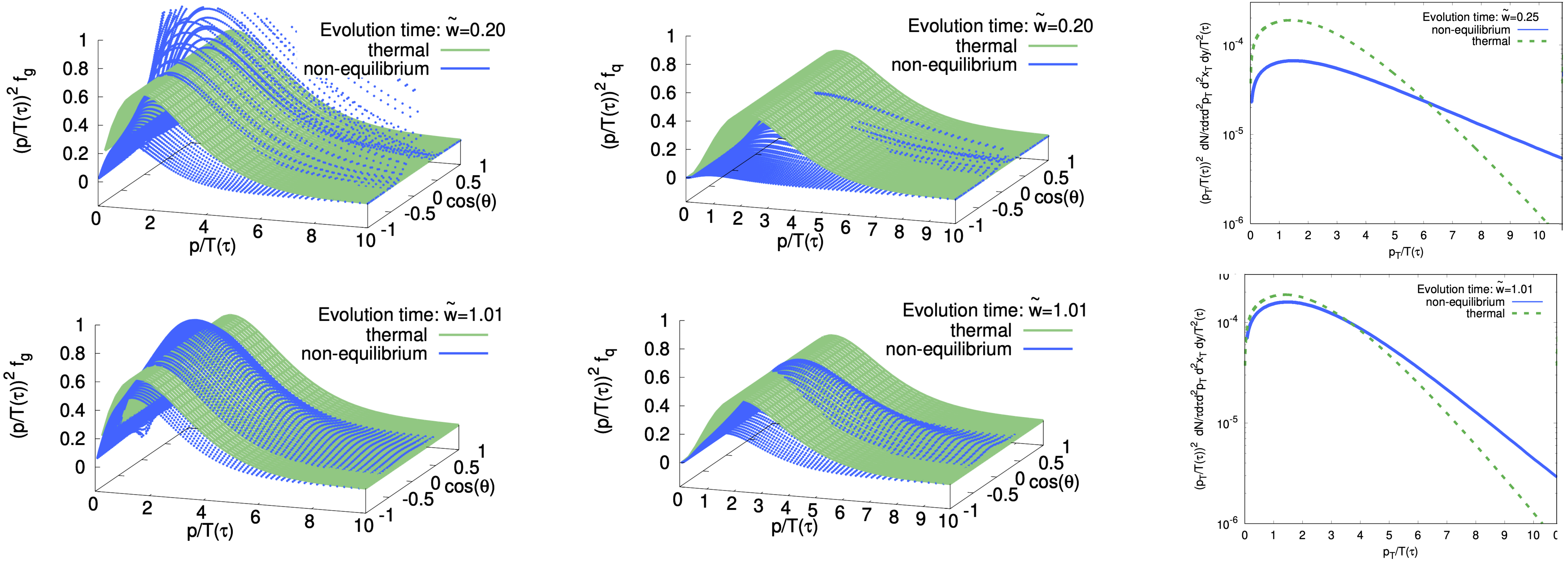

time

- The system starts with a gluon-dominated initial state; quarks are produced via gluon fusion $gg \to q\bar{q}$ and gluon splitting $g \to q\bar{q}$.
- Non-equilibrium spectrum is well below the thermal spectrum at low p_T and is much harder; thermalization is first achieved in the soft regime. [Note the p_T-dependence!]

Kurkela, Mazeliauskas, PRD 99 (2019) 054018; X. Du, Schlichting, PRD 104 (2021) 054011; Garcia-Montero, Mazeliauskas, Plaschke, Schlichting, JHEP03(2024)05

Garcia-Montero, 9:00 am, Tue

Anisotropic flows v_n as probe of equilibration

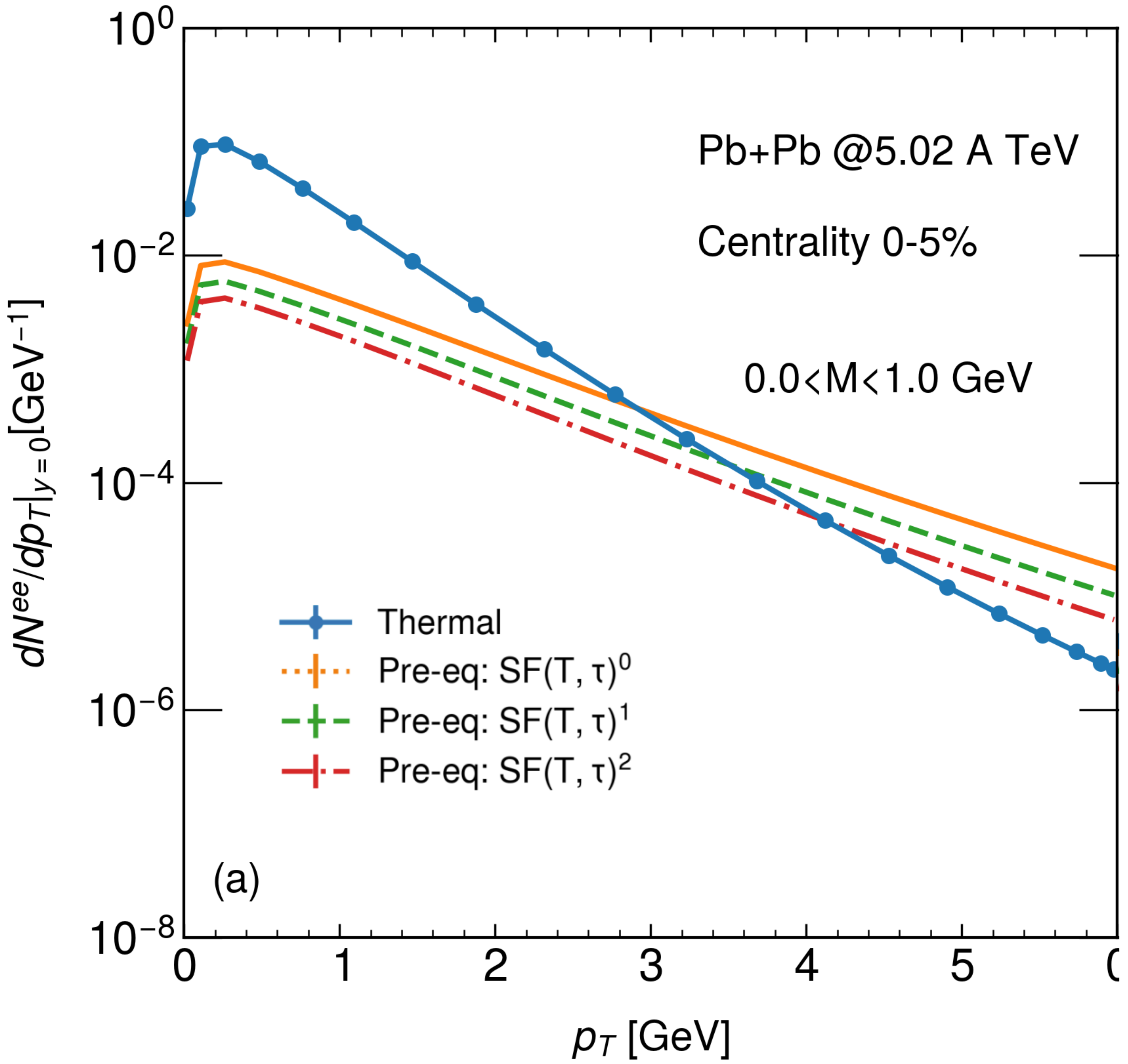

X.-Y. Wu, LD, Gale, Jeon, 2407.04156; Gale, Paquet, Schenke, Shen, PRC 105, 014909 (2022)

Xiang-Yu Wu, 9:40 am, Tue

Anisotropic flows v_n as probe of equilibration

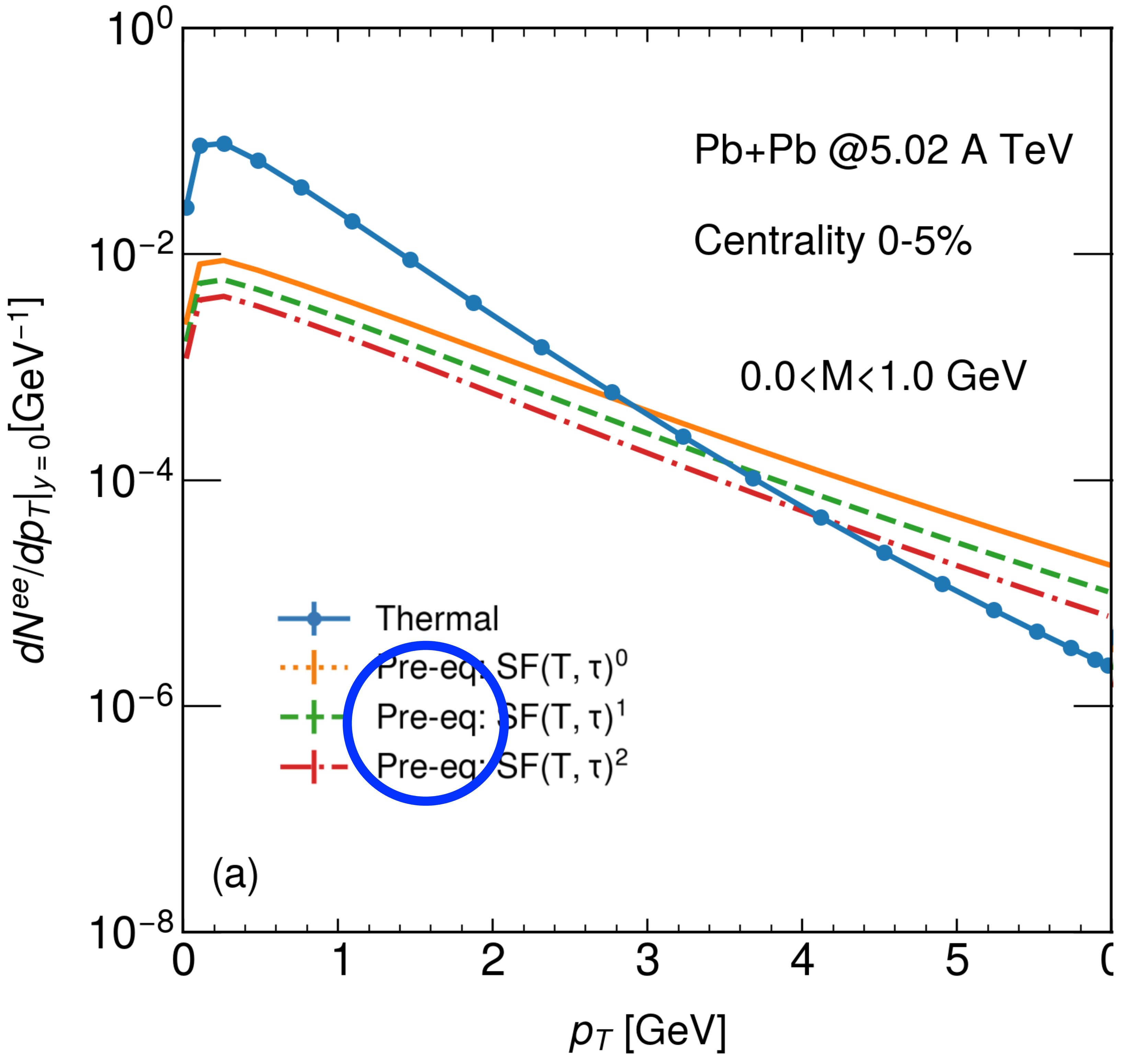

X.-Y. Wu, LD, Gale, Jeon, 2407.04156; Gale, Paquet, Schenke, Shen, PRC 105, 014909 (2022)

Xiang-Yu Wu, 9:40 am, Tue

Anisotropic flows v_n as probe of equilibration

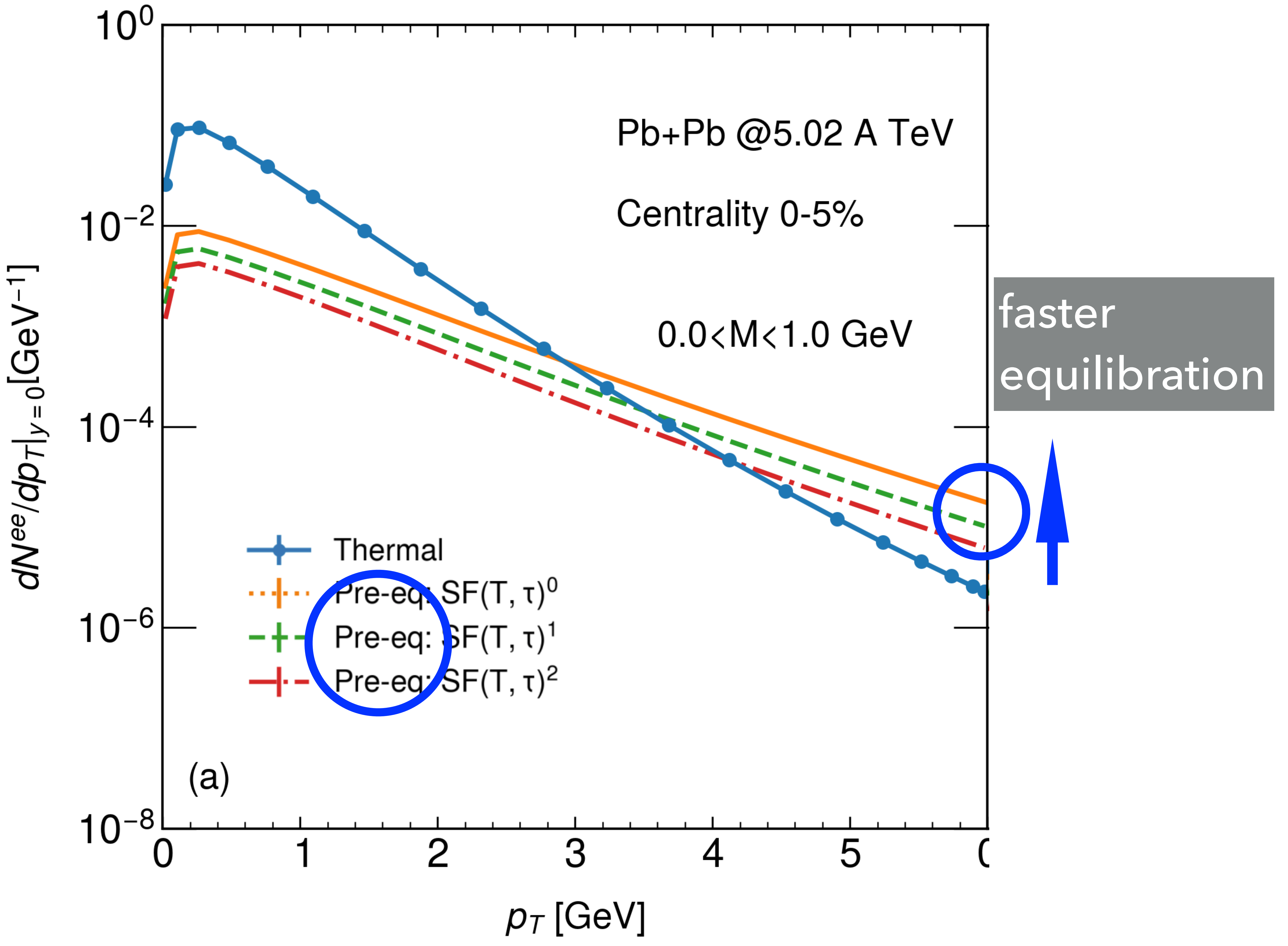

X.-Y. Wu, LD, Gale, Jeon, 2407.04156; Gale, Paquet, Schenke, Shen, PRC 105, 014909 (2022)

Xiang-Yu Wu, 9:40 am, Tue

Anisotropic flows v_n as probe of equilibration

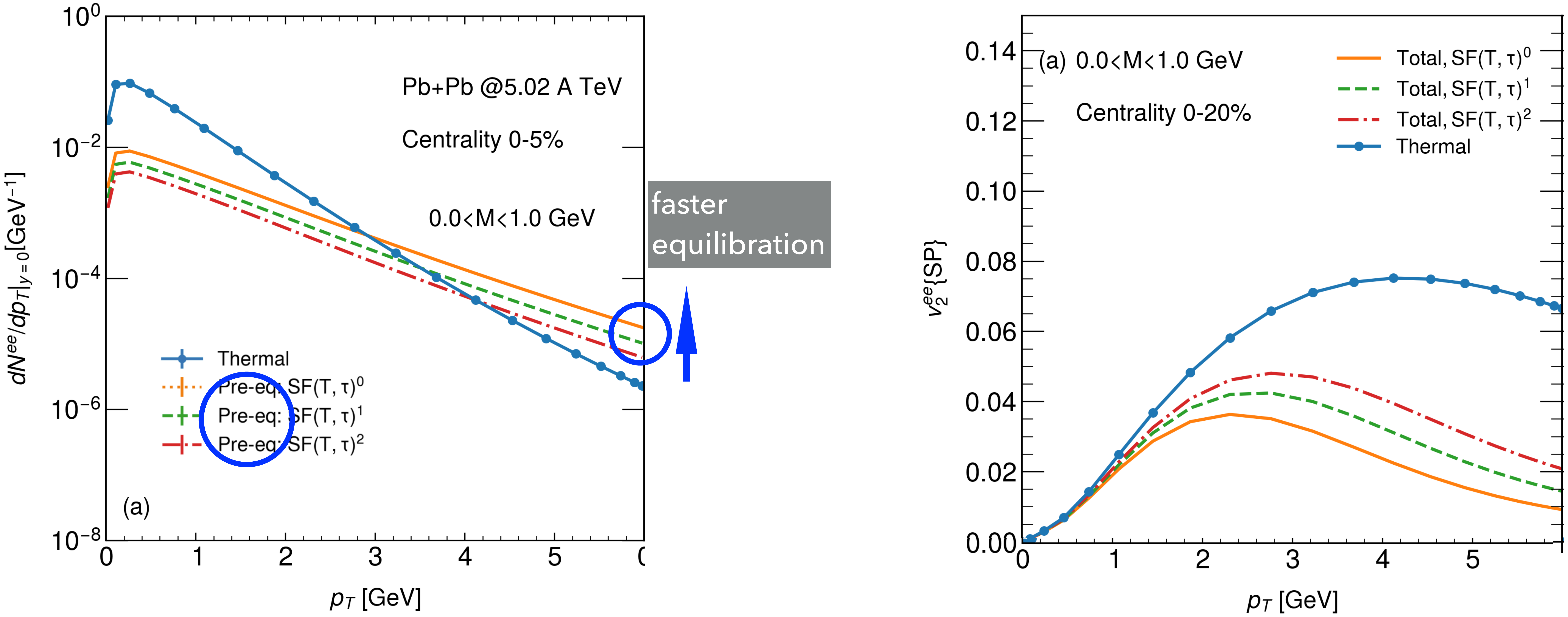

X.-Y. Wu, LD, Gale, Jeon, 2407.04156; Gale, Paquet, Schenke, Shen, PRC 105, 014909 (2022)

Xiang-Yu Wu, 9:40 am, Tue

Anisotropic flows v_n as probe of equilibration

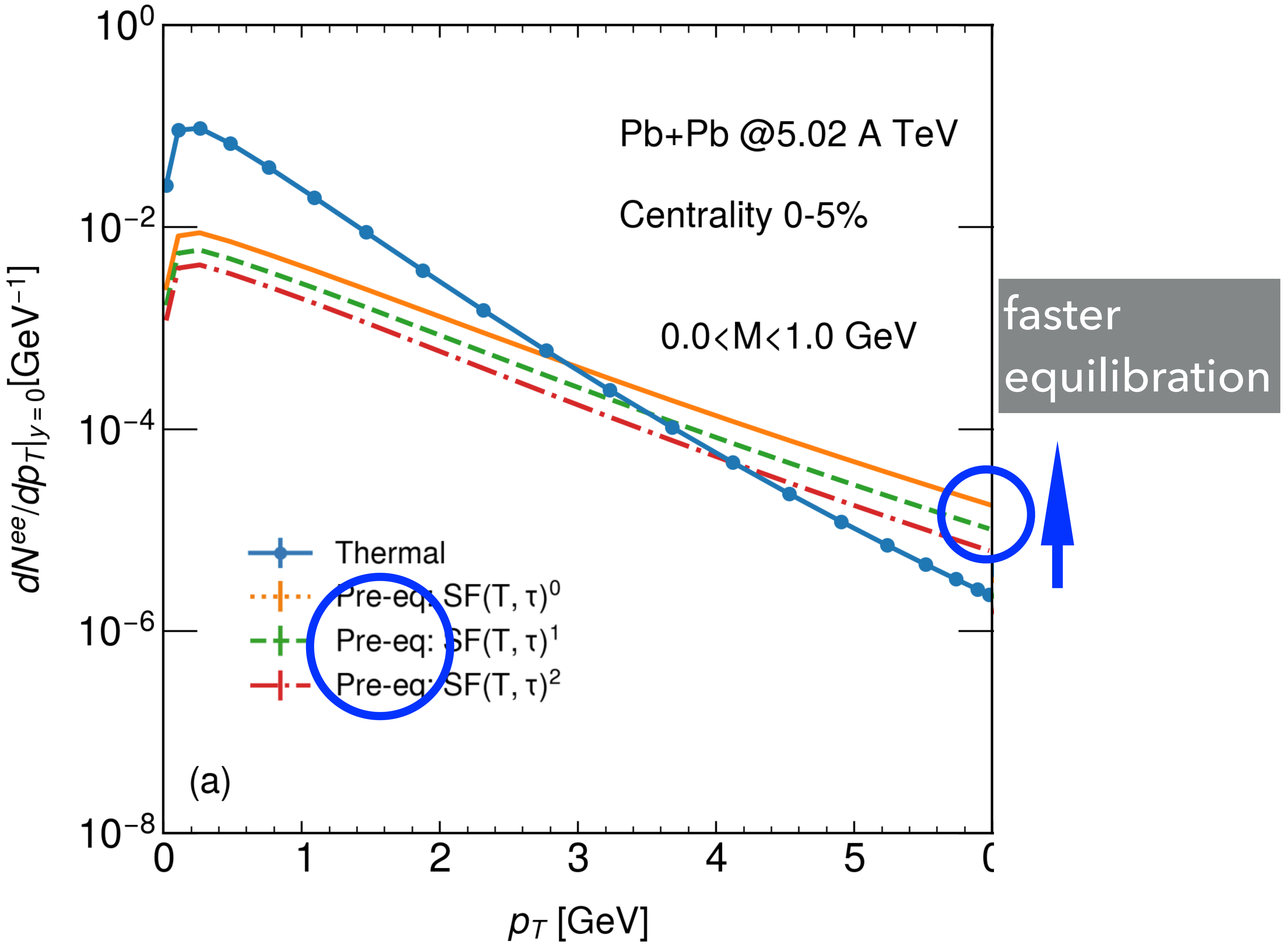

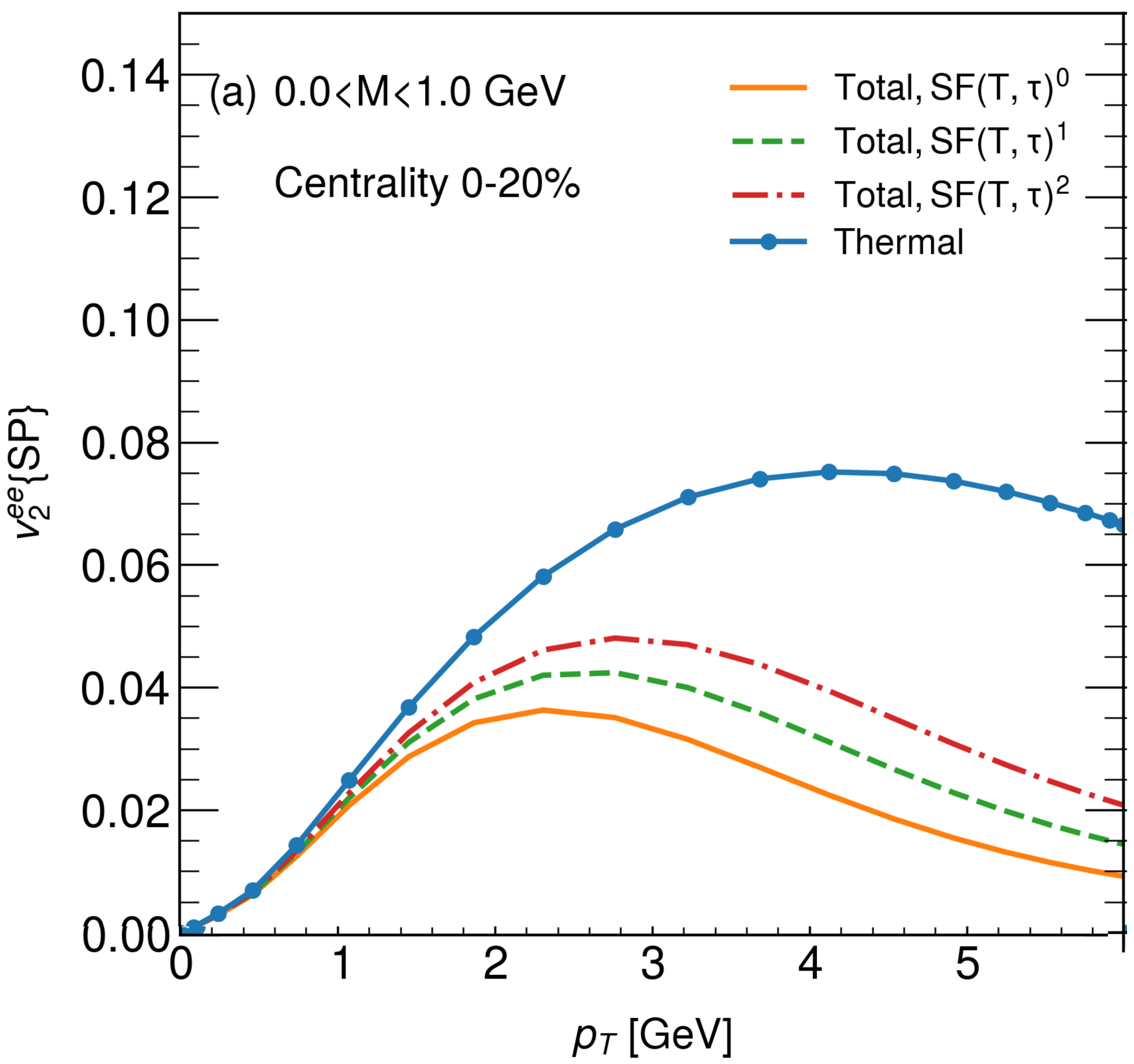

- EM radiations are penetrating but can obtain non-zero v_n, because of the anisotropically expanding emission source. [same as hadrons]

X.-Y. Wu, LD, Gale, Jeon, 2407.04156; Gale, Paquet, Schenke, Shen, PRC 105, 014909 (2022)

Xiang-Yu Wu, 9:40 am, Tue

Anisotropic flows v_n as probe of equilibration

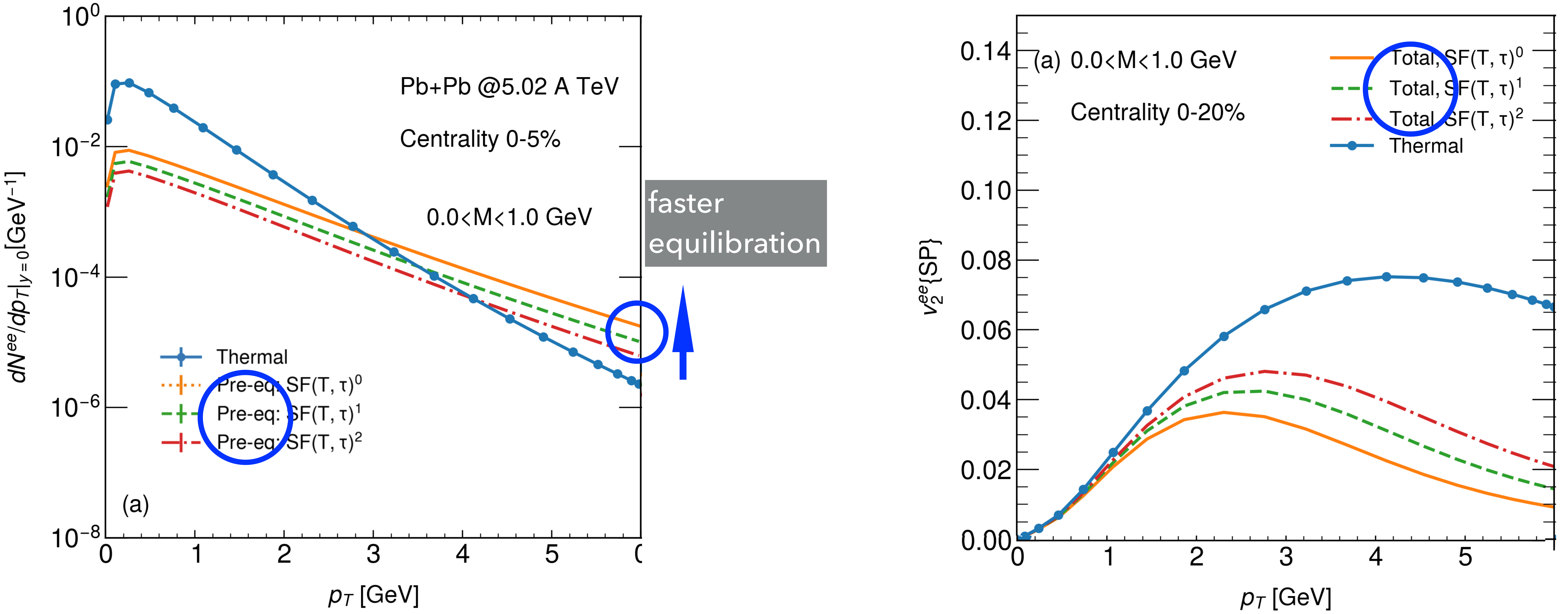

- EM radiations are penetrating but can obtain non-zero v_n, because of the anisotropically expanding emission source. [same as hadrons]

X.-Y. Wu, LD, Gale, Jeon, 2407.04156; Gale, Paquet, Schenke, Shen, PRC 105, 014909 (2022)

Xiang-Yu Wu, 9:40 am, Tue

Anisotropic flows v_n as probe of equilibration

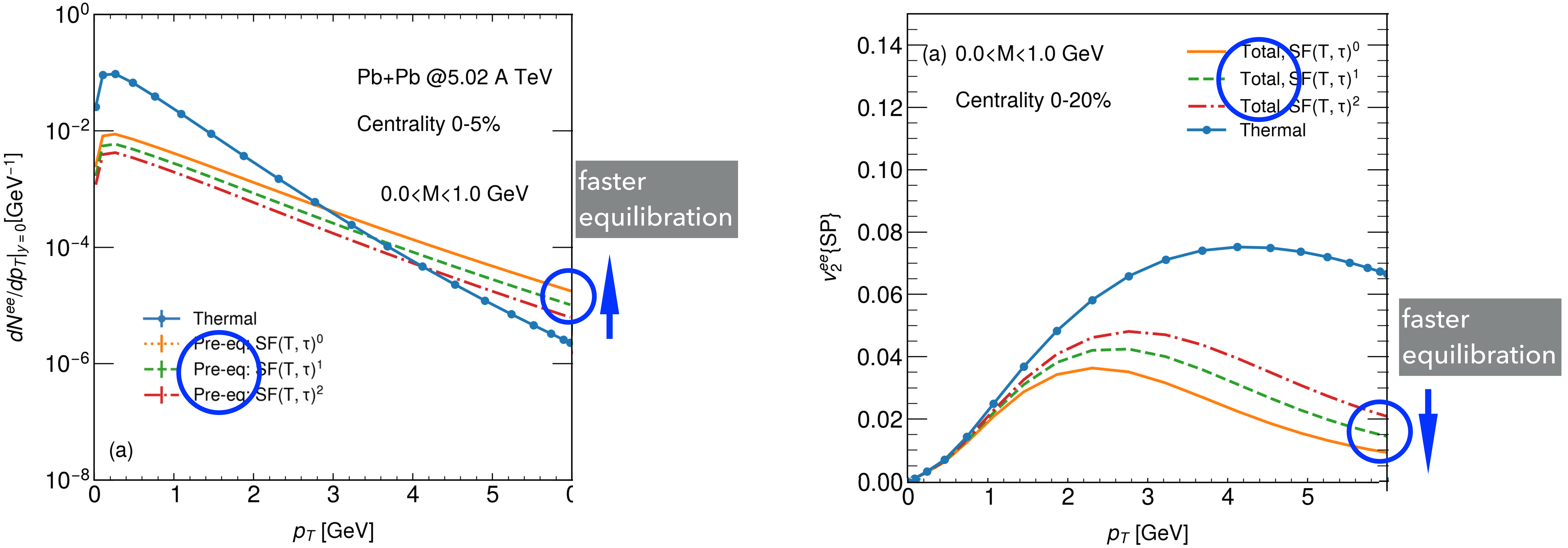

- EM radiations are penetrating but can obtain non-zero v_n, because of the anisotropically expanding emission source. [same as hadrons]
- After accounting for pre-equilibrium dileptons, the total dilepton flow is significantly suppressed relative to the thermal dilepton flow; the faster the equilibration is, the smaller the $v_n(p_T)$ are.

X.-Y. Wu, LD, Gale, Jeon, 2407.04156; Gale, Paquet, Schenke, Shen, PRC 105, 014909 (2022)

Xiang-Yu Wu, 9:40 am, Tue

Anisotropic flows v_n as probe of equilibration

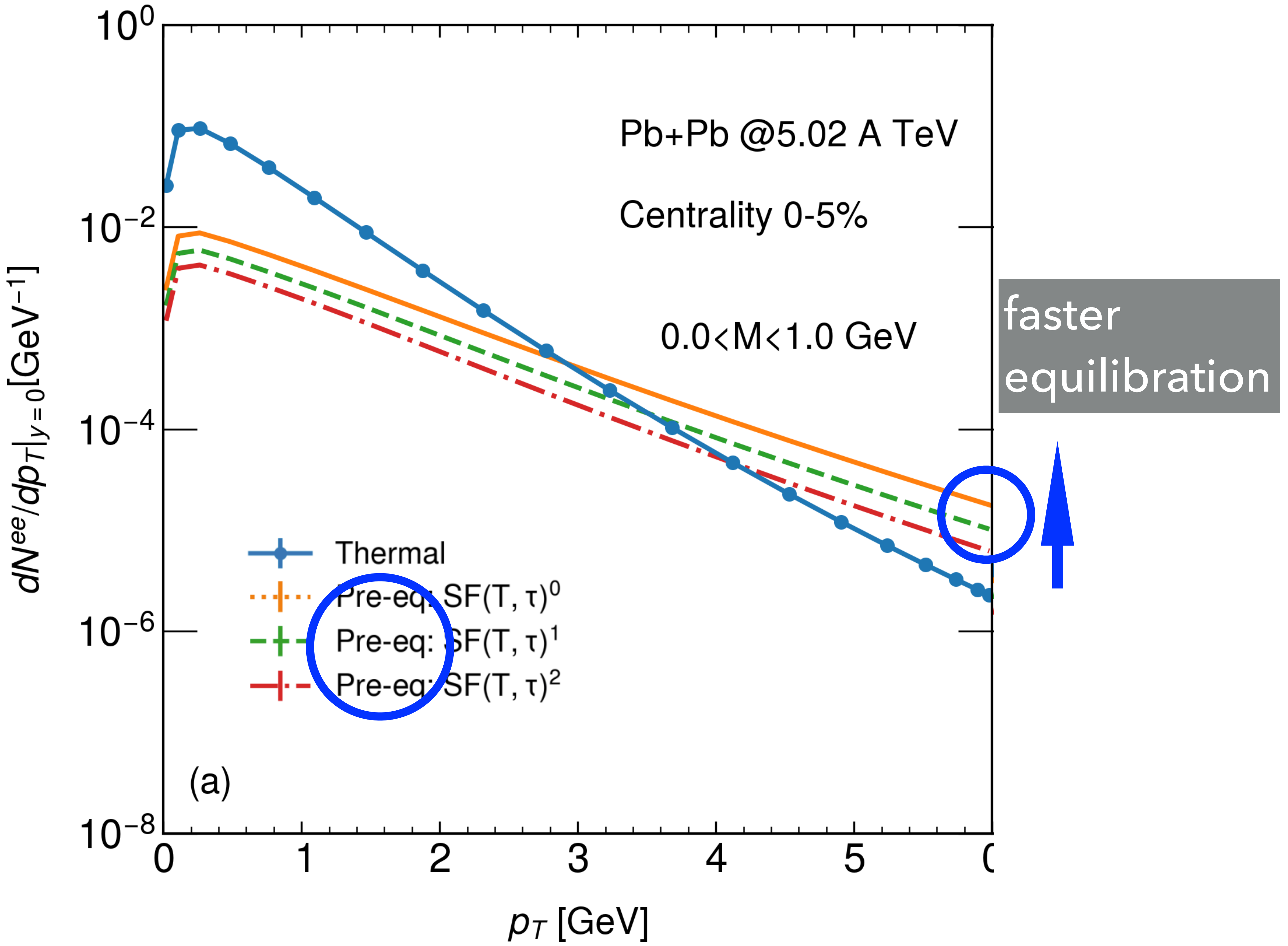

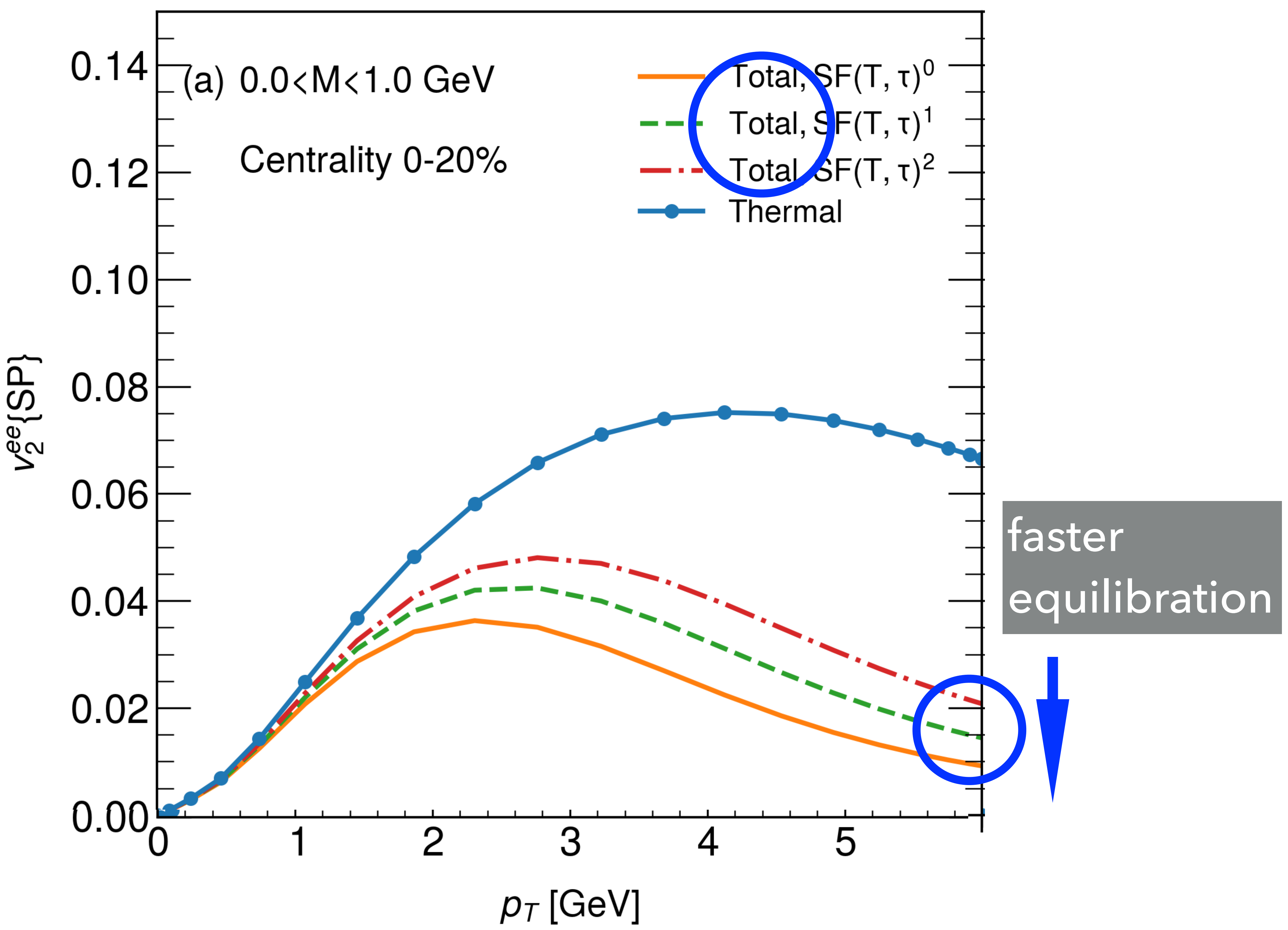

- EM radiations are penetrating but can obtain non-zero v_n, because of the anisotropically expanding emission source. [same as hadrons]
- After accounting for pre-equilibrium dileptons, the total dilepton flow is significantly suppressed relative to the thermal dilepton flow; the faster the equilibration is, the smaller the $v_n(p_T)$ are.
- Combining spectra and anisotropic flows helps to probe the equilibration. [similar story in photons]

X.-Y. Wu, LD, Gale, Jeon, 2407.04156; Gale, Paquet, Schenke, Shen, PRC 105, 014909 (2022)

Xiang-Yu Wu, 9:40 am, Tue

Angular distribution as probe of equilibration

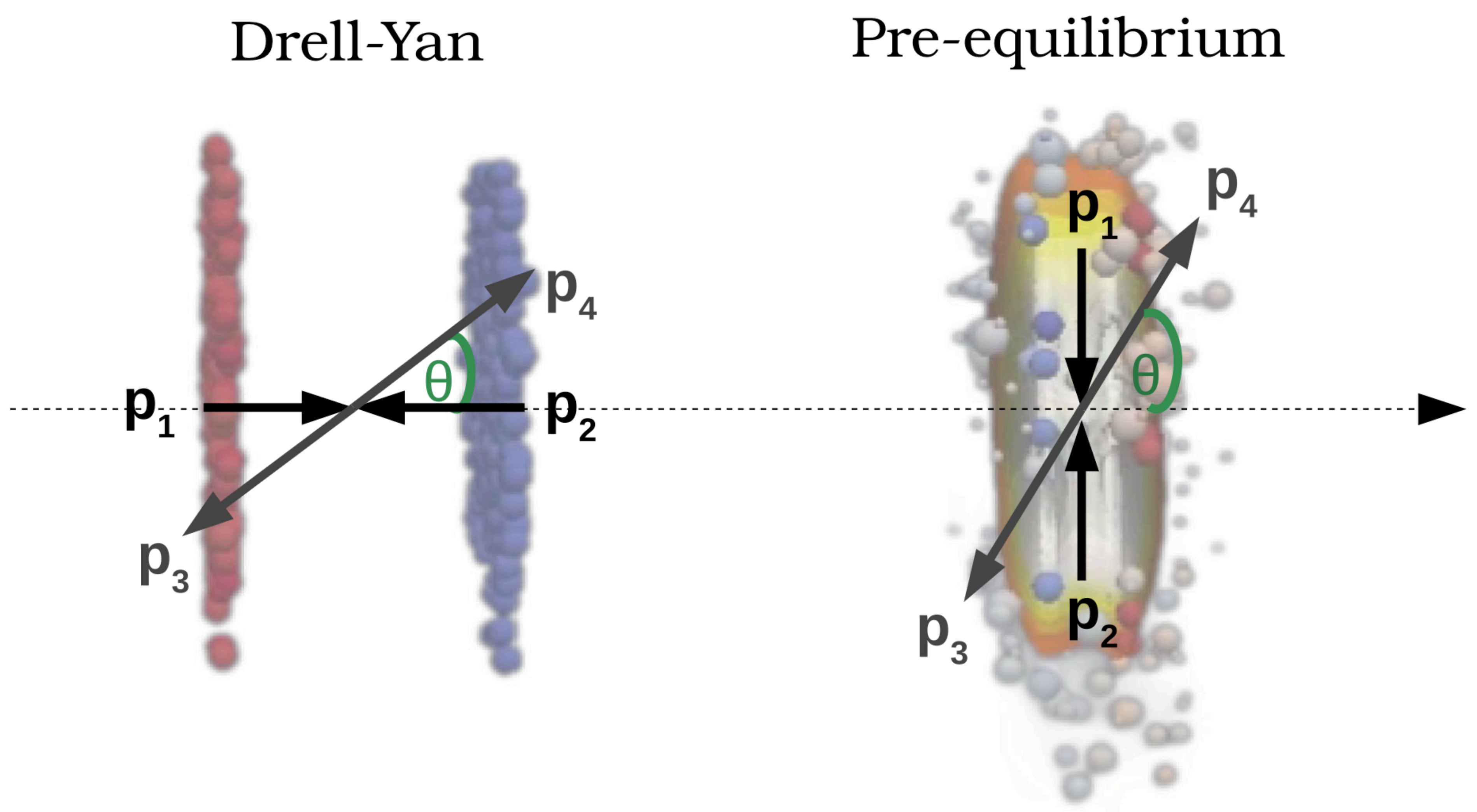

quadrupole moment

$$\left\langle \frac{3\cos^2\theta - 1}{2} \right\rangle$$

Coquet, Winn, X. Du, Ollitrault, Schlichting, PRL 132, 232301 (2024); see also: Seck, Friman, Galatyuk, van Hees, Speranza, Rapp, Wambach, 2309.03189

Angular distribution as probe of equilibration

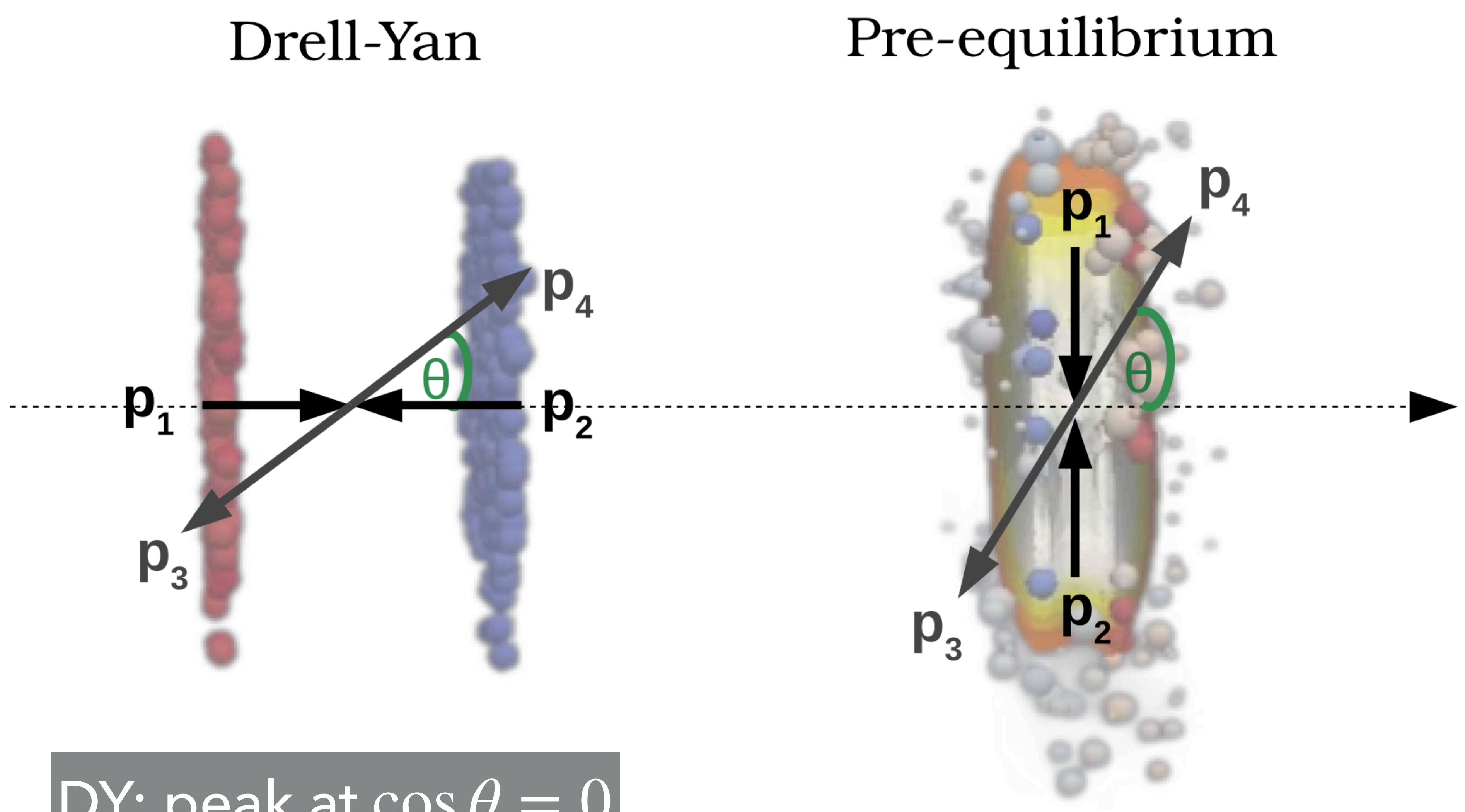

DY: peak at $\cos\theta = 0$

quadrupole moment

$$\left\langle \frac{3\cos^2\theta - 1}{2} \right\rangle$$

DY: positive

- Drell-Yan: quark momenta are mostly longitudinal; preferential emission of longitudinal leptons; negative quadrupole moment.

Coquet, Winn, X. Du, Ollitrault, Schlichting, PRL 132, 232301 (2024); see also: Seck, Friman, Galatyuk, van Hees, Speranza, Rapp, Wambach, 2309.03189

Angular distribution as probe of equilibration

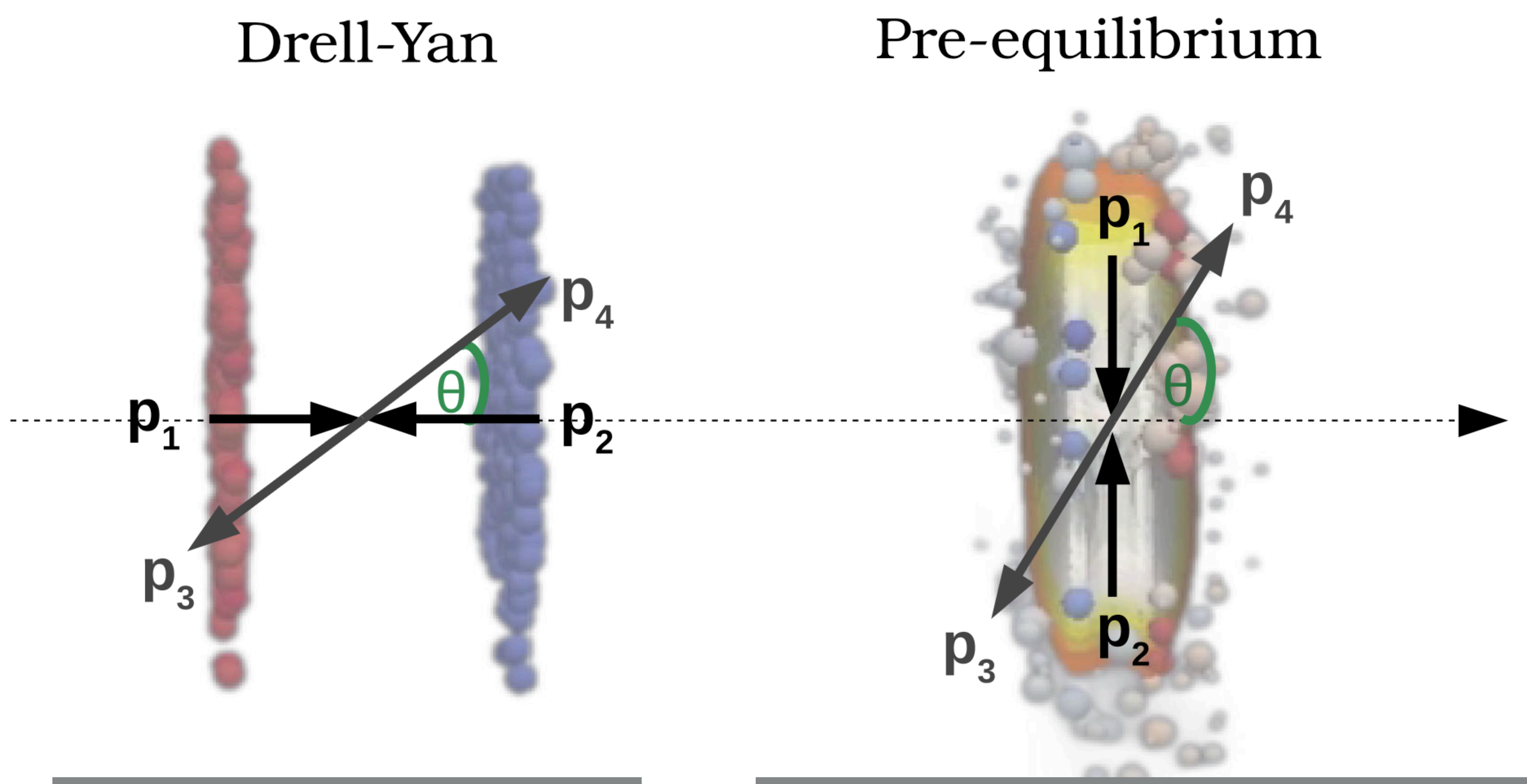

DY: peak at $\cos\theta = 0$

pre-eq. QGP: peak at $\cos\theta = \pm 1$

quadrupole moment

$$\left\langle \frac{3\cos^2\theta - 1}{2} \right\rangle$$

DY: positive

QGP: negative

- Drell-Yan: quark momenta are mostly longitudinal; preferential emission of longitudinal leptons; negative quadrupole moment.
- Pre-eq. QGP: quark momenta are mostly transverse; preferential emission of transverse leptons; positive quadrupole moment.

Coquet, Winn, X. Du, Ollitrault, Schlichting, PRL 132, 232301 (2024); see also: Seck, Friman, Galatyuk, van Hees, Speranza, Rapp, Wambach, 2309.03189

Angular distribution as probe of equilibration

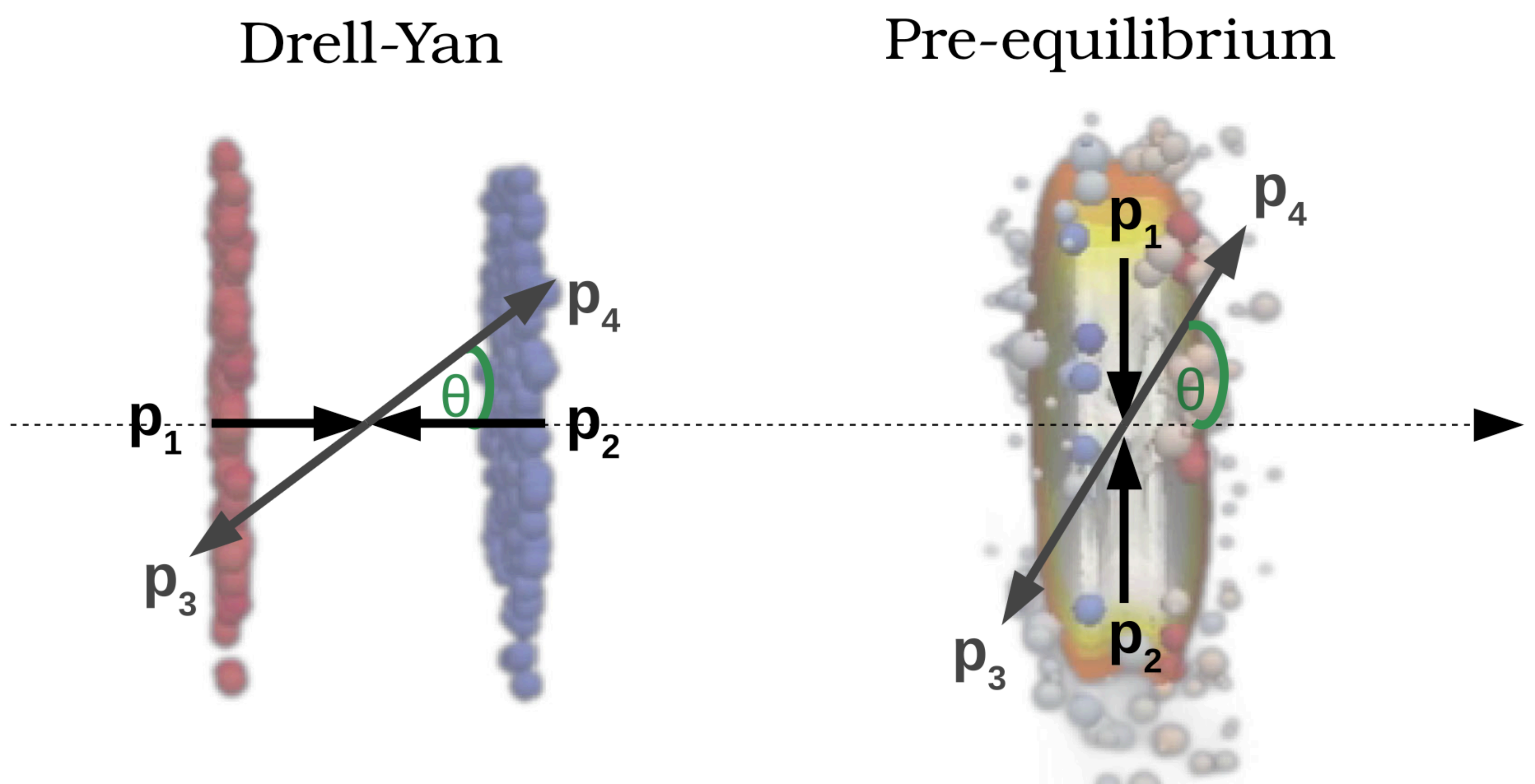

DY: peak at $\cos\theta = 0$

pre-eq. QGP: peak at $\cos\theta = \pm 1$

quadrupole moment

$$\left\langle \frac{3\cos^2\theta - 1}{2} \right\rangle$$

DY: positive

QGP: negative

total: DY+QGP

- Drell-Yan: quark momenta are mostly longitudinal; preferential emission of longitudinal leptons; negative quadrupole moment.
- Pre-eq. QGP: quark momenta are mostly transverse; preferential emission of transverse leptons; positive quadrupole moment.

Coquet, Winn, X. Du, Ollitrault, Schlichting, PRL 132, 232301 (2024); see also: Seck, Friman, Galatyuk, van Hees, Speranza, Rapp, Wambach, 2309.03189

Angular distribution as probe of equilibration

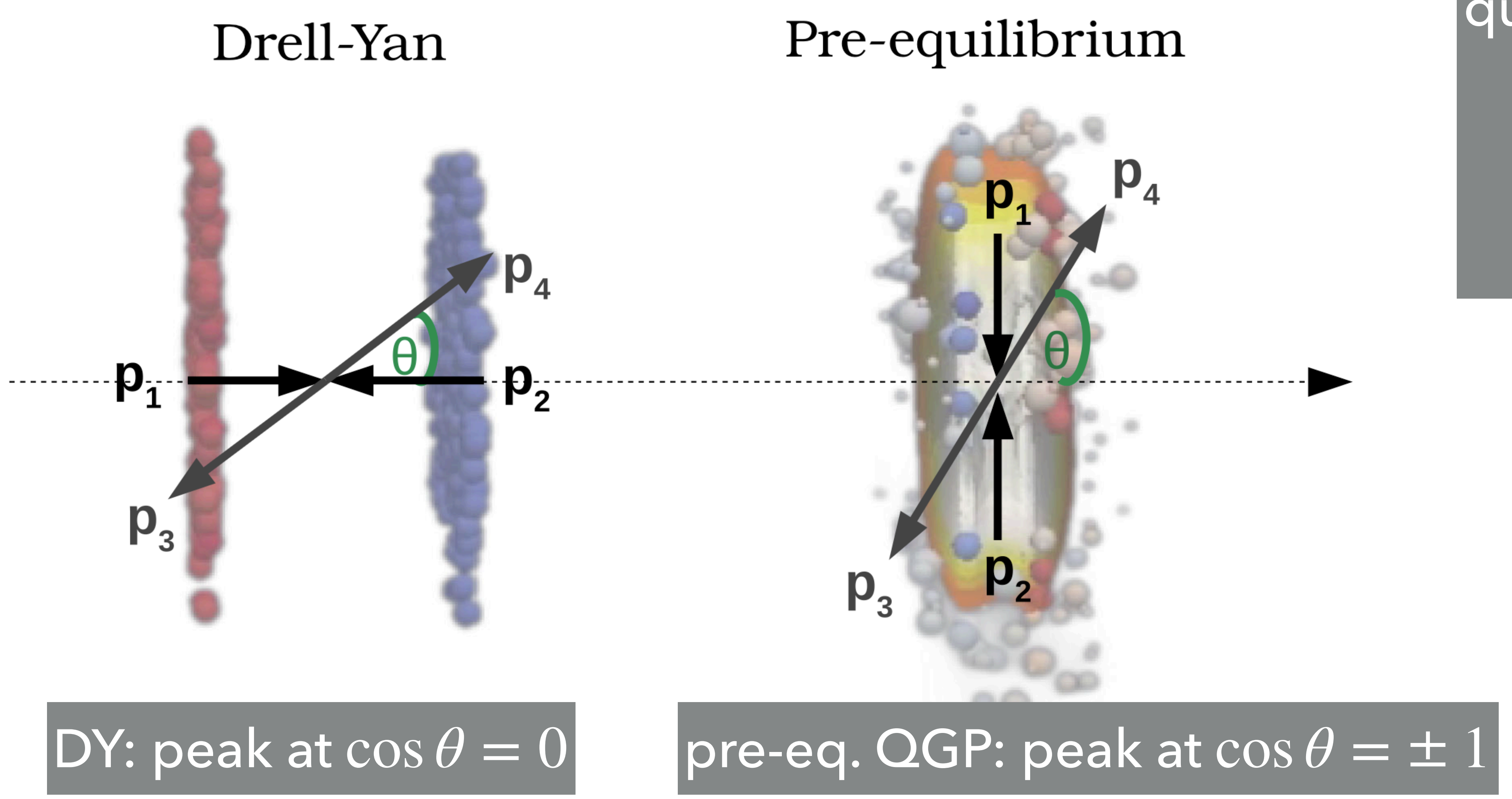

quadrupole moment

$$\left\langle \frac{3\cos^2\theta - 1}{2} \right\rangle$$

DY: positive

QGP: negative

total: DY+QGP

no initial quarks

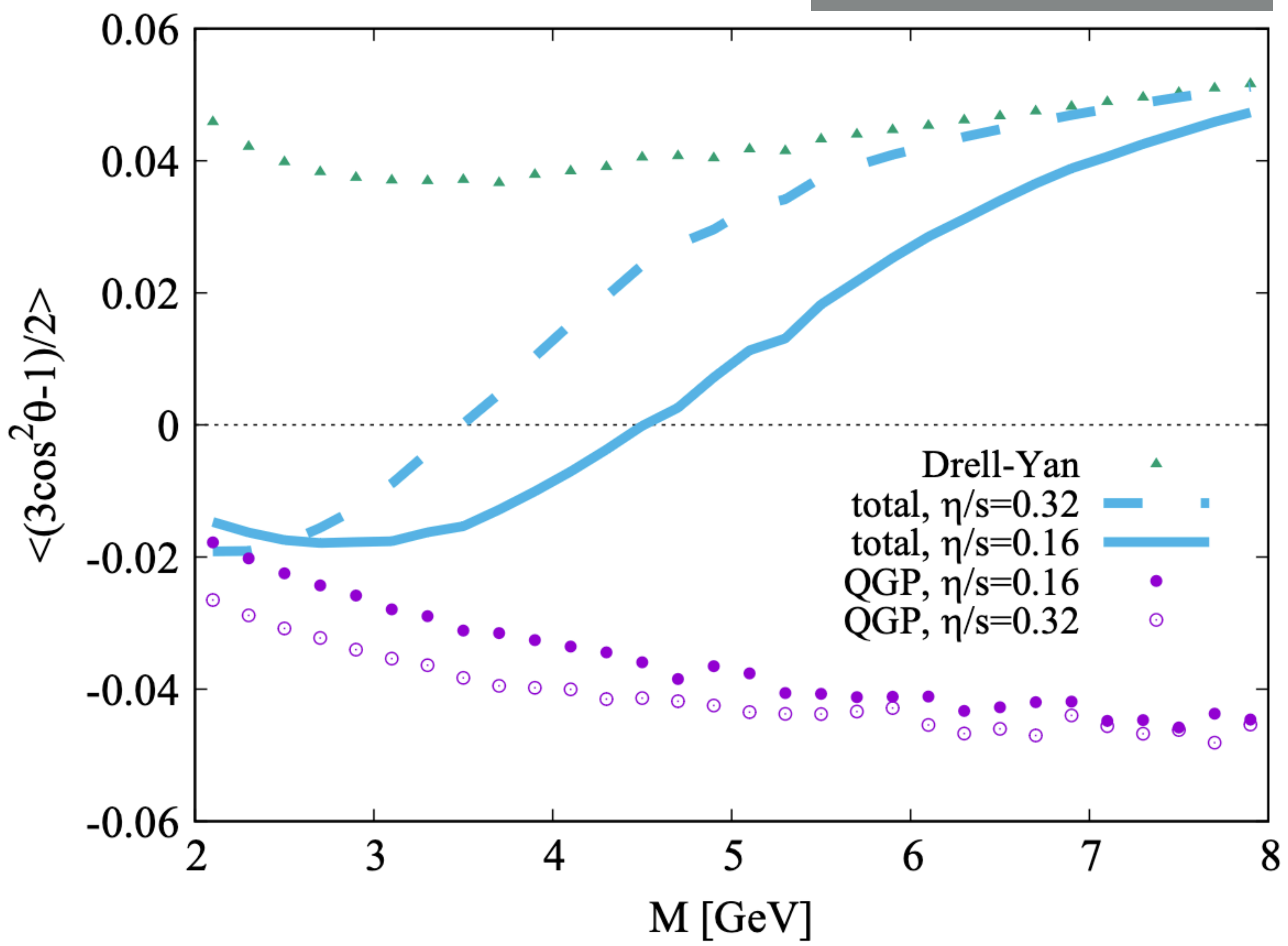

- Drell-Yan: quark momenta are mostly longitudinal; preferential emission of longitudinal leptons; negative quadrupole moment.
- Pre-eq. QGP: quark momenta are mostly transverse; preferential emission of transverse leptons; positive quadrupole moment.

Coquet, Winn, X. Du, Ollitrault, Schlichting, PRL 132, 232301 (2024); see also: Seck, Friman, Galatyuk, van Hees, Speranza, Rapp, Wambach, 2309.03189

Angular distribution as probe of equilibration

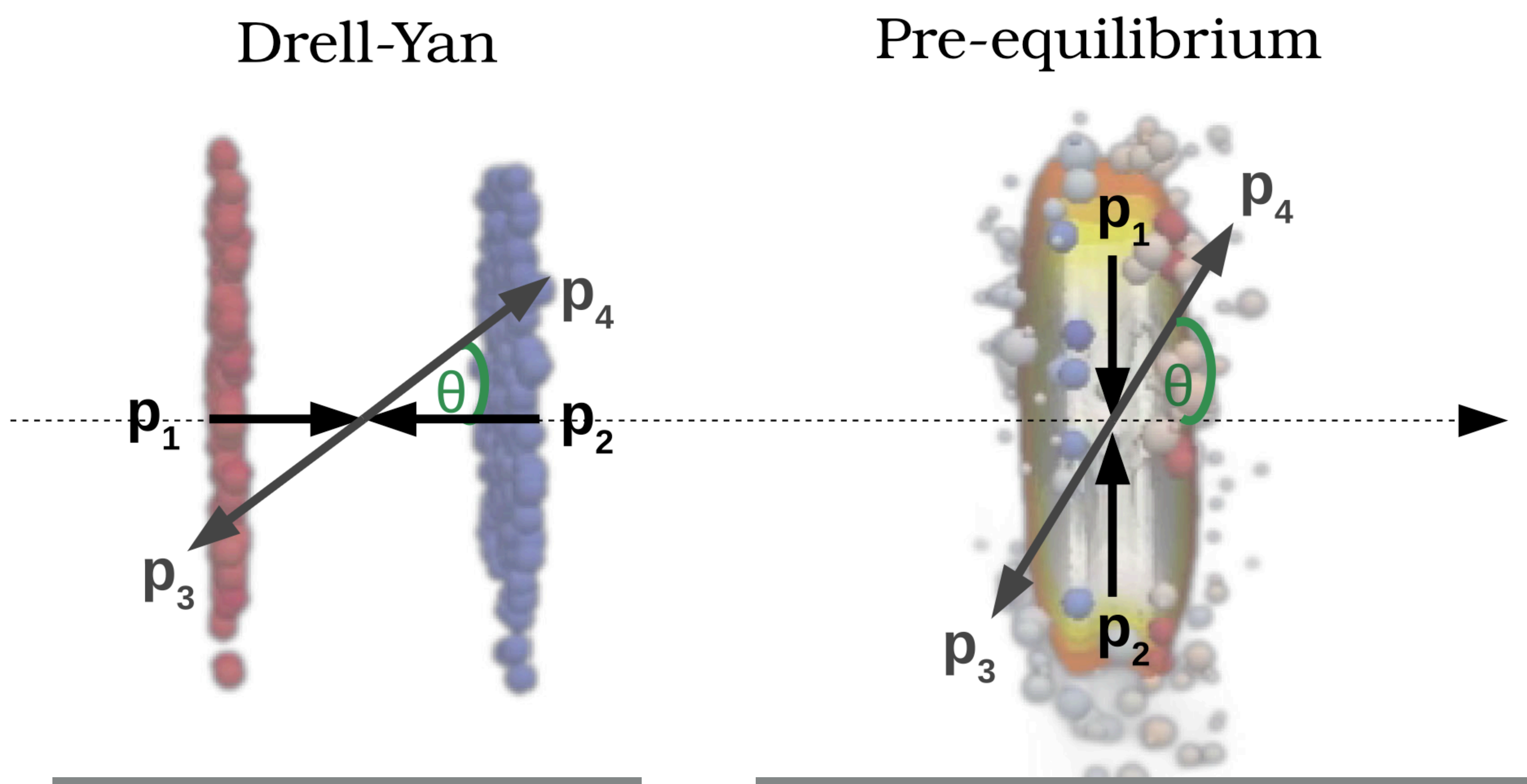

DY: peak at $\cos\theta = 0$

pre-eq. QGP: peak at $\cos\theta = \pm 1$

quadrupole moment

$$\left\langle \frac{3\cos^2\theta - 1}{2} \right\rangle$$

DY: positive

QGP: negative

total: DY+QGP

no initial quarks

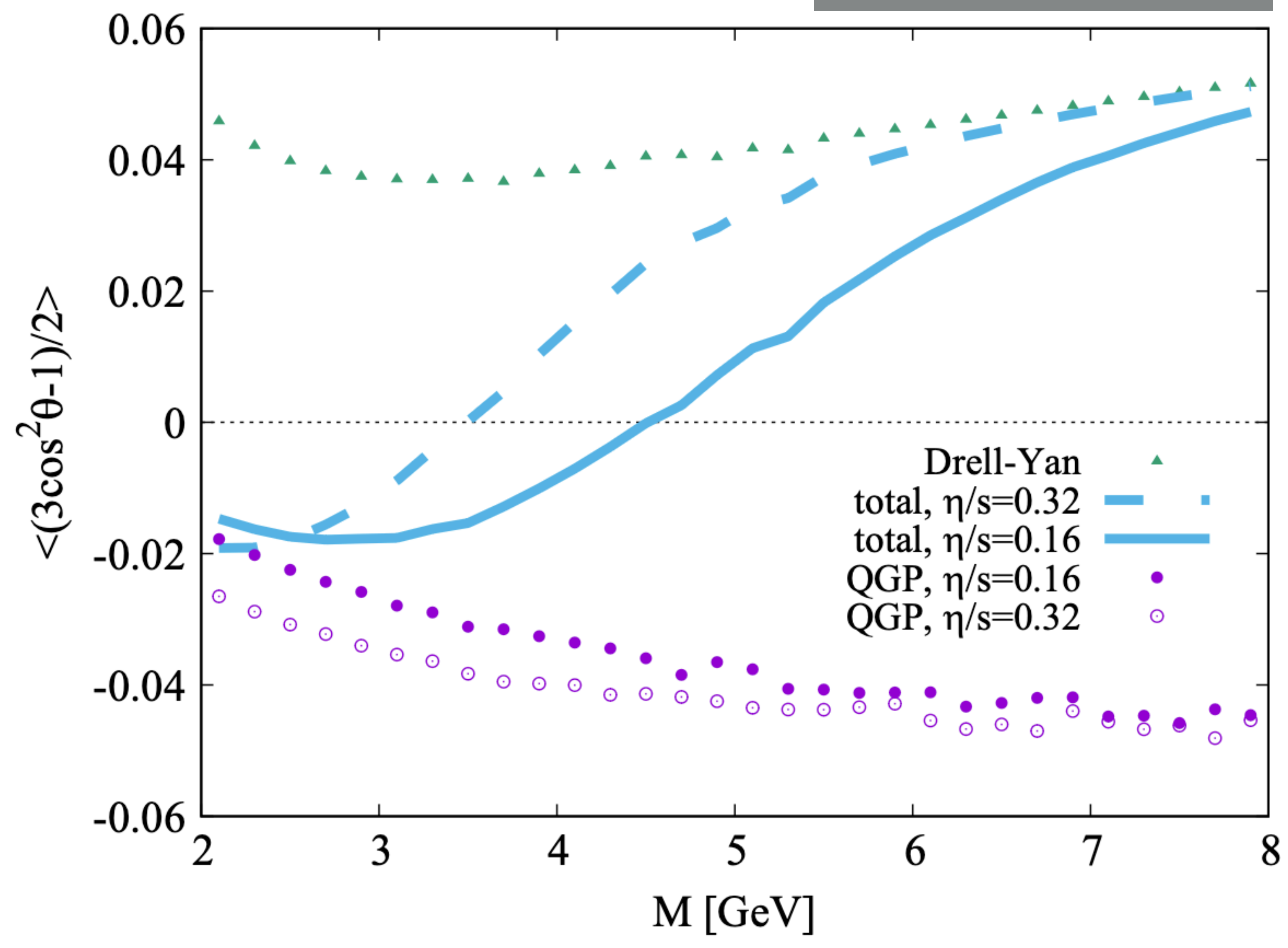

quarks equilibrated throughout

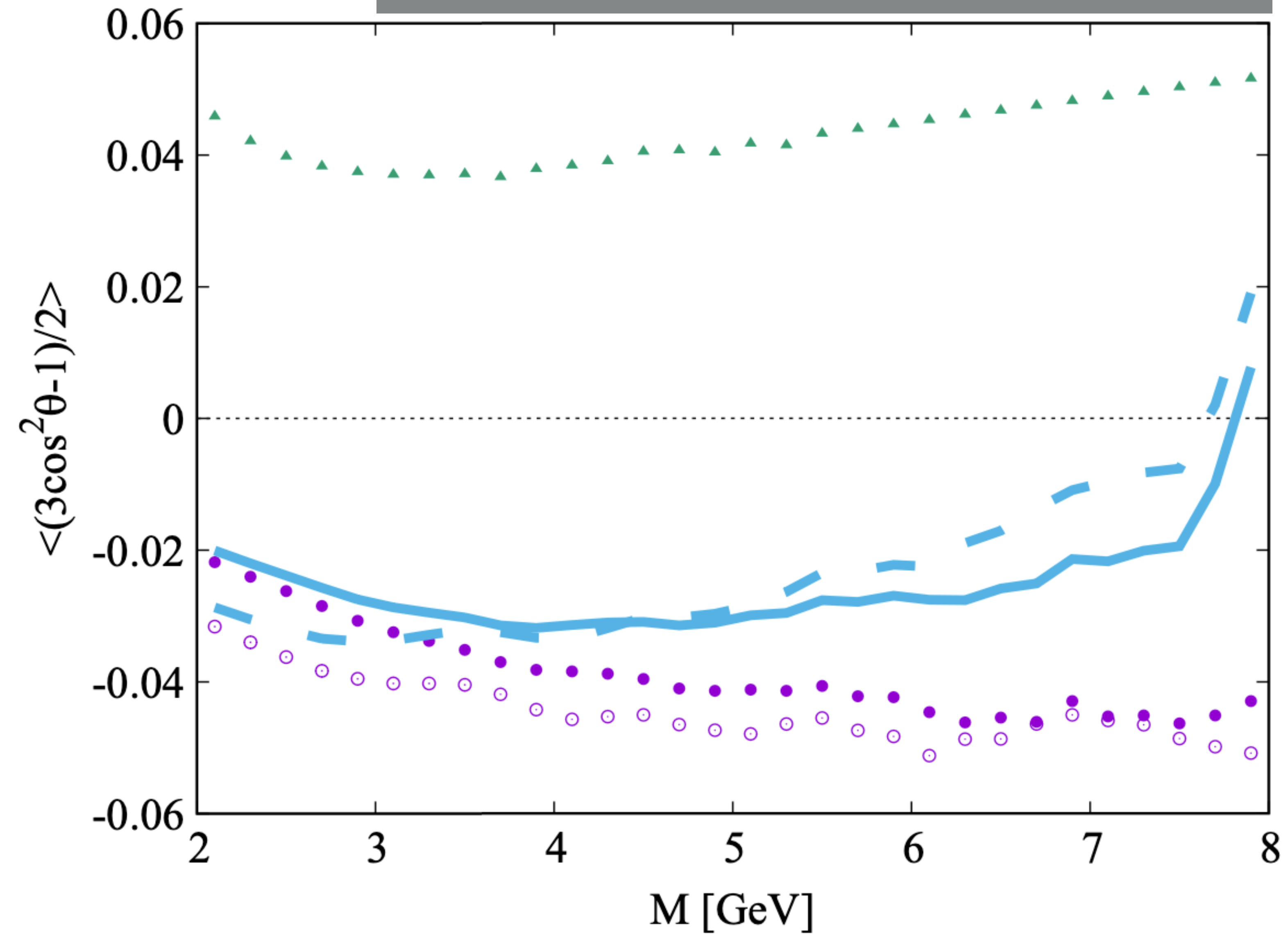

- Drell-Yan: quark momenta are mostly longitudinal; preferential emission of longitudinal leptons; negative quadrupole moment.
- Pre-eq. QGP: quark momenta are mostly transverse; preferential emission of transverse leptons; positive quadrupole moment.

Coquet, Winn, X. Du, Ollitrault, Schlichting, PRL 132, 232301 (2024); see also: Seck, Friman, Galatyuk, van Hees, Speranza, Rapp, Wambach, 2309.03189

Angular distribution as probe of equilibration

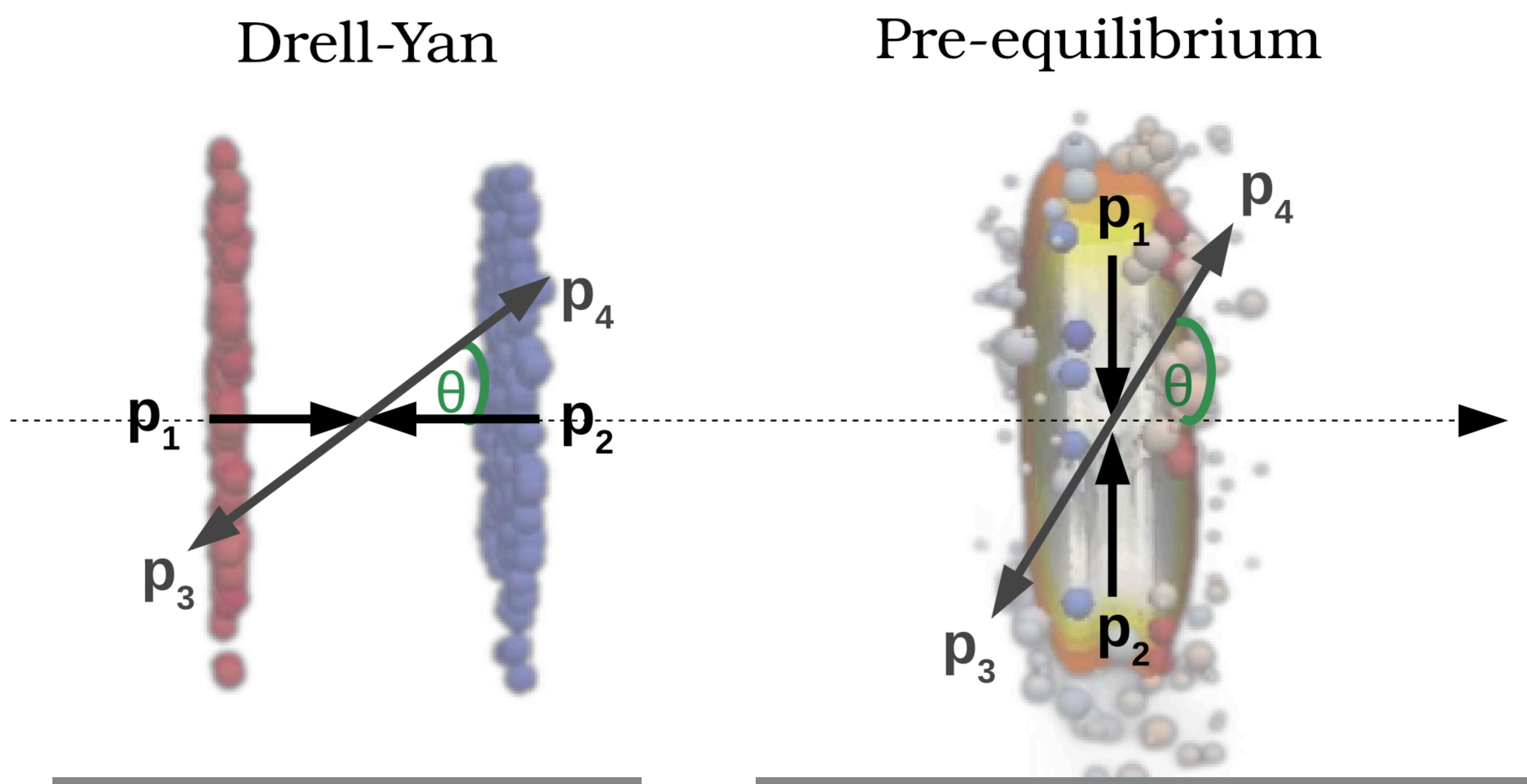

DY: peak at $\cos\theta = 0$

pre-eq. QGP: peak at $\cos\theta = \pm 1$

quadrupole moment

$$\left\langle \frac{3\cos^2\theta - 1}{2} \right\rangle$$

DY: positive

QGP: negative

total: DY+QGP

no initial quarks

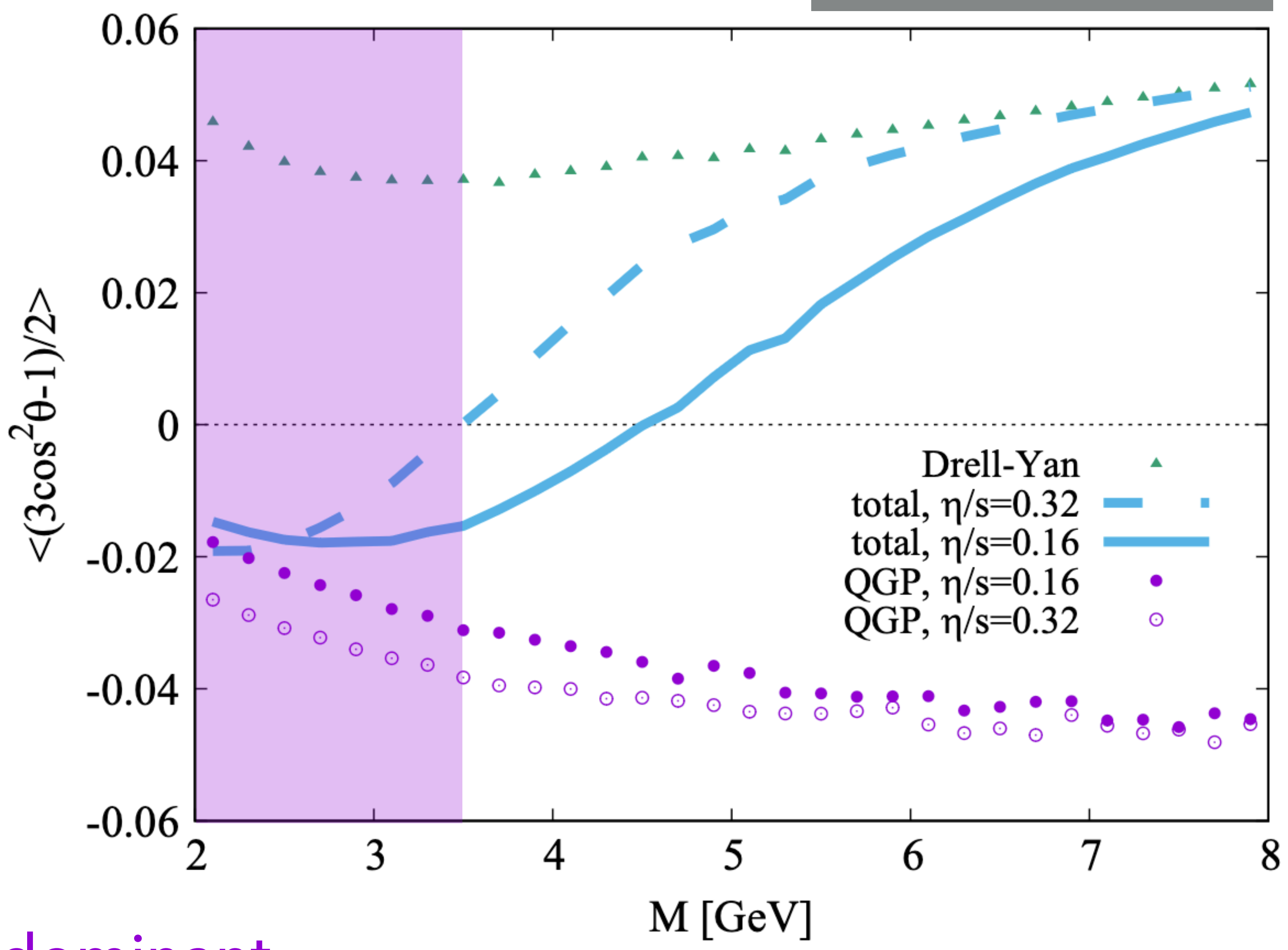

QGP-dominant

quarks equilibrated throughout

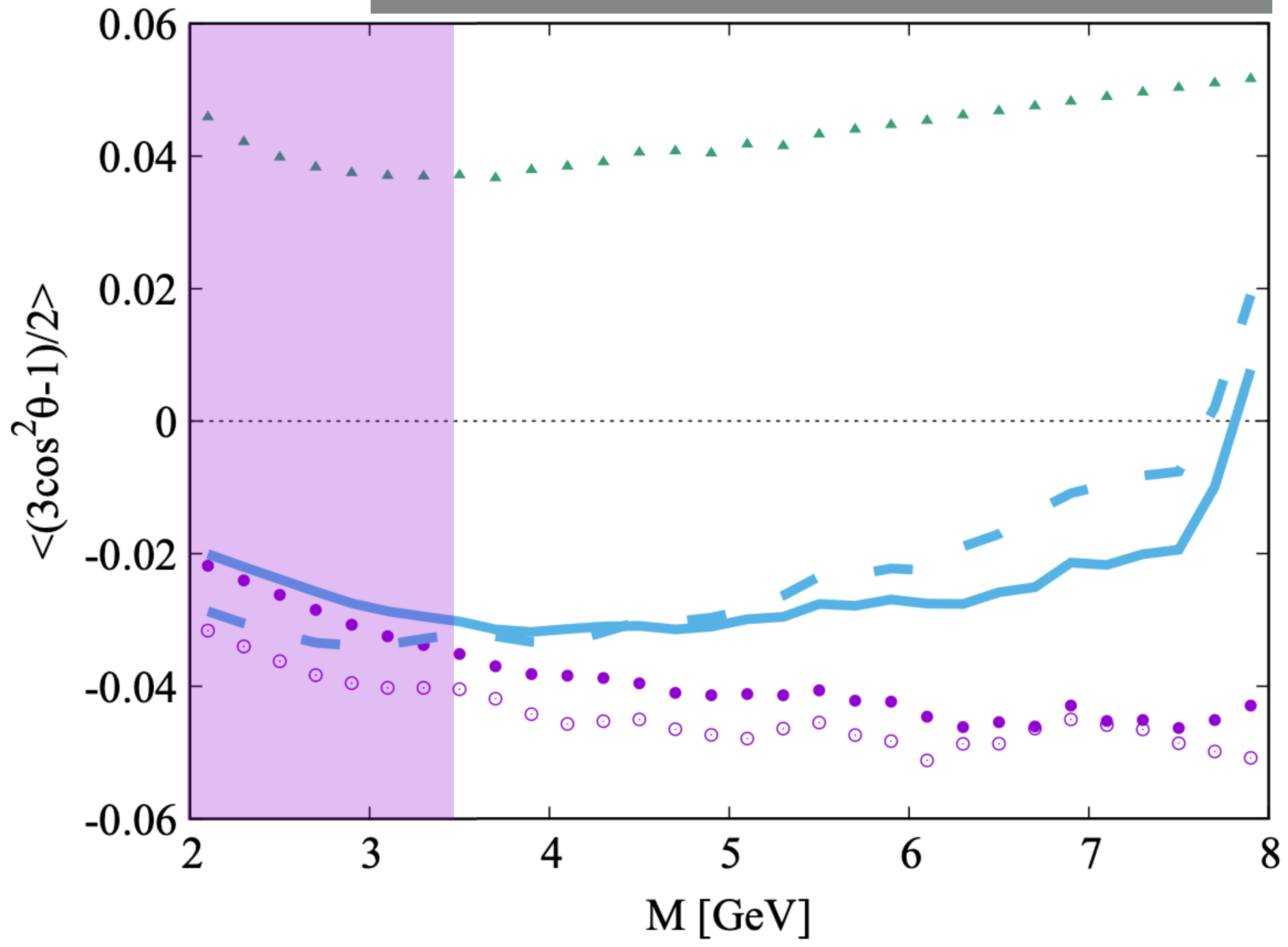

- Drell-Yan: quark momenta are mostly longitudinal; preferential emission of longitudinal leptons; negative quadrupole moment.
- Pre-eq. QGP: quark momenta are mostly transverse; preferential emission of transverse leptons; positive quadrupole moment.

Coquet, Winn, X. Du, Ollitrault, Schlichting, PRL 132, 232301 (2024); see also: Seck, Friman, Galatyuk, van Hees, Speranza, Rapp, Wambach, 2309.03189

Angular distribution as probe of equilibration

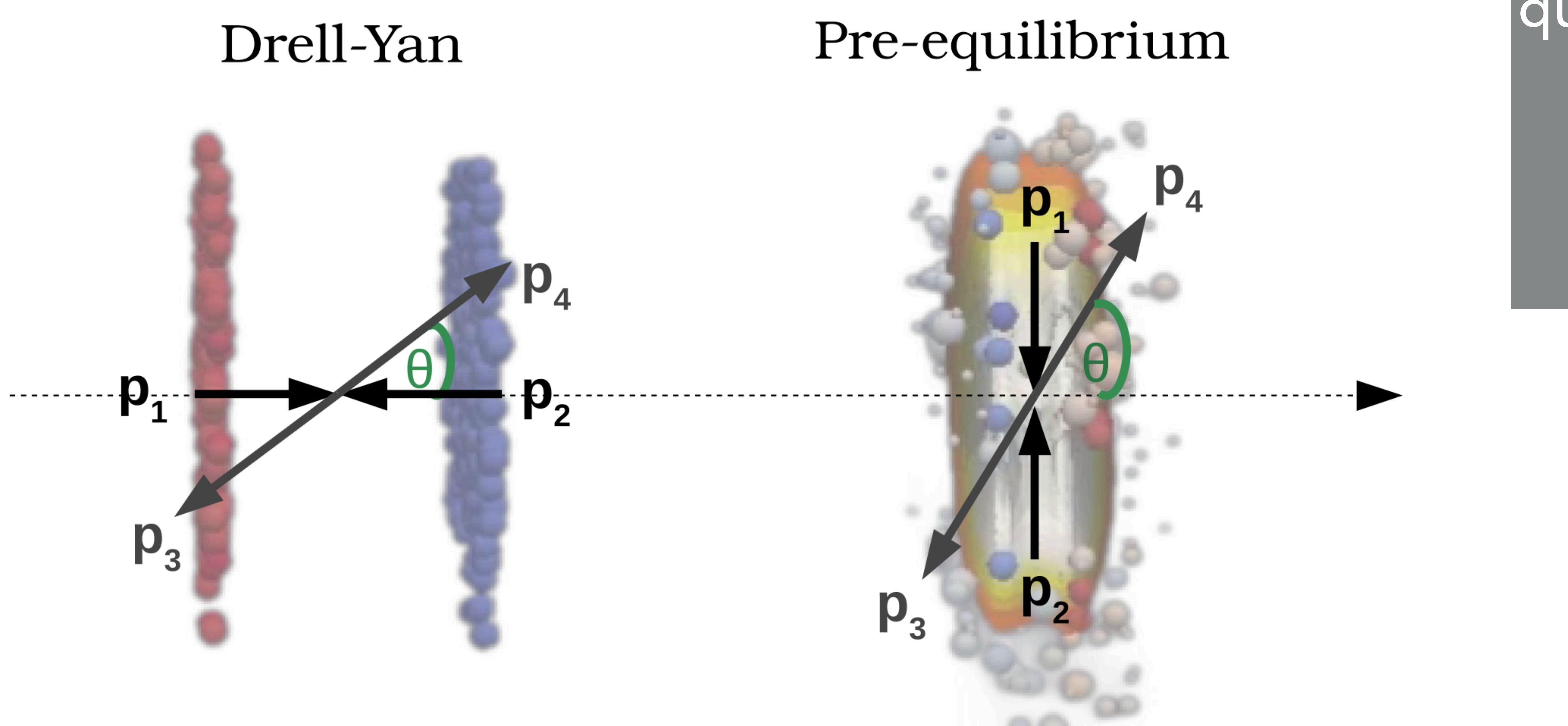

DY: peak at $\cos\theta = 0$

pre-eq. QGP: peak at $\cos\theta = \pm 1$

quadrupole moment

$$\left\langle \frac{3\cos^2\theta - 1}{2} \right\rangle$$

DY: positive

QGP: negative

total: DY+QGP

no initial quarks

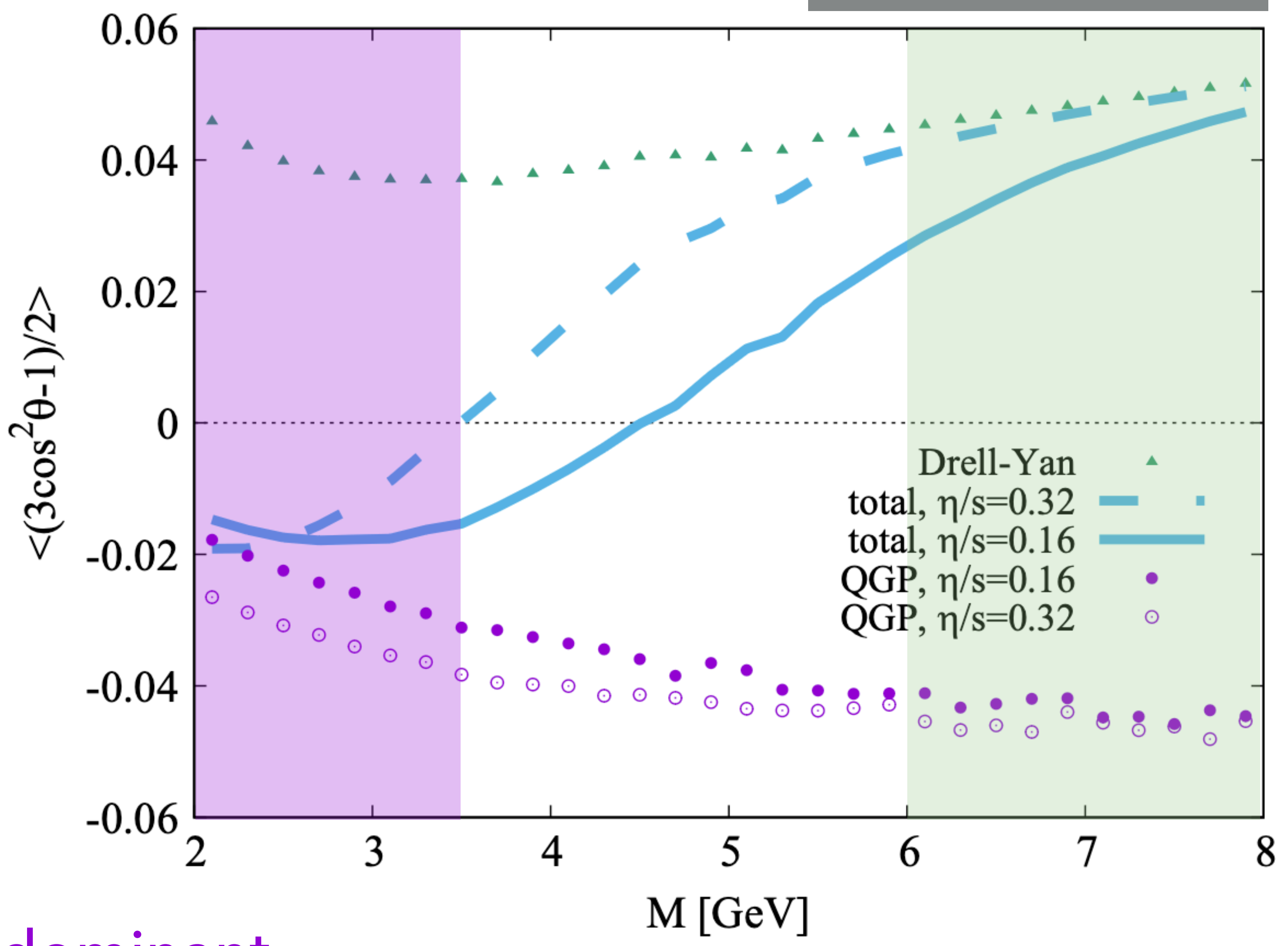

DY-dominant

QGP-dominant

quarks equilibrated throughout

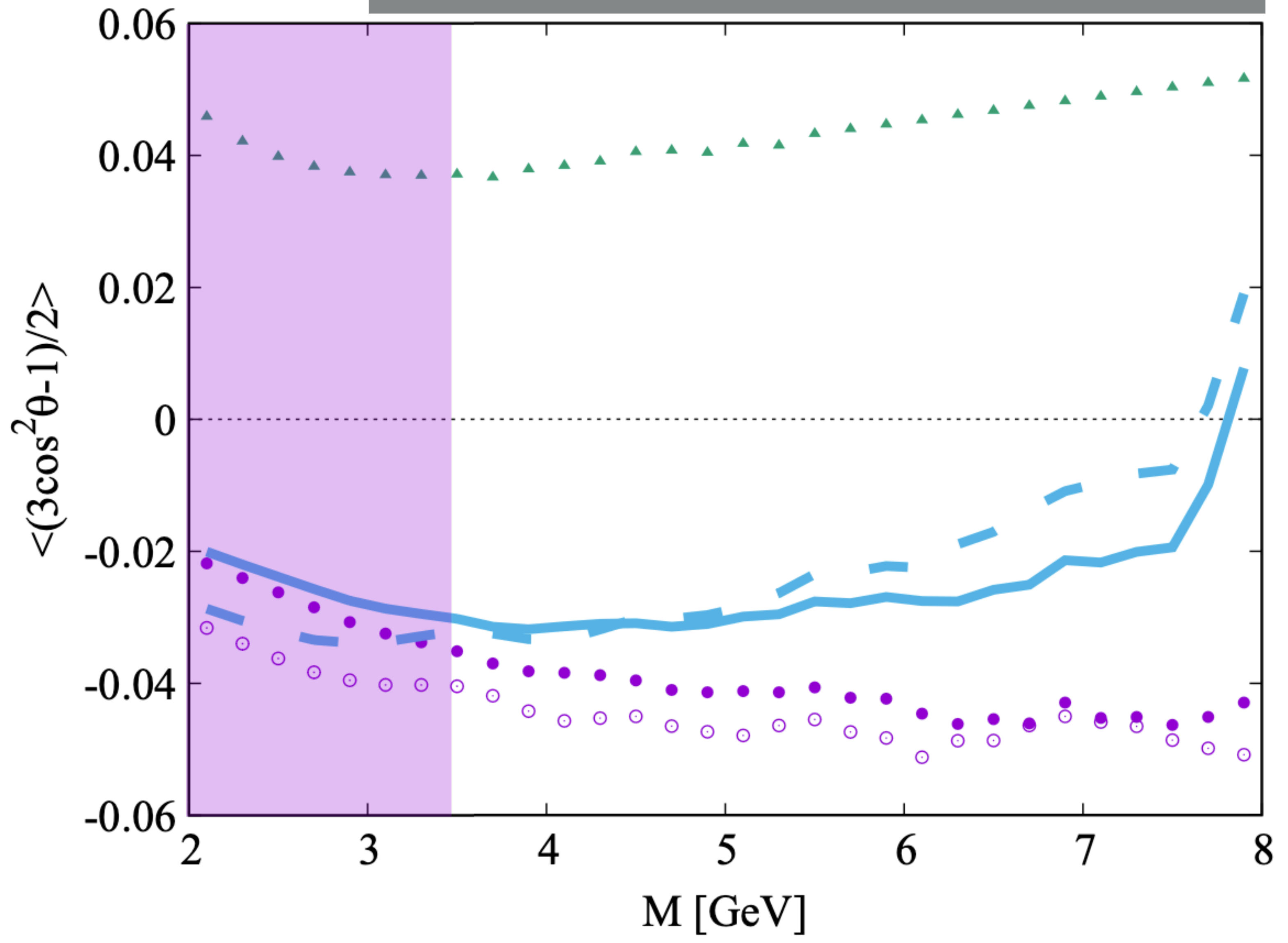

- Drell-Yan: quark momenta are mostly longitudinal; preferential emission of longitudinal leptons; negative quadrupole moment.
- Pre-eq. QGP: quark momenta are mostly transverse; preferential emission of transverse leptons; positive quadrupole moment.

Coquet, Winn, X. Du, Ollitrault, Schlichting, PRL 132, 232301 (2024); see also: Seck, Friman, Galatyuk, van Hees, Speranza, Rapp, Wambach, 2309.03189

Angular distribution as probe of equilibration

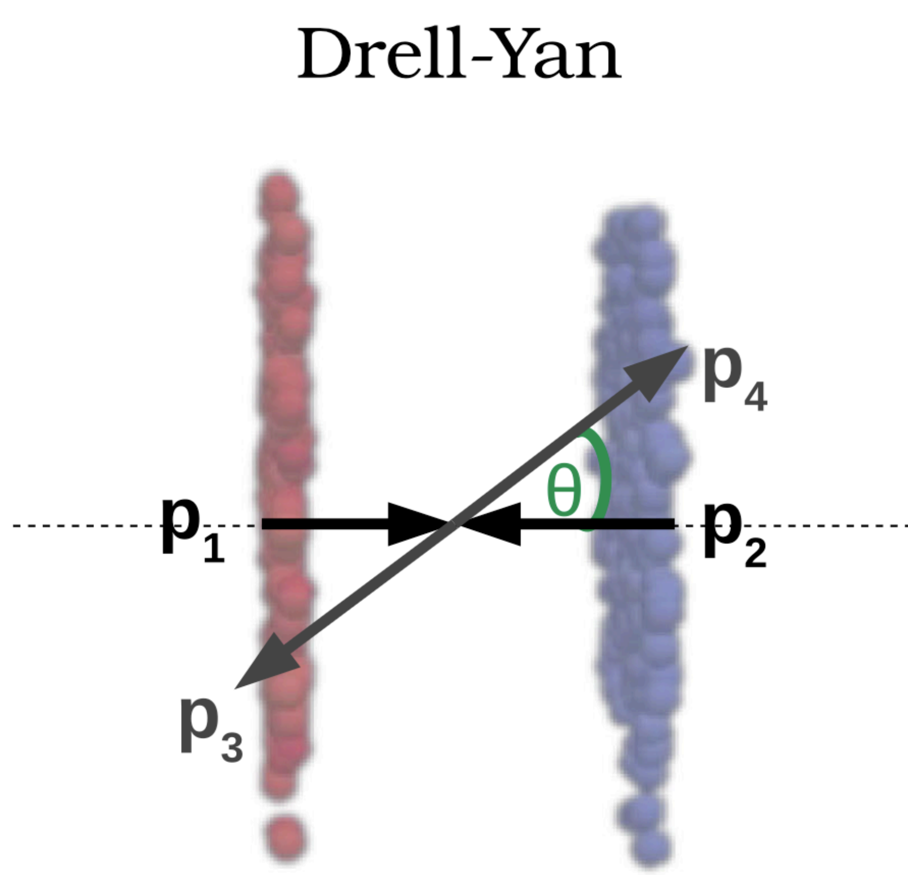

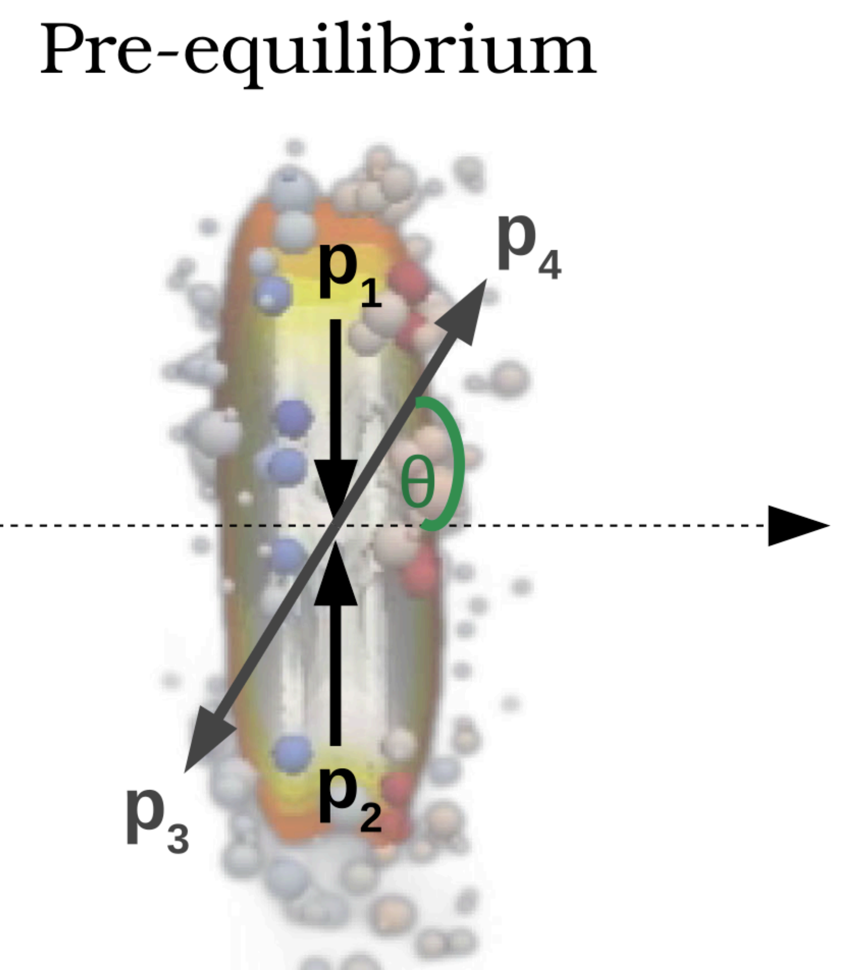

DY: peak at $\cos\theta = 0$

pre-eq. QGP: peak at $\cos\theta = \pm 1$

quadrupole moment

$$\left\langle \frac{3\cos^2\theta - 1}{2} \right\rangle$$

DY: positive

QGP: negative

total: DY+QGP

no initial quarks

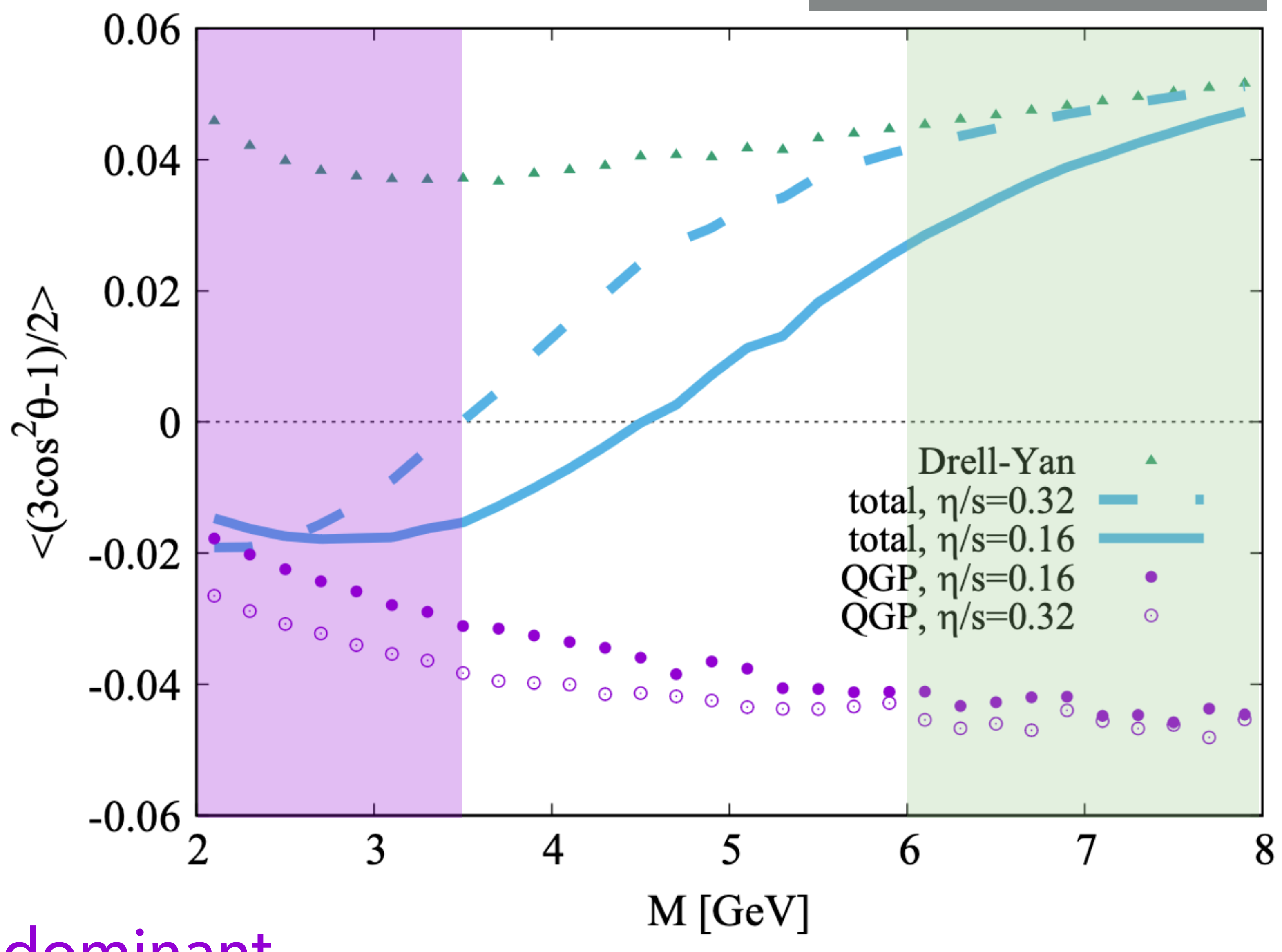

DY-dominant

QGP-dominant

quarks equilibrated throughout

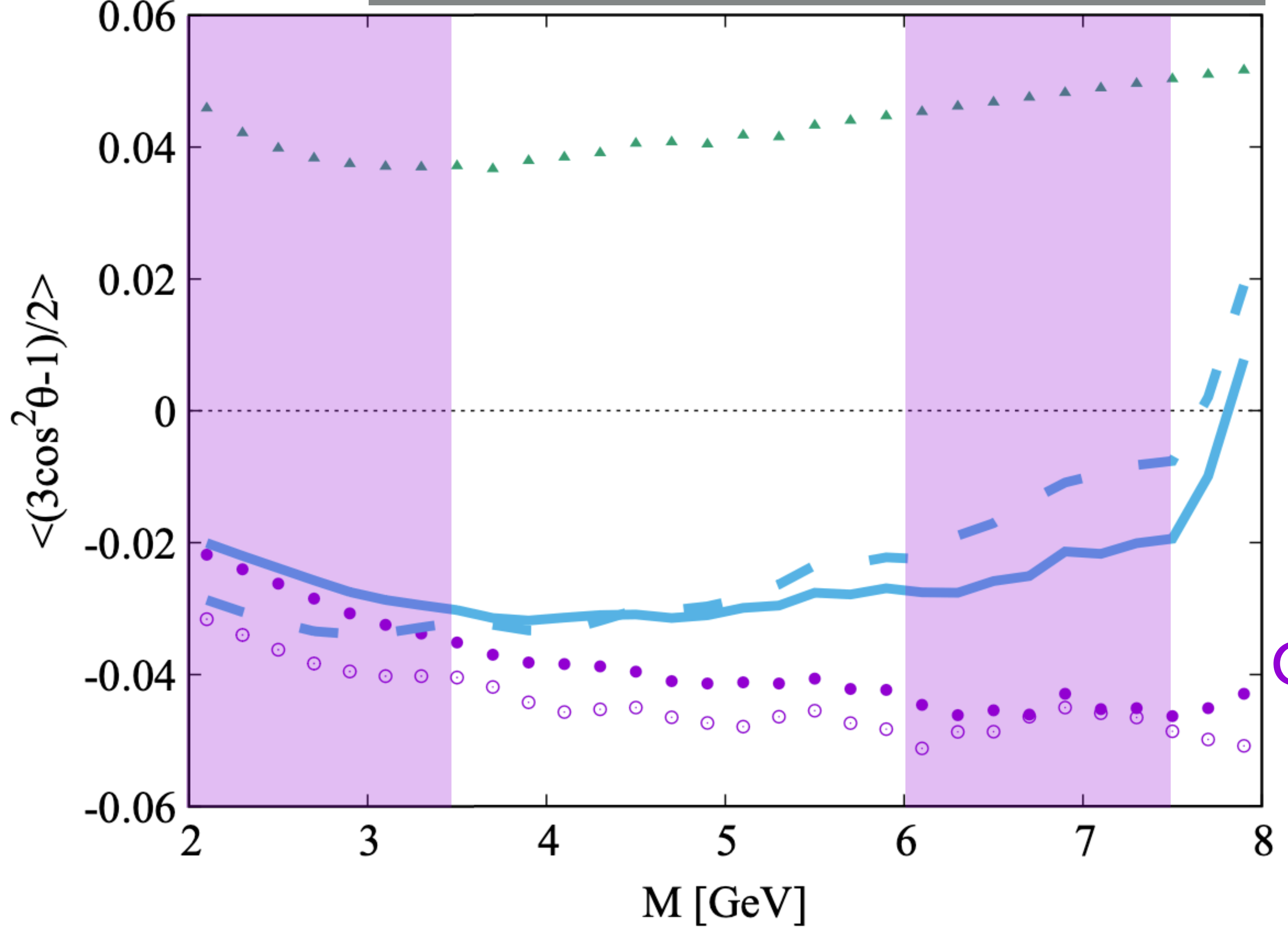

QGP-dominant

- Drell-Yan: quark momenta are mostly longitudinal; preferential emission of longitudinal leptons; negative quadrupole moment.
- Pre-eq. QGP: quark momenta are mostly transverse; preferential emission of transverse leptons; positive quadrupole moment.

Coquet, Winn, X. Du, Ollitrault, Schlichting, PRL 132, 232301 (2024); see also: Seck, Friman, Galatyuk, van Hees, Speranza, Rapp, Wambach, 2309.03189

Angular distribution as probe of equilibration

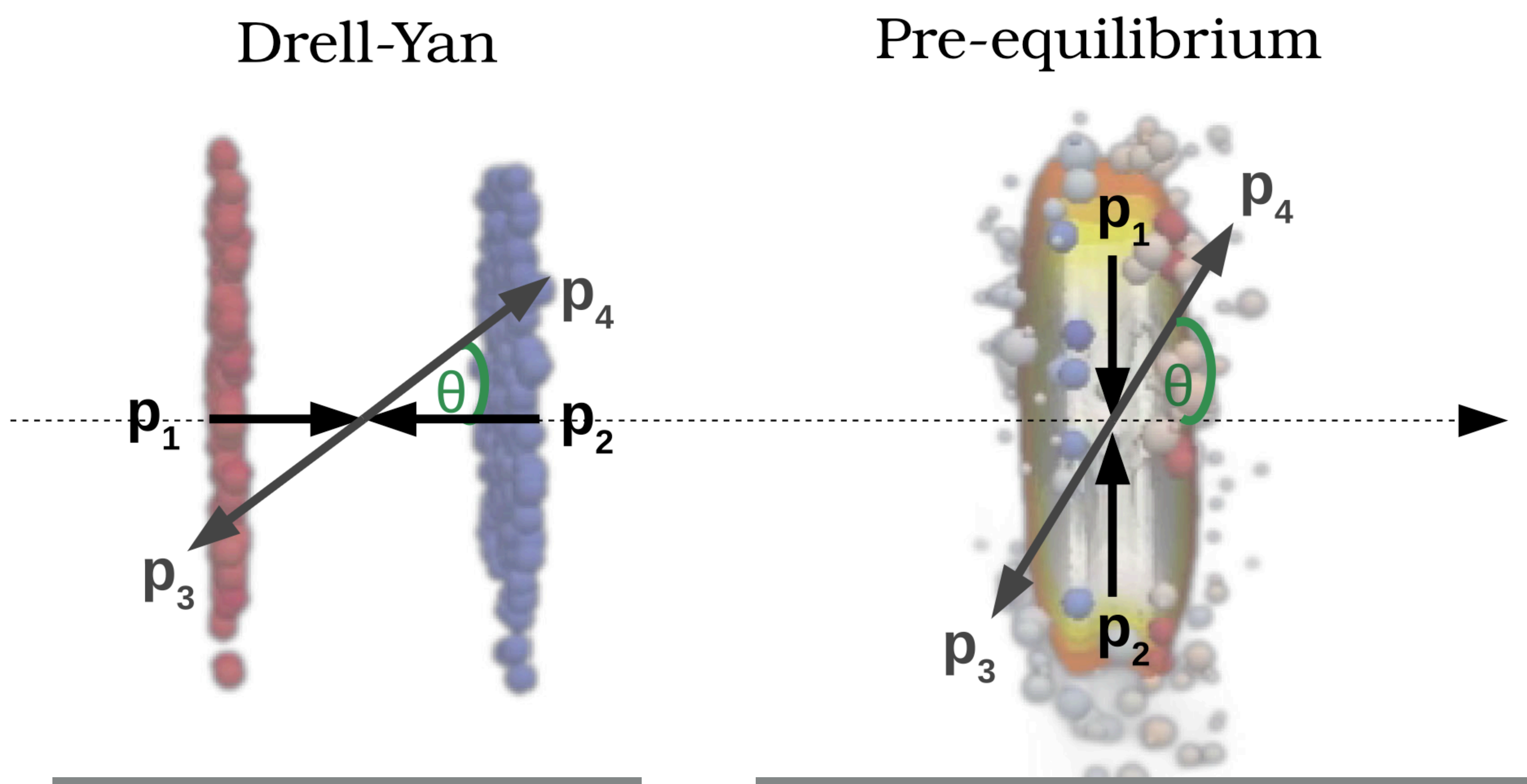

DY: peak at $\cos\theta = 0$

pre-eq. QGP: peak at $\cos\theta = \pm 1$

quadrupole moment

$$\left\langle \frac{3\cos^2\theta - 1}{2} \right\rangle$$

DY: positive

QGP: negative

total: DY+QGP

no initial quarks

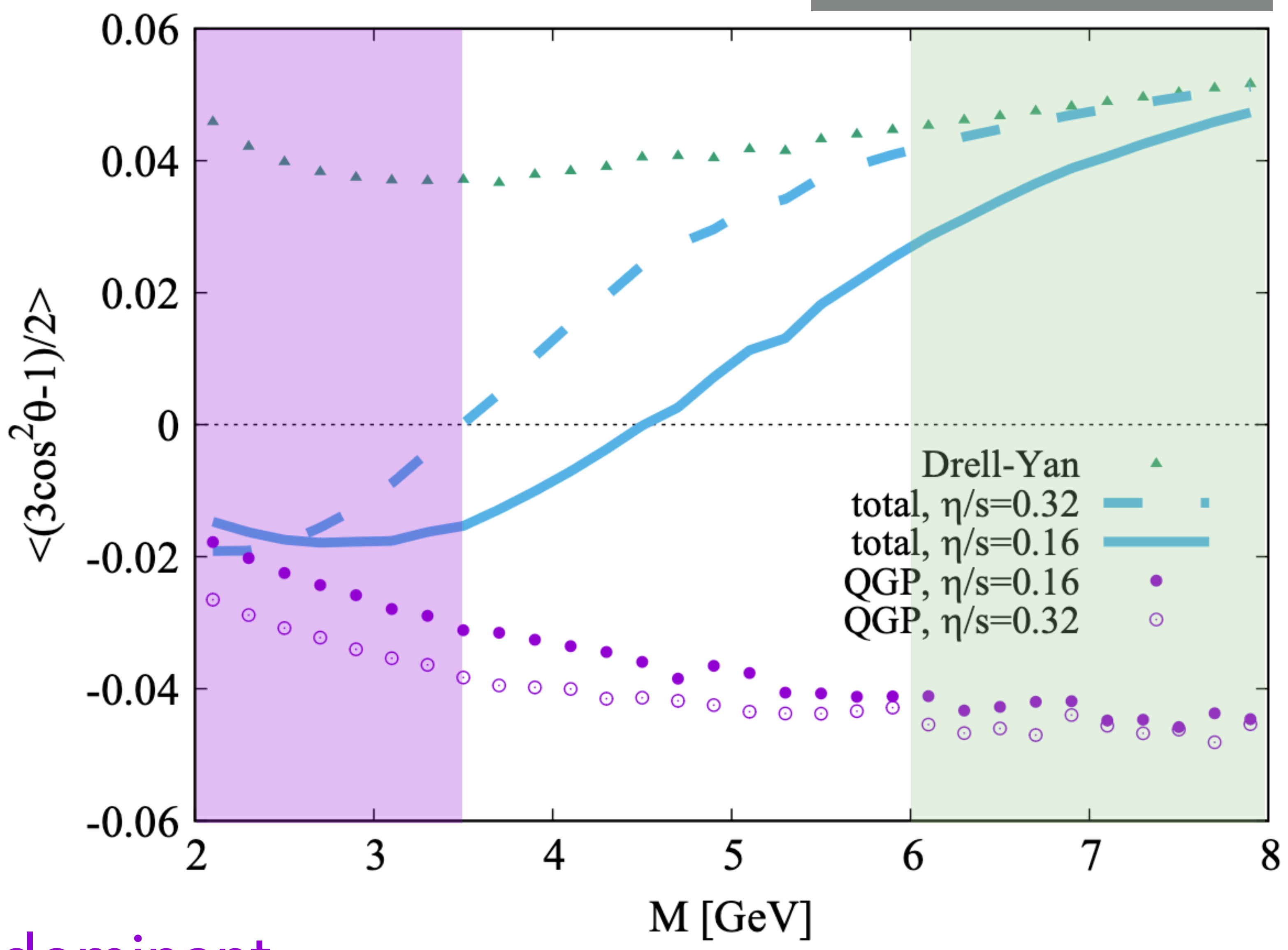

DY-dominant

QGP-dominant

quarks equilibrated throughout

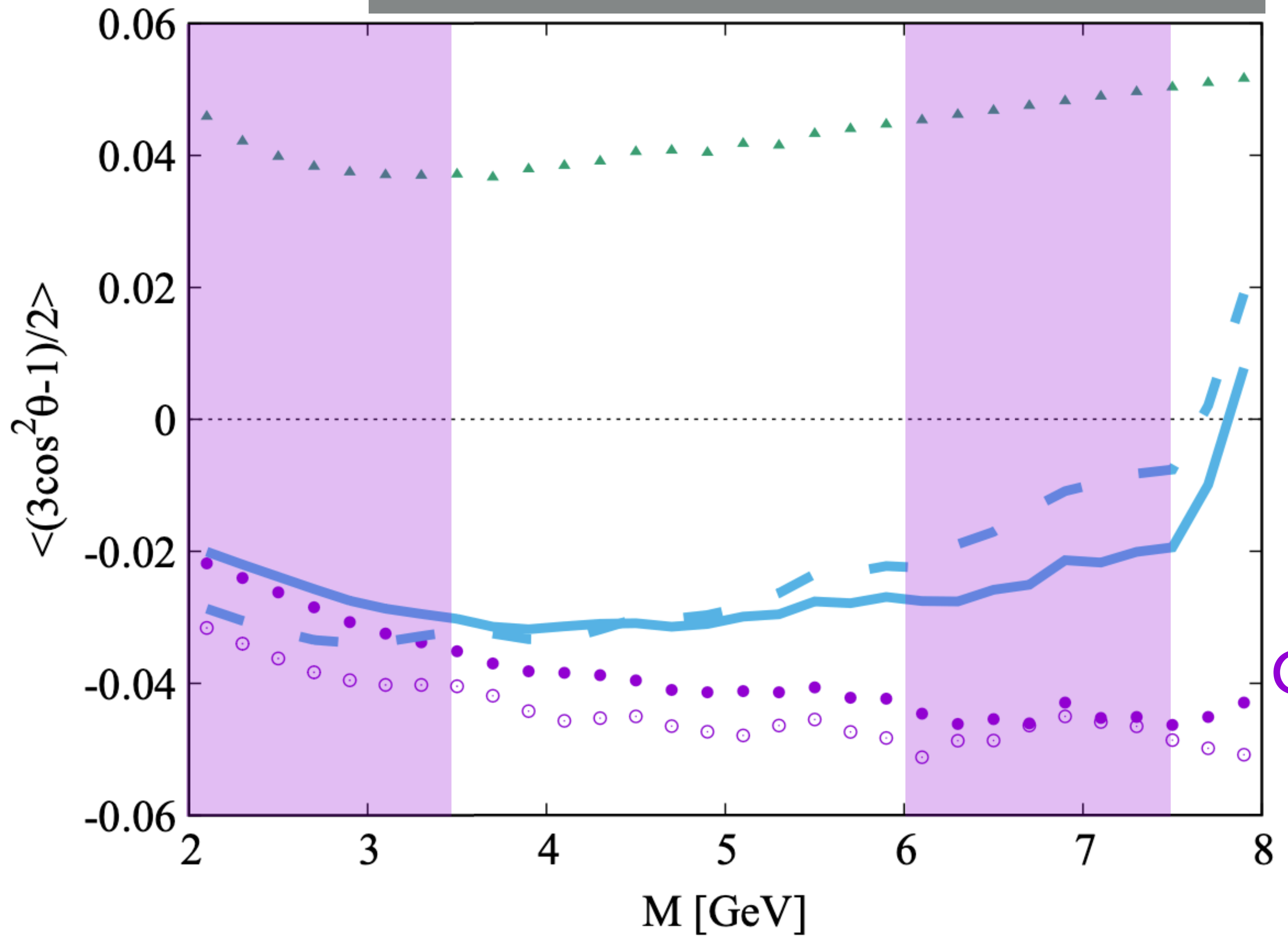

QGP-dominant

- Drell-Yan: quark momenta are mostly longitudinal; preferential emission of longitudinal leptons; negative quadrupole moment.
- Pre-eq. QGP: quark momenta are mostly transverse; preferential emission of transverse leptons; positive quadrupole moment.
- Total: at large values of M, the sign of the quadruple moment changes, depending on the dominance of the pre-eq. QGP emission, which further depends on the equilibration.

Coquet, Winn, X. Du, Ollitrault, Schlichting, PRL 132, 232301 (2024); see also: Seck, Friman, Galatyuk, van Hees, Speranza, Rapp, Wambach, 2309.03189

HYDRO STAGE

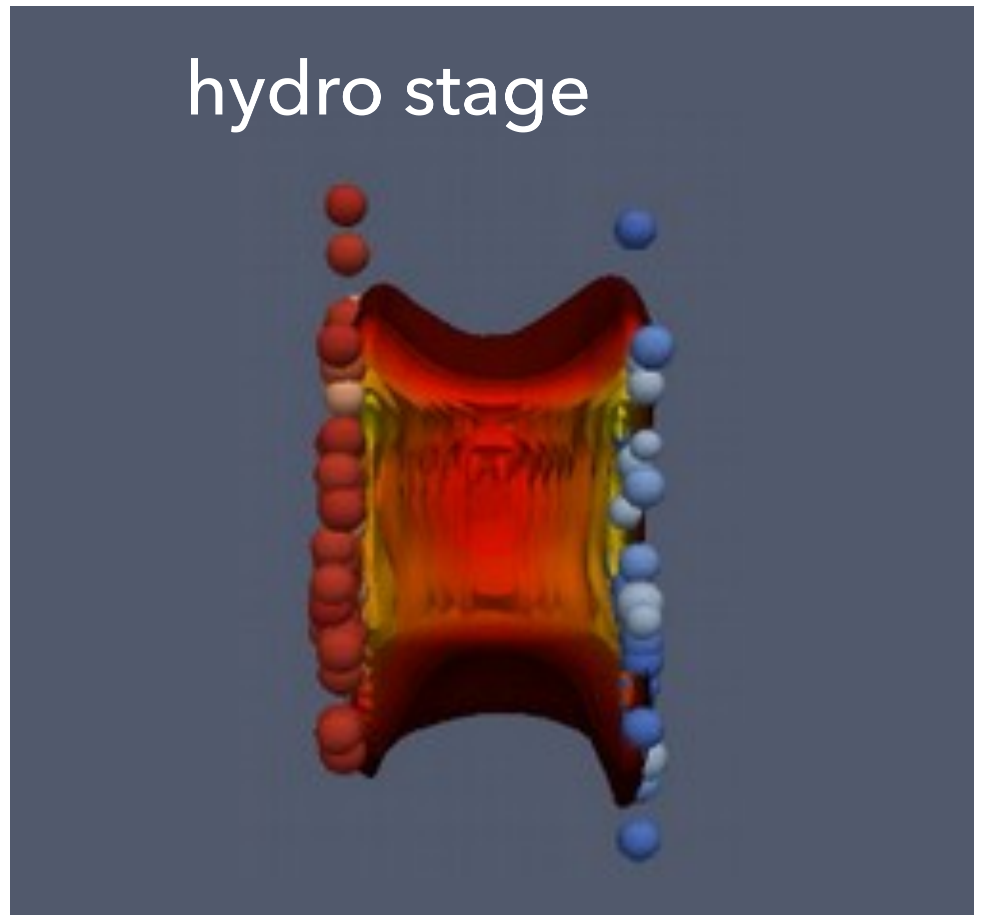

Thermal QGP dilepton production

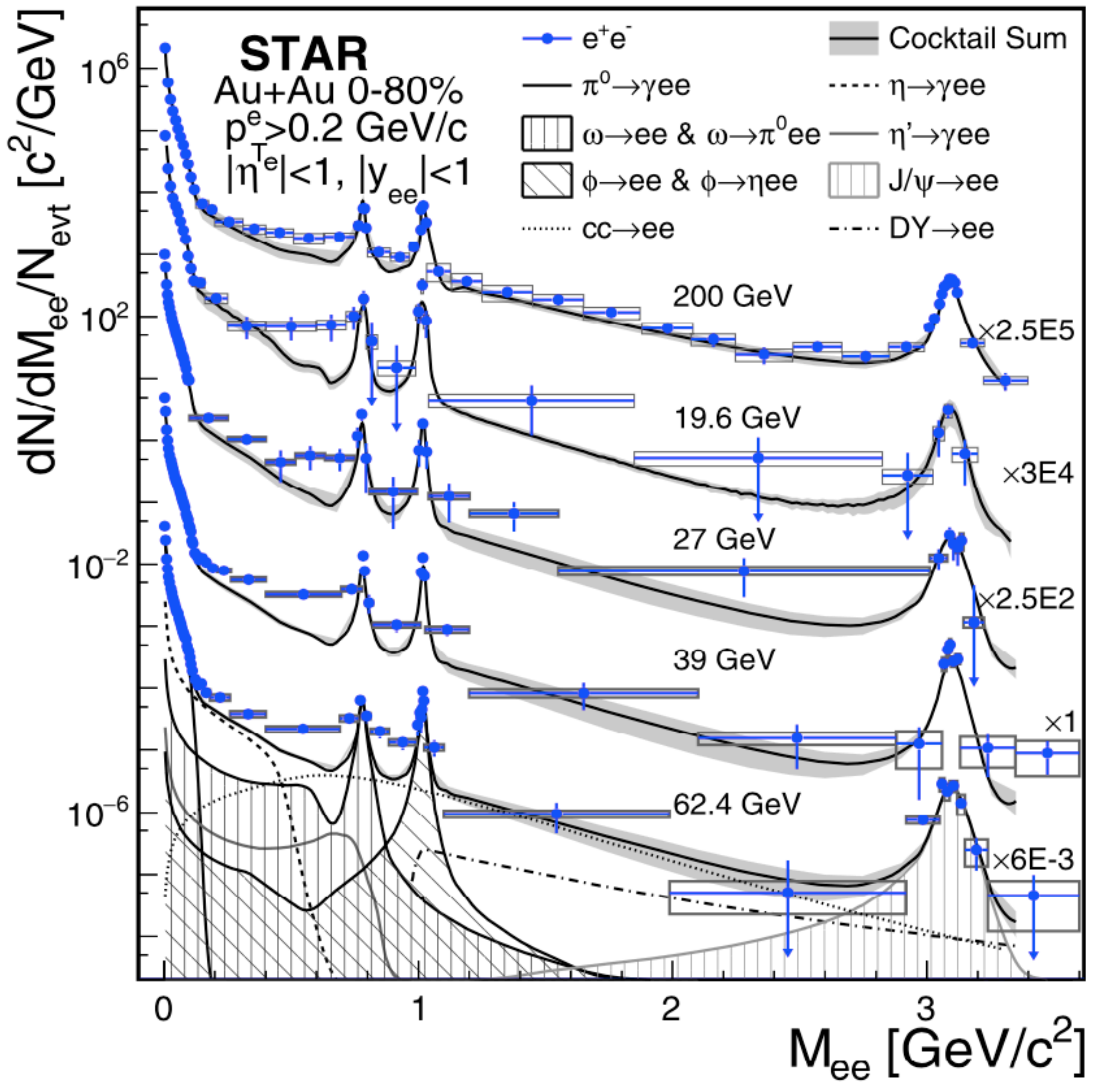

STAR, PRL113, 022301 (2014); PRC 92, 024912 (2015); PLB 750 (2015) 64–71; PRC 107, L061901 (2023); 2402.01998.

LD, Shen, Jeon, Gale, PRC 108 (2023) L041901; LD, Gao, Jeon, Gale, PRC 109, 014907 (2024); LD, Phys.Rev.C 110 (2024) 1, 014904

Thermal QGP dilepton production

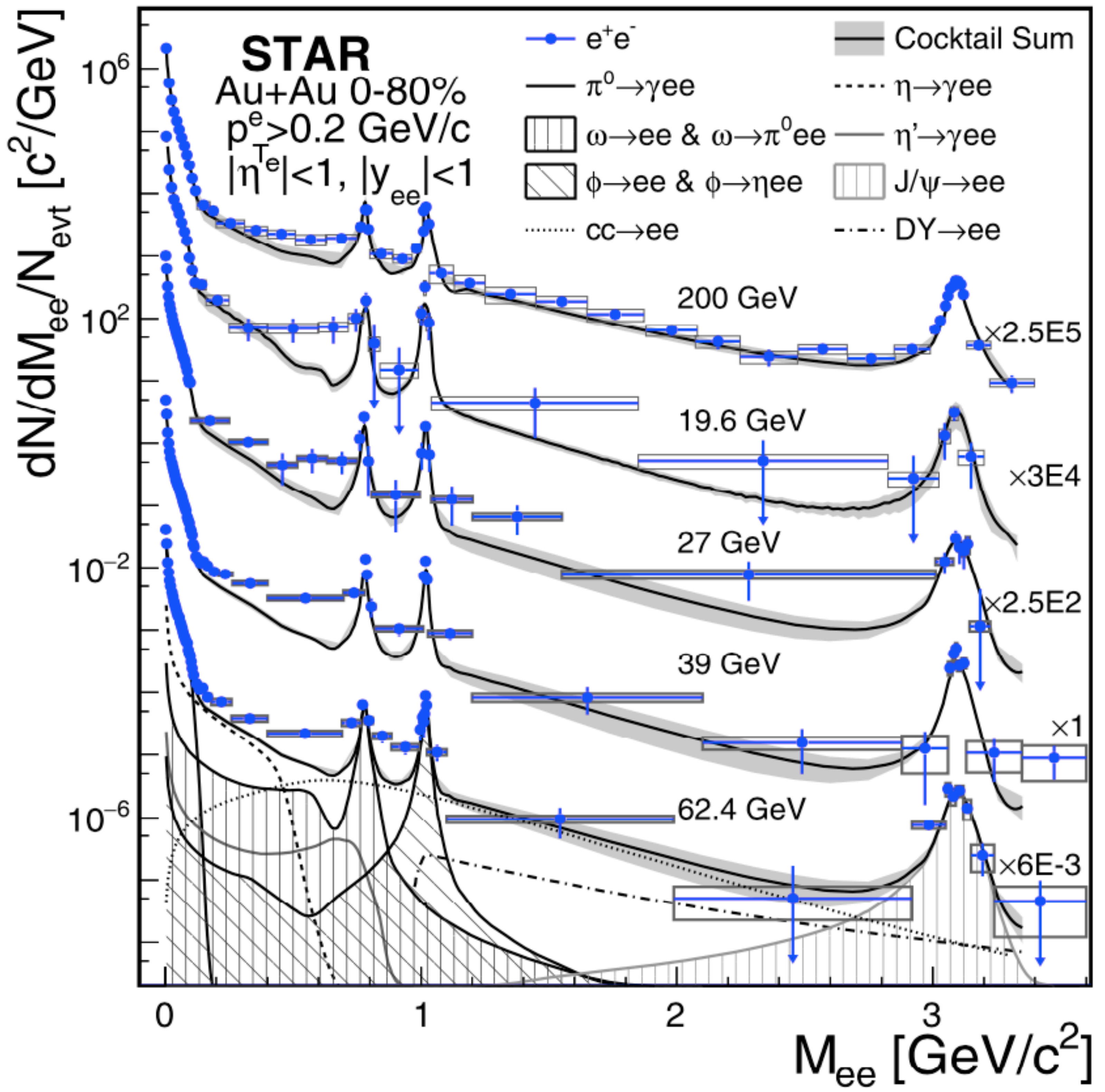

STAR, PRL113, 022301 (2014); PRC 92, 024912 (2015); PLB 750 (2015) 64–71; PRC 107, L061901 (2023); 2402.01998.

markers: excess = inclusive – cocktail

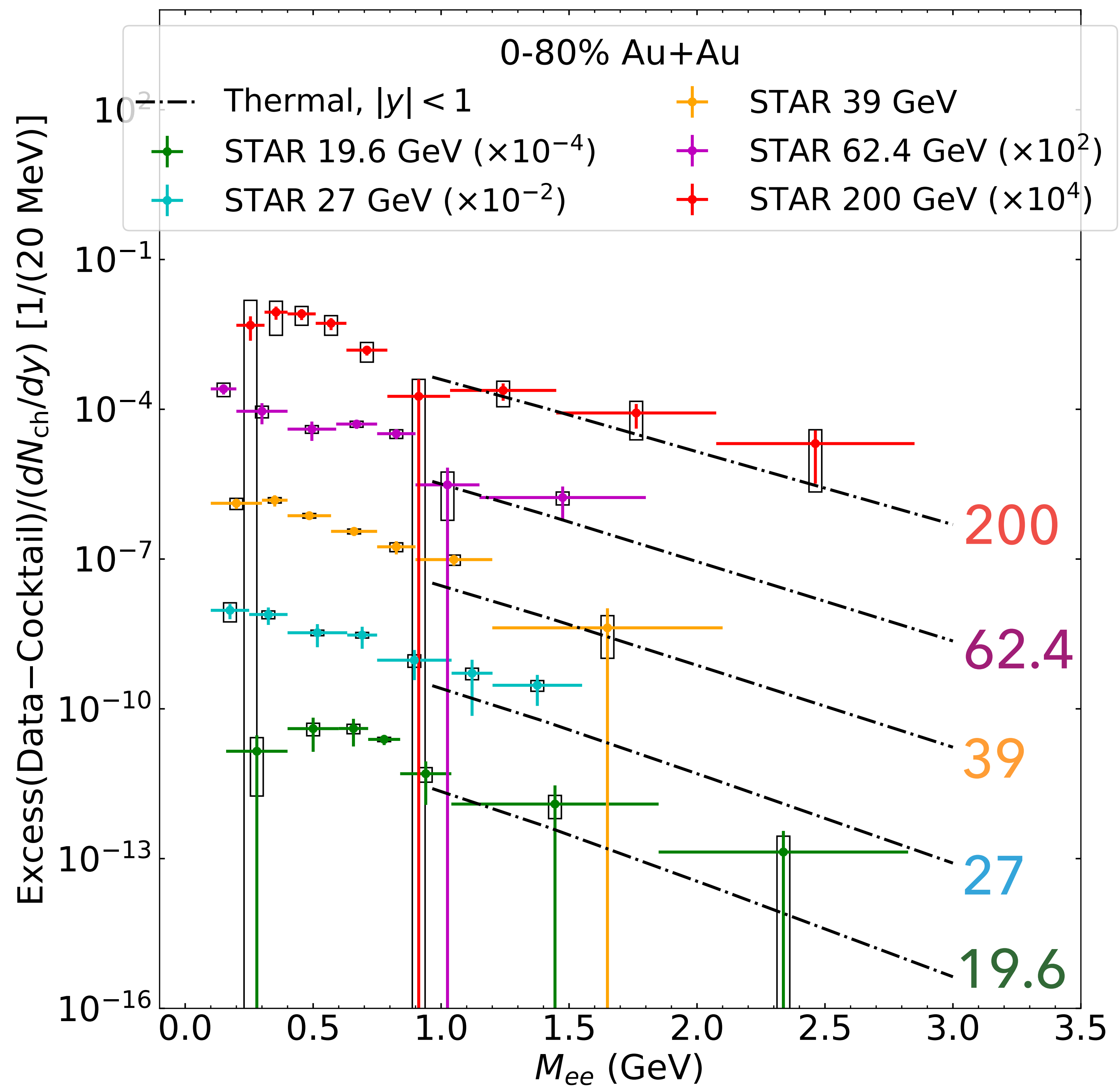

https://github.com/LipeiDu/DileptonEmission

Churchill, LD, Gale, Jackson, Jeon, PRC 109, 044915 (2024), PRL 132, 172301 (2024)

- First estimate of NLO dilepton emission at nonzero μ_B with (3+1)D multistage hydrodynamic model;
- The multistage model is calibrated using rapidity-dependent hadronic observables from the Beam Energy Scan.

LD, Shen, Jeon, Gale, PRC 108 (2023) L041901; LD, Gao, Jeon, Gale, PRC 109, 014907 (2024); LD, Phys.Rev.C 110 (2024) 1, 014904

QCD thermometer: experiments

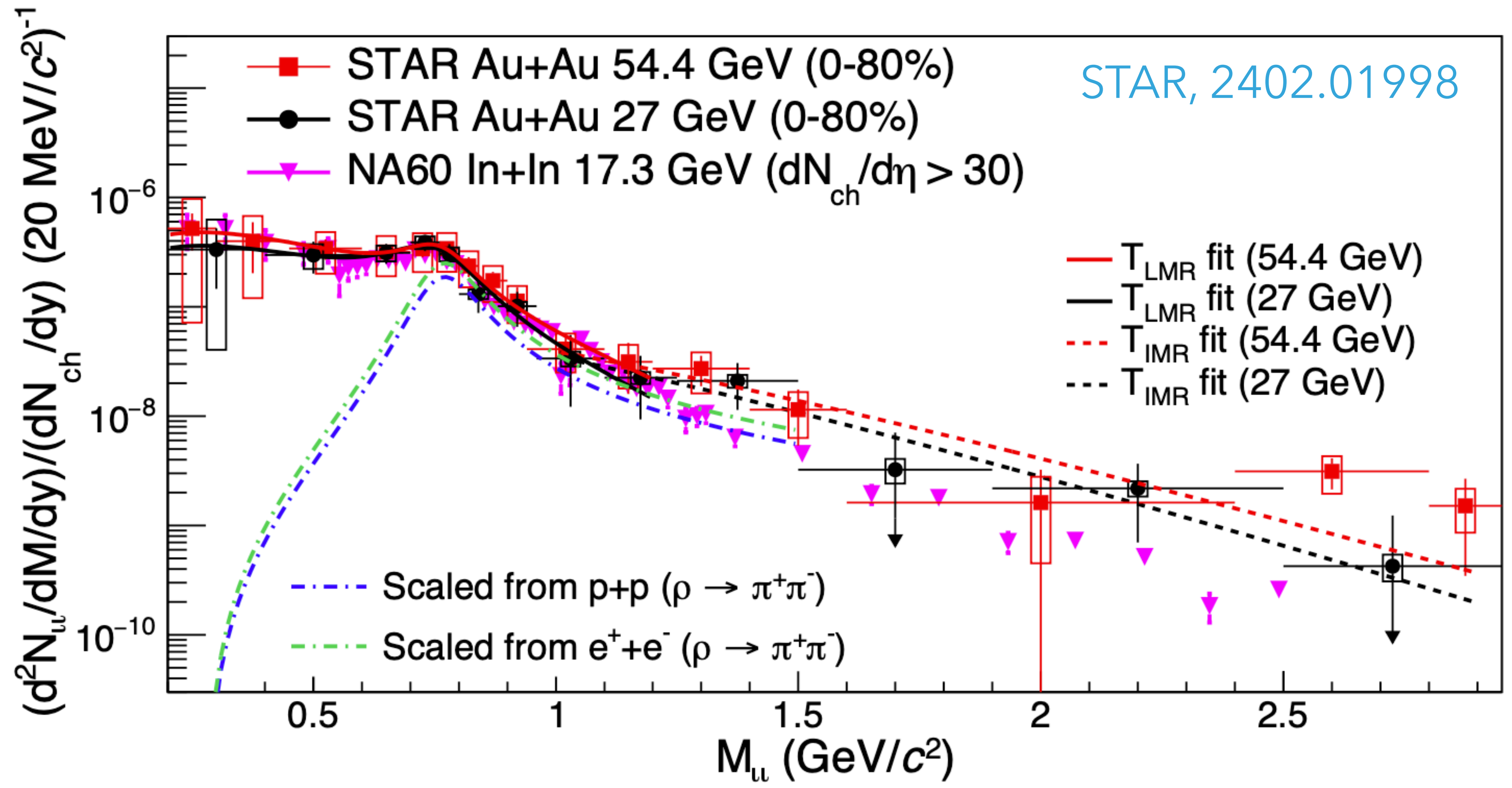

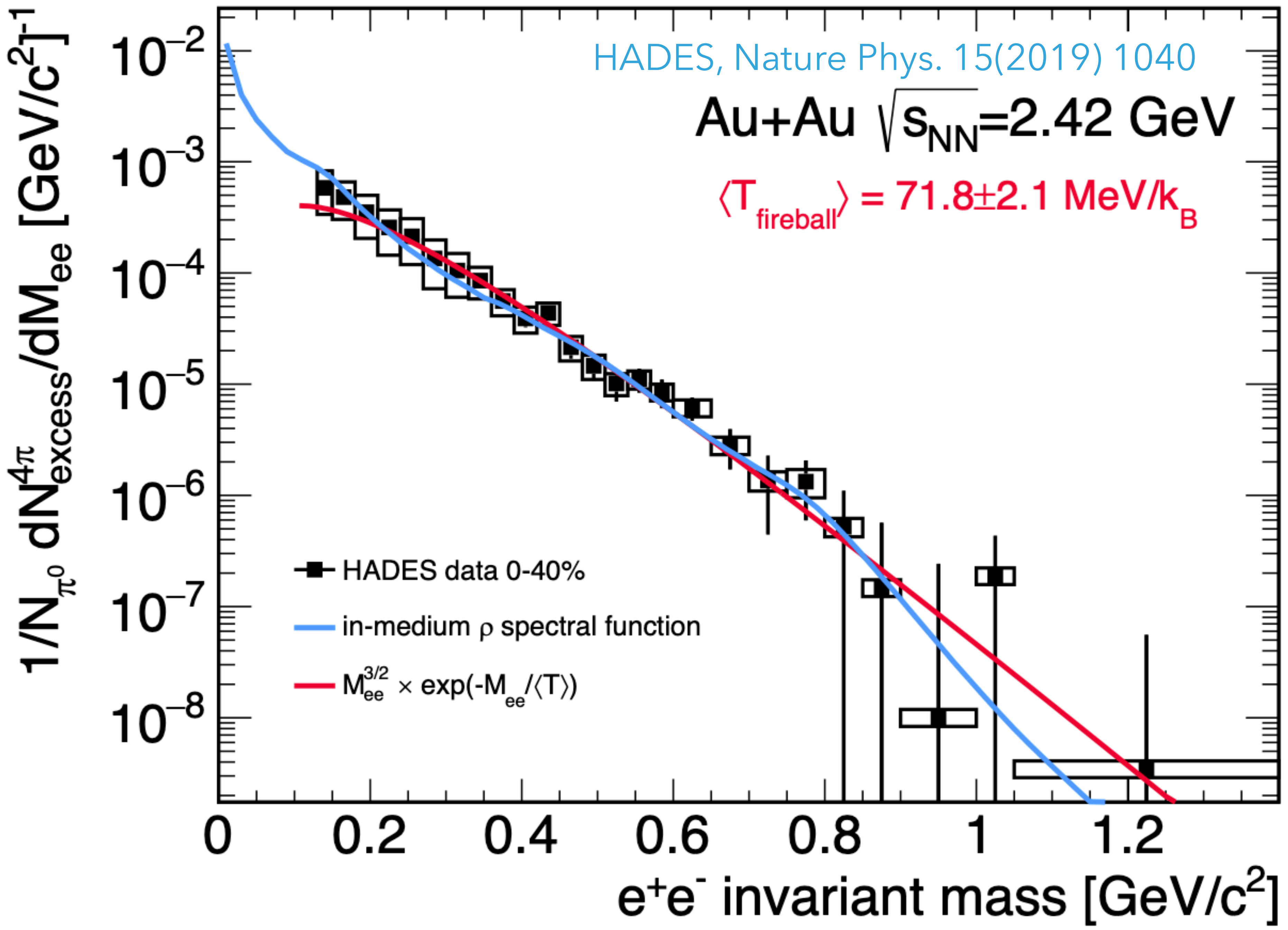

NA60, PRL 100, 022302 (2008); EPJC 59 607-623 (2009). STAR, 2402.01998. HADES, Nat. Phys.,1040–1045 (2019). Rapp and van Hees, PLB 753, 586 (2016)

QCD thermometer: experiments

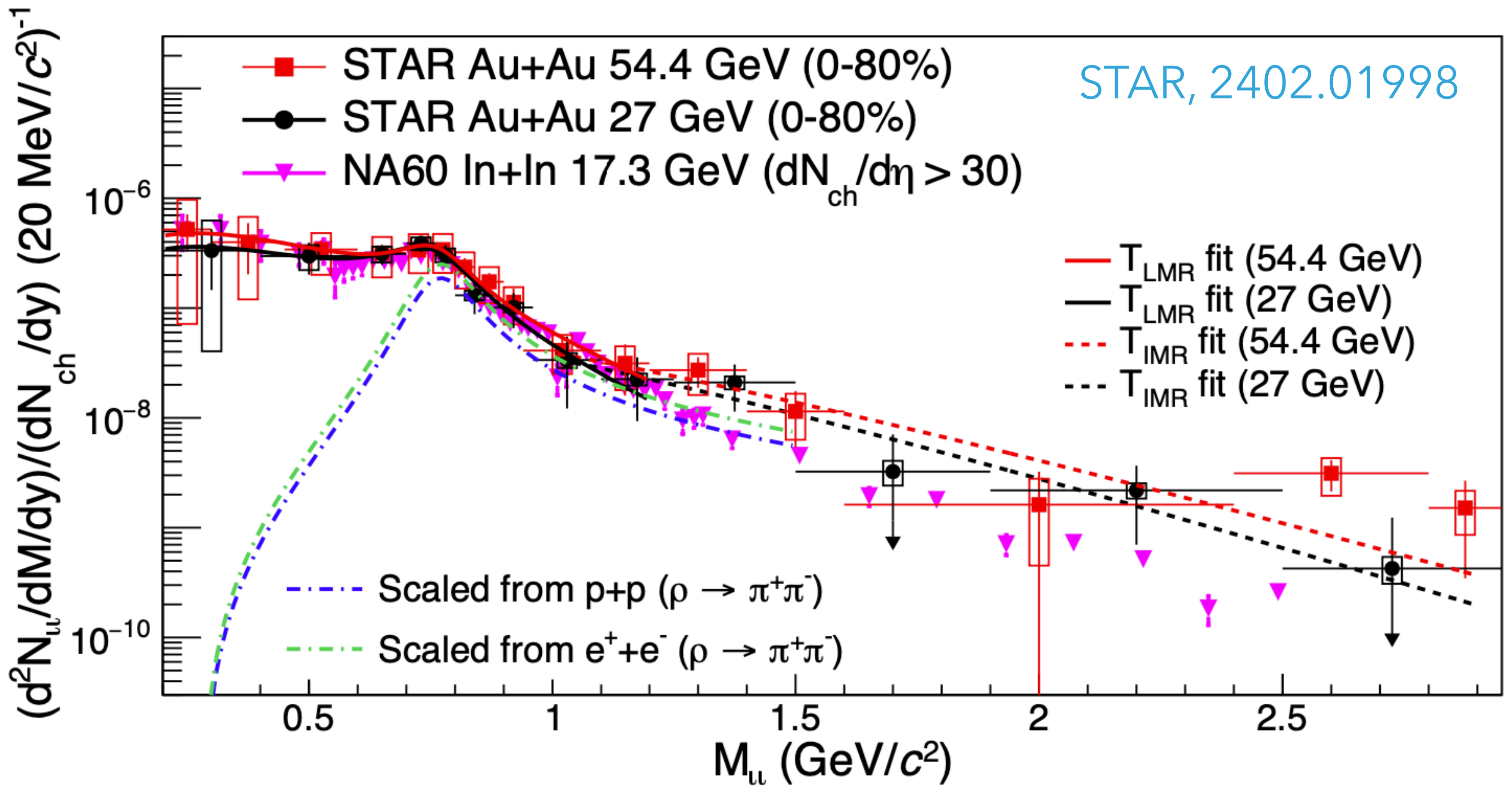

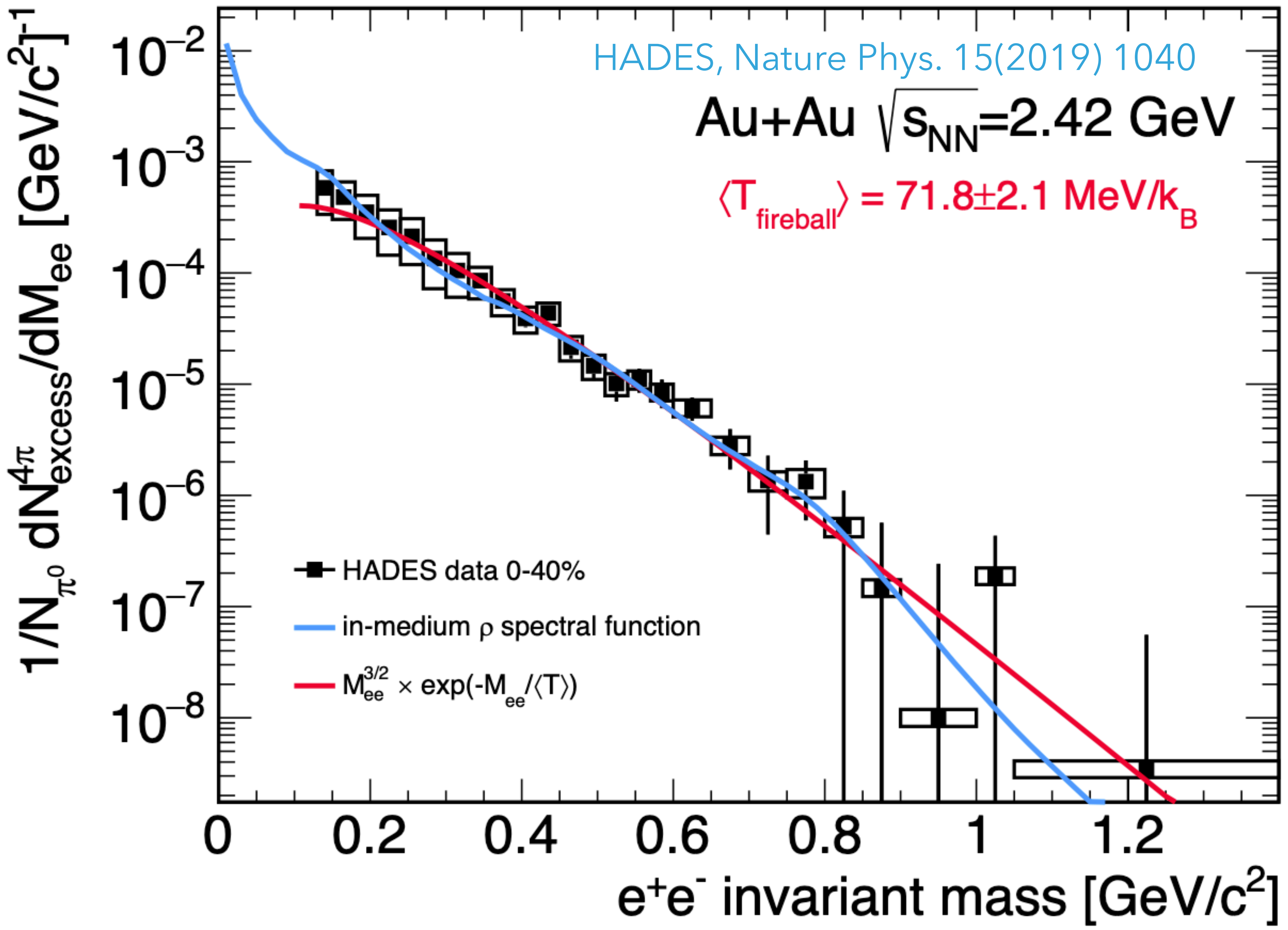

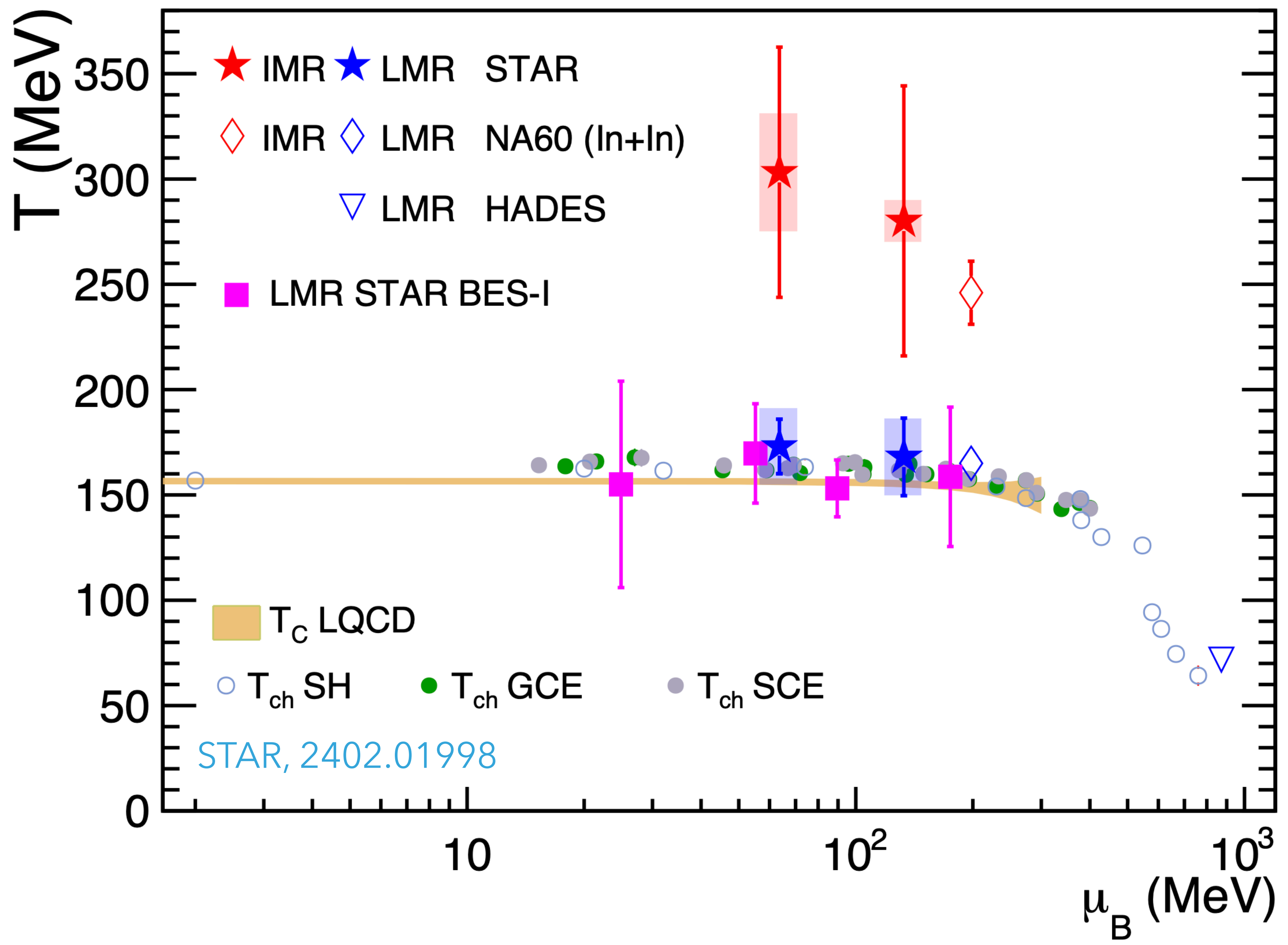

NA60, PRL 100, 022302 (2008); EPJC 59 607-623 (2009). STAR, 2402.01998. HADES, Nat. Phys.,1040–1045 (2019). Rapp and van Hees, PLB 753, 586 (2016)

QCD thermometer: experiments

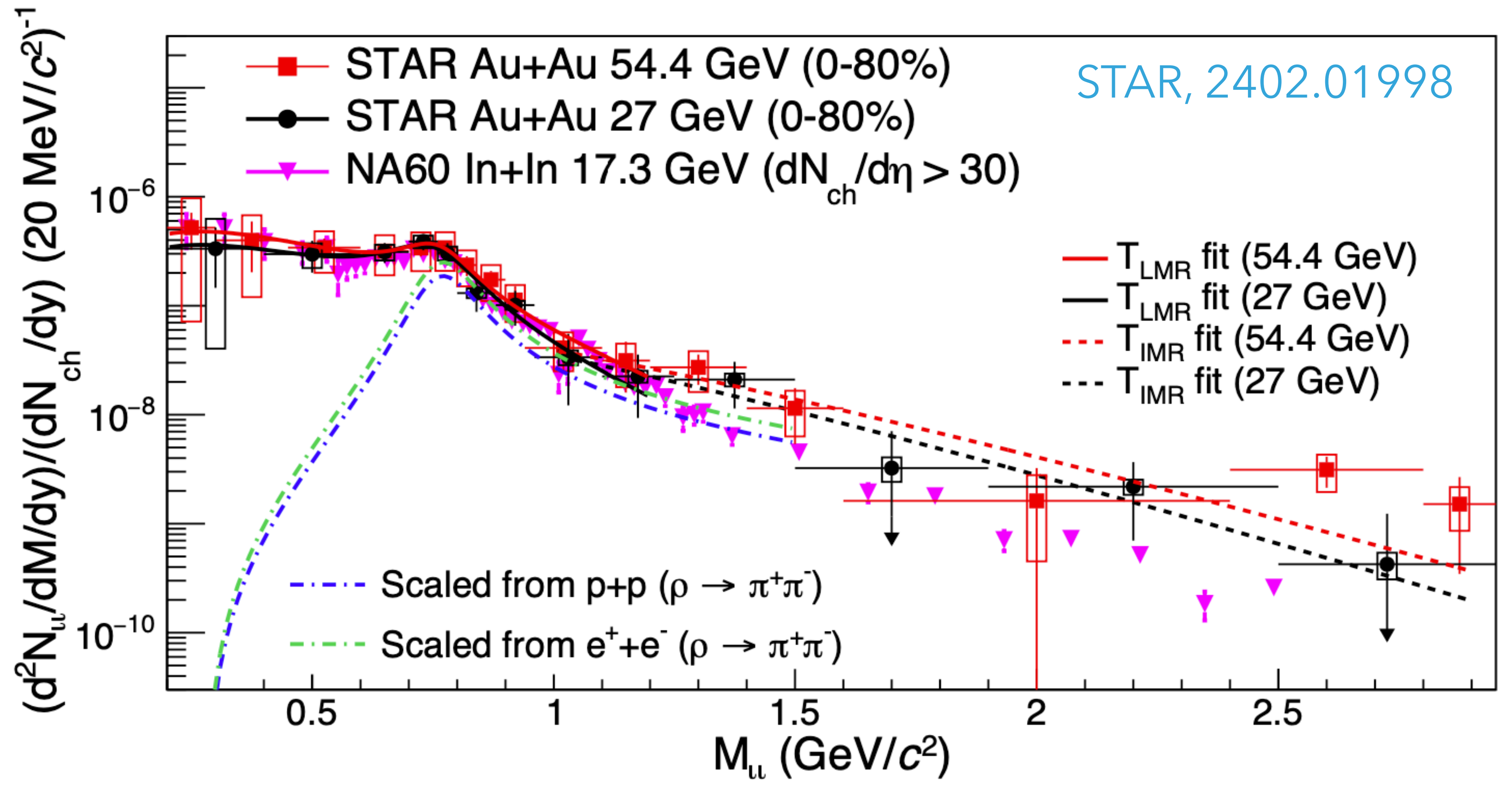

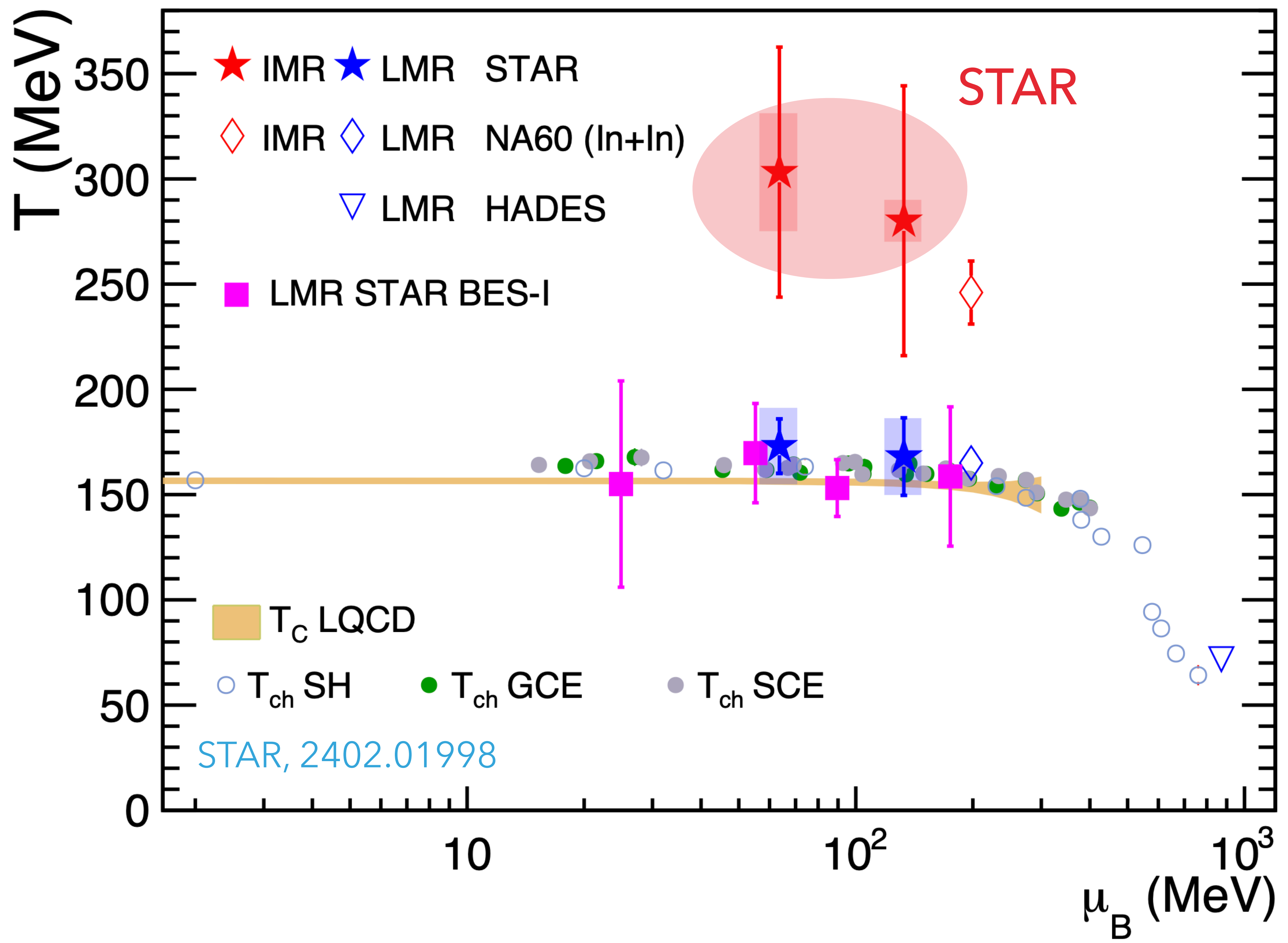

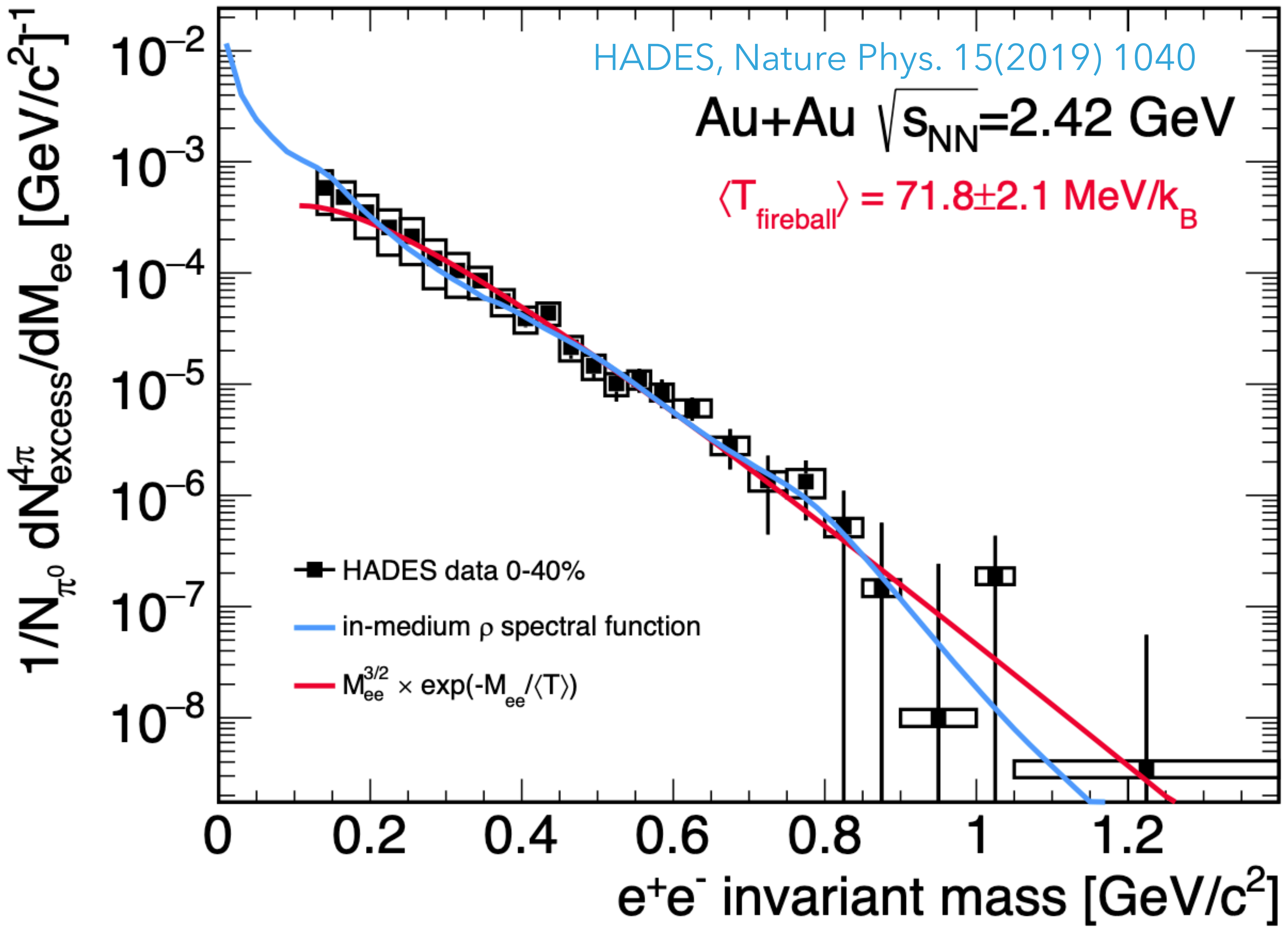

NA60, PRL 100, 022302 (2008); EPJC 59 607-623 (2009). STAR, 2402.01998. HADES, Nat. Phys.,1040–1045 (2019). Rapp and van Hees, PLB 753, 586 (2016)

QCD thermometer: experiments

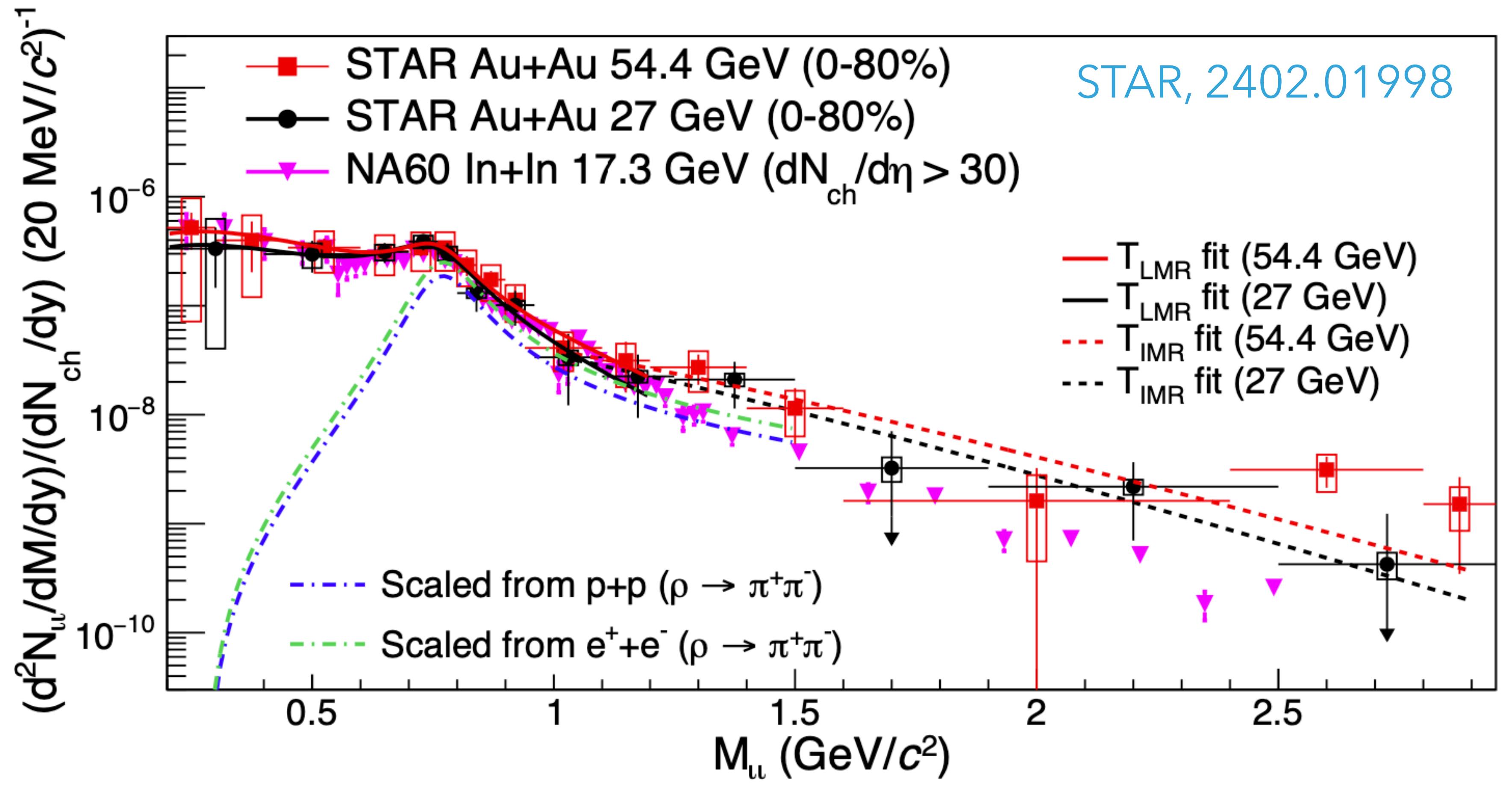

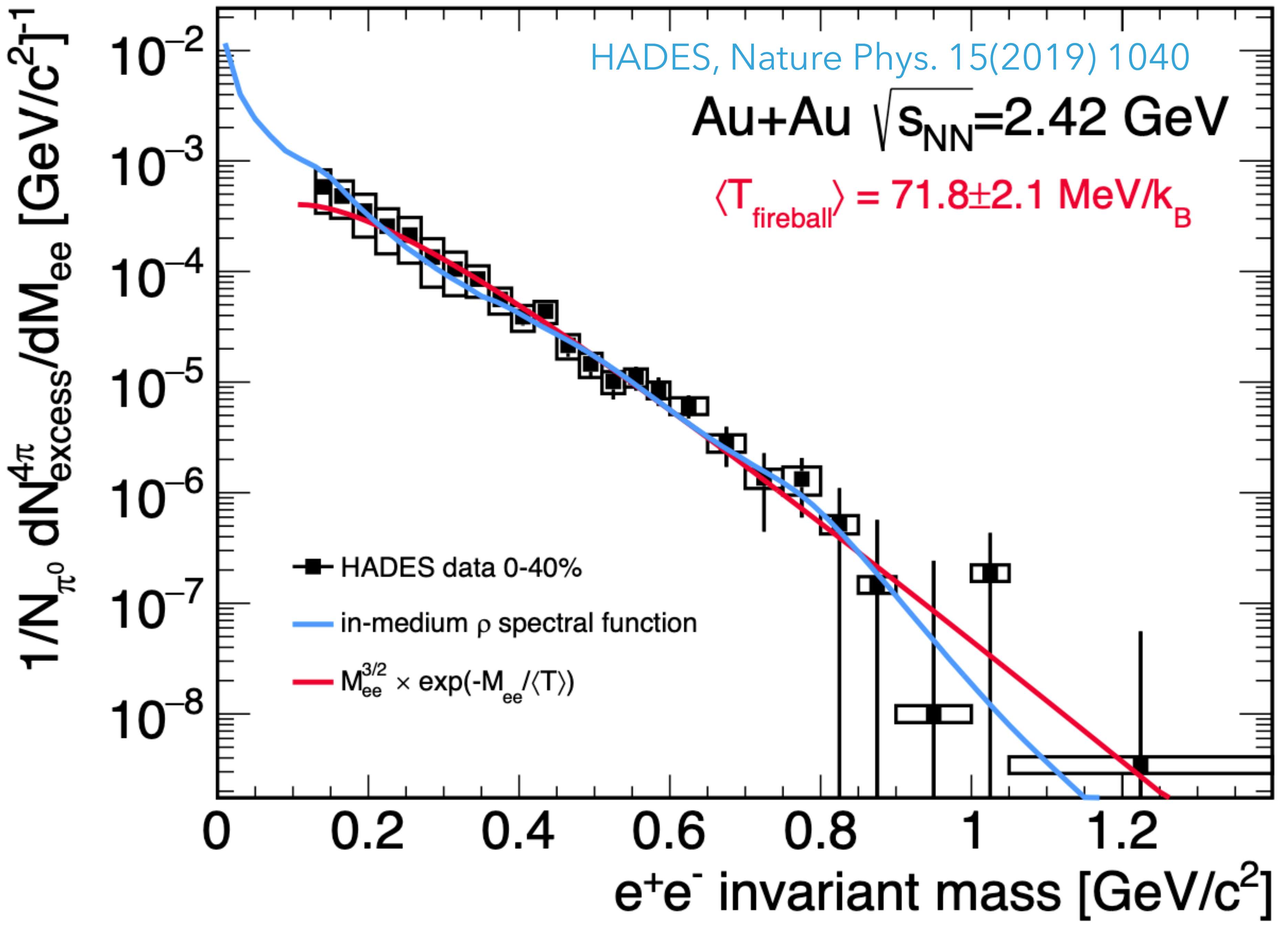

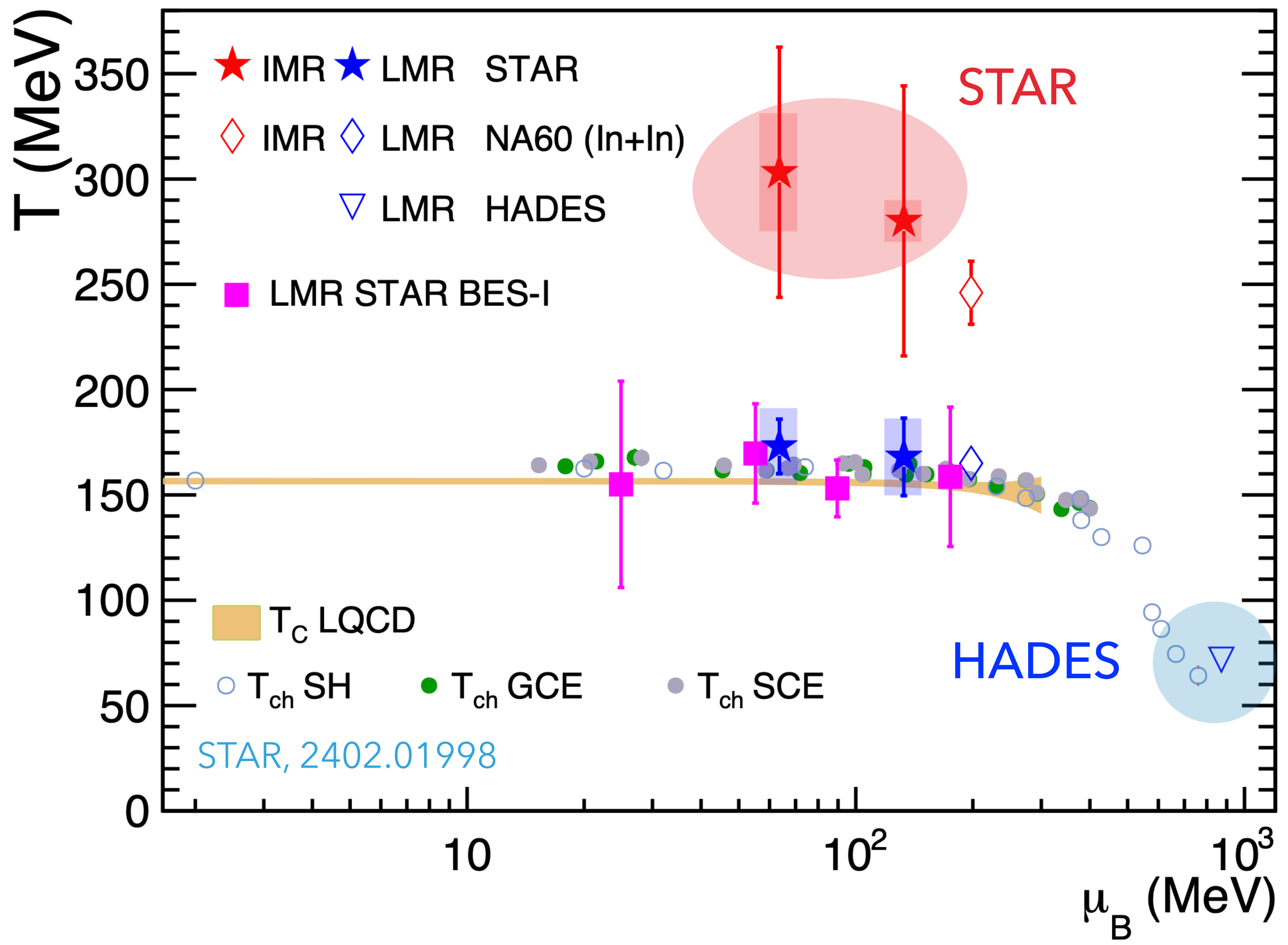

NA60, PRL 100, 022302 (2008); EPJC 59 607-623 (2009). STAR, 2402.01998. HADES, Nat. Phys.,1040–1045 (2019). Rapp and van Hees, PLB 753, 586 (2016)

QCD thermometer: experiments

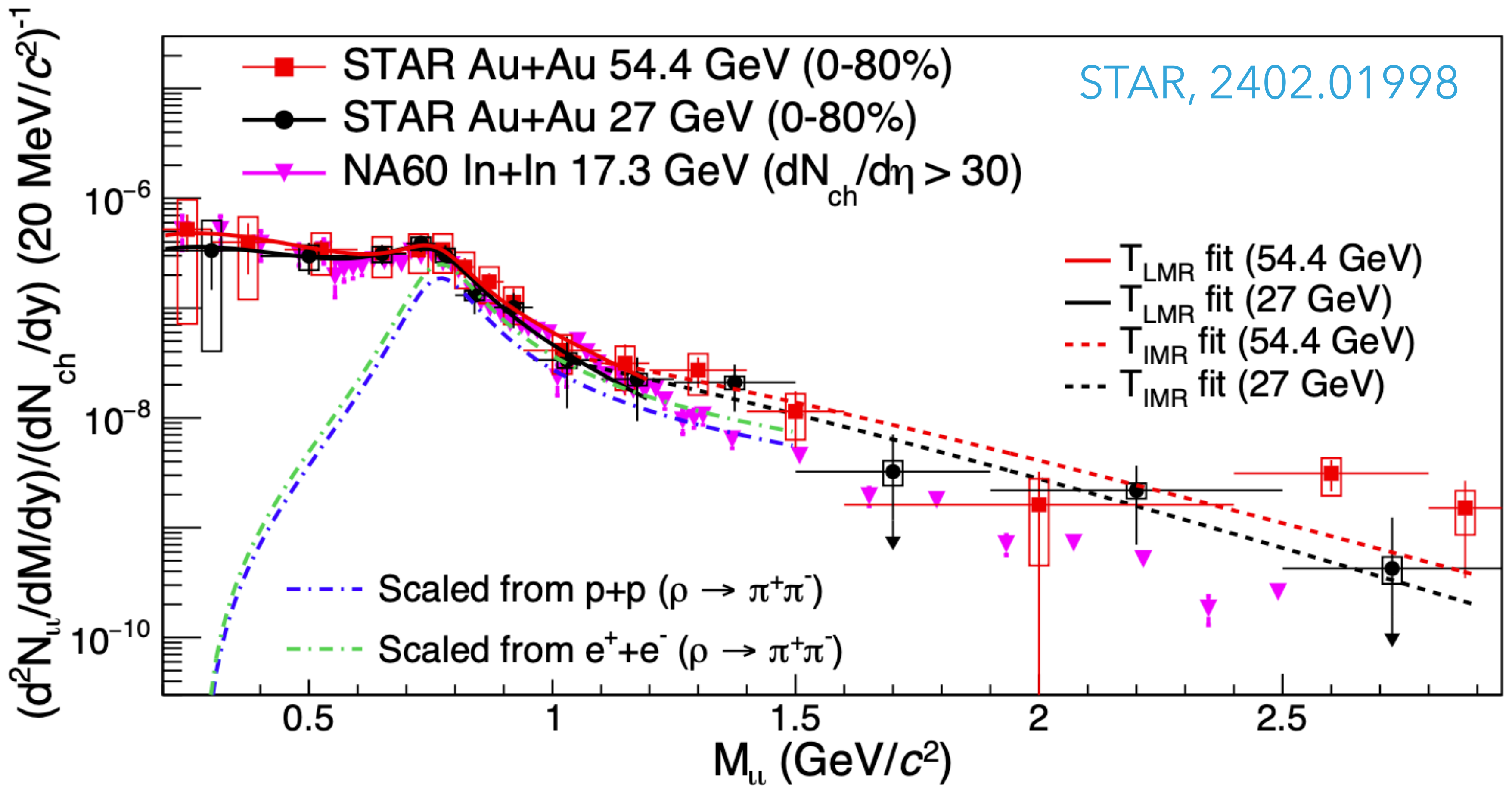

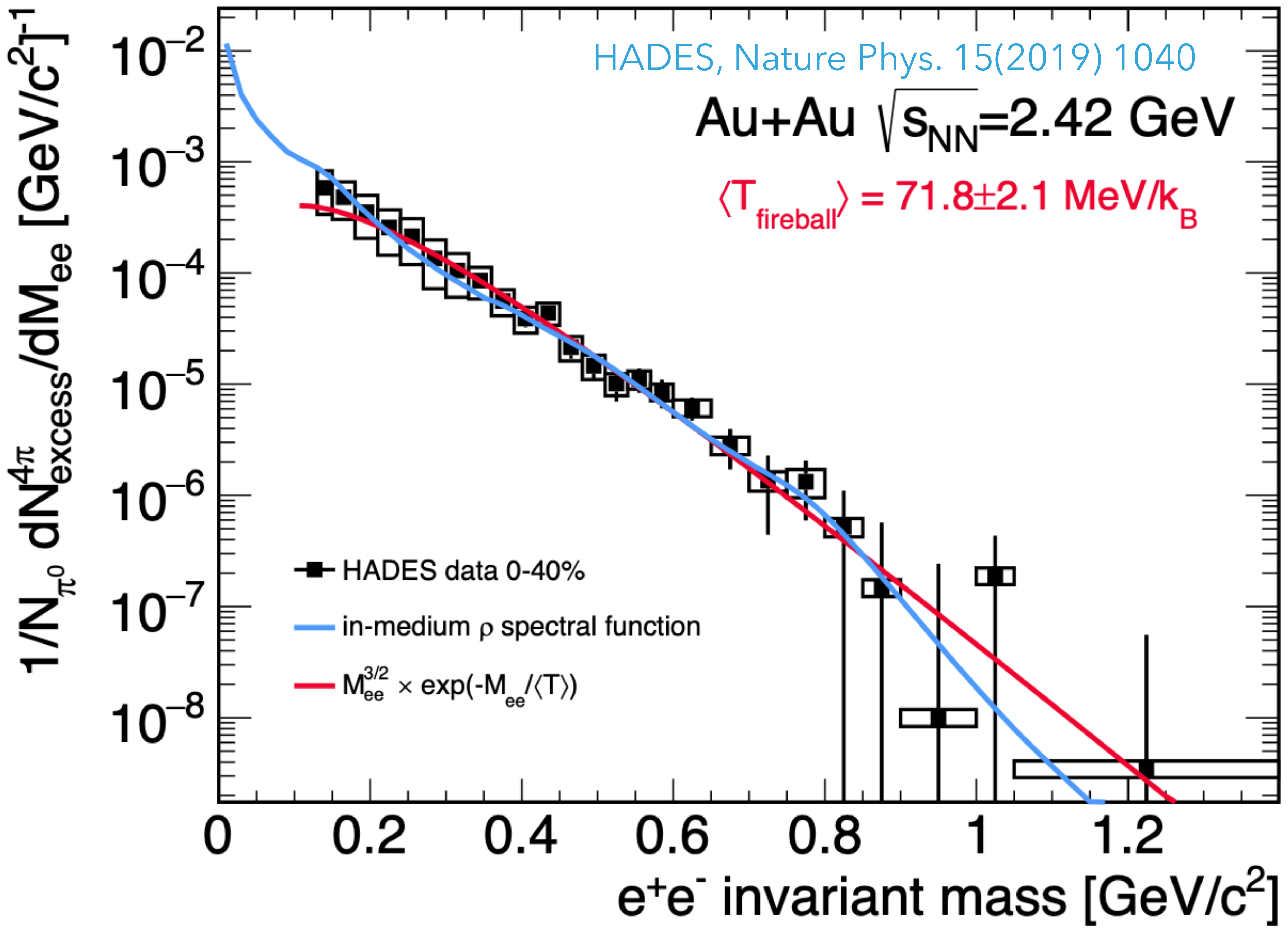

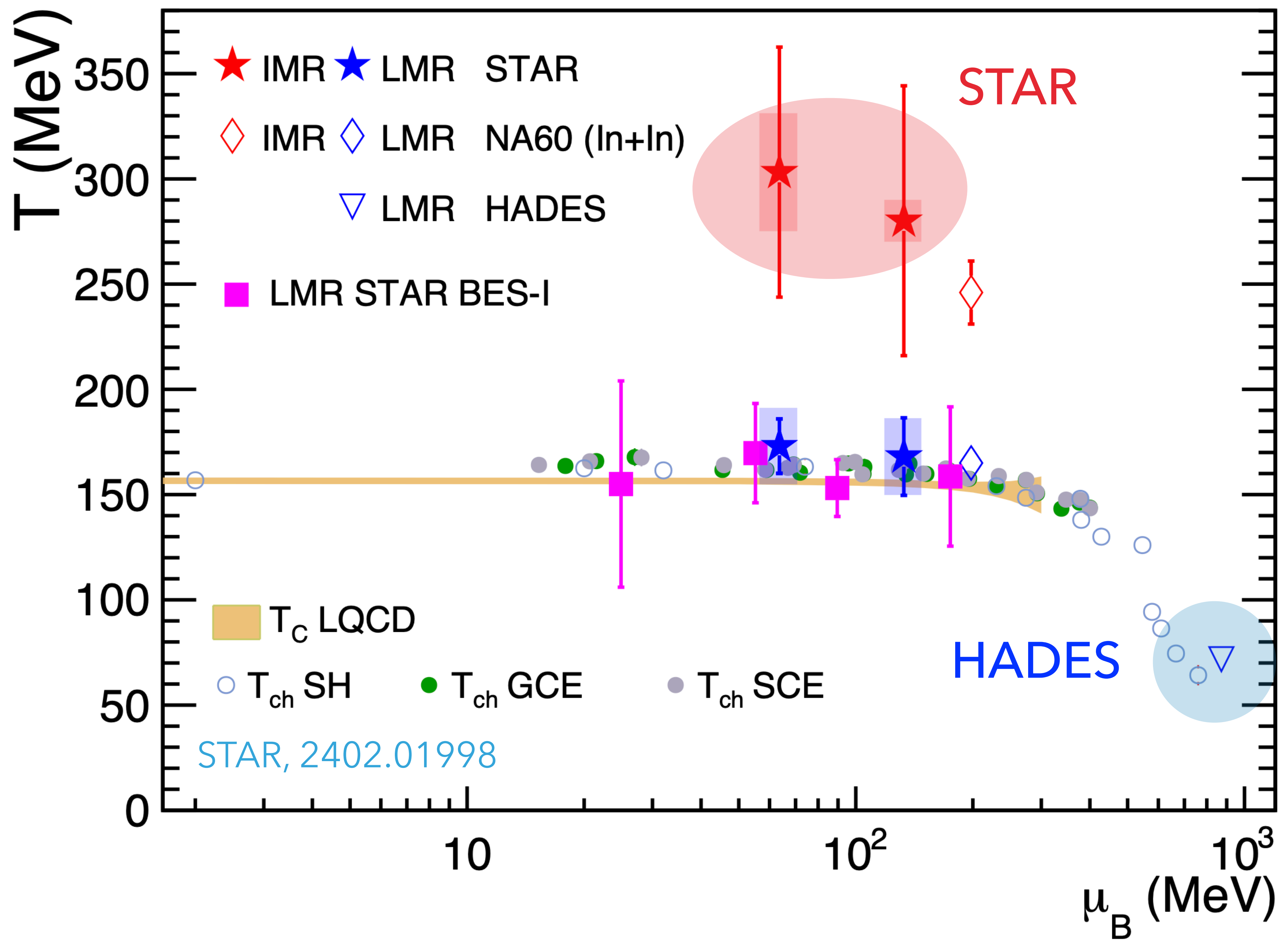

Questions:

NA60, PRL 100, 022302 (2008); EPJC 59 607-623 (2009). STAR, 2402.01998. HADES, Nat. Phys.,1040–1045 (2019). Rapp and van Hees, PLB 753, 586 (2016)

QCD thermometer: experiments

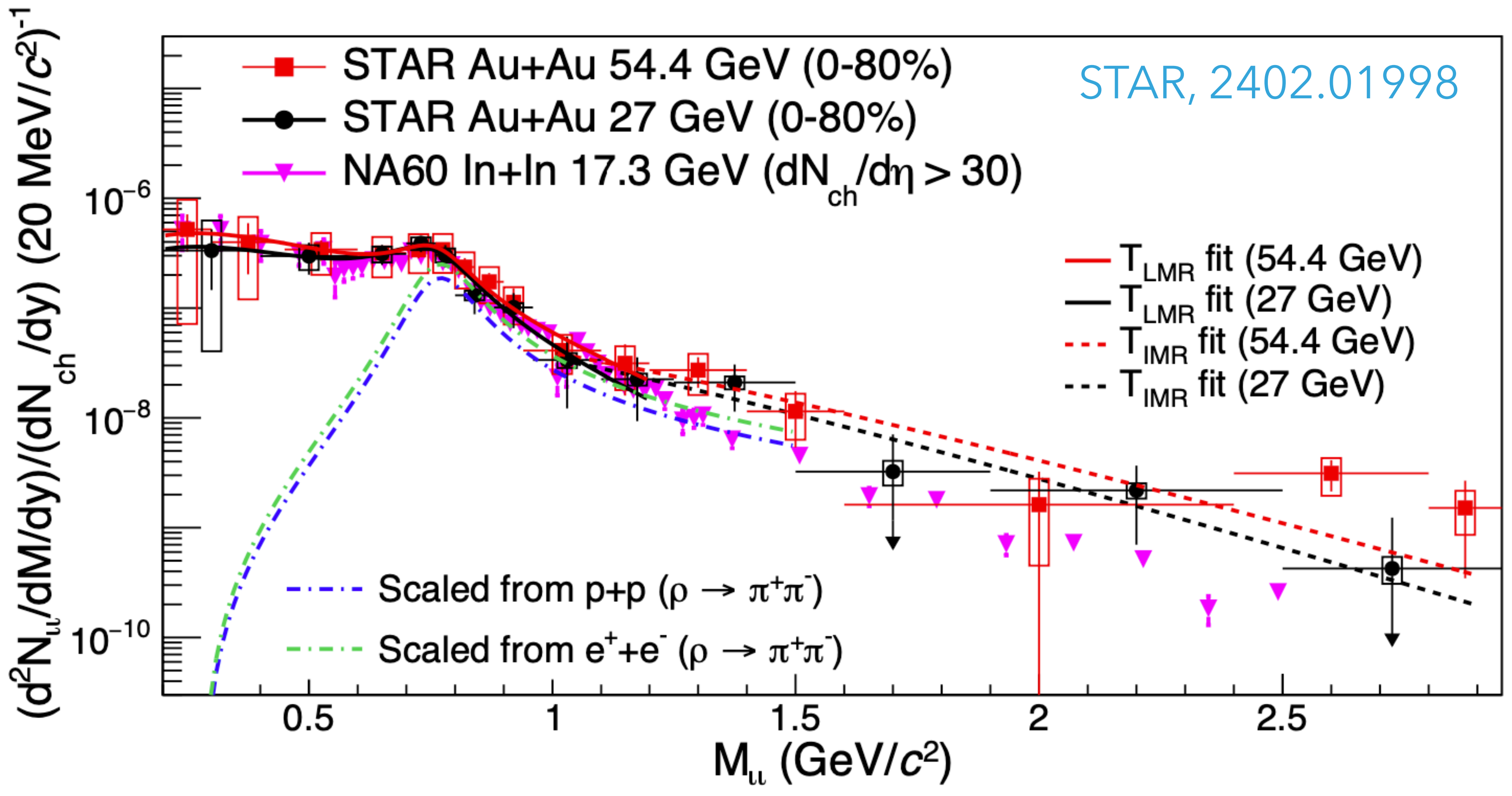

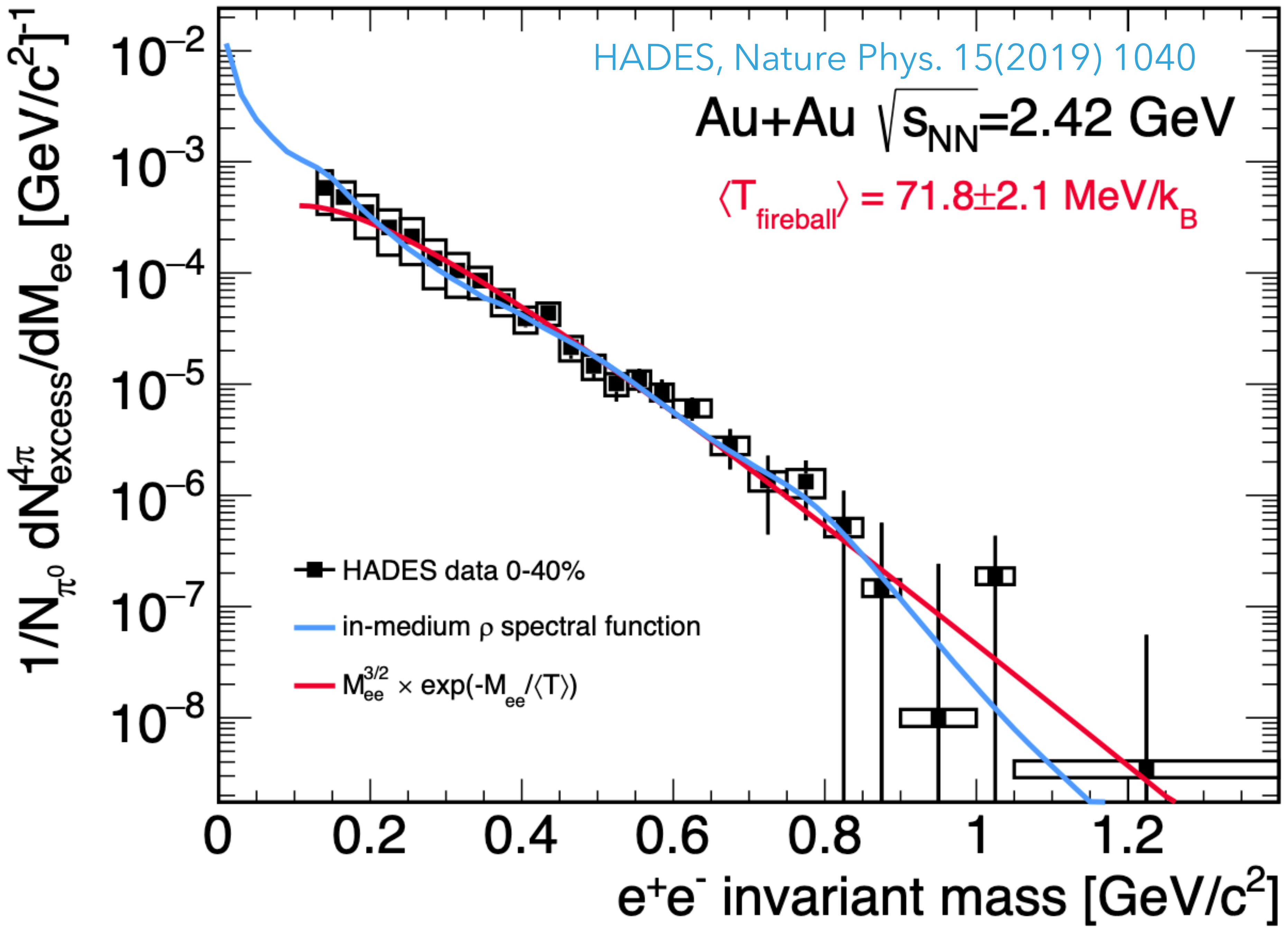

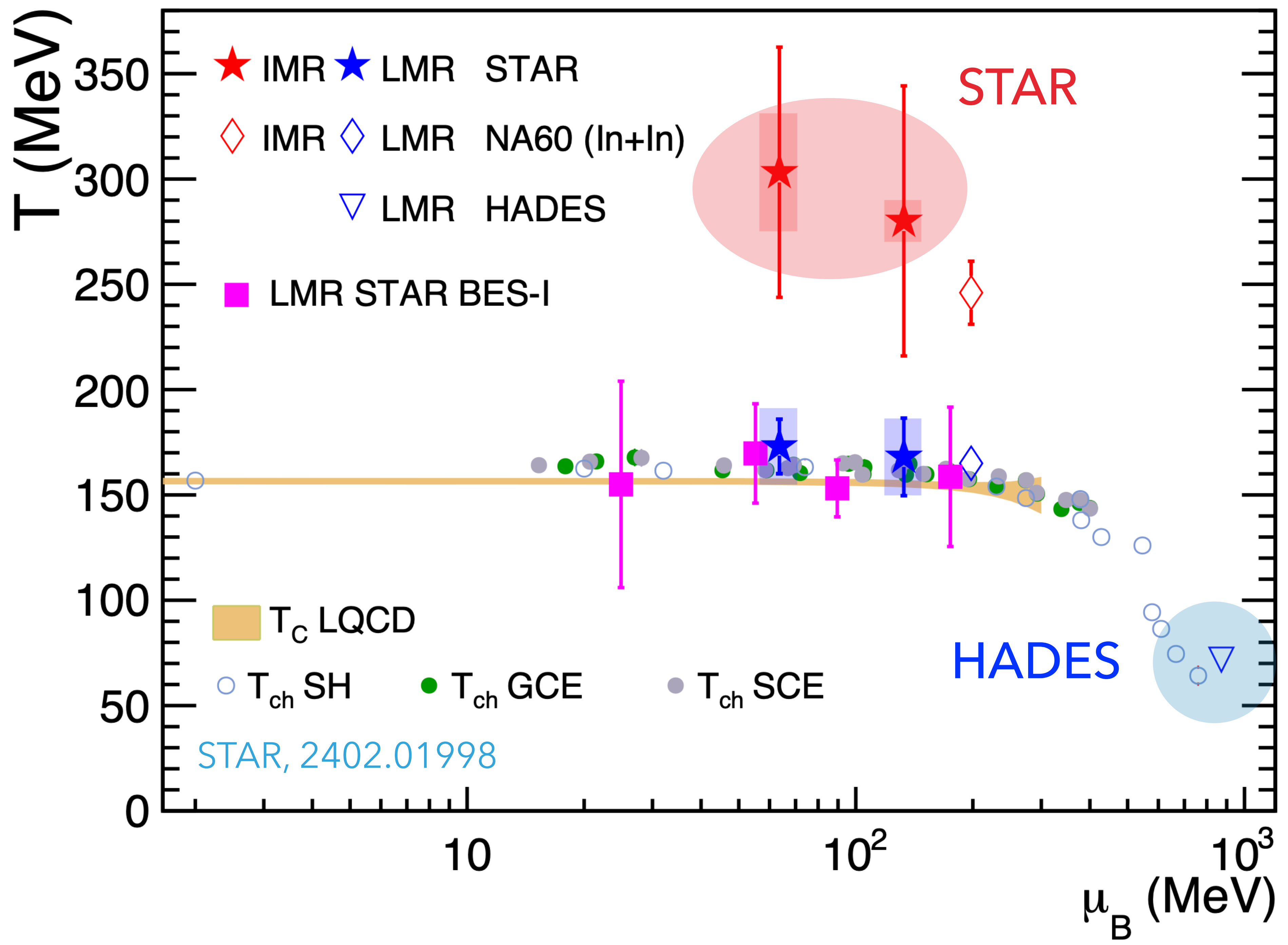

Questions:

- How do we know if the fitting method using $\frac{dN}{dM} \propto (MT)^{3/2} e^{-M/T}$ works?

NA60, PRL 100, 022302 (2008); EPJC 59 607-623 (2009). STAR, 2402.01998. HADES, Nat. Phys.,1040–1045 (2019). Rapp and van Hees, PLB 753, 586 (2016)

QCD thermometer: experiments

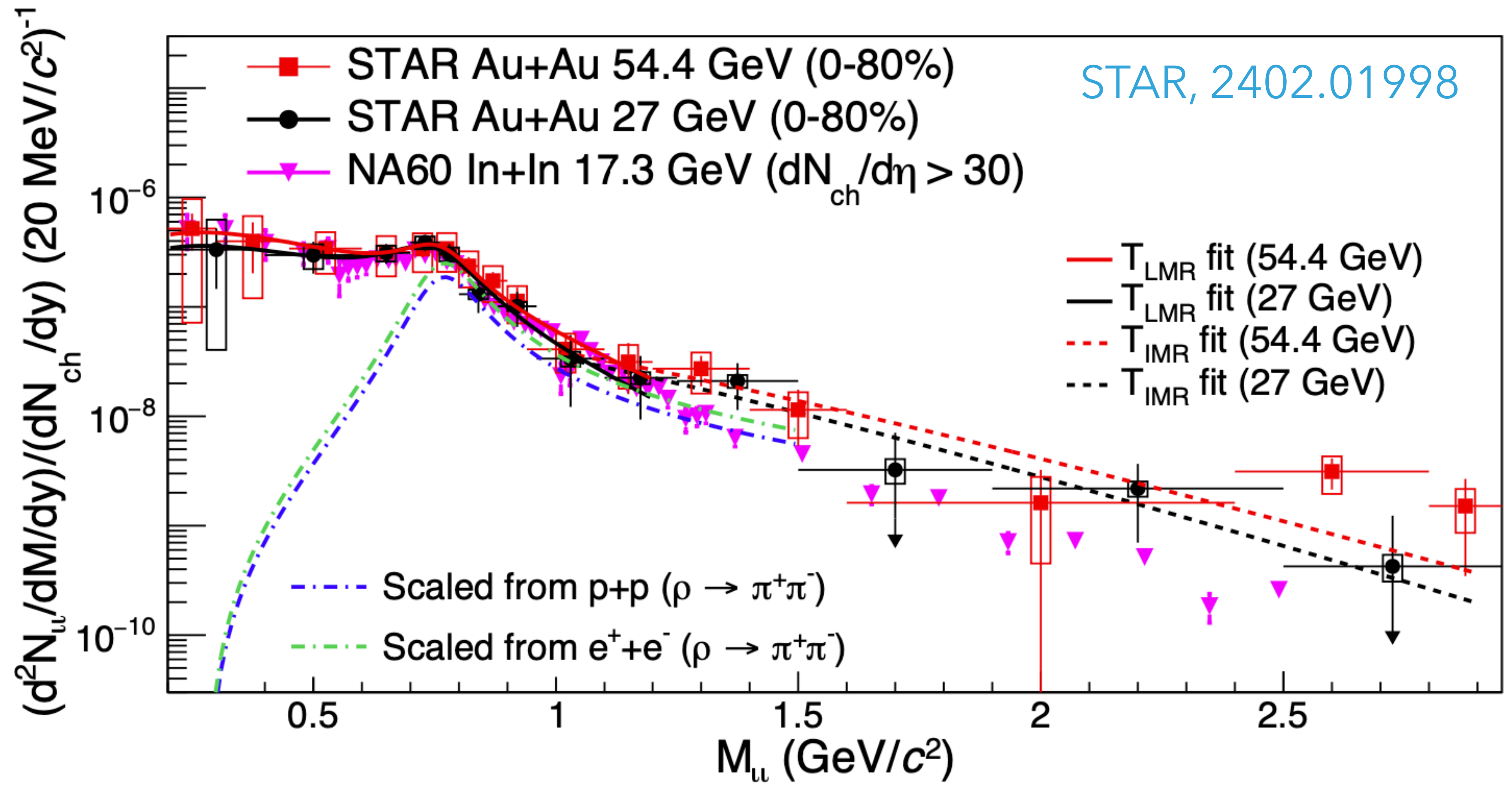

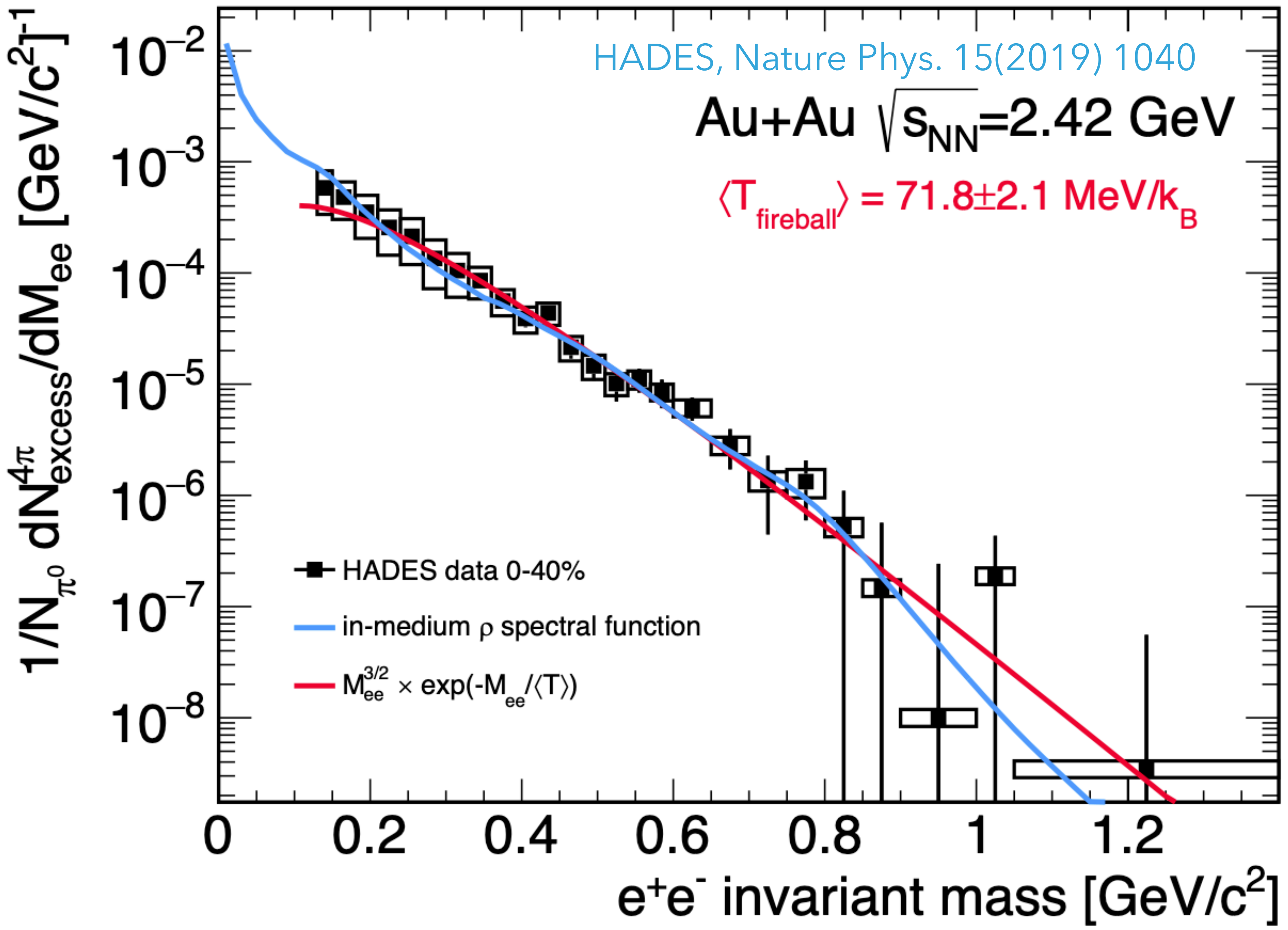

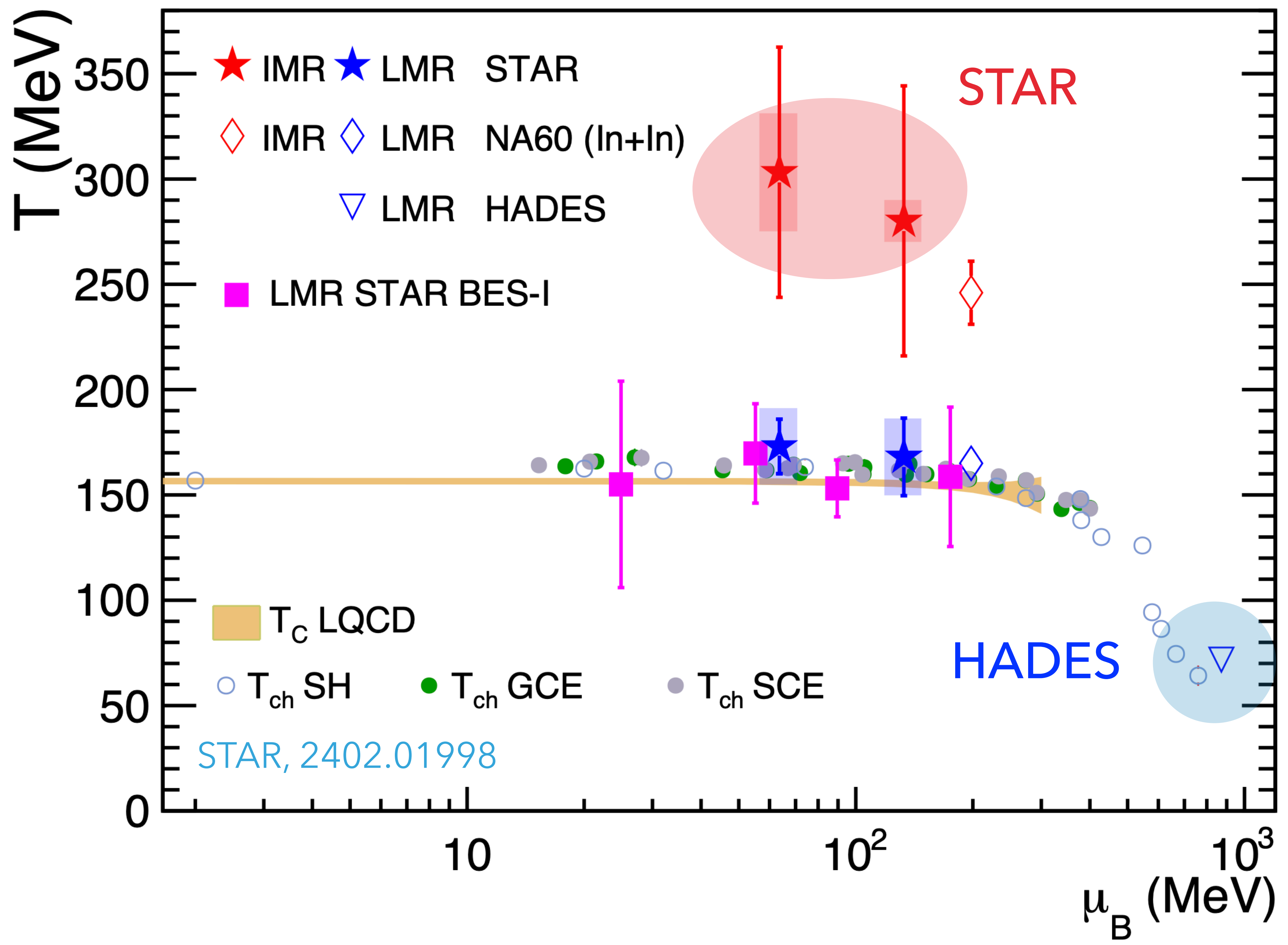

Questions:

- How do we know if the fitting method using $\frac{dN}{dM} \propto (MT)^{3/2} e^{-M/T}$ works?
- How do we interpret the extracted temperature?

NA60, PRL 100, 022302 (2008); EPJC 59 607-623 (2009). STAR, 2402.01998. HADES, Nat. Phys.,1040–1045 (2019). Rapp and van Hees, PLB 753, 586 (2016)

QCD thermometer: reexamined in models

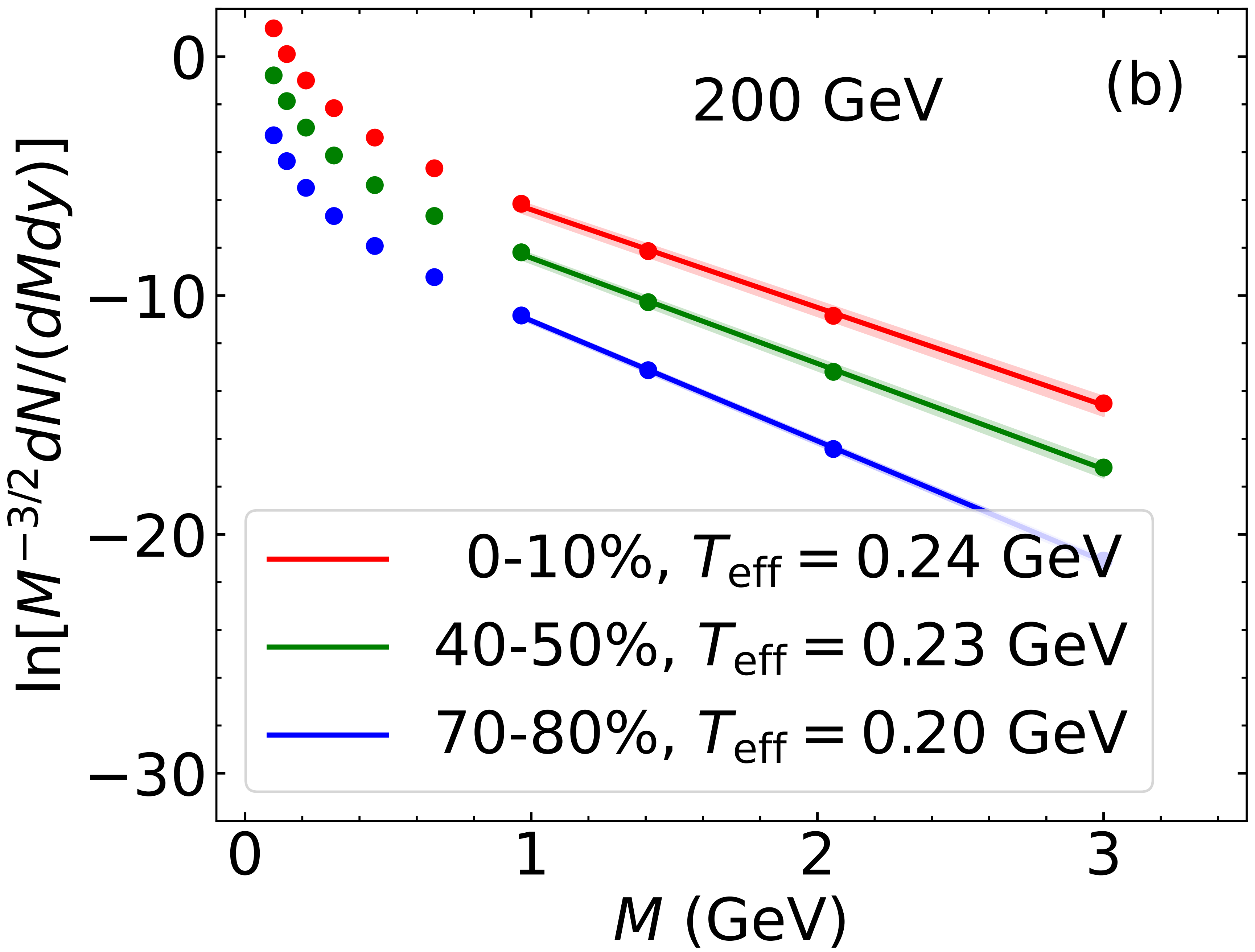

Churchill, LD, Gale, Jackson, Jeon, PRC 109, 044915 (2024), PRL 132, 172301 (2024)

QCD thermometer: reexamined in models

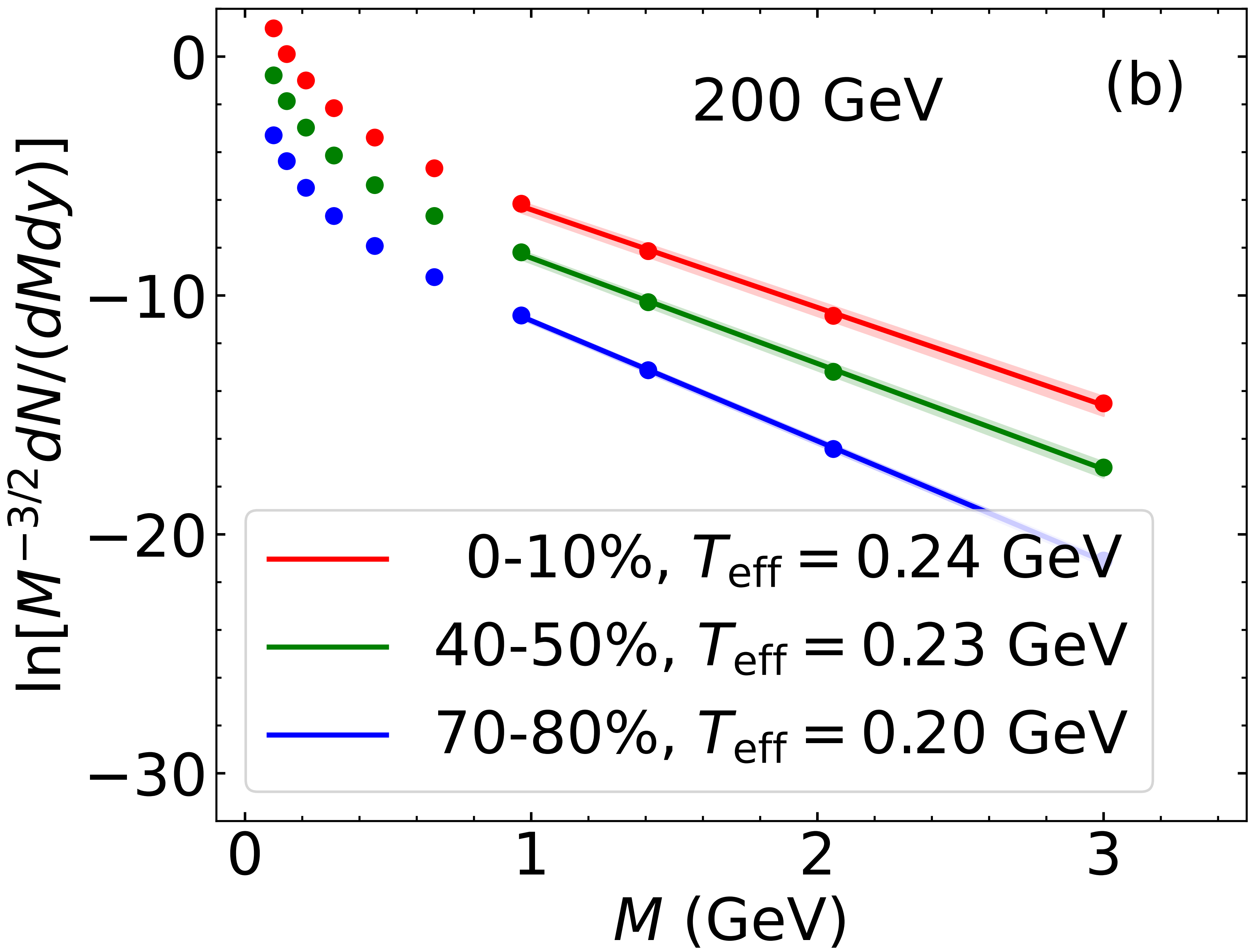

Churchill, LD, Gale, Jackson, Jeon, PRC 109, 044915 (2024), PRL 132, 172301 (2024)

- The fit quality of the exponential ansatz is good [✅ fitting method verified!]. Uncertainties are larger at higher beam energies and in central collisions since the fireball has larger temperature variations.

QCD thermometer: reexamined in models

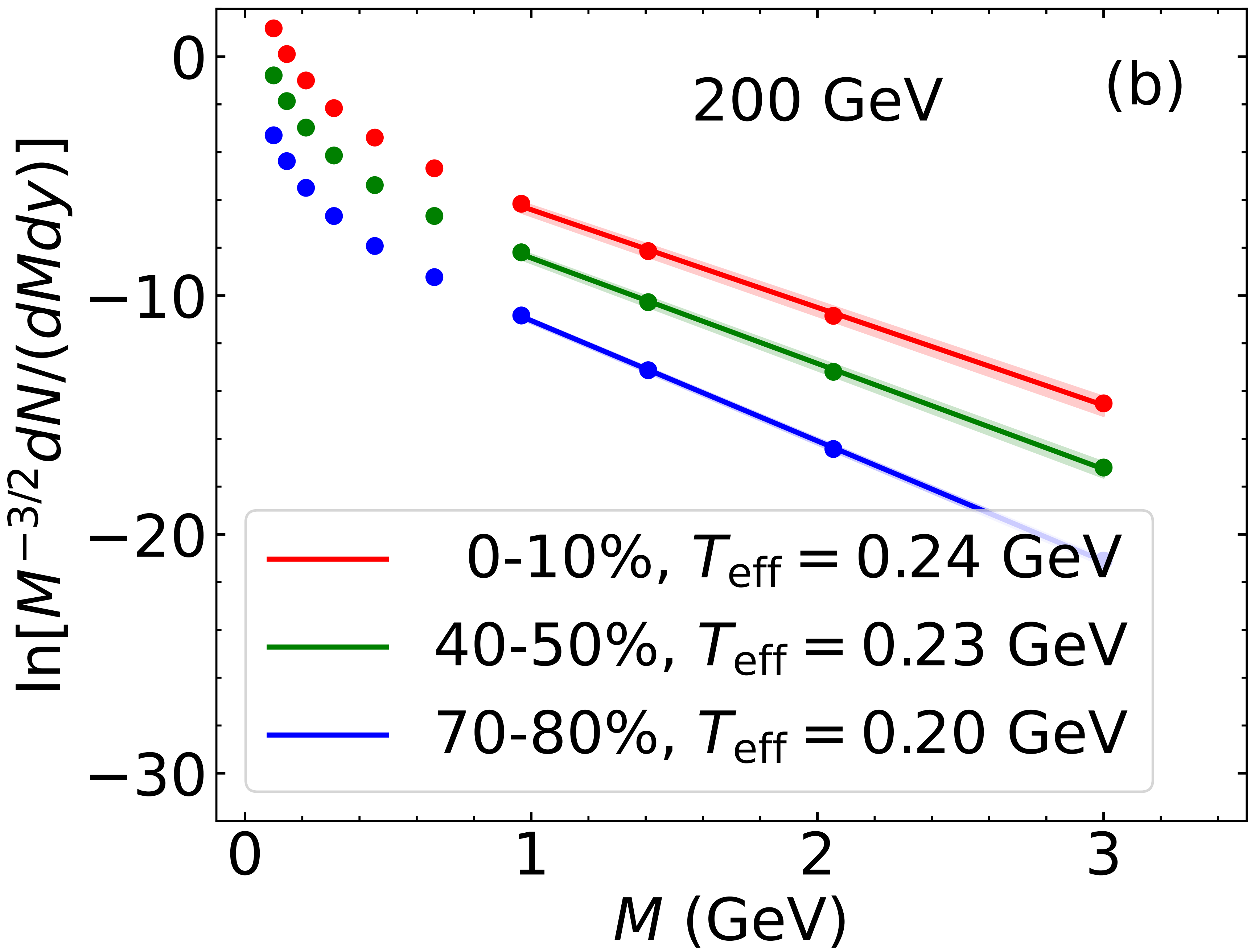

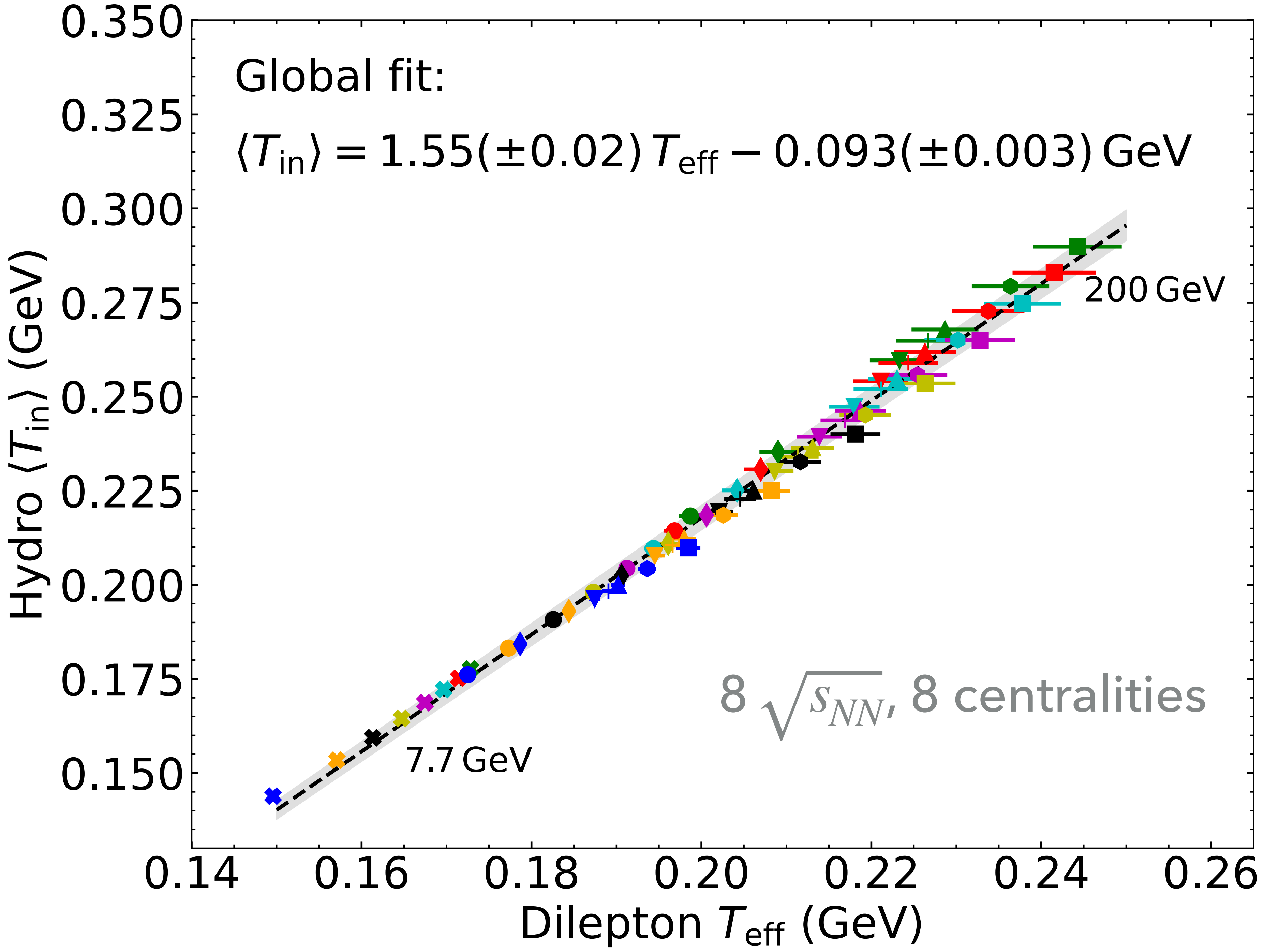

Churchill, LD, Gale, Jackson, Jeon, PRC 109, 044915 (2024), PRL 132, 172301 (2024)   https://github.com/LipeiDu/DileptonEmission

- The fit quality of the exponential ansatz is good [✅ fitting method verified!]. Uncertainties are larger at higher beam energies and in central collisions since the fireball has larger temperature variations.

QCD thermometer: reexamined in models

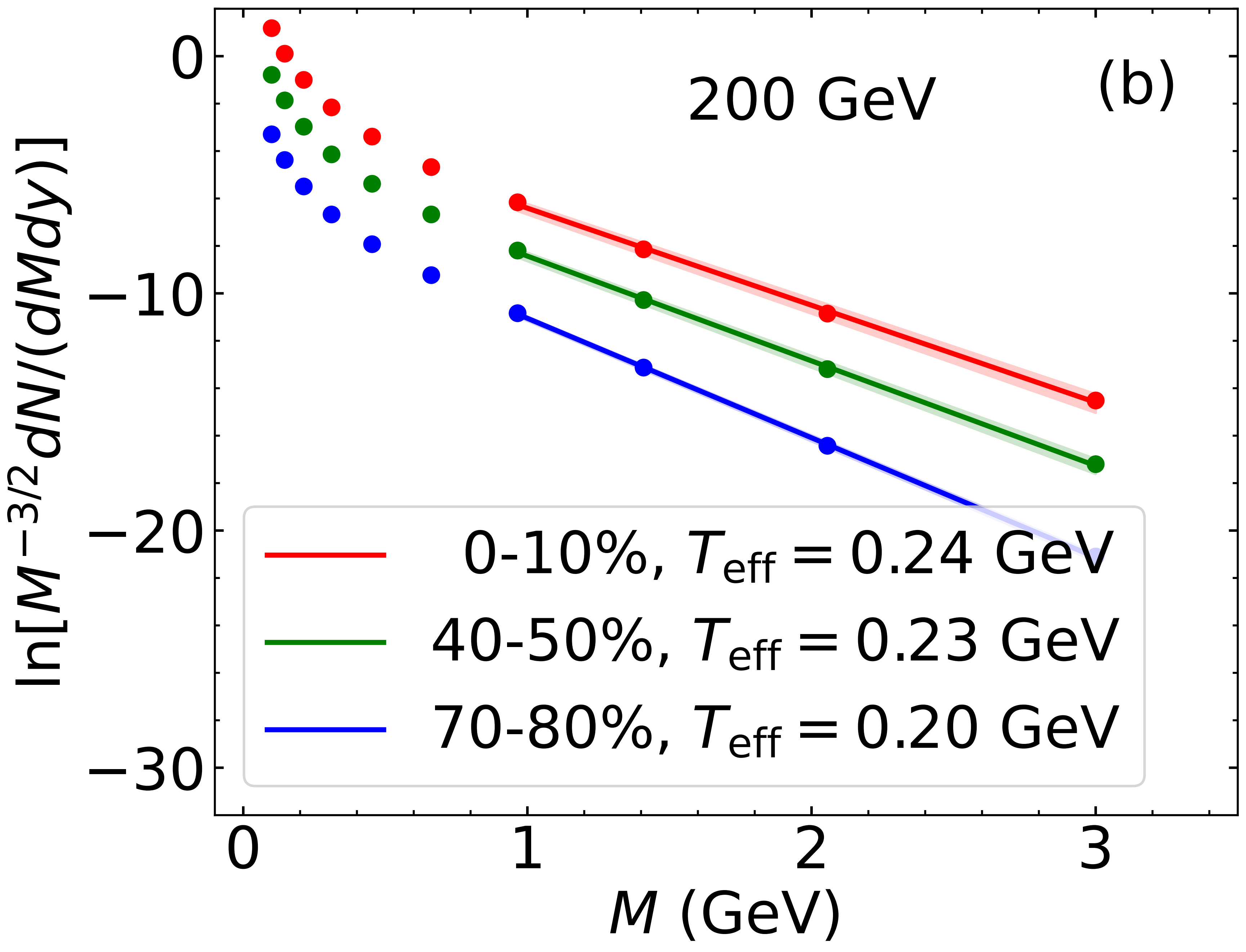

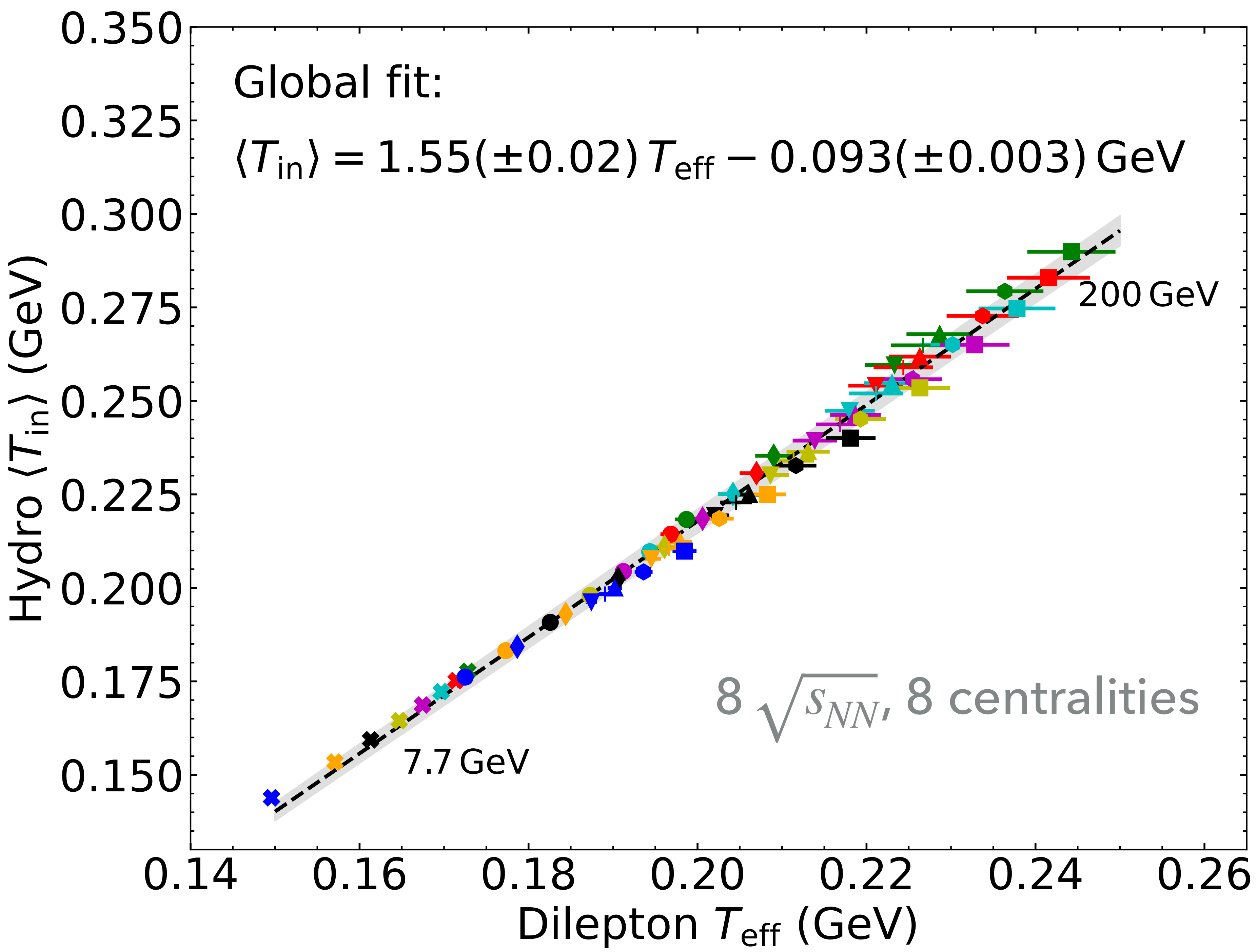

Churchill, LD, Gale, Jackson, Jeon, PRC 109, 044915 (2024), PRL 132, 172301 (2024)

https://github.com/LipeiDu/DileptonEmission

- The fit quality of the exponential ansatz is good [✅ fitting method verified!]. Uncertainties are larger at higher beam energies and in central collisions since the fireball has larger temperature variations.
- A correlation between the average temperature and the initial hydro temperature is identified [✅ interpretation of the extracted temperature found!].

QCD thermometer: reexamined in models

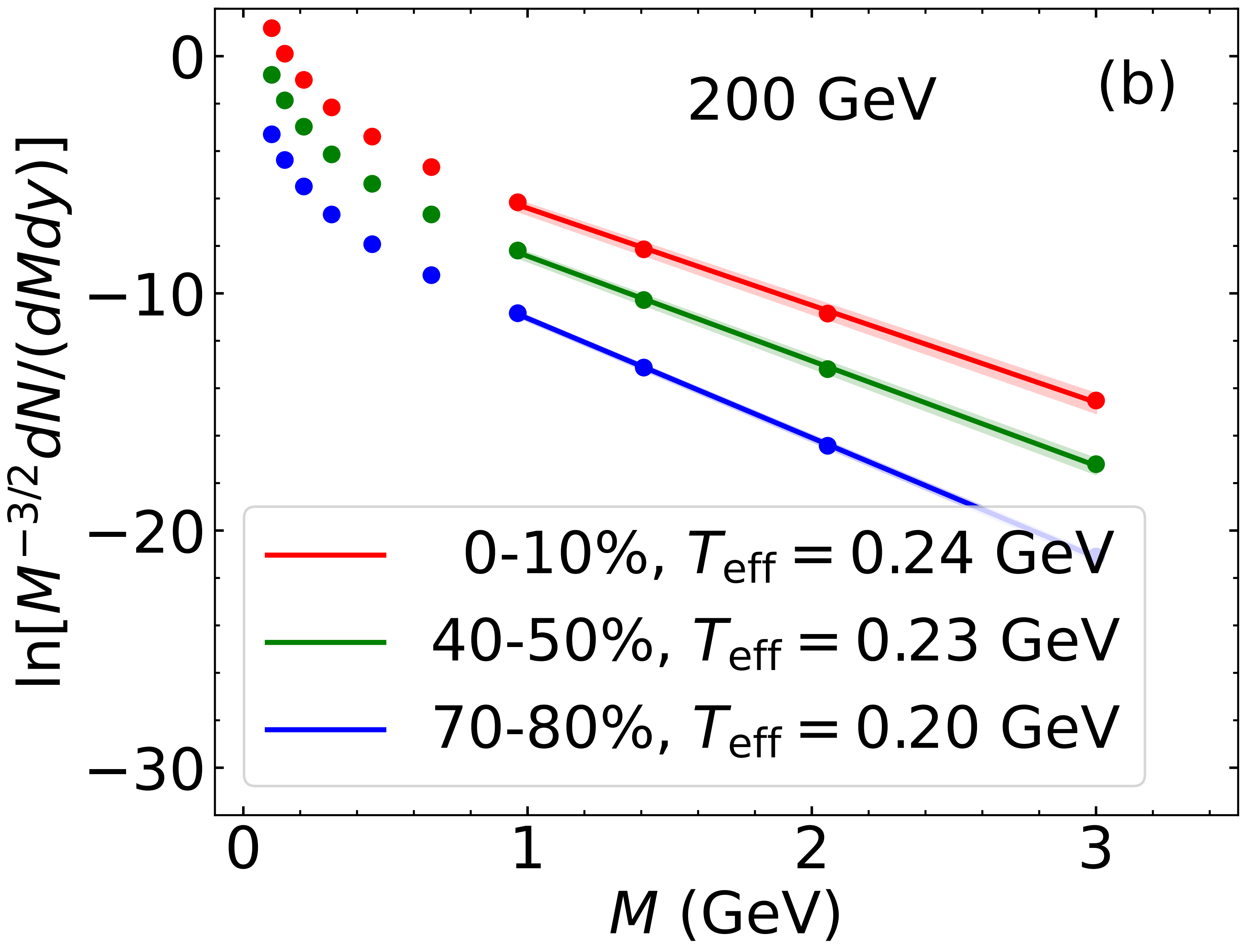

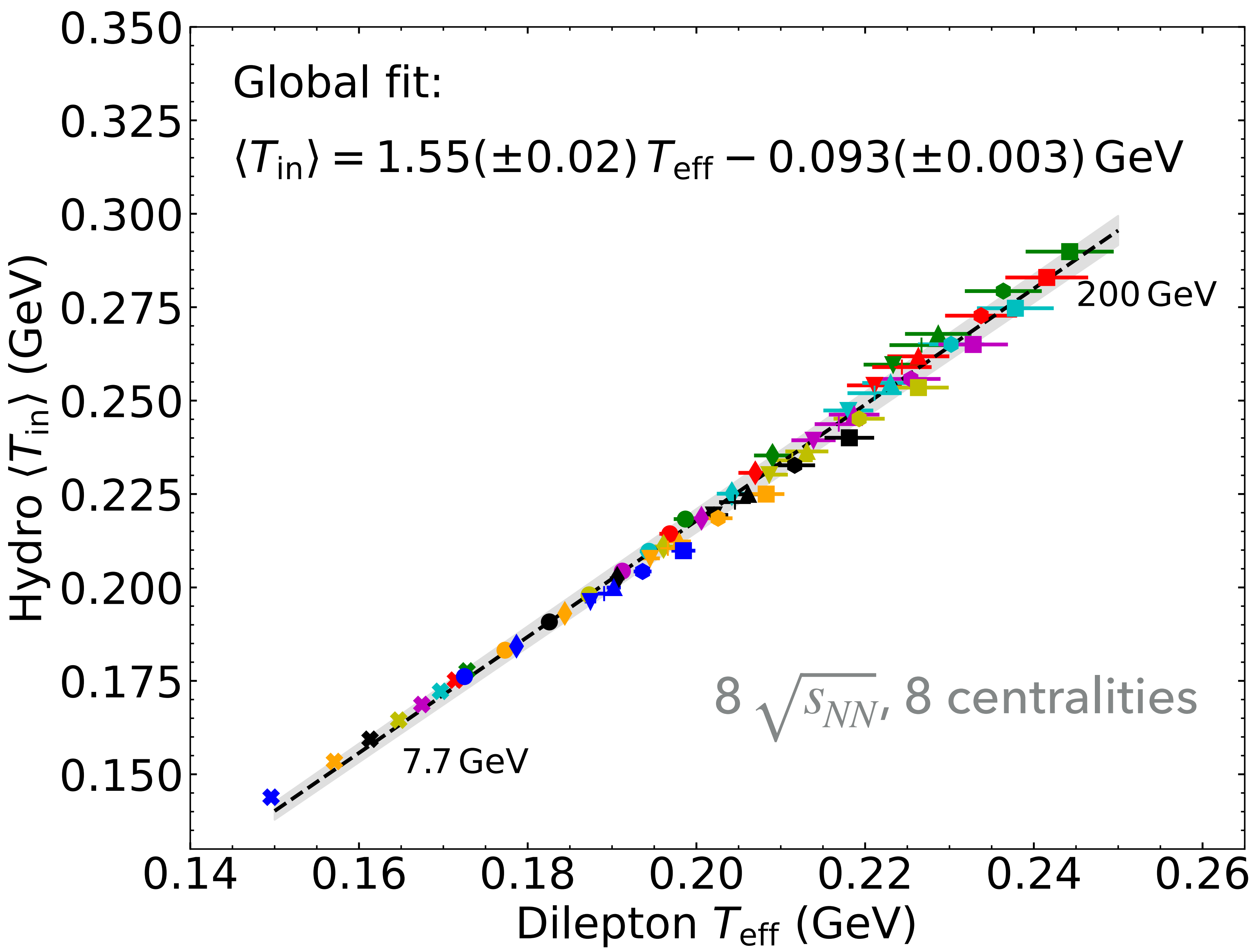

Churchill, LD, Gale, Jackson, Jeon, PRC 109, 044915 (2024), PRL 132, 172301 (2024)   https://github.com/LipeiDu/DileptonEmission

- The fit quality of the exponential ansatz is good [✅ fitting method verified!]. Uncertainties are larger at higher beam energies and in central collisions since the fireball has larger temperature variations.
- A correlation between the average temperature and the initial hydro temperature is identified [✅ interpretation of the extracted temperature found!].
- Measure the initial temperature of the evolving QCD fireball in a way that is unaffected by dynamical distortions.

Multi-messenger study

https://github.com/LipeiDu/DileptonEmission

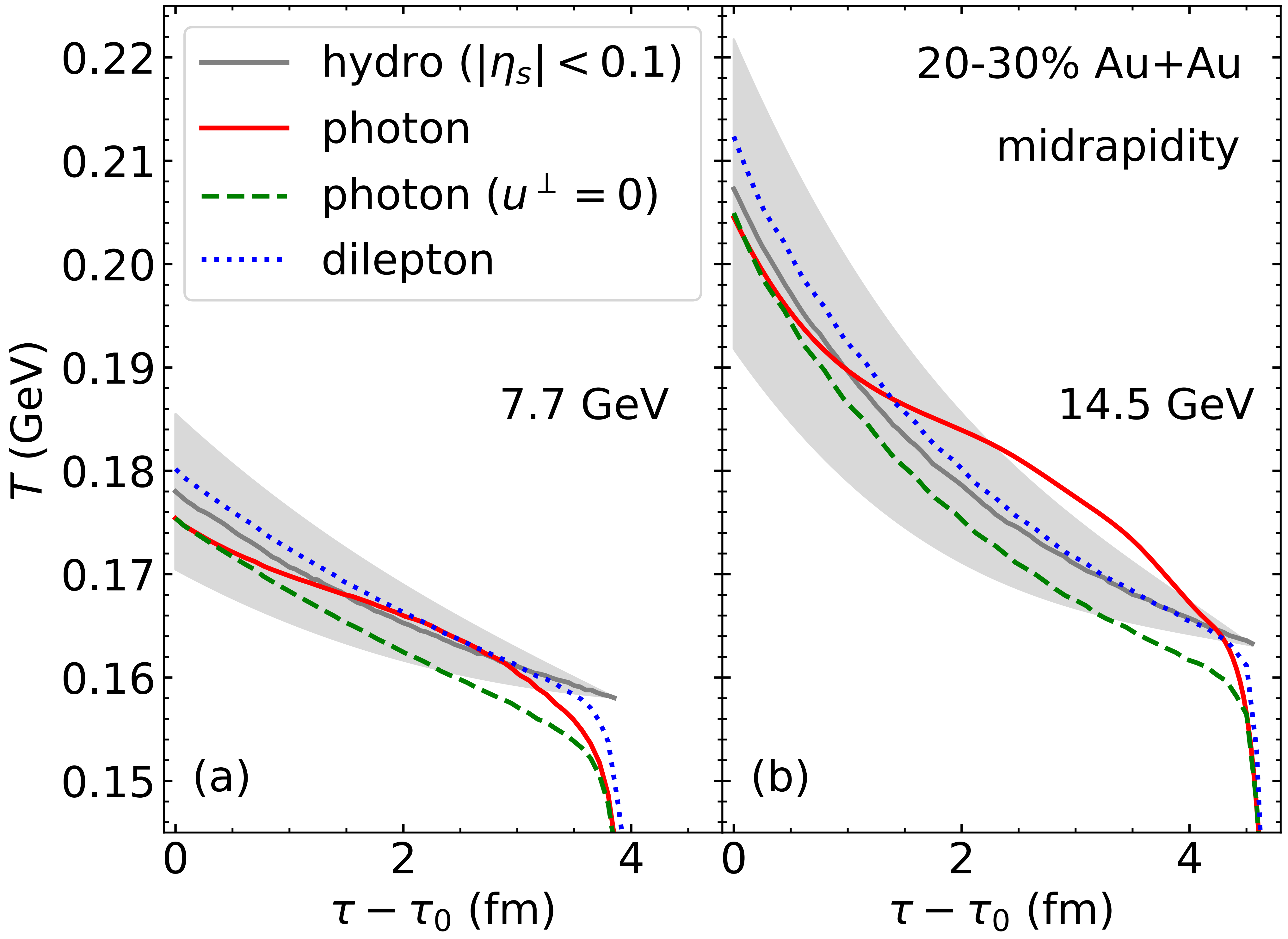

LD, arXiv: 2408.08501

Shen, Heinz, Paquet, Gale, Phys. Rev. C 89 (2014) 044910; Churchill, LD, Gale, Jackson, Jeon, PRC 109, 044915 (2024), PRL 132, 172301 (2024)

Multi-messenger study

https://github.com/LipeiDu/DileptonEmission

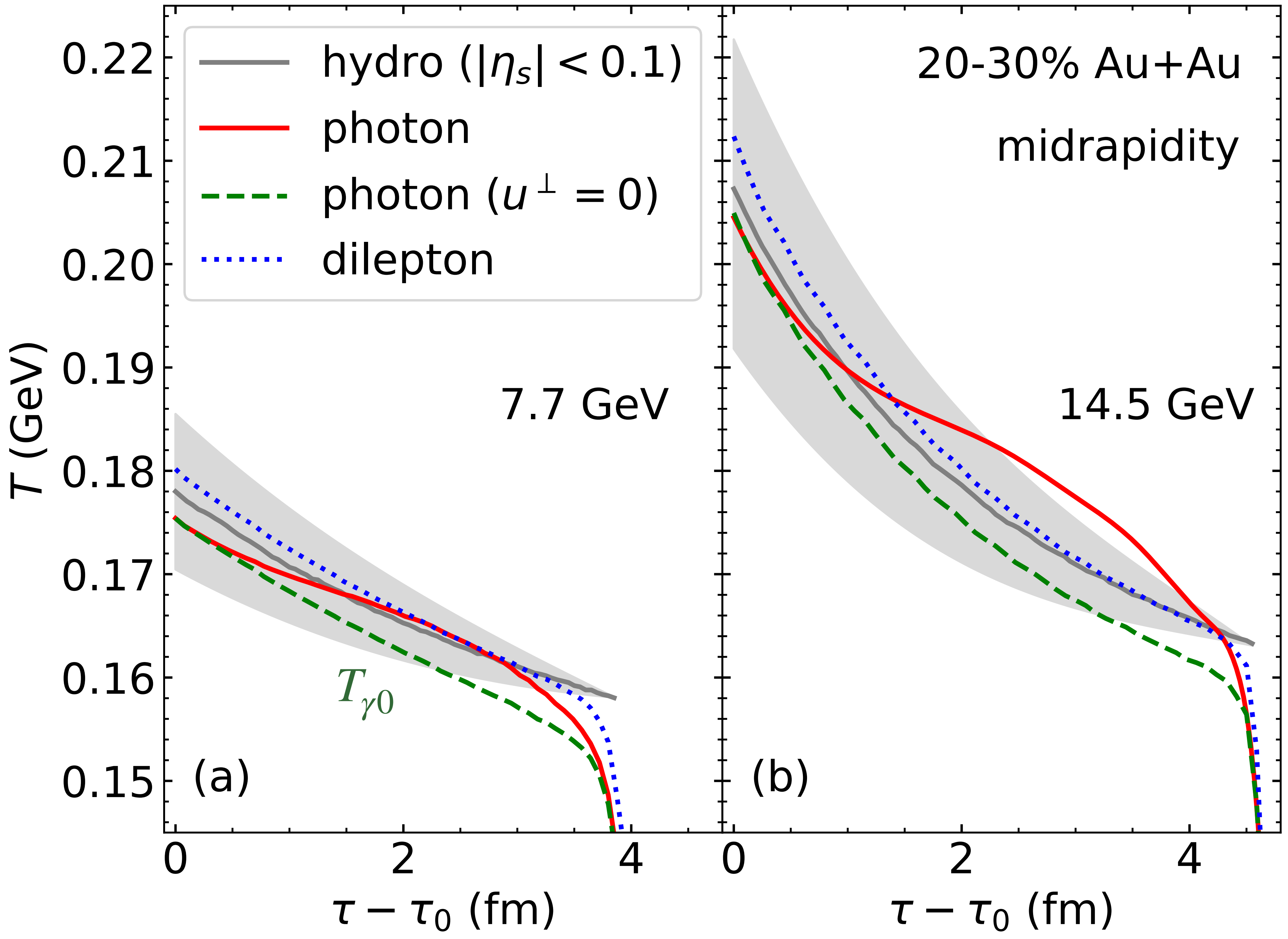

LD, arXiv: 2408.08501

Shen, Heinz, Paquet, Gale, Phys. Rev. C 89 (2014) 044910; Churchill, LD, Gale, Jackson, Jeon, PRC 109, 044915 (2024), PRL 132, 172301 (2024)

Multi-messenger study

https://github.com/LipeiDu/DileptonEmission

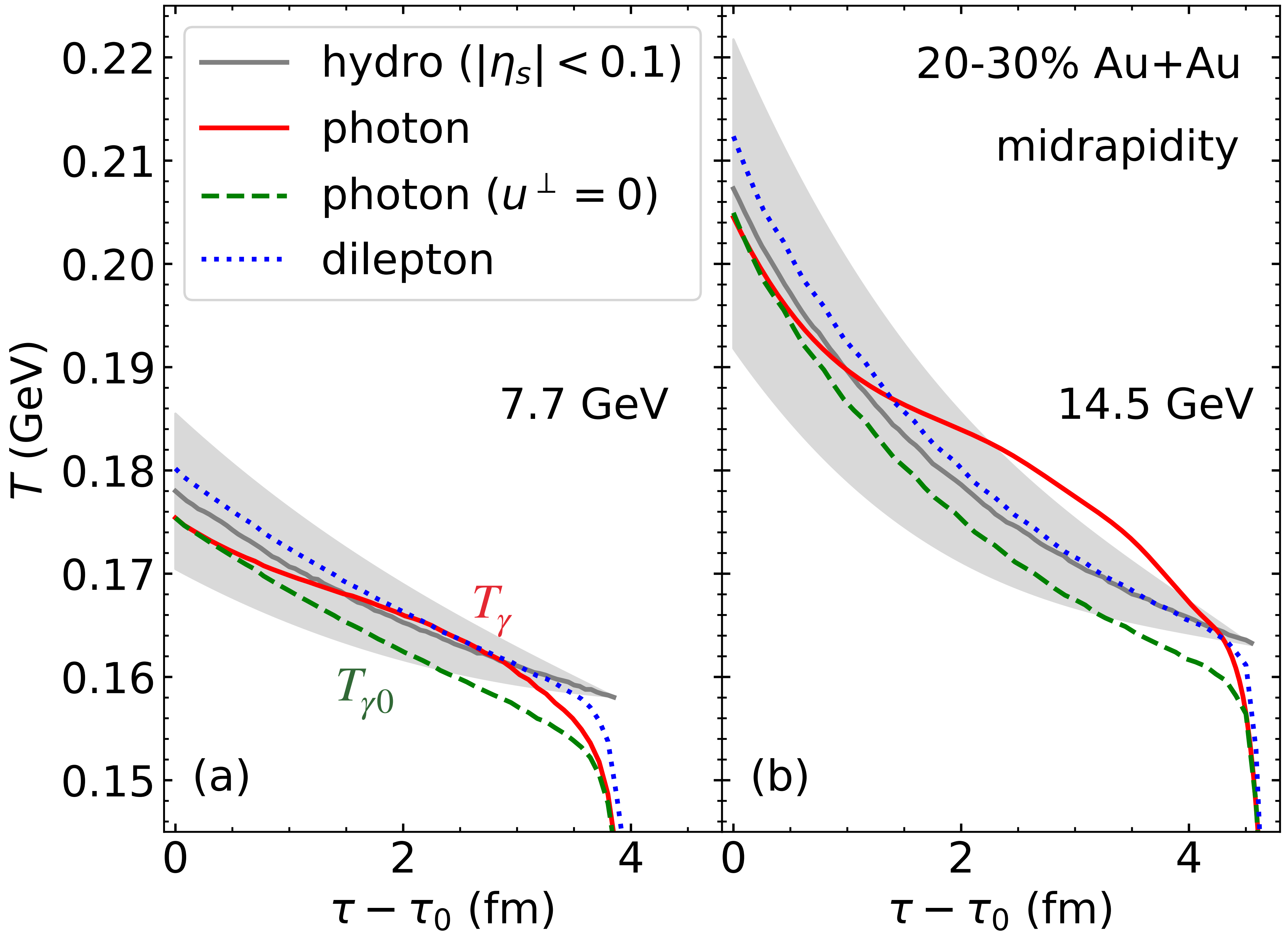

LD, arXiv: 2408.08501

Shen, Heinz, Paquet, Gale, Phys. Rev. C 89 (2014) 044910; Churchill, LD, Gale, Jackson, Jeon, PRC 109, 044915 (2024), PRL 132, 172301 (2024)

Multi-messenger study

https://github.com/LipeiDu/DileptonEmission

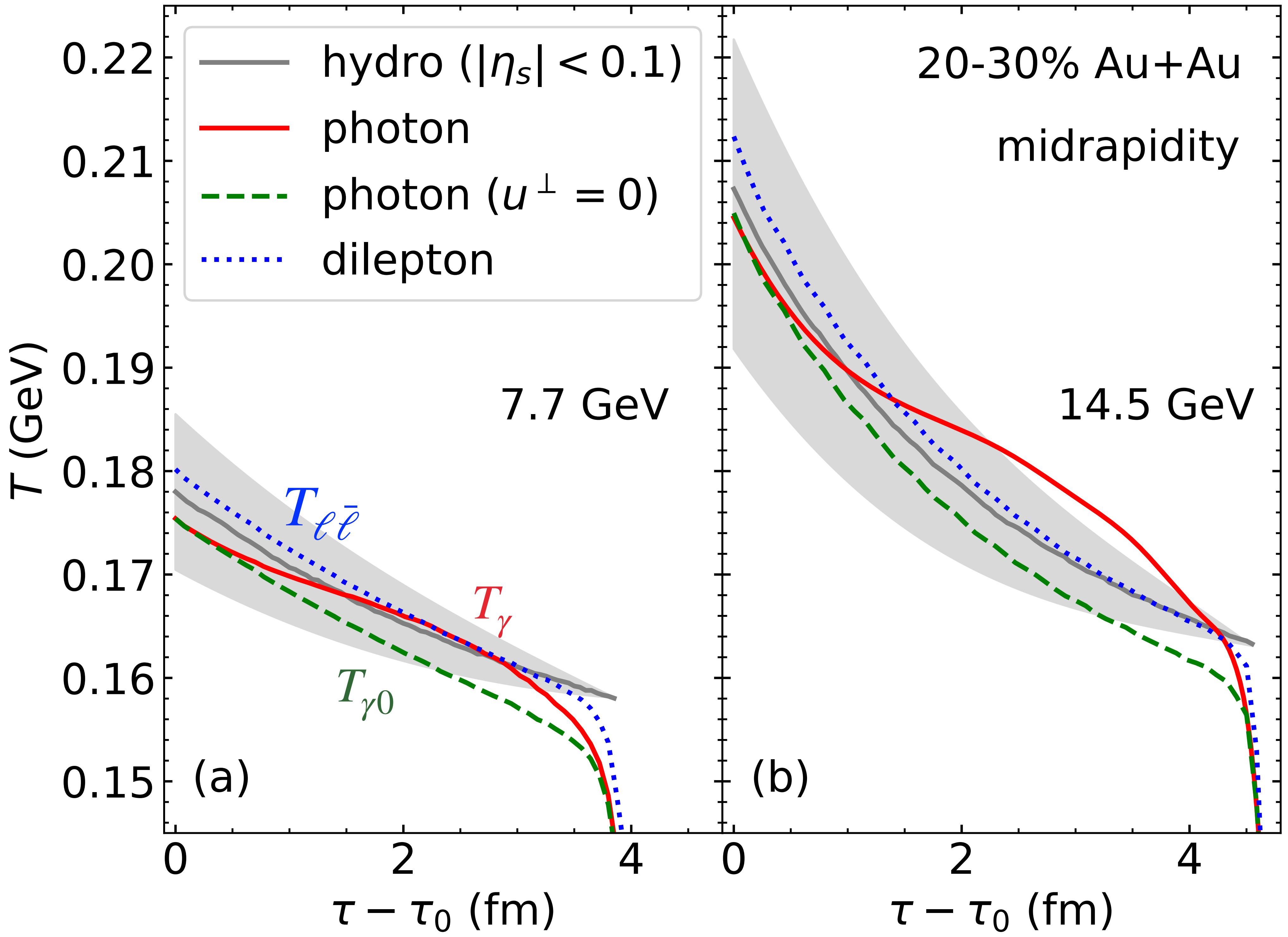

LD, arXiv: 2408.08501

Shen, Heinz, Paquet, Gale, Phys. Rev. C 89 (2014) 044910; Churchill, LD, Gale, Jackson, Jeon, PRC 109, 044915 (2024), PRL 132, 172301 (2024)

Multi-messenger study

https://github.com/LipeiDu/DileptonEmission

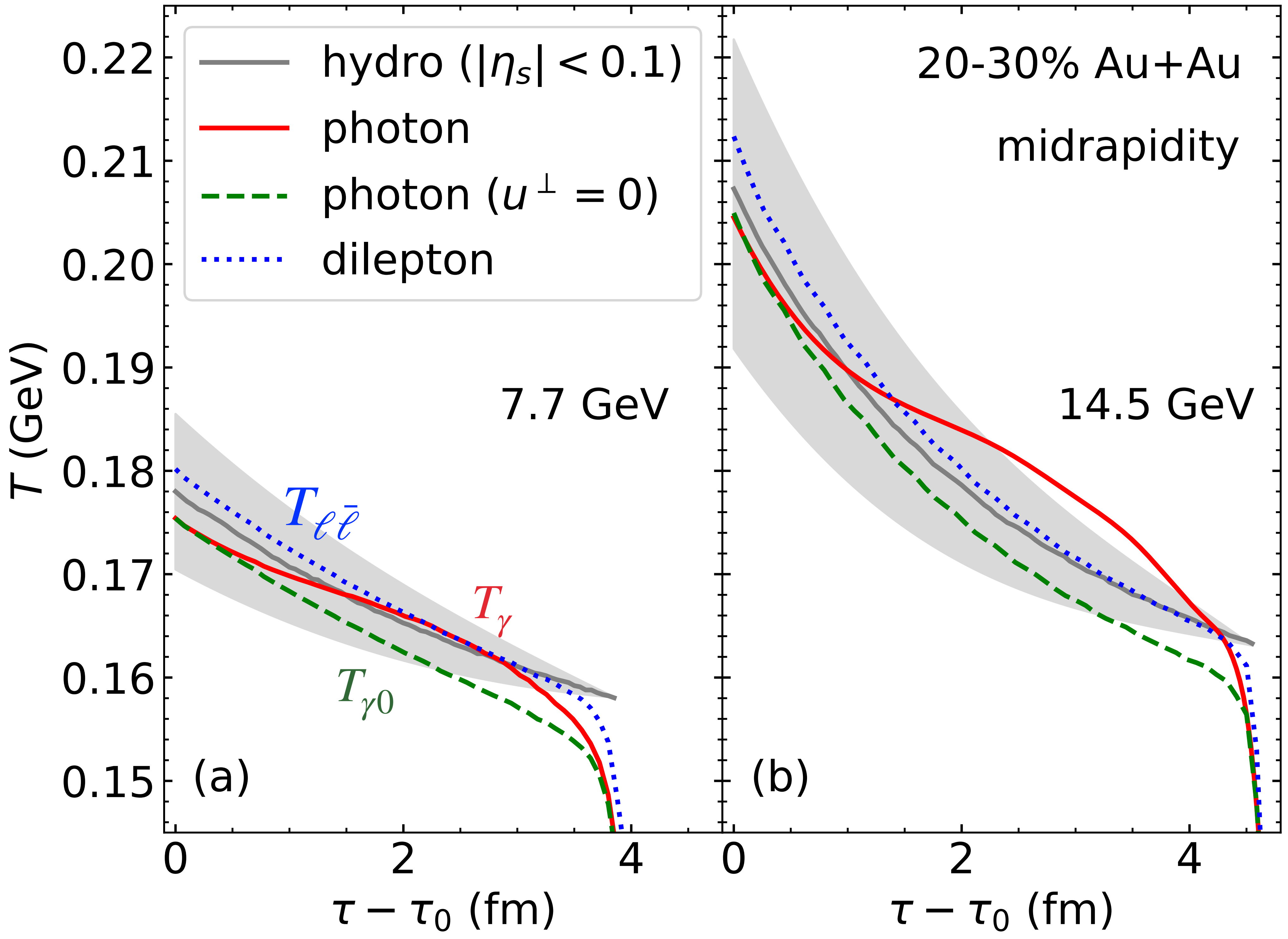

photon T

photon T w/o Doppler effect

$$T_\gamma \approx T_{\gamma 0}\sqrt{\frac{1+v_\perp}{1-v_\perp}}$$

LD, arXiv: 2408.08501

Shen, Heinz, Paquet, Gale, Phys. Rev. C 89 (2014) 044910; Churchill, LD, Gale, Jackson, Jeon, PRC 109, 044915 (2024), PRL 132, 172301 (2024)

Multi-messenger study

https://github.com/LipeiDu/DileptonEmission

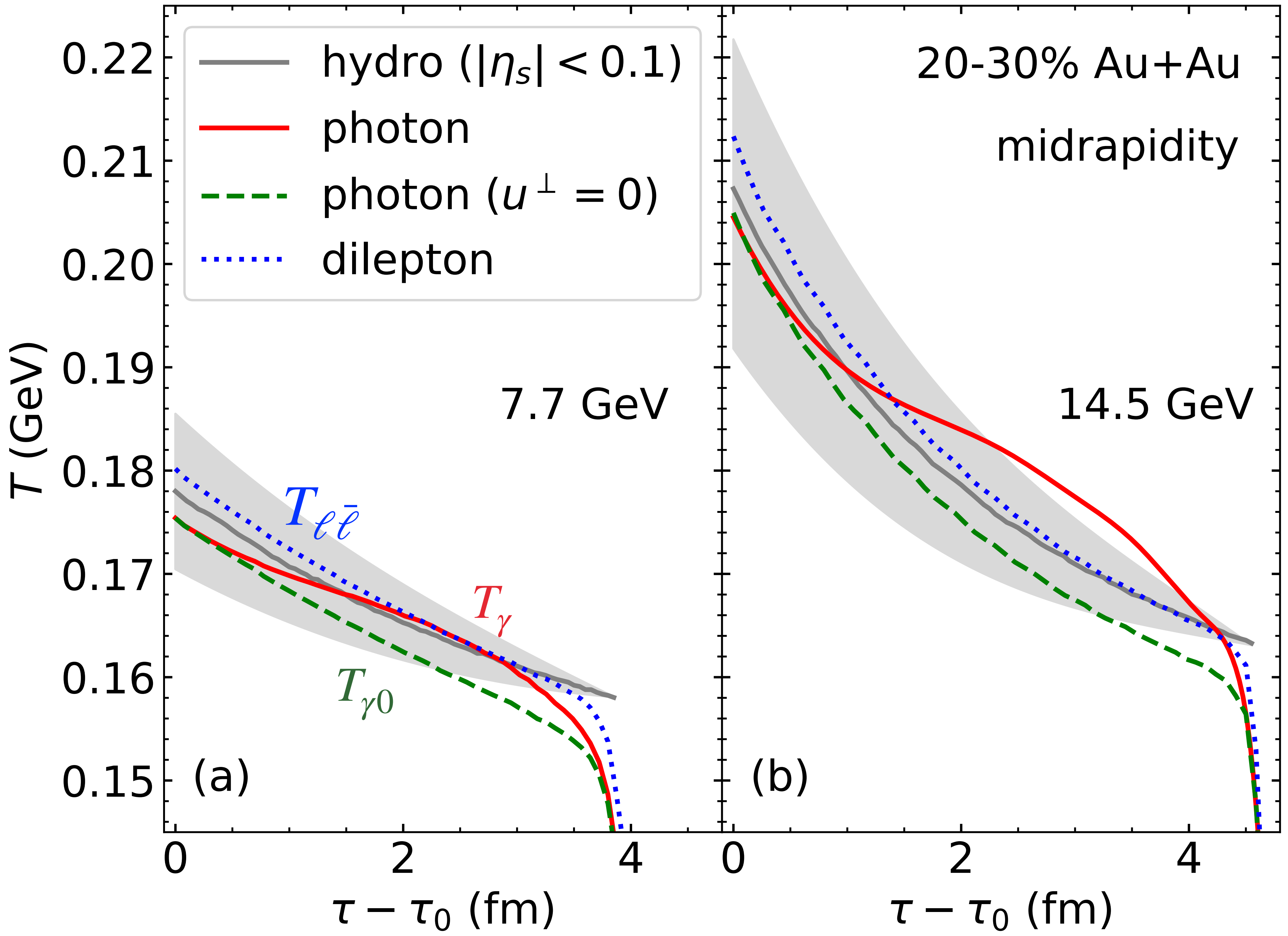

photon T

photon T w/o Doppler effect

$$T_\gamma \approx T_{\gamma 0}\sqrt{\frac{1+v_\perp}{1-v_\perp}}$$

LD, arXiv: 2408.08501

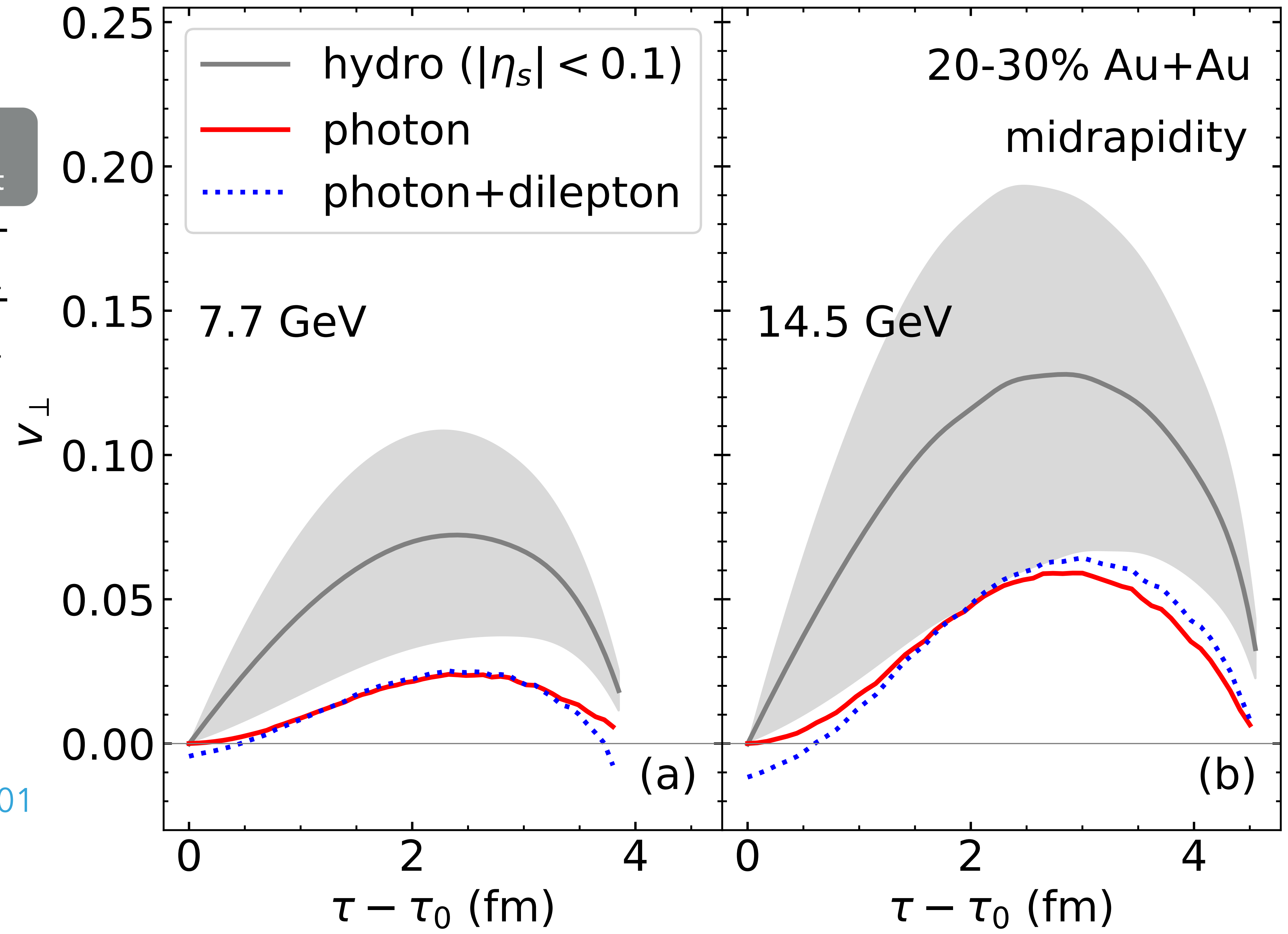

Shen, Heinz, Paquet, Gale, Phys. Rev. C 89 (2014) 044910; Churchill, LD, Gale, Jackson, Jeon, PRC 109, 044915 (2024), PRL 132, 172301 (2024)

Multi-messenger study

https://github.com/LipeiDu/DileptonEmission

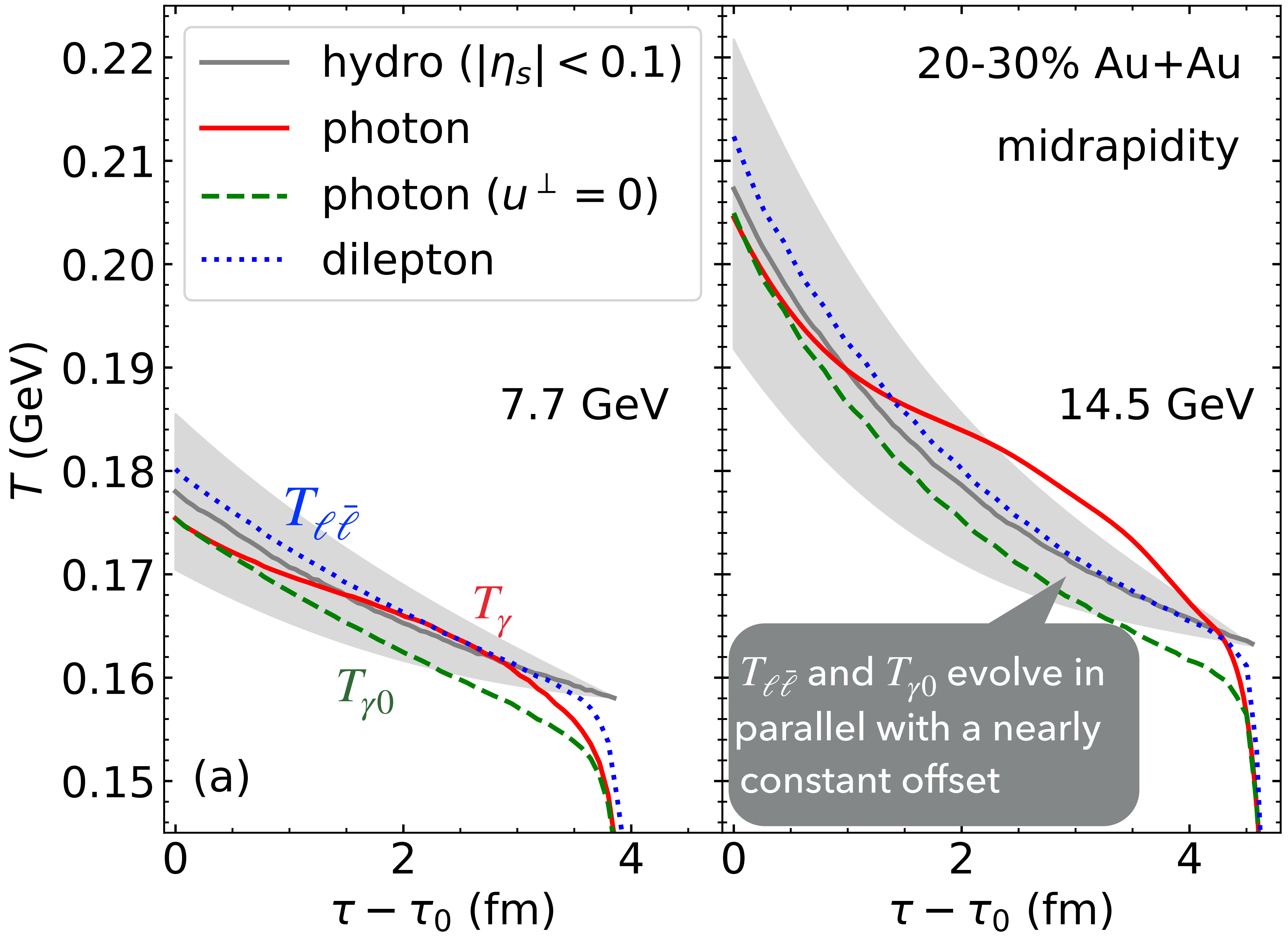

photon T

photon T w/o Doppler effect

$$T_\gamma \approx T_{\gamma 0}\sqrt{\frac{1+v_\perp}{1-v_\perp}}$$

LD, arXiv: 2408.08501

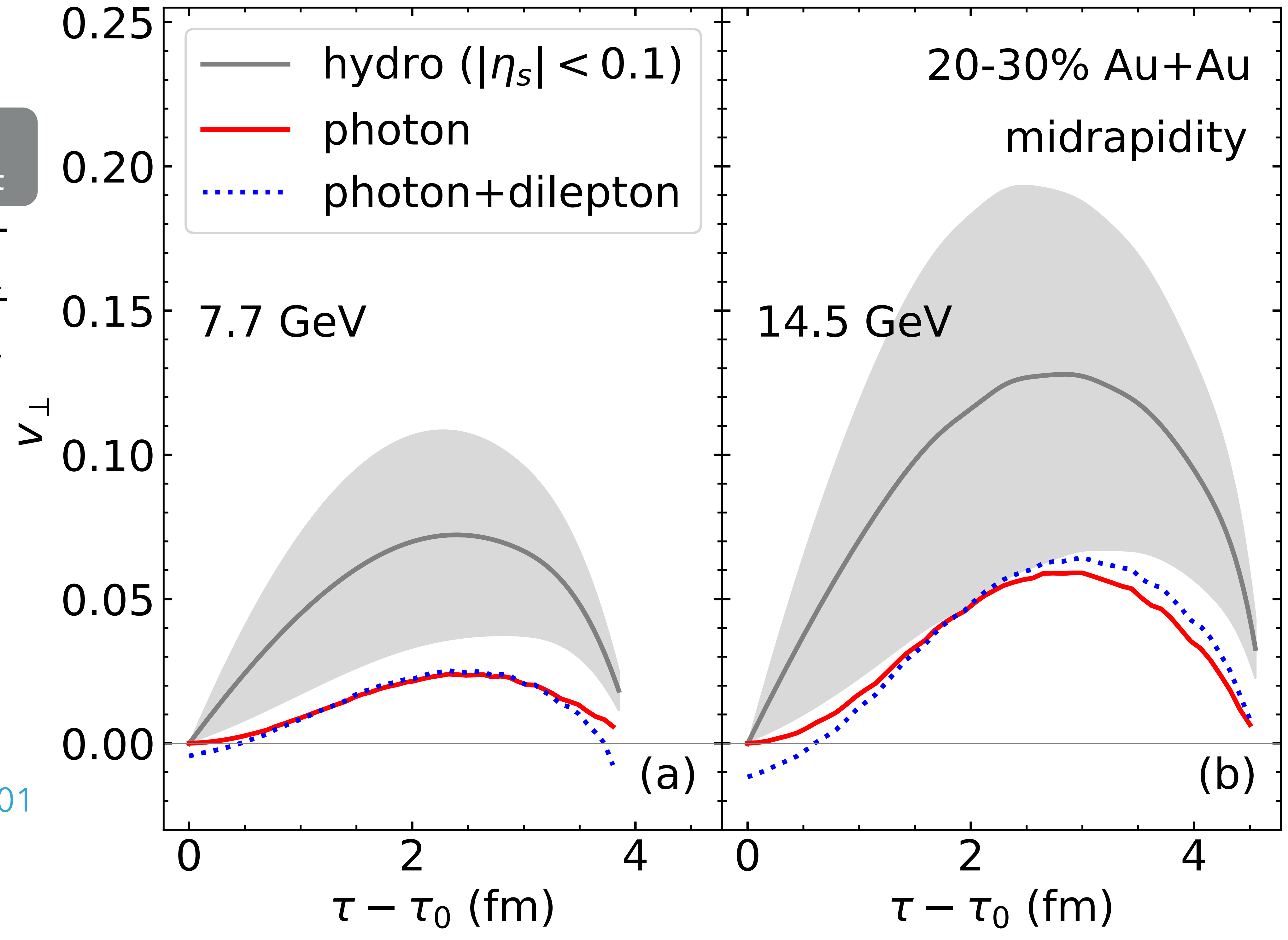

Shen, Heinz, Paquet, Gale, Phys. Rev. C 89 (2014) 044910; Churchill, LD, Gale, Jackson, Jeon, PRC 109, 044915 (2024), PRL 132, 172301 (2024)

Multi-messenger study

https://github.com/LipeiDu/DileptonEmission

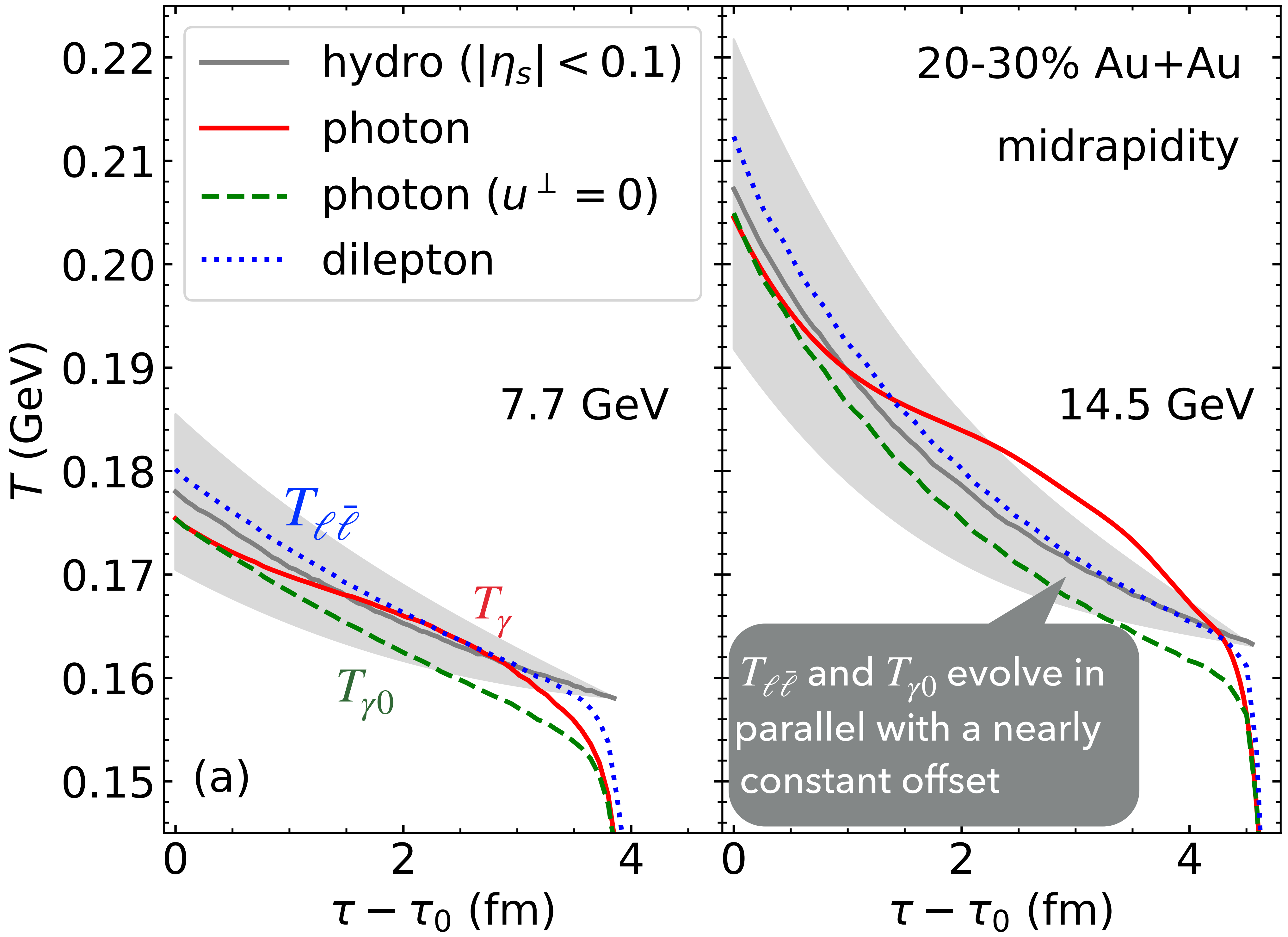

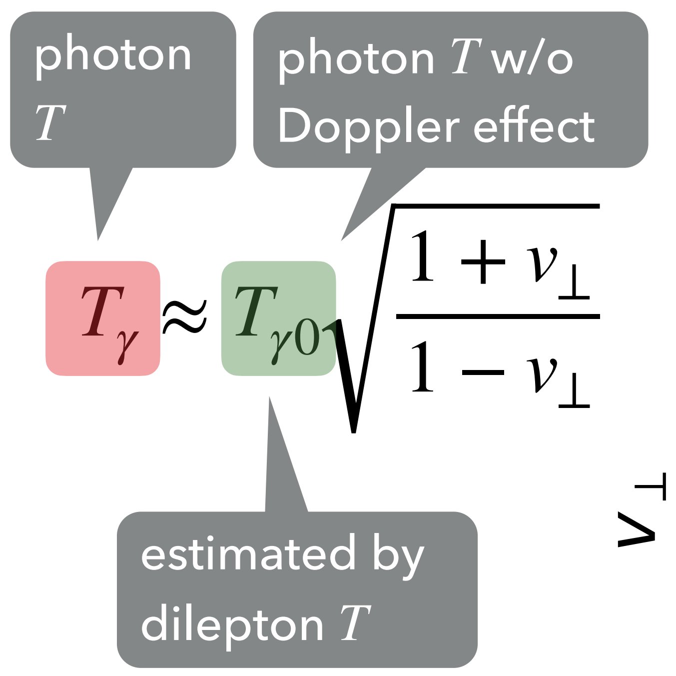

$$T_\gamma \approx T_{\gamma 0}\sqrt{\frac{1+v_\perp}{1-v_\perp}}$$

LD, arXiv: 2408.08501

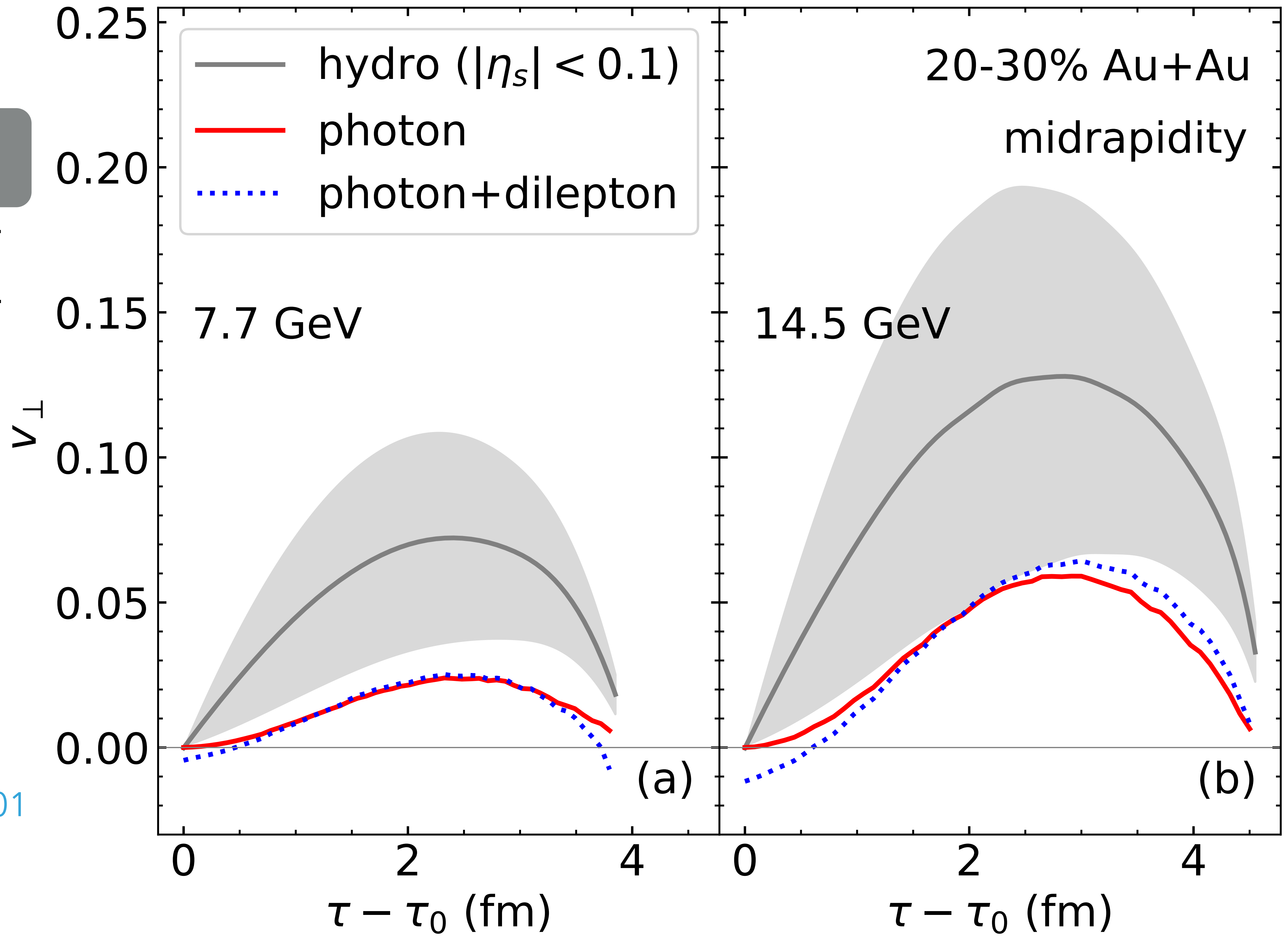

Shen, Heinz, Paquet, Gale, Phys. Rev. C 89 (2014) 044910; Churchill, LD, Gale, Jackson, Jeon, PRC 109, 044915 (2024), PRL 132, 172301 (2024)

Multi-messenger study

https://github.com/LipeiDu/DileptonEmission

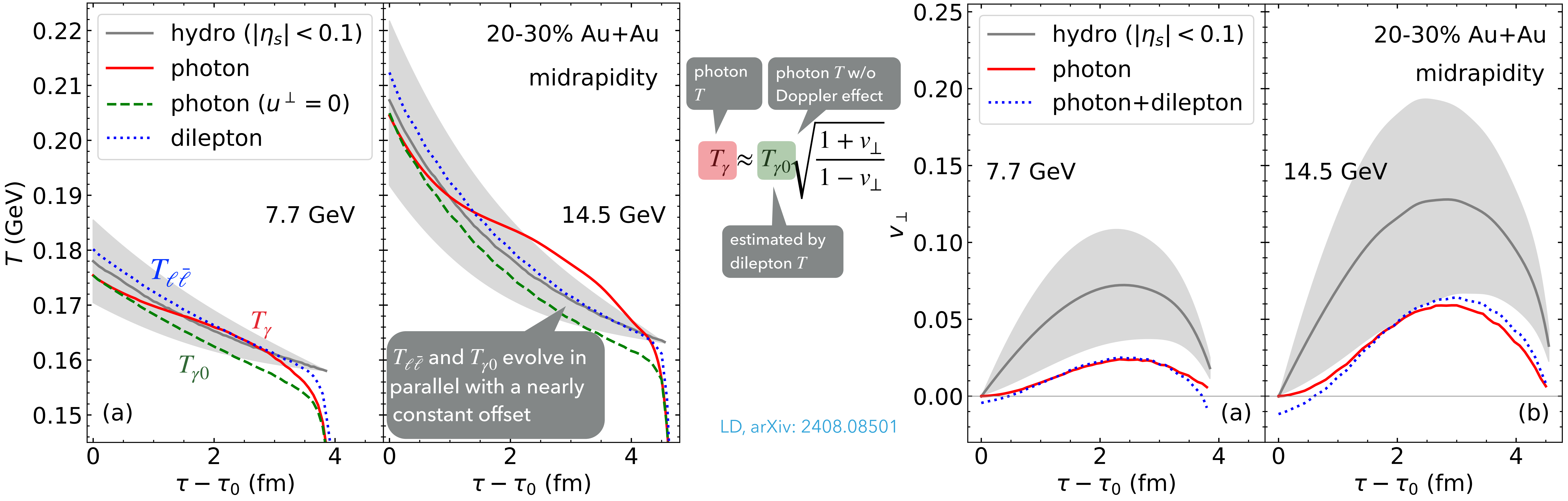

- A correlation between the temperatures extracted from photon spectra (without Doppler shift) and dilepton spectra is identified, leading to the possibility of combining measurable photon and dilepton spectra to extract radial flow.

Shen, Heinz, Paquet, Gale, Phys. Rev. C 89 (2014) 044910; Churchill, LD, Gale, Jackson, Jeon, PRC 109, 044915 (2024), PRL 132, 172301 (2024)

Multi-messenger study

https://github.com/LipeiDu/DileptonEmission

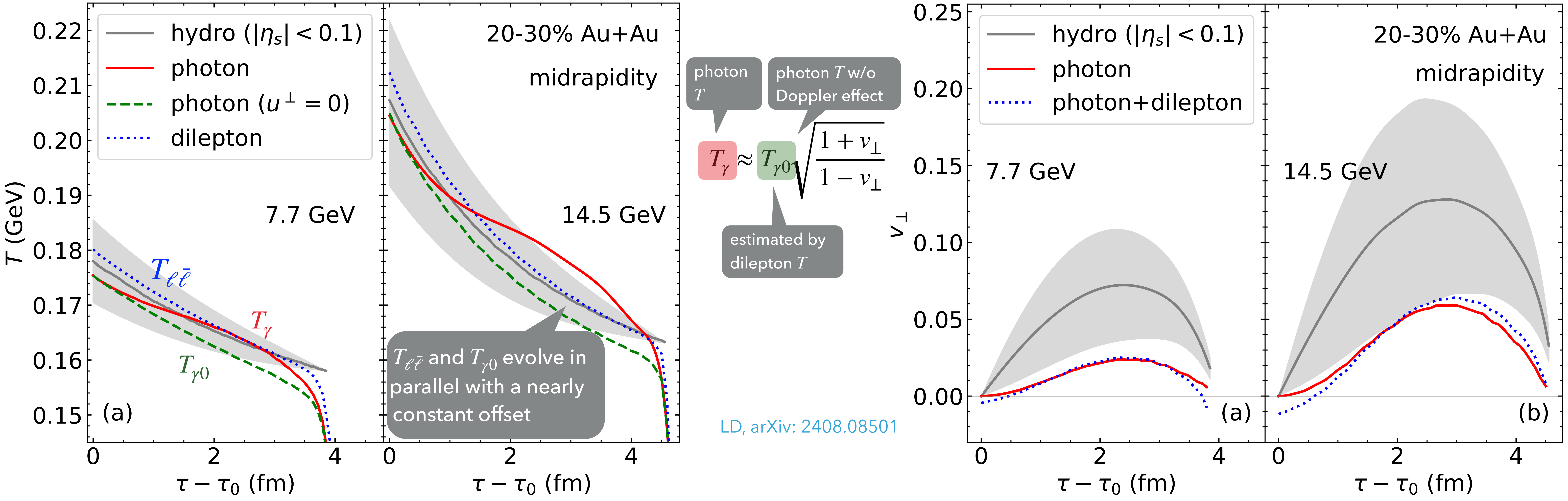

- A correlation between the temperatures extracted from photon spectra (without Doppler shift) and dilepton spectra is identified, leading to the possibility of combining measurable photon and dilepton spectra to extract radial flow.
- Measuring the thermodynamic properties of the created systems in heavy-ion collisions using multiple messengers through two fundamental interactions within the same framework.

Shen, Heinz, Paquet, Gale, Phys. Rev. C 89 (2014) 044910; Churchill, LD, Gale, Jackson, Jeon, PRC 109, 044915 (2024), PRL 132, 172301 (2024)

SUMMARY

Summary

- EM radiations from the early stages offer insights into thermalization and chemical equilibration processes.
- EM radiation from both the QGP and hadronic matter reveals the thermodynamic properties of QCD matter.
  - Various thermodynamic measures have been proposed; they should be examined in realistic simulations.
- We are entering a new era of multi-messenger studies in heavy-ion collisions.
  - More systematic measurements: hadrons, photons, and dileptons
  - More advanced theoretical modeling

THANKS FOR YOUR ATTENTION!

Application of perturbative QCD

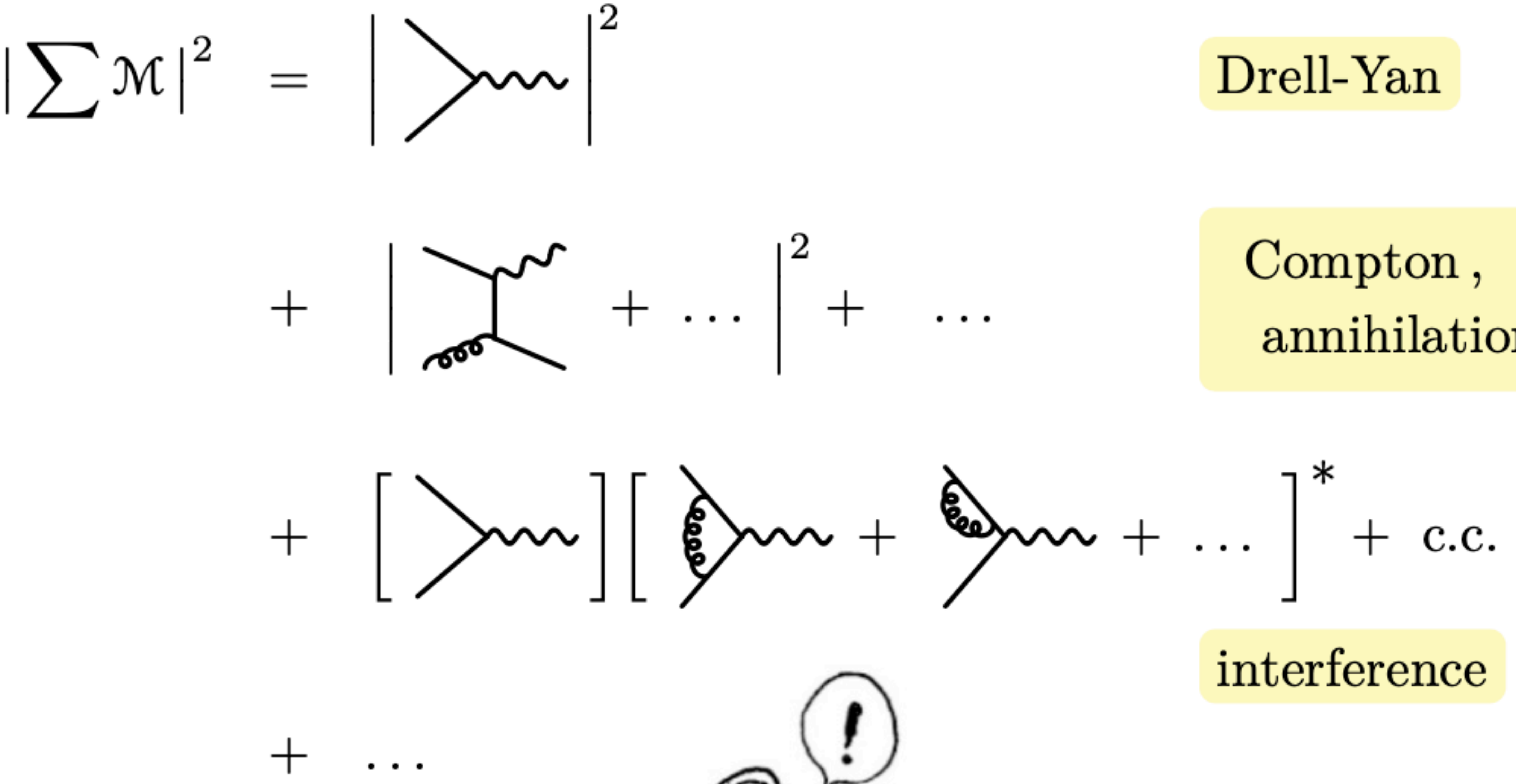

Drell-Yan

Compton, annihilation, ...

interference

G. Jackson

Application of perturbative QCD

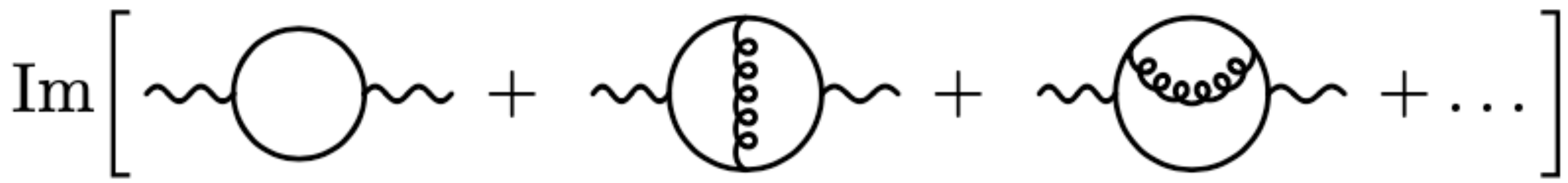

self-energy, $\Pi_{\mu\nu}$

[Weldon (1990)] , [Bödeker, Sangel, Wörmann (2015)]

NLO emission rates

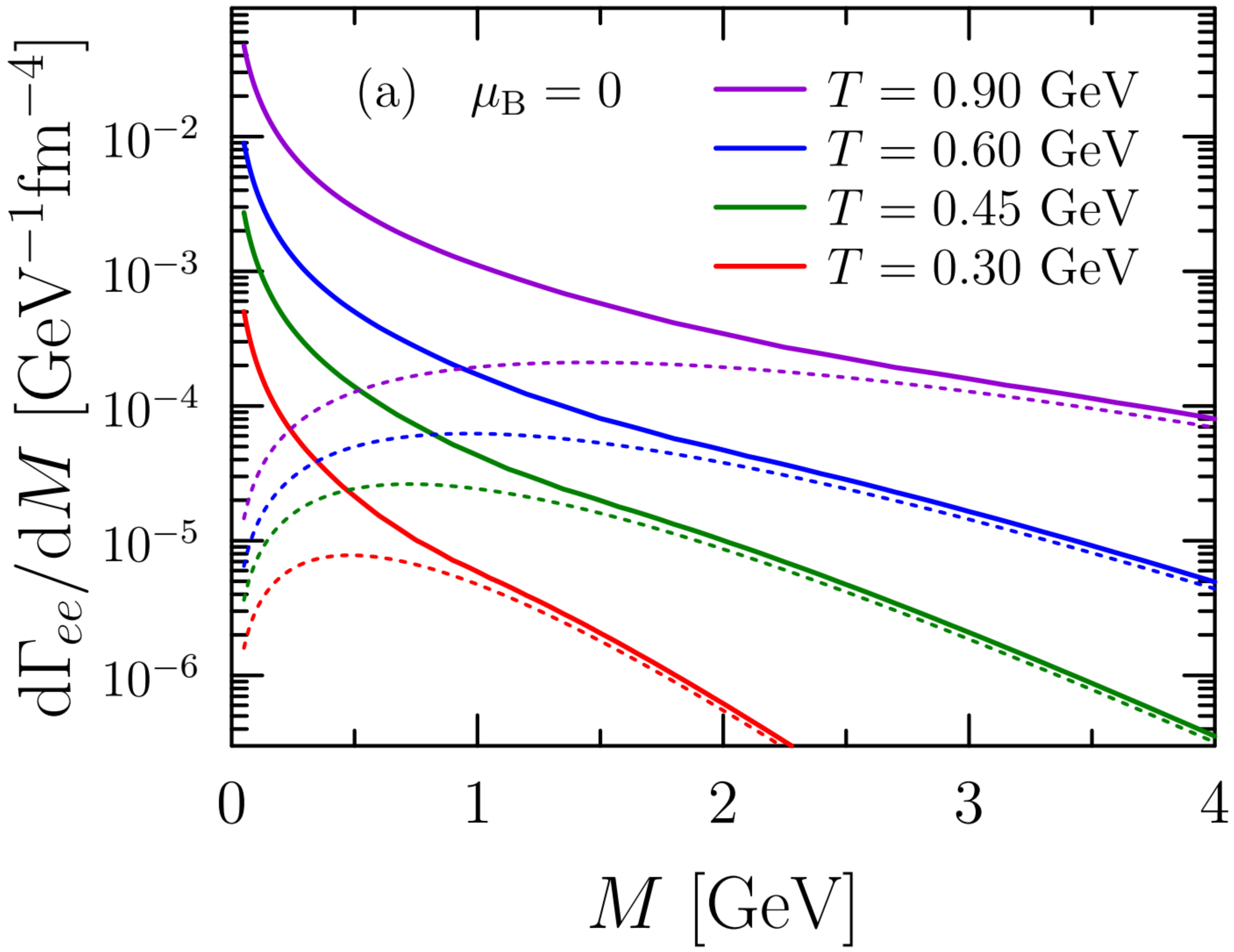

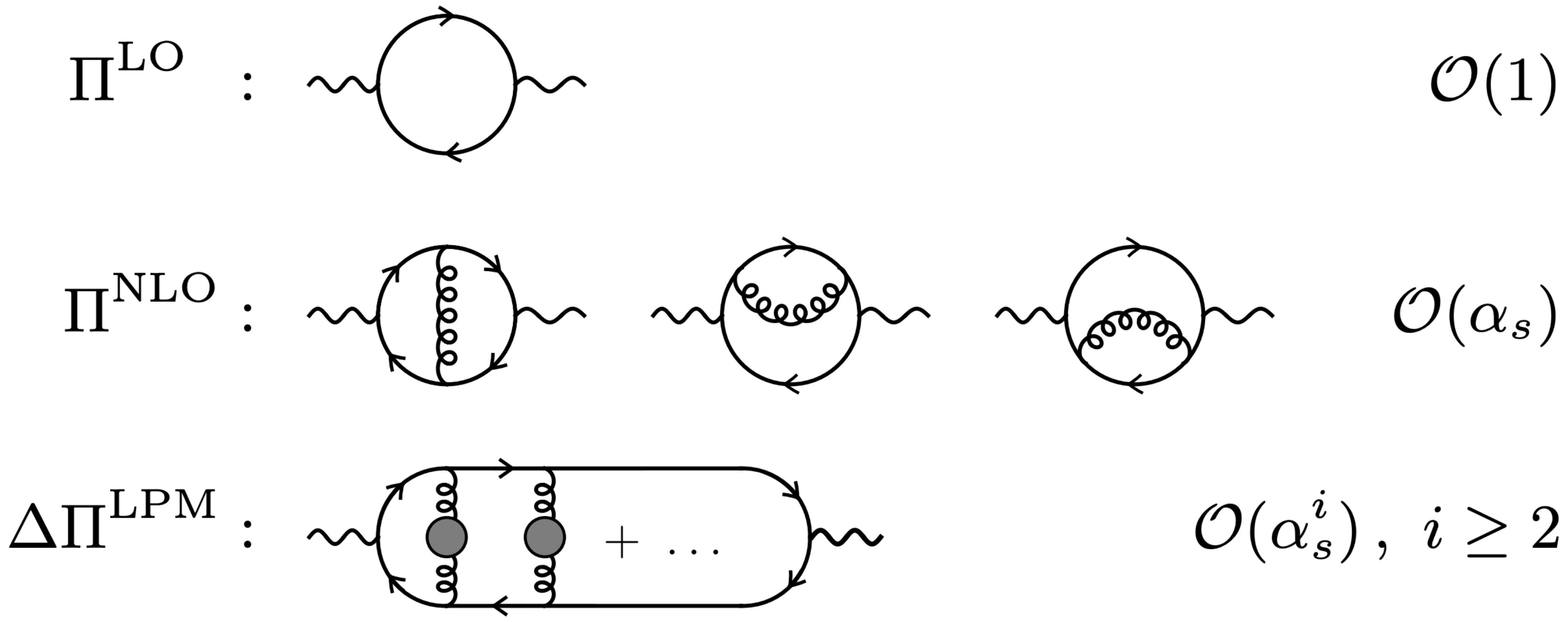

Churchill, LD, Gale, Jackson, Jeon, PRC 109, 044915 (2024), PRL 132, 172301 (2024)

Extraction of electric conductivity $\sigma_{\rm el}$

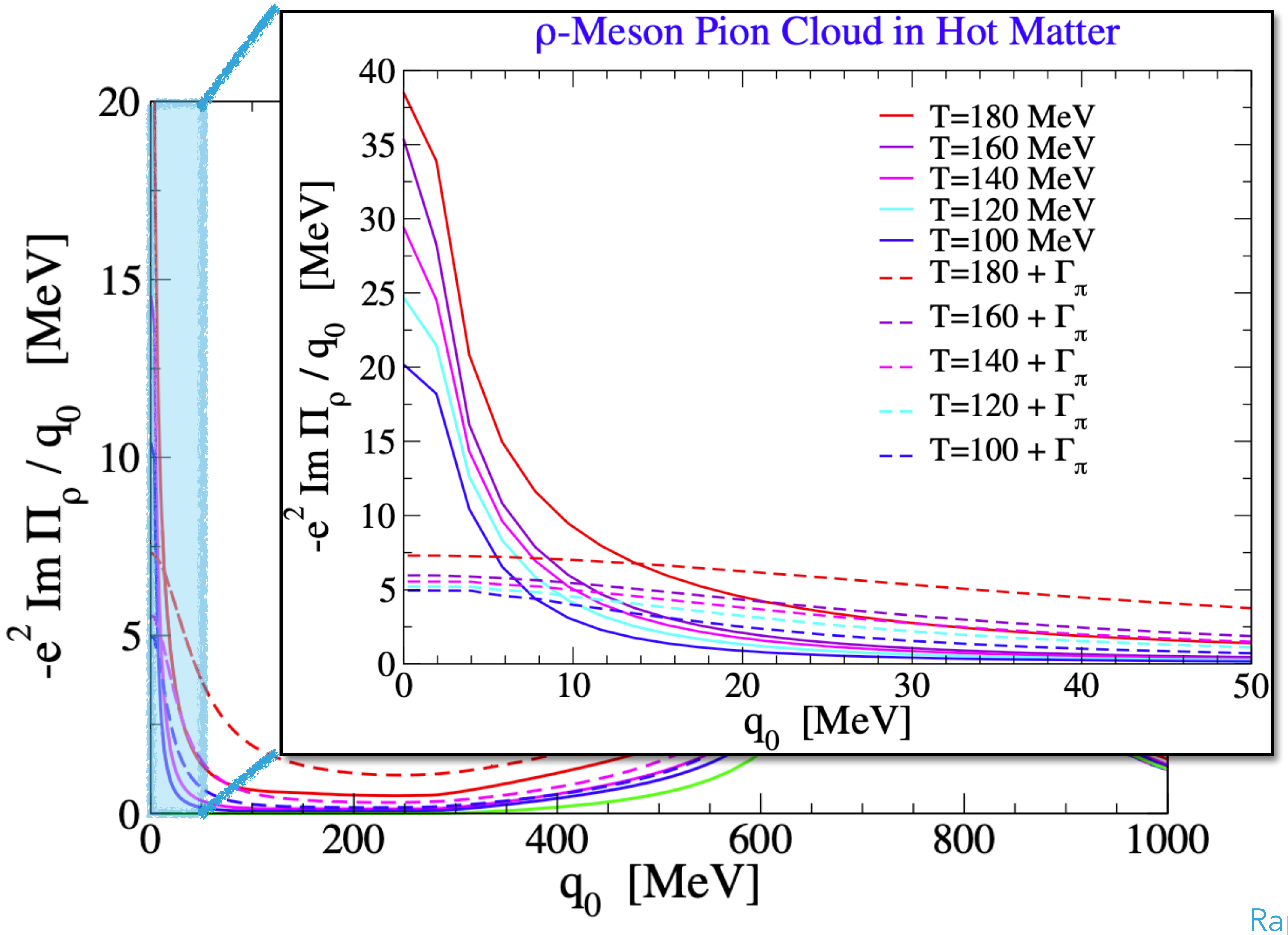

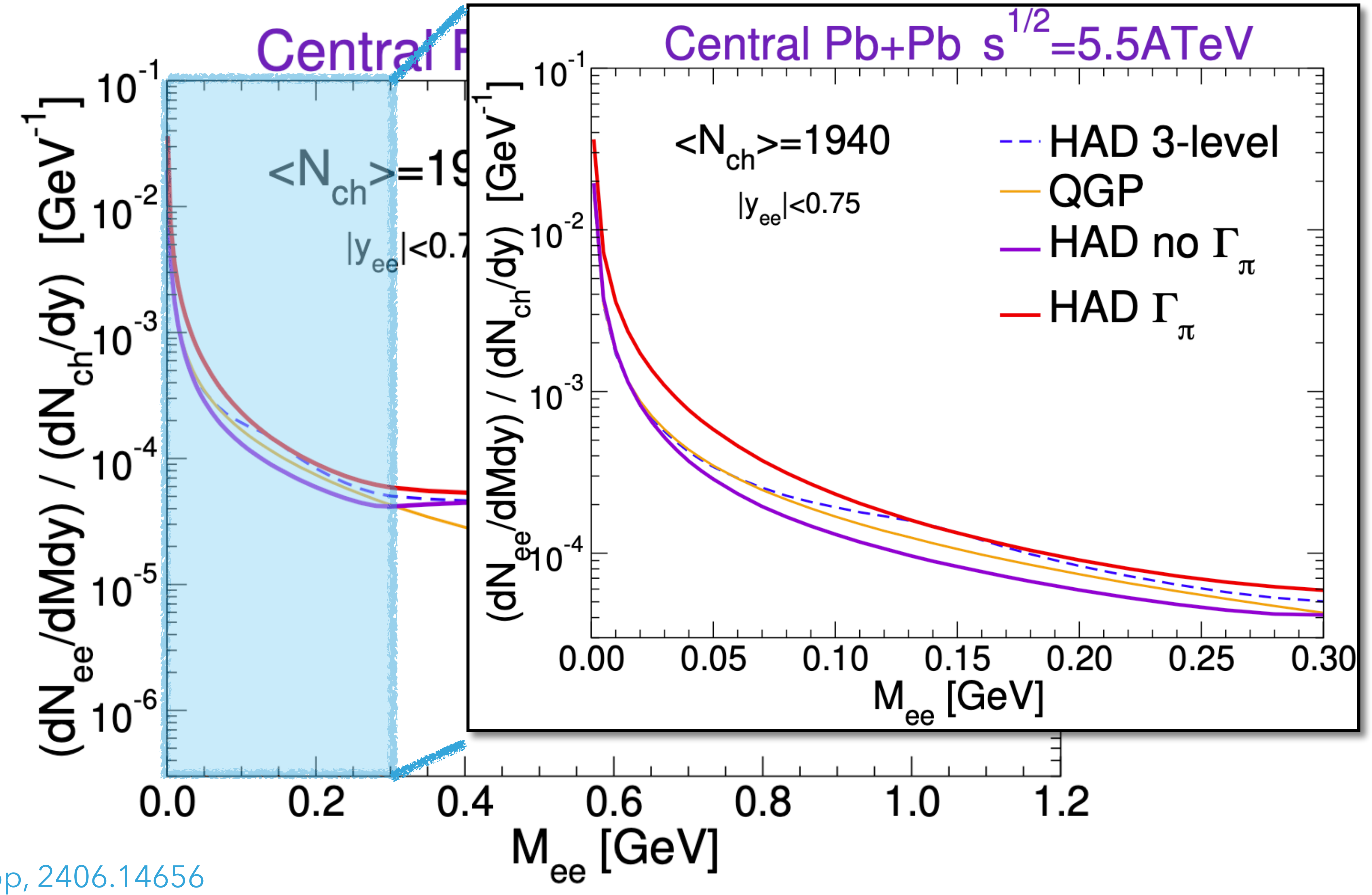

Rapp, 2406.14656

- Electric conductivity $\sigma_{\rm el}$ manifests in low-mass thermal dilepton spectra: $\sigma_{\rm el}(T) = \dfrac{e^2}{2} \lim\limits_{q_0 \to 0} \rho_{\rm em}(q_0, q = 0)/q_0$
- The inclusion of thermal pion widths significantly broadens the conductivity peak near zero energy.
- A key signature of a small conductivity is the enhanced dilepton yields in the very-low-mass region.

Floerchinger, Gebhardt, Reygers, PLB 837 (2023) 137647; Rapp, 2406.14656; Atchison, Han, Geurts, 2408.1017